University of Alberta

Plant residue decomposition in soil: interactions among substrates, decomposers and the soil environment

by

Desirée Candace Jans-Hammermeister

A thesis submitted

to the Faculty of Graduate Studies and Research

in partial fulfillment of the requirements for the degree of

Doctor of Philosophy

in

Soil Biology and Biochemistry

Department of Soil Science

Edmonton, Alberta

Fall 1995

ISBN 0-612-06229-5

Canada

University of Alberta

Library Release Form

Name of Author: Desiree Candace Jans-Hammermeister

Title of Thesis: Plant residue decomposition in soil: interactions among substrates, decomposers and the soil environment

Degree: Doctor of Philosophy

Year this Degree Granted: 1995

9517 - 84 Street
Fort Saskatchewan, Alberta
T8L 2T5

Date: August 10, 1995

There are more things in heaven
and earth, Haratio, than are
dreamt of in your philosophy

Shakespeare

University of Alberta

Faculty of Graduate Studies and Research

The undersigned certify that they have read, and recommend to the Faculty of Graduate Studies and Research for acceptance, a thesis entitled 'Plant residue decomposition in soil: interactions among substrates, decomposers and the soil environment' submitted by Desirée Candace Jans-Hammermeister in partial fulfillment of the requirements for the degree of Doctor of Philosophy in Soil Biology and Biochemistry.

W.B. McGill
(Supervisor)

M.J. Dudas

R.F. Grant

N.R. Knowles

R.C. Izaurralde
(Departmental Reader)

J.A.E. Molina
(External Examiner)

Date: June 22, 1995

ABSTRACT

Interactions among substrates, decomposers and the soil environment determine the dynamics of energy and nutrients within soil systems. Comprehensive prediction of soil response in varied agro-ecosystems requires elucidation of basic transformation mechanisms and the influence of controlling factors on these mechanisms. Pea residue decomposition in soil was investigated in the field, under controlled laboratory conditions and with mechanistic simulation models. In each case, the emphasis was on the microbial biomass as mediator of organic matter transformations. Field incorporation of full bloom pea residues resulted in a slower initial release of N and a greater recovery of pea-derived ^{15}N in the straw and roots of a subsequent barley crop (closer synchrony between the appearance of pea-derived mineral N and barley demand) compared to 10% bloom residues. The more mature residue was postulated to contain a smaller proportion of water-soluble N and/or a larger proportion of resistant components which physically limited microbial accessibility. In the laboratory, decomposition of the water-soluble and insoluble fractions of ^{15}N-labelled pea residues were further investigated. Evidence was found to suggest that decomposition was enhanced by maintaining a physical association between soluble and insoluble components, possibly the result of increasing decomposer efficiency by supplying both a readily available energy source and a hospitable habitat (in the form of insoluble residues). In addition to substrate quality, soil characteristics also influence plant residue decomposition. Our observations supported previous reports of higher normalized mineralization rates (e.g. N mineralization per unit biomass N) in Luvisolics compared to Chernozemics and were consistent with the hypothesis that higher rates of decomposition are associated with soils of lower clay content. Three mathematical representations of the decomposition process in soil were compared. All of the models appeared more sluggish than the natural system and none could account for differences in decomposition resulting from the spatial arrangement of residue components within the soil matrix. The importance of appropriate quantitative techniques and representative experimental data for model evaluation is discussed.

ACKNOWLEDGEMENTS

To my supervisor, Dr. W.B. McGill, a special thanks for sharing his knowledge, wisdom and sense of humor, and for always having time to 'chat'.

To my committee, Dr. M.J. Dudas, Dr. N.R. Knowles and especially Dr. R.F. Grant (who spent many hours sharing his expertise in simulation modelling), for guidance and suggestions.

To my departmental reader, Dr. R.C. Izaurralde and my external examiner, Dr. J.A.E. Molina, for helping to make the end a pleasant experience.

To my fellow McGillians, for camaraderie and friendly criticism and to the Friends of the Pedon for much needed recreation-time.

To Tom Jensen for encouraging me to begin my graduate program and for his generosity in sharing ideas, resources and hard work.

To C.T.K. Nguyen, C.T. Figueiredo, G.D. Dinwoodie, G.A. McGregor, L.D. Watson, E.W. Oosterhuis, and G. Braebrook for technical assistance.

To the Farming For the Future Program of the Alberta Agriculture Research Institute and the Natural Sciences and Engineering Research Council of Canada for financial support.

Finally, a sincere thanks to my husband, Andy, and my mother, Anita, for their love and support and to my dog, Kailey, for taking me out on long walks and keeping me in touch with the 'real world'!

TABLE OF CONTENTS

CHAPTER 1

Introduction

1.1 Residue decomposition and nutrient cycling ____ 1
1.2 Research objectives ____ 2
1.3 Literature cited ____ 3

CHAPTER 2

Nitrogen accumulations and relative rates of mineralization in two soils following legume green manuring

2.1 Introduction ____ 4
2.2 Materials and methods ____ 5
2.3 Results and discussion ____ 7
2.4 Literature cited ____ 13

CHAPTER 3

Dynamics of ^{15}N in two soil-plant systems following incorporation of 10% bloom and full bloom field pea

3.1 Introduction ____ 16
3.2 Materials and methods ____ 17
3.3 Results ____ 19
3.4 Discussion ____ 25
3.5 Literature cited ____ 27

CHAPTER 4

Is there a correlation among factors used to estimate soil microbial biomass?

4.1 Introduction ____ 30
4.2 Materials and methods ____ 30
4.3 Results and discussion ____ 31
4.4 Literature cited ____ 35

CHAPTER 5

Decomposition of pea shoot in soil: a laboratory incubation

5.1 Introduction ____ 37
5.2 Materials and methods ____ 38
5.3 Results ____ 40
5.4 Discussion ____ 44
5.5 Literature cited ____ 50

CHAPTER 6

Evaluation of three simulation models used to describe plant residue decomposition in soil

6.1 Introduction ____ 53
6.2 Materials and methods ____ 54
6.3 Results ____ 65
6.4 Discussion ____ 75
6.5 Literature cited ____ 85

CHAPTER 7
Spatial relationships and decomposition
7.1 Introduction ____ 87
7.2 Materials and methods ____ 88
7.3 Results ____ 92
7.4 Discussion ____ 96
7.5 Literature cited ____ 101

CHAPTER 8
Synthesis
8.1 Decomposition within an ecosystem framework ____ 103
8.2 Conclusions ____ 104
8.3 Further considerations ____ 106
8.4 Literature cited ____ 106

APPENDIX A
Simulation model equations and schematics ____ 107

LIST OF TABLES

Table 2-1. Properties of Provost and Rimbey soils ____ 5

Table 2-2. Mean square of analysis of variance for N accumulation as soil N, NH_4^+-N, NO_3^--N, mineral N (NH_4^+-N + NO_3^--N), and microbial N in Provost and Rimbey soil samples ____ 6

Table 2-3. Net N mineralization rates (estimated from non-fumigated soil samples incubated for 10 days) and normalized N mineralization rates in Provost and Rimbey soil samples on three 1990 sampling dates ____ 10

Table 2-4. Mean square of analysis of variance for net ^{14}N mineralized, net ^{15}N mineralized and normalized N mineralization rates in Provost and Rimbey soil samples ____ 11

Table 3-1. Composition of ^{15}N-labelled pea shoots (means of 8 samples) ____ 18

Table 3-2. Barley yield on two 1990 sampling dates following 10% bloom or full bloom legume incorporation ____ 20

Table 3-3. Mean square of analysis of variance for barley yield and nitrogen content ____ 20

Table 3-4. Mean square of analysis of variance for percent ^{15}N recovery in barley, legume residue and soil components (0-30 cm) ____ 23

Table 3-5. Regression coefficients of the relation between ln(proportion ^{15}N retained in the recalcitrant fraction of the legume) and decomposition period ____ 24

Table 4-1. Flushes of CO_2-C, mineral N and NRN and corresponding biomass C and N estimates ____ 32

Table 5-1. Properties of the Chernozemic and Luvisolic soils used in the laboratory incubation ____ 40

Table 5-2. ANOVA results for combined 81 day incubation data ____ 42

Table 5-3. First order decay parameters for microbial biomass ____ 43

Table 5-4. Change in microbial biomass upon incubation as reported in the literature ____ 45

Table 6-1. Initialization values for simulations of plant residue decomposition ____ 64

Table 6-2. Goodness of fit method to evaluate submodels (DBC and GLL experimental data) ____ 69

Table 6-3. Chi-square method to rank the submodels' overall correspondence to experimental data ____ 70

Table 6-4. Comparison of simulated N fluxes after 81 days (g N Mg^{-1} soil) ____ 74

Table 6-5. Mineralization response to amendment with pea shoot at 81 days ____ 75

Table 7-1. Characteristics of pea components ____ 89

Table 7-2. Initialization values for simulations of plant residue decomposition ____ 91

LIST OF FIGURES

Figure 1-1. Simplified N dynamics of legume green manure. 2

Figure 2-1. Nitrogen accumulation in the whole soil and soil fractions in (A) Provost and (B) Rimbey soil on four sampling dates. 8

Figure 2-2 Net N mineralization rates under controlled environments in (A) Provost and (B) Rimbey soils on three 1990 sampling dates. **Units: ^{14}N = g m^{-2} $10days^{-1}$; ^{15}N = mg m^{-2} $10days^{-1}$. 10

Figure 3-1. Recovery of ^{15}N in barley at (A) Provost and (B) Rimbey on two 1990 sampling dates following 10% bloom and full bloom incorporation. 21

Figure 3-2. Recovery of ^{15}N in legume residue and soil fractions on four sampling dates between 1989 and 1990 (A) Provost soil, (B) Rimbey soil following 10% bloom incorporation and (C) Provost soil, (D) Rimbey soil following full bloom incorporation. NMO = non-microbial organic. 22

Figure 4-1. Correlation among flushes of CO_2-C, mineral N and NRN following fumigation of a DBC (■) and a GLL (□) soil at the 0-15 cm sampling depth (A-C) and the 15-30 cm sampling depth (D-F). 33

Figure 5-1. Microbial biomass N in (A) DBC and (B) GLL; mineral N in (C) DBC and (D) GLL; CO2 evolved from (E) DBC and (F) GLL. ■, amended with pea shoot; □, non-amended. Error bars indicate standard deviation, n=3. 41

Figure 5-2 ^{15}N recovery in (A) DBC and (B) GLL soils. ◆, microbial biomass N; ◇, mineral N. Error bars indicate standard deviation, n=3. 42

Figure 5-3. Transformation of plant residue ^{15}N in (A) DBC and (B) GLL soils. ◆, Total ^{15}N - mineral ^{15}N; ◇, Total ^{15}N - (microbial biomass ^{15}N + mineral ^{15}N). 42

Figure 5-4. Ninhydrin-reactive N extracted from non-fumigated DBC soil (A) non-amended and (B) amended with pea residue. 46

Figure 6-1. Structure of plant residue decomposition submodels: (A) ECO, (B) PHO and (C) VER. Microbial biomass, adsorbed and active organic matter are components of the base model shown in Figure 6-2. 55

Figure 6-2. General structure of base model for soil functions. As shown here, 'microbial biomass' represents both live and inactivated biomass. The *respiration* flow is used for C simulation and the *mineralization immobilization* flow is used for N simulation. Note: *sorption* refers to both adsorption/precipitation and desorption/dissolution. 56

Figure 6-3. The concept of active biomass (55% labile + 45% resistant). 56

Figure 6-4. Observed (■) and simulated values (◆, ECO; ◇, PHO; +, VER) of (A) microbial biomass N, (B) mineral N, (C) ^{15}N recovery in microbial biomass N, (D) ^{15}N recovery in mineral N and (E) CO_2 evolved from a Dark Brown Chernozemic soil amended with ^{15}N-labelled pea shoots. 66

Figure 6-5. Observed (■) and simulated values (◆, ECO; ◇, PHO; +, VER) of (A) N mineralization rate and (B) respiration rate in a Dark Brown Chernozemic soil amended with ^{15}N-labelled pea shoots ____ 68

Figure 6-6. Observed (■) and simulated values (◆, ECO; ◇, PHO; +, VER) of (A) microbial biomass N and (B) ^{15}N recovery in microbial biomass N of a silty clay loam soil amended with ^{15}N-labelled wheat straw. Observed data from Ocio et al. (1991). ____ 71

Figure 6-7. Observed (■) and simulated values (◆, ECO; ◇, PHO; +, VER) of (A) ^{15}N recovery in microbial biomass N and (B) ^{15}N recovery in mineral N of a vertisol amended with ^{15}N-labelled medic leaves. Observed data from Amato and Ladd (1980). ____ 72

Figure 6-8. Simulated values (◆, ECO; ◇, PHO; +, VER) of (A) C and (B) N remaining in plant residue during simulated incubation of a Dark Brown Chernozemic soil amended with ^{15}N-labelled pea residue. ____ 73

Figure 6-9. Schematic of simulated N fluxes (see Table 6-4). 'Soil organic matter' represents soluble, adsorbed, active and passive organic matter and 'microbial biomass' represents both live and inactivated biomass. ____ 74

Figure 7-1. Scanning electron microscopy images of freeze-dried, ground pea shoot. For reference, a spherical bacterial cell is approximately 1 um in diameter. ____ 90

Figure 7-2. ^{15}N recovery (as a percent of total soil ^{15}N) in the mineral, microbial and non-microbial organic (NMO) fractions of a Dark Brown Chernozemic soil amended with the (A) whole, (B) soluble component, (C) insoluble component, (D) soluble + insoluble components of ^{15}N-labelled pea shoots and ^{15}N-labelled pea roots. ____ 93

Figure 7-3. Rate of CO_2 evolution (corrected for basal rate) following amendment with (A) pea shoots and shoot components and (B) pea roots and root components. ____ 94

Figure 7-4. Respiratory response to amendment with (A) pea shoots and shoot components and (B) pea roots and root components. Values were calculated by subtracting the non-amended respiration from the respiration of amended incubations and dividing by the mass of residue C added (x 100%). ____ 94

Figure 7-5. Simulated values of (A) pea shoot C remaining and (B) pea root C remaining. ◆, ECO and ■, PHO whole plant residue; ◇, ECO and □, PHO sum of soluble and insoluble components of plant residue. ____ 95

CHAPTER 1

Introduction

1.1 RESIDUE DECOMPOSITION AND NUTRIENT CYCLING

The soil matrix and its living inhabitants are integral parts of the energy and nutrient cycles which enable ecosystems to function. C from organic residues is utilized by heterotrophic organisms within food webs and may be dissipated as CO_2 or incorporated into heterogeneous humic materials. Nutrients contained in the residues, such as N, are also transformed and may be recycled within the soil system through repeated mineralization-immobilization reactions. Although organic matter decomposition dynamics have been studied extensively, the complex nature of the soil matrix precludes direct measurement of changes in the decomposing materials. Consequently, our understanding of the process is based on indirect methods of investigation ranging from simple measurements of C and N mineralization to the development of integrated mechanistic simulation models.

Input of organic matter into agro-ecosystems[1] may be less than that lost by crop removal, gaseous losses and leaching. The result is a decrease in the organic matter content of cultivated soils and an eventual increase in N fertilizer requirements. The use of annual legumes as green manures has been suggested as a management strategy to increase soil organic matter, particularly stable organic N reserves (Jensen and Timmermans, 1987). Legumes used as a summerfallow substitute may also reduce N-fertilizer and tillage requirements (Rice et al., 1993). To optimize potential benefits of legume green manures, it is necessary to understand the dynamics of legume-derived N in the soil (Figure 1-1).

Decomposition and subsequent mineralization-immobilization reactions are mediated by the soil microbial biomass. The biomass changes in size and activity in response to substrate availability and environmental conditions. Therefore, the chemical properties of a substrate, such as the proportion of readily metabolizable soluble organics (Muller et al., 1988), as well as the physical accessibility of the substrate (McGill and Myers, 1987) influence the rate of

---

[1] agro-ecosystem refers to an ecosystem manipulated by frequent, marked anthropogenic modifications of its biotic and abiotic environments (Coleman and Hendrix, 1988).

decomposition. Soil physico-chemical properties also influence the rate of organic matter transformation. For example, residual organic matter from decomposing legumes is positively correlated with soil clay content and cation exchange capacity (Amato and Ladd, 1992). Consequently, soils with contrasting pedogenic histories have characteristic responses to agronomic practices.

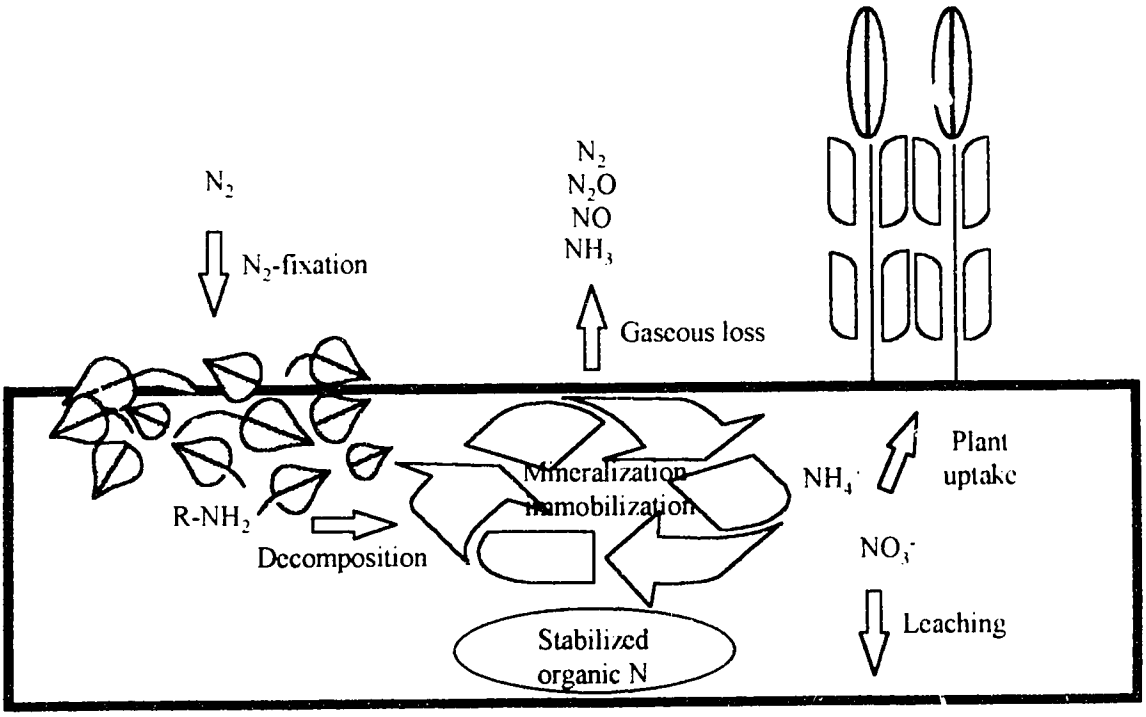

Figure 1-1. Simplified N dynamics of legume green manure.

1.2 RESEARCH OBJECTIVES

The objective of this research was to study plant residue decomposition in soil: specifically, the interactions among substrates, decomposers (primarily the microbial biomass), and the soil environment. To elucidate mechanisms and regulatory factors involved in this process, dynamics of N and C following soil incorporation of pea residues were studied in field experiments, laboratory incubations, and computer simulation models. Specific objectives were:

(Chapter 2) To compare the accumulation and dynamics of N in the microbial, mineral and non-microbial organic fractions of a Chernozemic and a Luvisolic soil following pea incorporation under field conditions; to compare normalized N mineralization rates (e.g. mg N mineralized g^{-1} microbial N); and to relate N dynamics to soil properties.

(Chapter 3) To compare barley yield and legume-derived N dynamics following incorporation of ^{15}N-labelled pea residues at two bloom stages and at two field sites.

(Chapter 4) To examine the correlation among factors (flush of CO_2-C, mineral N, NRN) used to estimate soil microbial biomass.

(Chapter 5) To obtain and analyze critically sets of independent experimental data from laboratory incubations of ^{15}N-labelled plant residues in soil which would be used for evaluation of simulation models.

(Chapter 6) To evaluate systematically the plant residue decomposition algorithms from three published simulation models.

(Chapter 7) To compare microbial utilization and mineralization of spatially associated or spatially separated plant components (water soluble/insoluble) in soil; to assess the ability of two plant residue decomposition models to account for differences in the spatial arrangement of plant residue components.

1.3 LITERATURE CITED

Amato, M. and Ladd, J.N. 1992. Decomposition of ^{14}C-labelled glucose and legume material in a range of soils: Properties influencing the accumulation of organic residues and microbial biomass C. Soil Biol. Biochem. 24:455-464.

Coleman, D.C. and Hendrix, P.F. 1988 Agroecosystem processes. Pages 149-170 *in* L.R. Pomeroy and J.J. Alberts, eds. Concepts of Ecosystem Ecology: A Comparitive View. Springer-Verlag, New York, USA.

Jensen, T.L. and Timmermans, J. 1987. Conservation Tillage. Alberta Agriculture Agdex 516-3.

McGill, W.B. and Myers, R.J.K. 1987. Controls on dynamics of soil and fertilizer nitrogen. Pages 73-99 *in* Soil Fertility and Organic Matter as Critical Components of Production Systems. SSSA Spec. Pub. no. 19.

Muller, M.M., Sundman, V., Soininvaara, O. and Merilainen, A. 1988. Effect of chemical composition on the release of nitrogen from agricultural plant materials decomposing in soil under field conditions. Biol. Fertil. Soils 6:78-83.

Rice, W.A., Olsen, P.E., Bailey, L.D., Biederbeck, V.O. and Slinkard, A.E. 1993. The use of annual legume green-manure crops as a substitute for summerfallow in the Peace River region. Can. J. Soil Sci. 73:243-252.

CHAPTER 2

Nitrogen accumulations and relative rates of mineralization in two soils following legume green manuring[1]

2.1 INTRODUCTION

Dark Brown Chernozemic and Gray Luvisol Luvisolic soils are used extensively for cereal production in Alberta. These soils are susceptible to degradation and must be carefully managed to maintain productivity. One management strategy for soil conservation involves green manuring of annual legumes in place of cultivated summerfallow (Jensen and Timmermans, 1987). Legumes are particularly useful as green manures because, in addition to supplying organic matter to the soil, they also supply nitrogen obtained through symbiotic N_2-fixation.

Organic C and N dynamics do not follow the same patterns in Chernozemic and Luvisolic soils (Dinwoodie and Juma, 1988; Rutherford and Juma, 1989) and, consequently, these soils have their own characteristic responses to agronomic practices such as green manuring. C and N dynamics can best be compared among soils when transformation rates are expressed on the basis of common soil components. Here we use the term 'normalized rates' to describe net N mineralization rates expressed as proportions of the N present in the whole soil or in selected soil fractions (e.g. mg N mineralized g^{-1} soil microbial N).

Residue decomposition and subsequent mineralization-immobilization processes are affected by substrate type and location (McGill and Myers, 1987), climate (Amato et al., 1987; Ladd et al., 1981), soil texture (Campbell and Souster, 1982; Amato and Ladd, 1992; Ladd et al., 1992), pH and pore space (Amato and Ladd, 1992). These factors influence not only the quantity of N in soil fractions but also the flux of N between fractions. The objectives of this study were: (i) to compare the accumulation and dynamics of N in the mineral, microbial and non-microbial organic fractions of a Chernozemic and a Luvisolic soil following pea incorporation under field conditions; (ii) to compare normalized N mineralization rates; and (iii) to relate N dynamics to soil properties.

---

[1] A version of this chapter has been published in the Canadian Journal of Soil Science 74:23-28.

2.2 MATERIALS AND METHODS

Site Descriptions

Field sites were established in 1989 near the towns of Provost and Rimbey, Alberta. The Provost site (52° 21' N, 110° 16' W) was 260 km southeast of Edmonton, Alberta on a Chernozemic (Dark Brown) soil with a 30 year mean growing season (May-September) precipitation of 285 mm. Total precipitation over the one year study period (legume incorporation to barley harvest) was 480 mm. The cropping history from 1985 to 1988 was: fallow, wheat, fallow, canola. The Rimbey site (52° 38' N, 114° 16' W) was 110 km southwest of Edmonton on a Luvisolic (Gray Luvisol) soil with a 30 year mean growing season (May-September) precipitation of 351 mm. Total precipitation over the one year study period was 860 mm. The cropping history of the Rimbey site included rotations with forages and the land was in forages from 1985 to 1987 followed by wheat in 1988. Soil properties for both sites are shown in Table 2-1.

Table 2-1. Properties of Provost and Rimbey soils

Sample	Total C[a] (%)	Total N[b] (%)	pH[c]	D_b (Mg m^{-3})	Clay[d] (%)	Texture
Provost (0 - 15cm)	2.07	0.160	7.2	1.24	35.54	Clay loam
Provost (15 - 30cm)	2.22	0.115	8.3	1.58	42.82	Clay loam
Rimbey (0 - 15cm)	2.46	0.183	6.0	1.19	15.04	Silty loam
Rimbey (15 - 30cm)	0.94	0.099	6.4	1.57	29.53	Loam

[a] Determined by dry oxidation in LECO induction furnace.
[b] Determined by Kjeldahl digestion.
[c] Determined in 1:2 soil:H_2O (mass:volume) mixture by glass electrode.
[d] Determined by hydrometer method.

In May of 1989, four blocks were established at each site in a factorial split-split-plot design with incorporation of legume at two bloom stages (10% bloom or full bloom) as main plots split by four sampling dates and further split by two sampling depths (0-15 cm and 15-30 cm). Data reported here are from the full bloom treatment only. Sites were managed as recommended for annual legume green manuring. The Provost site was fertilized with 7.4 kg P ha^{-1} as triple superphosphate and 11 kg S ha^{-1} as elemental sulfur and the Rimbey site was fertilized with 9.6 kg P ha^{-1} as triple superphosphate, 28 kg K ha^{-1} as potassium sulfate and 11 kg S ha^{-1} as potassium sulfate and elemental sulfur. Both sites were treated with Treflan 545EC (545 g trifluralin L^{-1}) at 2

L ha^{-1} and seeded to 'Type C' inoculated field pea (*Pisum sativum* 'Sirius') at 80 kg ha^{-1}. In early August, full bloom field-grown peas were incorporated to approximately 10 cm with a discing implement.

Sampling and Analysis of Soils

Four open-ended plastic cylinders (30 cm diameter, 50 cm length) were installed in each plot and non-labelled plant material removed from within the cylinders by hand-picking to a depth of approximately 15 cm. ^{15}N-labelled full bloom pea shoots were incorporated into the cylinder soil to a depth of 10 cm. Details of ^{15}N procedures are reported in Chapter 3. Briefly, peas were grown in sterile sand troughs fed with nutrient solution including the equivalent of 100 kg N ha^{-1} as $^{15}NH_4{}^{15}NO_3$ (10% ^{15}N atom abundance).

In May of 1990, the entire plot area was seeded to barley (*Hordeum vulgare* 'Bonanza'). Cylinders were hand weeded and thinned to contain 12 barley plants each giving a density of 170 plants m^{-2}. Pulled vegetation was left on the soil surface within the cylinders.

One cylinder from each plot was removed from the field: 1) in the fall following legume incorporation; 2) at the time of barley seeding; 3) when barley was at Zadoks Growth Stage 39 (flag leaf) (Tottman and Broad, 1987); and 4) when the barley was at Zadoks Growth Stage 75 (ripening). At Provost, samples were taken September 18, 1989 and May 24, July 13 and August 21, 1990. At Rimbey, samples were taken September 21, 1989 and May 23, August 2 and September 5, 1990. Barley roots and partially decomposed legume residues were removed from each of two soil layers (0-15 and 15-30 cm) by hand picking and soil sieving (2 mm). Recovered roots were washed in distilled water on a 1 mm mesh sieve. Total N of the remaining soil was measured on a Carlo Erba Model 1500 Automatic Nitrogen Analyzer.

Soil mineral N was extracted from moist sieved soil (2 mm) with 2 *M* KCl (25 g soil:125 mL KCl) for 1 hour and then filtered through Whatman 42 filter paper. The extracts were frozen until time of analysis. A Technicon AutoAnalyzer was used to quantify NH_4^+-N and NO_3^--N (Keeney and Nelson, 1982). The ^{15}N diffusion method of Brooks et al. (1989) was used to prepare mineral N in the extracts for isotope ratio analysis on a VG Isogas ANA-SIRA (Automatic Nitrogen Analyzer - Stable Isotope Ratio Analyzer) Dumas combustion - mass spectrometer system in which samples were dispensed into a Carlo Erba Model 1500 ANA, combusted, analyzed for N content and the effluent introduced directly into the mass spectrometer for isotope ratio analysis.

Microbial biomass N was determined by the chloroform fumigation-incubation method of Jenkinson and Powlson (1976) on moist, sieved (2 mm) soil adjusted to 55% water-holding capacity and incubated at 23°C. The formula of Shen et al. (1984) was used to calculate biomass N as $B_n = F_n/k_n$, where F_n is {[NH_4^+ + NO_3^- in fumigated soil incubated for 10 days] - [NH_4^+ + NO_3^- in non-fumigated control soil incubated for 10 days]} and $k_n = 0.68$. The change in mineral N during the 10 day incubation of non-fumigated samples was used as a measure of net N mineralization. Mineral N samples were prepared for isotope ratio analysis on the ANA-SIRA system by the ^{15}N diffusion method (Brooks et al., 1989). Non-microbial organic N (NMO N) was calculated as the difference between total soil N and the sum of microbial N and mineral N.

Statistical Analysis

All experimental data were analyzed using the General Linear Model procedure of SAS (SAS Institute, 1985). The probabilities presented are Greenhouse-Geisser (Greenhouse and Geisser, 1959) adjusted probabilities which correct for unequal variances of the means.

2.3 RESULTS AND DISCUSSION

Overall, the quantities of soil N, mineral N and microbial N were not significantly different between sites (Figure 2-1; Table 2-2). A survey of Alberta soils reported that, in the top 15 cm of cultivated A horizons, the mean concentrations of organic carbon are 2.7% and 2.3% for Dark Brown and Gray Luvisol soils, respectively (McGill et al., 1988). The C content of the Provost soil (2.07%) was slightly below the mean value for a Dark Brown, possibly reflecting the frequent summerfallow; and that of the Rimbey soil (2.46%) was slightly above the mean for Gray Luvisols, which is consistent with the history of forage production at this site. Consequently, the Provost and Rimbey soils had similar C and N concentrations in the top 15 cm. The similarity in microbial N ($g\ m^{-2}$) between sites was expected as microbial biomass is positively correlated with total soil organic C and N (Carter, 1986). Microbial N generally decreased with depth but followed different trends over time at each depth (significant date x depth interaction), generally increasing with time in the 0-15 cm layer while decreasing in the 15-30 cm layer. Both sites had soil concentrations of NH_4^+ and NO_3^- near zero at the time of grain ripening which indicated that the crop uptake and microbial immobilization of mineral N were equal to or greater than the rate of N mineralization in both soils.

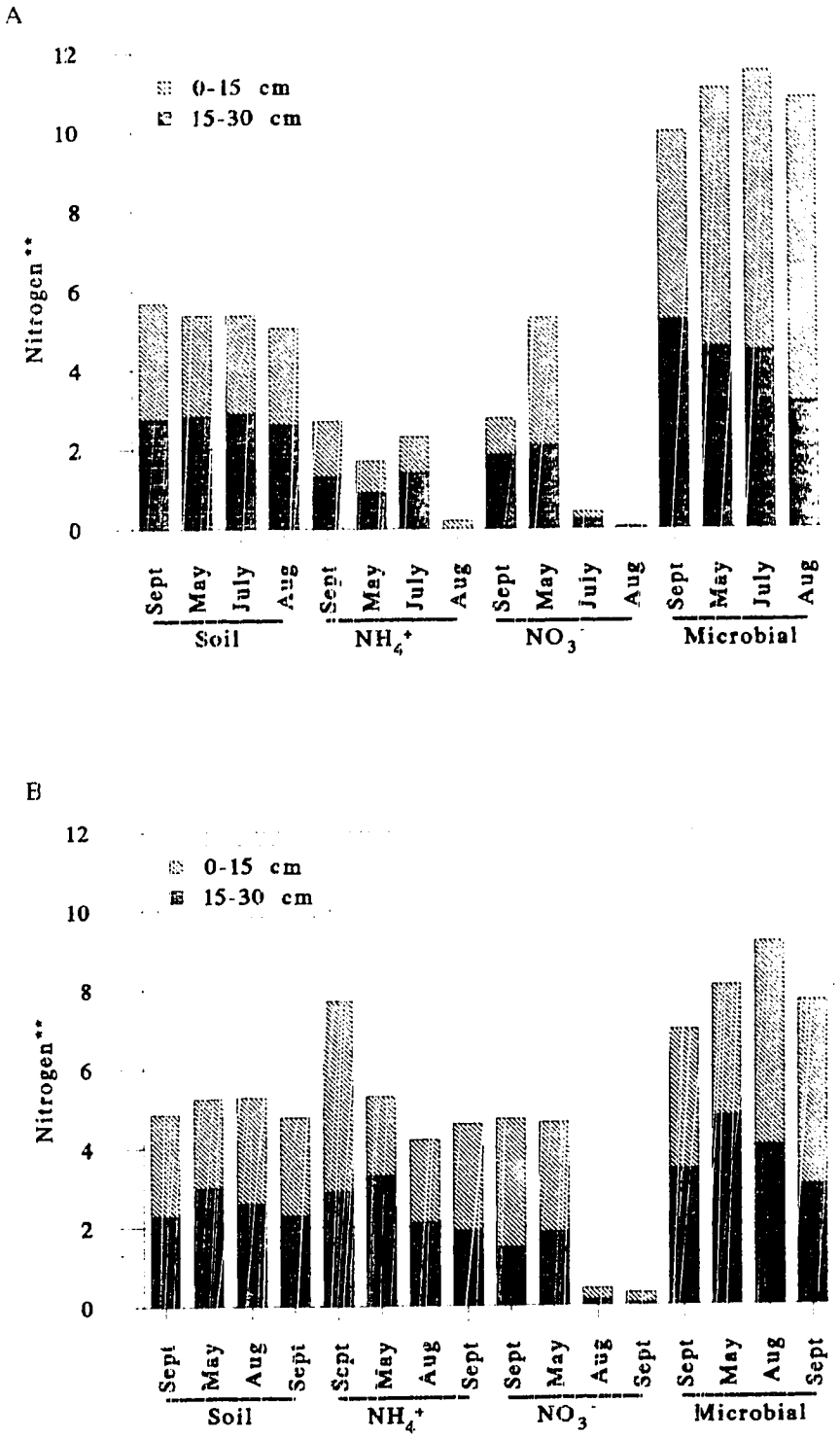

Figure 2-1. Nitrogen accumulation in the whole soil and soil fractions in (A) Provost and (B) Rimbey soil on four sampling dates. **Units: Soil = 10^3kg ha^{-1}, NH_4^+ = kg ha^{-1}; NO_3^- = 10^1kg ha^{-1}; Microbial = 10^1kg ha^{-1}.

Table 2-2 Mean square of analysis of variance for N accumulation as soil N, NH_4^+-N, NO_3^--N, mineral N (NH_4^+-N + NO_3^--N), and microbial N in Provost and Rimbey soil samples

Source of Variation	df	Soil N	NH_4^+-N	NO_3^--N	Mineral N	Microbial N
Site	1	2966	0.5550 **	0.60	2.33	29.44
Error 1	6	10149	0.0149	0.66	0.75	12.79
Date	3	2132	0.0543 *	23.13 **	24.58 **	2.75
Date x Site	3	1686	0.0193	1.26 *	1.46 *	0.14
Error 2	18	1237	0.0135	0.34	0.39	1.07
Depth	1	912	0.0020	2.83 **	2.98 *	30.10 *
Depth x Site	1	1678	0.0068	2.01 *	2.22 *	16.41
Error 3	6	729	0.0051	0.20	0.22	3.38
Depth x Date	3	2731	0.0220 *	0.80 *	0.69 *	11.08 **
Depth x Date x Site	3	782	0.0142	1.81 **	2.07 **	3.99
Error 4	18	948	0.0052	0.17	0.20	1.27

* The difference between the means is significant at: **, P<0.01; *, P<0.05.

Soil fractions with the highest turnover rates react most rapidly to changes in substrate availability (McGill et al., 1988). For example, mineralizable N declines faster than total N in response to increased fallow frequency (Janzen, 1987) and microbial biomass is more affected by crop rotations and amendments than are total C and N (McGill et al., 1986; Powlson et al., 1987). It is the kinetic state of these rapidly cycling fractions which determines the short term fate of N from decomposing residues. Consequently, comparisons among dynamic parameters such as rates and normalized rates of soil processes yield greater insights than do comparisons among static parameters such as the absolute sizes of these fractions. Dinwoodie and Juma (1988) express the rates of C transformations on a soil C basis, rather than a soil mass basis, so that the distribution of C among, and flow of C between, soil components can be compared across soils. Similarly, potentially mineralizable N makes up a larger proportion of total N in cultivated Luvisolics compared to Chernozemics (Campbell and Souster, 1982). Our observations support these findings with an overall greater net N mineralization rate, as well as greater net N mineralization rate normalized o soil N, microbial N, or NMO N in the Rimbey soil samples (Table 2-3; 2-4). N distribution did not distinguish between these soils, but transformation rates did.

Table 2-3. Net N mineralization rates (estimated from non-fumigated soil samples incubated for 10 days) and normalized N mineralization rates in Provost and Rimbey soil samples on three 1990 sampling dates[a]

Site and depth	Provost (0-15 cm)						Rimbey (0-15 cm)					
Sampling date	May		July		August		May		August		September	
Net ^{14}N mineralized (kg ha^{-1} soil 10d^{-1})	8.10	(1.0)	14.4	(3.7)	2.70	(0.8)	14.7	(1.5)	8.60	(2.2)	11.0	(2.1)
Net ^{15}N mineralized (kg ha^{-1} soil 10d^{-1})	0.059	(0.031)	0.061	(0.006)	0.014	(0.008)	0.048	(0.056)	0.023	(0.009)	0.027	(0.004)
Net N mineralized (mg g^{-1} soil N 10d^{-1})	3.25	(0.64)	5.82	(1.48)	1.11	(0.21)	5.87	(0.79)	3.25	(0.95)	4.43	(0.75)
Net N mineralized (mg g^{-1} microbial N 10d^{-1})	125.36	(24.39)	213.40	(68.62)	35.92	(7.96)	464.87	(133.41)	169.37	(50.30)	240.88	(68.11)
Net N mineralized (mg g^{-1} NMO N 10d^{-1})	3.38	(0.68)	5.99	(1.52)	1.15	(0.22)	6.02	(0.81)	3.32	(0.97)	4.52	(0.76)
Site and depth	Provost (15-30 cm)						Rimbey (15-30 cm)					
Sampling date	May		July		August		May		August		September	
Net ^{14}N mineralized (kg ha^{-1} soil 10d^{-1})	3.60	(3.3)	9.80	(3.9)	3.80	(1.8)	15.7	(2.3)	5.40	(1.8)	3.60	(0.9)
Net ^{15}N mineralized (kg ha^{-1} soil 10d^{-1})	-0.018	(0.011)	0.004	(0.002)	0.003	(0.004)	0.020	(0.010)	0.005	(0.003)	0.002	(0.001)
Net N mineralized (mg g^{-1} soil N 10d^{-1})	1.30	(1.11)	3.54	(1.07)	1.42	(0.41)	5.49	(1.66)	2.08	(0.63)	1.61	(0.29)
Net N mineralized (mg g^{-1} microbial N 10d^{-1})	76.87	(66.81)	271.81	(155.32)	117.42	(26.81)	340.53	(87.05)	141.37	(58.08)	120.87	(11.61)
Net N mineralized (mg g^{-1} NMO N 10d^{-1})	1.34	(1.14)	1.07	(3.59)	1.43	(0.42)	5.63	(1.73)	2.12	(0.64)	1.63	(0.30)

[a] Means of three replicates and (standard deviation)

Table 2-4 Mean square of analysis of variance for net ^{14}N mineralized, net ^{15}N mineralized and normalized N mineralization rates in Provost and Rimbey soil samples

Source of		Net mineralization				N mineralization rates normalized to					
Variation	df	^{14}N		^{15}N		Soil N		Microbial N		NMO N	
Site	1	0.9324	*	0.016		13.209	*	135308	*	13.462	*
Error 1	6	0.0715		2.831		1.055		10399		1.090	
Date	3	1.2307	**	10.503		15.466	**	61045	**	16.595	**
Date x Site	3	2.1387	**	11.137		30.798	**	151192	**	32.283	**
Error 2	18	0.0695		2.890		0.838		5010		0.881	
Depth	1	1.0296	*	155.502	**	22.908	**	10915		24.941	**
Depth x Site	1	0.0094		18.674		0.068		44105	*	0.037	
Error 3	6	0.0798		4.735		1.340		5348		1.428	
Depth x Date	3	0.0472		12.190		0.357		10683		0.397	
Depth x Date x Site	3	0.5091	**	11.546		6.704	**	4858		7.139	**
Error 4	18	0.0178		4.671		0.587		4799		0.636	

* The difference between the means is significant at: **, P<0.01; *, P<0.05.

In addition to allowing comparisons among soils, normalized rates also yield information on the dynamics of active soil fractions. For example, all soil N which becomes mineralized must pass through the microbial biomass. Therefore, net N mineralization rate normalized to microbial N is an index of microbial activity. Furthermore, net N mineralization rate normalized to NMO N may give insight to the kinetic state of the organic N. Both of these normalized rates were greater in Rimbey soil samples which may be indicative of a more active biomass and a more dynamic organic N fraction. Dinwoodie and Juma (1988) also report greater microbial respiration per unit of biomass C in a Luvisolic soil compared to a Chernozemic soil. Rutherford and Juma (1989) report comparable N mineralization rates normalized to soil N with a significantly higher rate in a Luvisolic compared to a Chernozemic soil (2.0 mg g^{-1} soil N $10d^{-1}$ for a Chernozemic and 3.9 mg g^{-1} soil N $10d^{-1}$ for a Luvisolic soil, calculated from Tables 2 and 4). N mineralization normalized to biomass N, however, was not significantly different between soils (170 mg g^{-1} microbial N $10d^{-1}$ for a Chernozemic and 200 mg g^{-1} microbial N $10d^{-1}$ for a Luvisolic soil, calculated from Table 4) (Rutherford and Juma, 1989).

From an extensive study of 23 Australian soils, Amato and Ladd (1992) suggest that, for soils of neutral to alkaline pH, the residual organic ^{14}C from decomposing (^{14}C)-*Medicago*

littoralis is positively correlated with soil clay content and cation exchange capacity but is not significantly correlated with soil organic C and N content. Therefore, the higher clay content at Provost (mean of 39.2% in the 0-30 cm layer compared to 22.3% at Rimbey) was expected to result in greater retention of organic N and slower decomposition rate. The lower net N mineralization rate and lower normalized N mineralization rates per unit of NMO- or microbial-N in Provost soil samples are consistent with this hypothesis (Table 2-3; 2-4).

N mineralization is microbially mediated and, therefore, soil physical properties which influence the interaction between microorganisms and their substrate will also influence N mineralization. Soils with high clay content have several associated properties including high cation exchange capacity, greater total pore space and a greater proportion of small pores, which make them more likely to have slower decomposition and mineralization rates. Organic matter in the soil may be protected from microbial attack by adsorption to clay surfaces and by its location within aggregates or small pores (<0.2 μm) which are inaccessible to the decomposers (Hassink, 1993; Van Veen and Kuikman, 1990). Besides mediating the mineralization of organic soil N, the microbial biomass is also a potential source of mineral N. Therefore, if the biomass has a slow turnover rate, then the organic N held within it will also have a slow turnover rate. The greater proportion of small pores in clay soils protect the microorganisms in two ways: more water is retained in the pores at a given matric potential and, therefore, cellular dehydration is less likely (Van Veen and Kuikman, 1990), and soil fauna cannot prey on microbes located within the small pores (0.2 - 6 μm) (Hassink, 1993). Predation increases N mineralization because the C:N ratio of the fauna is greater than that of their prey and excess N is released into the soil as NH_4 (Hunt et al., 1987).

Pre-incubation soil conditions appear to influence N mineralization rates as determined from the incubation of non-fumigated soil samples under laboratory conditions. Soil ^{14}N dynamics, represented by net ^{14}N mineralization rates, showed significant but contrasting variation between sampling dates (Table 2-3; 2-4). Provost reached a peak rate at the July sampling date while Rimbey reached a peak rate at the May sampling date. These mineralization rates were determined in laboratory incubations under controlled conditions without further amendments to the soils in the field following initial legume incorporation other than growth of a barley crop. Consequently, the significant 'date' effect and date x site interaction must be indicative of changes either in the nature of the substrate, its accessibility or the microbial communities - or perhaps all three. Furthermore, these changes occurred at different times at the two sites. Such observations emphasize the

importance of considering pre-incubation soil conditions, as well as the timing of soil sampling when interpreting results from studies under controlled environments.

In contrast to net ^{14}N mineralization rates, net ^{15}N mineralization rates did not differ significantly between sites or dates (Table 2-3; 2-4). Although not statistically significant, observations in Provost soil samples (15-30 cm) at the May sampling date suggest that the two isotopes followed distinctly different trends with apparent net ^{15}N immobilization accompanied by net ^{14}N mineralization. Similar observations have been reported in which considerable quantities of labelled N are immobilized when soil is incubated with labelled inorganic N even if there is net mineralization of N in soil (Jenkinson et al., 1985). Such observations are attributed to an apparent 'added nitrogen interaction' caused by substitution of mineral ^{15}N for mineral ^{14}N in the immobilization process during concurrent N mineralization and immobilization. Contrasting flows between the two N isotopes are further evidence in favor of a kinetic approach to investigating element cycling patterns in soil systems.

In summary, accumulations of N in the whole soil and in the mineral and microbial fractions were similar between Provost and Rimbey soils. N mineralization rates under controlled environments were strongly influenced by pre-incubation soil conditions. We obtained additional evidence to confirm that the fate of N from plant residues is distinguished best among diverse soils on the basis of normalized rates of flow through selected soil components (e.g. mg N mineralized g^{-1} soil microbial N), rather than on the basis of accumulation in them. Our observations supported previous reports of higher normalized N mineralization rates in Luvisolics compared to Chernozemics under controlled environments and were consistent with the hypothesis that higher rates of decomposition processes are associated with soils of lower clay content.

2.4 LITERATURE CITED

Amato, M. and Ladd, J.N. 1992. Decomposition of ^{14}C-labelled glucose and legume material in a range of soils: Properties influencing the accumulation of organic residues and microbial biomass C. Soil Biol. Biochem. 24:455-464.

Amato, M., Ladd, J.N, Ellington, A., Ford, G., Mahoney, J.E., Taylor, A.C. and Walsgott, D. 1987. Decompositon of plant material in Australian soils. IV: Decomposition *in situ* of ^{14}C and ^{15}N-labelled legume and wheat materials in a range of southern Australian soils. Aust. J. Soil Res. 25:95-105.

Brooks, P.D., Stark, J.M., McInteer, B.B. and Preston, T 1989. Diffusion method to prepare soil extracts for automated nitrogen-15 analysis. Soil Sci. Soc. Am. J. 53:1707-1711.

Campbell, C.A. and Souster, W. 1982. Loss of organic matter and potentially mineralizable nitrogen from Saskatchewan soils due to cropping. Can. J. Soil Sci. 62:651-656.

Carter, M.R. 1986. Microbial biomass as an index for tillage-induced changes in soil biological properties. Soil Tillage Res. 7:29-40.

Dinwoodie, G.D. and Juma, N.G. 1988. Allocation and microbial utilization of C in two soils cropped to barley. Can. J. Soil Sci. 68:495-505.

Greenhouse, S.W. and Geisser, S. 1959. On methods in the analysis of profile data. Psychometrika 24:95-112.

Hassink, J., Bouwman, L.A., Zwart, K.B. and Brussaard, L. 1993. Relationships between habitable pore space, soil biota and mineralization rates in grassland soils. Soil Biol. Biochem. 25:47-55.

Hunt, H.W., Coleman, D.C., Ingham, E.R., Ingham, R.E., Elliott, E.T., Moore, J.C., Rose, S.L., Reid, C.P.P. and Morley, C.R. 1987. The detrital food web in a shortgrass prairie. Biol. Fertil. Soils 3:57-68.

Janzen, H.H. 1987. Soil organic matter characteristics after long-term cropping to various spring wheat rotations. Can. J. Soil Sci. 67:845-856.

Jenkinson, D.S., Fox, R.H. and Rayner, J.H. 1985. Interactions between fertilizer nitrogen and soil nitrogen - the so-called 'priming' effect. J. Soil Sci. 36:425-444.

Jenkinson, D.S. and Powlson, D.S. 1976. The effects of biocidal treatments on metabolism in soil V. A method for measuring soil biomass. Soil Biol. Biochem. 8:209-213.

Jensen, T.L. and Timmermans, J. 1987. Conservation Tillage. Alberta Agriculture Agdex 516-3.

Keeney, D.R. and Nelson, D.W. 1982. Nitrogen-Inorganic Forms. Pages 643-693 *in* A.L. Page, R.H. Miller, D.R. Keeney, eds. Methods of Soil Analysis. Part 2-Chemical and Microbiological Properties, 2nd Ed. ASA-SSSA, Madison, WI, USA.

Ladd, J.N., Jocteur-Monrozier, L. and Amato, M. 1992. Carbon turnover and nitrogen transformations in an alfisol and vertisol amended with [U-^{14}C] glucose and [^{15}N] ammonium sulfate. Soil Biol. Biochem. 24:359-371.

Ladd, J.N., Oades, J.M. and Amato, M. 1981. Distribution and recovery of nitrogen from legume residues decomposing in soils sown to wheat in the field. Soil Biol. Biochem. 13:251-256.

McGill, W.B., Dormaar, J.F. and Reinl-Dwyer, E. 1988. New perspectives on soil organic matter quality, quantity and dynamics on the Canadian prairies. Pages 30-48 *in* Proceedings of the 34th Annual CSSS/AIC Meeting, Aug. 21-24, Calgary, Alberta.

McGill, W.B. and Myers, R.J.K. 1987. Controls on dynamics of soil and fertilizer N. Pages 73-99 *in* R. Follett, ed. Soil Fertility and Organic Matter as Critical Components of Production Systems. Spec. Publ. 19, ASA-SSSA, WI, USA.

McGill, W.B., Cannon, K.R., Robertson, J.A. and Cook, F.D. 1986. Dynamics of soil microbial biomass and water-soluble organic C in Breton L after 50 years of cropping to two rotations. Can. J. Soil Sci. 66:1-19.

Powlson, D.S., Brookes, P.C. and Christensen, B.T. 1987. Measurement of soil microbial biomass provides and early indication of changes in total soil organic matter due to straw incorporation. Soil Biol. Biochem. 19:159-164.

Rutherford, P.M. and Juma, N.G. 1989. Shoot, root, soil and microbial nitrogen dynamics in two contrasting soils cropped to barley (*Hordeum vulgare* L.). Biol. Fertil. Soils 8:134-143.

SAS Institute. 1985. SAS User's Guide: Statistics, Version 5. SAS Institute, Cary, North Carolina, U.S.A.

Shen, S.M., Pruden, G. and Jenkinson, D.S. 1984. Mineralization and immobilization of nitrogen in fumigated soil and the measurement of microbial biomass nitrogen. Soil Biol. Biochem. 16:437-444.

Tottman, D.R. and Broad, H. 1987. The decimal code for the growth stages of cereals, with illustrations. Ann. Appl. Biol. 110:441-454.

Van Veen, J.A. and Kuikman, P.J. 1990. Soil structural aspects of decomposition of organic matter by micro-organisms. Biogeochem. 11:213-233.

CHAPTER 3

Dynamics of ^{15}N in two soil-plant systems following incorporation of 10% bloom and full bloom field pea[1]

3.1 INTRODUCTION

Green manuring of annual legumes is recommended as a soil conservation measure to replace cultivated summerfallow (Jensen and Timmermans, 1987). Extensive field studies in southern Saskatchewan screened several legumes for their potential as green manures and concluded that field pea (*Pisum sativum* 'Sirius') was among the most promising, producing more dry matter and protein at a higher water-use efficiency and fixing more N than most of the other legumes tested (Biederbeck and Slinkard, 1988). The primary goal of summerfallow is to conserve soil moisture. Although green manure legumes are typically incorporated at full bloom, earlier incorporation could conserve more moisture and still benefit the soil by producing surface cover and additions of organic matter and N. Earlier incorporation, however, would allow more extensive residue decomposition in the fall and may result in substantial leaching losses of released mineral N. Furthermore, the chemical composition of the younger plant material may make it more susceptible to microbial degradation thus influencing the timing and extent of N release.

Previous investigations into green manuring of ^{15}N-labelled legume material in the field indicate that 10-34% of legume N is recovered in the first subsequent barley or wheat crop (Azam et al., 1986; Ladd et al., 1981, 1983; Muller and Sundman, 1988; Ta and Faris, 1990). Few field studies, however, detail the dynamics of legume N in the soil-plant system during early decomposition or compare these dynamics between soil types. Theoretically, plant residue decomposition may be described by double exponential decay equations in which heterogeneous substrates are partitioned into labile and resistant fractions each of which exhibit exponential decay (Hunt, 1977; McGill et al., 1981; Wieder and Lang, 1982). Thus, the net amount of ^{15}N mineralized from decomposing plant residues is suggested to be proportional to the amount of plant ^{15}N in labile, readily metabolizable forms. Relationships of this type have been noted among plant

---

[1] A version of this chapter has been published in the Canadian Journal of Soil Science 74:99-107.

species (Amato et al., 1987), plant parts (Amato et al., 1983) and stages of maturity (Muller and Sundman, 1988).

Our objectives in the present study were to compare barley yield and legume-derived N dynamics following incorporation of ^{15}N-labelled pea residues at two bloom stages and at two field sites.

3.2 MATERIALS AND METHODS

Site Descriptions

Plots were established at two Alberta field sites, one on a Dark Brown Chernozemic soil (Provost) and the other on a Gray Luvisol Luvisolic soil (Rimbey). Detailed site descriptions are given in Chapter 2. The experimental design was a factorial split-split-plot with four blocks each with two treatments (legume incorporation at 10% bloom or full bloom) split by four sampling dates and two soil depths. To reduce the number of factors and thus emphasize treatment effects, data from the 0-15 cm and 15-30 cm sampling depths have been combined in this chapter. In May of 1989 both field sites were seeded to 'Type C' inoculated field pea (*Pisum sativum* 'Sirius') at 80 kg ha^{-1}. In late July and early August, field-grown peas were incorporated to approximately 10 cm with a discing implement at 10% bloom or full bloom in the appropriate plots.

Growth and Incorporation of ^{15}N-labelled Legume Material

Labelled pea material for eventual field incorporation was obtained by growing *Pisum sativum* 'Sirius' in open-air troughs (0.85 m x 0.55 m x 0.25 m) filled with sterile sand. Peas were seeded on June 14, 1989 and fed with a nutrient solution (adapted from Amato et al.(1987)) which included the equivalent of 100 kg N ha^{-1} as $^{15}NH_4{}^{15}NO_3$ (10% ^{15}N atom abundance). The solution was poured on the surface of the sand and excess solution collected at the drainage port to be recycled with each watering. Plants were harvested at either 10% bloom or full bloom and the roots separated from the shoots. Subsamples of shoot material were dried at 70°C and ground in a Brinkmann ultra high speed mill. Total C was determined by dry oxidation in a LECO induction furnace. Total N and ^{15}N analyses were performed on a VG Isogas ANA-SIRA (Automatic Nitrogen Analyzer-Stable Isotope Ratio Analyzer) Dumas combustion-mass spectrometer system. The composition of the shoot materials is shown in Table 3-1.

Table 3-1. Composition of ^{15}N-labelled pea shoots (means of 8 samples)

Bloom stage	C content (%)	N content (%)	C:N ratio	Water content (%)	% ^{15}N atom abundance
10% bloom	40.96 a	2.56 a	16.00 a	79.69 a	8.9939 a
Full bloom	41.40 a	2.75 a	15.05 a	76.86 a	9.0696 a

[a] Means in the same column followed by the same letter do not differ significantly according to Student's t test (alpha = 0.01).

Following incorporation of field-grown peas, four open-ended plastic cylinders (30 cm diameter, 50 cm length) were inserted in each plot and non-labelled plant material removed from within the cylinders by hand-picking to a depth of approximately 15 cm. Fresh ^{15}N-labelled pea shoots were incorporated into the soil within the cylinder to a depth of 10 cm (equivalent to dry mass of approximately 1040 kg ha^{-1}). At Provost, incorporation of 10% bloom occurred on August 7 and full bloom on August 22, 1989. The corresponding dates at Rimbey were August 15 (10% bloom) and August 24, 1989 (full bloom). The input of legume N was approximately equivalent to 27.6 kg ha^{-1}.

In May of 1990, the entire plot area was seeded to barley (*Hordeum vulgare* 'Bonanza') without additional fertilization. Cylinders were hand weeded and thinned to contain 12 barley plants each. Pulled vegetation was left on the soil surface within the cylinders.

Sampling and Analysis of Plants and Soils

Sampling details are given in Chapter 2. Briefly, one cylinder from each replicate was removed from the field: 1) in the fall following legume incorporation; 2) at the time of barley seeding; 3) when barley was at Zadoks Growth Stage 39 (flag leaf) (Tottman and Broad, 1987); and, 4) when barley was at Zadoks Growth Stage 75 (ripening). Barley plants, when present, were cut above the root crowns and, in the case of mature barley tops, were hand separated into grain and straw. Barley roots and partially decomposed legume residues were removed from the soil by hand picking and soil sieving (2 mm). Recovered roots were washed in distilled water on a 1 mm mesh sieve. Plant materials and soil subsamples were dried at 70°C and ground in a Brinkmann ultra high speed mill. Total N and ^{15}N in barley, legume residues and remaining whole soils were analyzed as described for legume shoot materials.

Soil mineral N was extracted from moist sieved soil (Keeney and Nelson, 1982) and prepared for isotope ratio analysis by the ^{15}N diffusion method (Brooks et al., 1989). Microbial

biomass N was determined by the chloroform fumigation-incubation method of Jenkinson and Powlson (1976) and calculated from the formula of Shen et al. (1984). Microbial ^{15}N excess was assumed to be the same as the ^{15}N excess of NH_4^+ extracted from the fumigated samples after a 10-day incubation. The non-microbial organic ^{15}N (NMO-^{15}N) was calculated as the difference between total soil ^{15}N and the sum of microbial ^{15}N and mineral ^{15}N. The recovery of legume ^{15}N in each soil and plant component was calculated as mass of ^{15}N above background level in the component (e.g. dry mass of soil sample x %N x (%^{15}N atom abundance in soil sample - %^{15}N atom abundance in control soil sample)) divided by the mass of legume ^{15}N added to the sample (dry mass of legume x %N x %^{15}N atom abundance in legume).

Statistical Analysis

All experimental data were analyzed using the General Linear Model procedure of SAS (SAS Institute, 1985). The probabilities presented are Greenhouse-Geisser (Greenhouse and Geisser, 1959) adjusted probabilities which correct for unequal variances of the means. Regression equations were developed with CA-Cricket Graph (Computer Associates, 1990). Independent regressions were analyzed for homogeneity as described by Steel and Torrie (1980).

3.3 RESULTS

Shoot dry mass (kg ha^{-1}) of peas grown in the field in 1989 was 519 for 10% bloom and 618 for full bloom at Provost compared to 1489 for 10% bloom and 1686 for full bloom at Rimbey (means of 4 samples). Statistical analysis revealed no significant difference ($P<0.01$) between the yields of 10% and full bloom plant shoots at either site. Furthermore, there was no significant difference in the C and N content of the two bloom stages. Pea plants grown in sterile sand were also not statistically different between bloom stages in terms of percent C and N, C:N ratio, water content and percent ^{15}N atom abundance (Table 3-1).

The 1990 growing season precipitation was 81% of the 30 year mean at Provost and 138% of the 30 year mean at Rimbey (70% of this fell during June and July). Barley development at Rimbey was delayed and the plants lacked vigor. Grain, straw and root yields were all significantly greater at Provost but were coupled with lower N concentrations compared to barley at Rimbey (Tables 3-2; 3-3). Although the bloom stage of the legume at incorporation had no significant influence on the yield or N content of grain or straw, overall barley root production, especially at Provost, was greater following incorporation of full bloom peas (Table 3-2; 3-3).

Table 3-2. Barley yield on two 1990 sampling dates following 10% bloom or full bloom legume incorporation

			Dry matter (kg ha^{-1})			Nitrogen (%)		
Site	Date	Bloom	Grain	Straw	Root	Grain	Straw	Root
Provost	July	10%	0	3290	1080	0	1.8	0.6
		full	0	4430	1810	0	1.8	0.6
	August	10%	5930	4460	1200	1.4	0.4	0.5
		full	5940	4600	1370	1.5	0.5	0.5
Rimbey	August	10%	0	1700	620	0	1.8	0.7
		full	0	1910	610	0	2.2	0.7
	September	10%	2000	2450	580	1.8	1.2	0.8
		full	2290	2190	560	1.6	1.1	0.7

Table 3-3. Mean square of analysis of variance for barley yield and nitrogen content

Source of		Yield						% N					
Variation	df	Grain		Straw		Root		Grain		Straw		Root	
Site	1	573855	**	363628	**	47739	**	0.268	**	1.524	*	0.1770	**
Error 1	6	32716		19382		1054		0.014		0.161		0.0013	
Bloom[a]	1	839		7733		3829	*	0.002		0.049		0.0003	
Bloom x Site	1	839		8957		4162	*	0.055	*	0.025		0.0015	
Error 2	6	13044		3756		362		0.005		0.062		0.0097	
Date	3			27956		844				9.915	**	0.0120	
Date x Site	3			487		250				0.558		0.0630	
Error 3	18			11273		1964				0.180		0.0148	
Date x Bloom	3			10617		1695				0.079		0.0045	
Date x Bloom x Site	3			1409		1542				0.083		0.0066	
Error 4	18			6393		400				0.067		0.1076	

[a] 'Bloom' refers to bloom stage of legume at incorporation.
[b] Straw and root samples taken summer and harvest, grain samples at harvest only.
[c] The difference between the means is significant at: **, P<0.01; *, P<0.05.

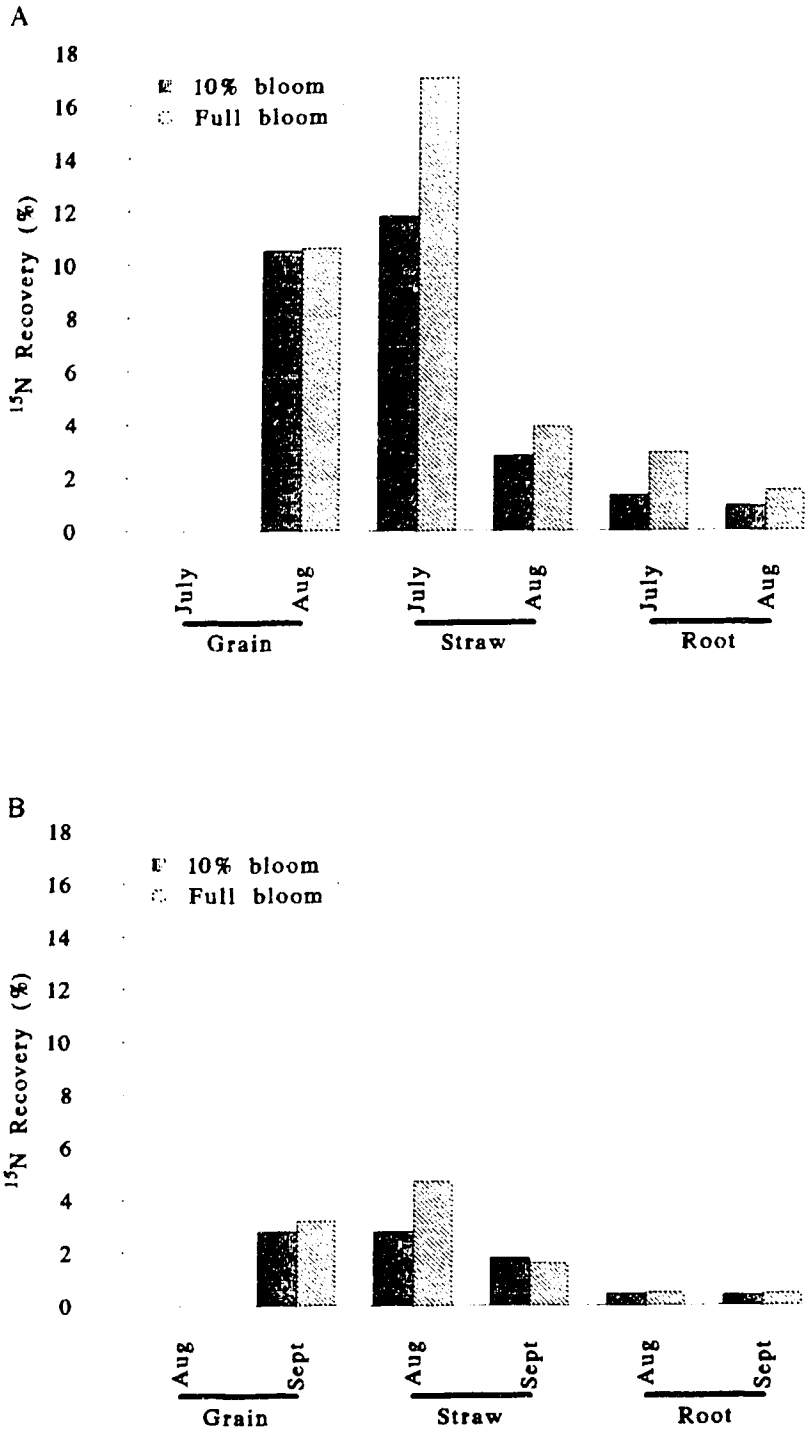

Figure 3-1. Recovery of ^{15}N in barley at (A) Provost and (B) Rimbey on two 1990 sampling dates following 10% bloom and full bloom incorporation.

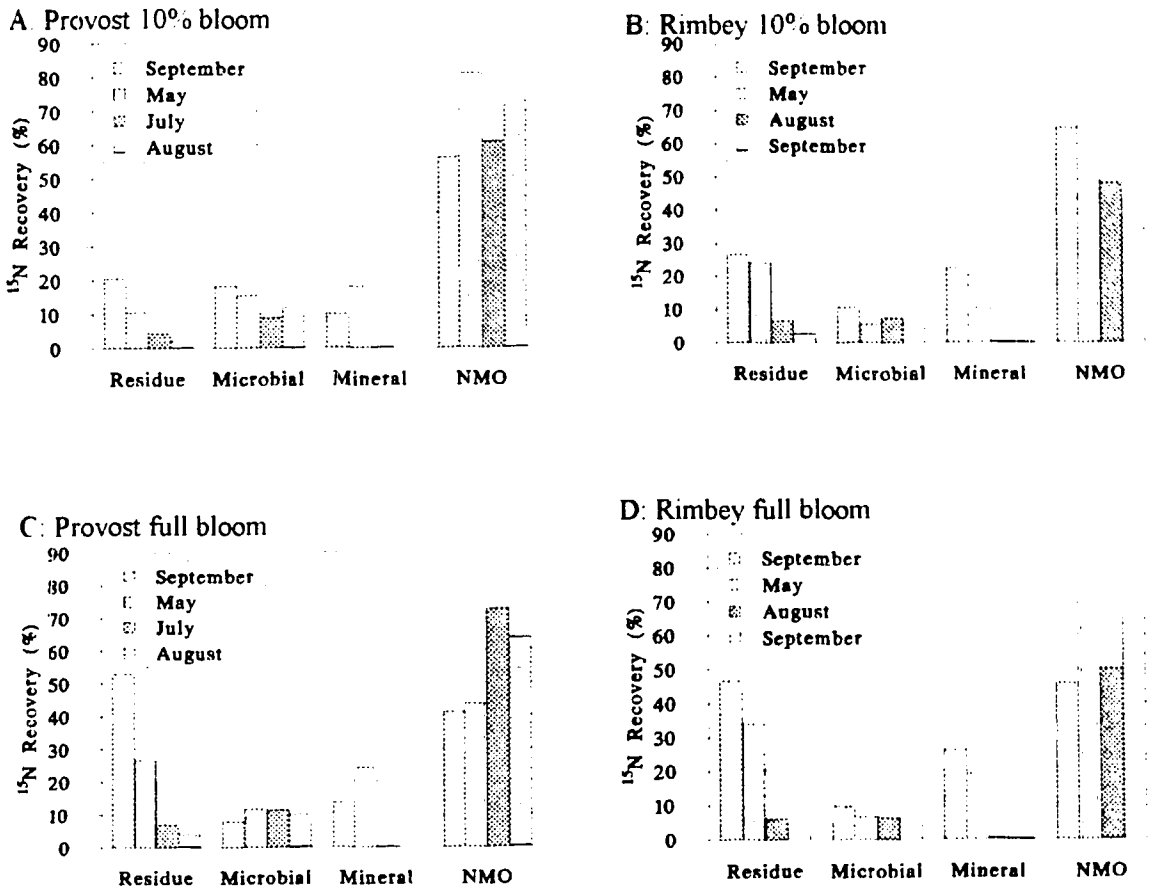

Figure 3-2. Recovery of ^{15}N in legume residue and soil fractions on four sampling dates between 1989 and 1990 (A) Provost soil, (B) Rimbey soil following 10% bloom incorporation and (C) Provost soil, (D) Rimbey soil following full bloom incorporation. NMO = non-microbial organic.

Total recovery of legume-derived ^{15}N in the plant-soil system (0-30 cm) ranged from 88-125% at Provost and 70-125% at Rimbey. The low recoveries at Rimbey occurred on the August and September sampling dates and were evident with incorporation of both bloom stages.

Significantly more ^{15}N was recovered in the Provost grain, straw and root samples (Figure 3-1; Table 3-4). Recovery of ^{15}N in the grain did not vary with bloom stage at either site. Significantly more ^{15}N from the full bloom residues was, however, recovered in the barley straw and roots. Grain ^{15}N accounted for 66% and 60% of total ^{15}N recovered in the barley at Provost and Rimbey, respectively while root ^{15}N accounted for 10% of the total at both sites.

Table 3-4. Mean square of analysis of variance for percent ^{15}N recovery in barley, legume residue and soil components (0-30 cm)

Source of Variation	df	Grain		Straw[b]		Root[b]		Residue		Soil[c]		Mineral		Microbial		NMO	
Site	1	229.1	**	300.6	**	6.08	**	106.4		94.7		23.7		169.6	*	35.9	
Error 1	6	7.8		7.2		0.18		65.4		604.0		16.2		15.4		525.5	
Bloom[a]	1	0.4		32.3	*	1.31	**	1654.7	**	124.2		64.3	**	24.4		196.8	
Bloom x Site	1	0.1		11.2		1.13	**	150.3		699.5	*	1.1		19.4		448.2	*
Error 2	6	2.3		4.7		0.05		97.6		60.1		4.3		6.9		52.1	
Date	3			344.8	**	0.99		4063.5	**	2016.8	**	846.0	**	17.0	**	494.4	*
Date x Site	3			161.1	**	0.69		116.2		724.2	**	123.4	**	8.4	*	550.9	*
Error 3	18			4.0		0.20		38.9		124.4		14.9		2.4		120.6	
Date x Bloom	3			19.3		0.24		589.7	**	345.3		25.2		16.2		382.4	
Date x Bloom x Site	3			2.1		0.24		22.3		376.5		0.9		15.1		321.3	
Error 4	18			9.3		0.08		62.3		1991.0		40.6		36.4		1247.1	

[a] 'Bloom' refers to bloom stage of legume at incorporation.
[b] Straw and root samples taken at summer and harvest only, therefore, date df = 1, bloom x date df = 1 and error 2 df = 6.
[c] 'Soil' refers to ^{15}N recovery in mineral + microbial + NMO components.
[d] The difference between the means is significant at: **, P<0.01; *, P<0.05.

Both soil and NMO had significant bloom x site interactions. At Provost, ^{15}N recoveries in the whole soil and NMO fraction were higher in the 10% bloom treatment while at Rimbey, they were higher in the full bloom treatment. Significantly more ^{15}N was recovered as mineral N in the full bloom treatment. This effect was only evident at the September and May sampling dates as mineral N and consequently mineral ^{15}N were near zero by mid summer and barley harvest in both treatments and at both sites. A significant date x site interaction emphasized the earlier peak ^{15}N recovery in the mineral N at Rimbey (September) compared to Provost (May). Significantly more ^{15}N was recovered in the Provost microbial biomass.

Significantly more ^{15}N was retained in the full bloom residues over the decomposition period investigated (Figure 3-2; Table 3-4). There was, however, no significant difference in ^{15}N recovery in the legume residues between sites. Analysis of the natural log values of ^{15}N recovery in legume residues over the post-winter sampling dates (Provost = May, July, August, 1990 and Rimbey = May, August, September, 1990) revealed that, in all cases, a simple linear equation gave the closest fitting regression (Table 3-5). Analyzing the independent regressions for homogeneity (Steel and Torrie, 1980) showed no significant difference ($P<0.05$) between the decomposition rate constants associated with the 10% bloom compared to full bloom residues at either site. Furthermore, no significant difference ($P<0.05$) was found between the overall site rate constants calculated from the combined 10% bloom and full bloom data.

Table 3-5. Regression coefficients of the relation between ln(proportion ^{15}N retained in the recalcitrant fraction of the legume)[a] and decomposition period[b]

Site	Bloom stage	a	k (day^{-1})	r^2
Provost	10% bloom	2.82	-0.017 a	0.999
Provost	full bloom	4.54	-0.022 a	0.972
Rimbey	10% bloom	4.46	-0.021 a	0.988
Rimbey	full bloom	6.32	-0.027 a	0.991
Provost	combined	4.04	-0.021 a	0.921
Rimbey	combined	5.32	-0.024 a	0.962

[a] Natural log (proportion ^{15}N retained) = a+kt

[b] First four entries based on three data points: Provost in May, July, August 1990 and Rimbey in May, August, September 1990. Other entries based on six data points.

[c] Pairs of rate constants (k) within a section followed by the same letter do not differ significantly according to independent regression analysis (alpha = 0.05).

3.4 DISCUSSION

Due to physiological similarities, green manuring 10% bloom or full bloom peas represented similar additions of organic matter and N to the soil. Possibly for this reason, barley yield and N content were not influenced by legume bloom stage at incorporation. Grain yield was much less than expected at Rimbey and was only 38% of the previous year's yield on an adjacent field (unpublished). Yield may have been lost to bird and insect predation which were more prevalent at Rimbey compared to Provost. In addition, Rimbey's high growing season precipitation (138% of the 30 year mean May - September precipitation), especially in June and July, delayed barley development which possibly had a deleterious effect on grain yield. The distribution of dry matter among plant parts was, however, similar at both sites. Grain yield accounted for 57% and 53% of the dry matter of barley tops at Provost and Rimbey, respectively and the ratios of dry matter in the tops:roots were 7.8:1 and 7.9:1. These ratios were higher than expected (Ladd et al., 1981) and may be the result of incomplete root recovery in the 0-30 cm layer and non-sampled roots at greater depths. The proportion of legume ^{15}N recovered in various barley parts at both sites, however, agreed with values reported for wheat (Azam et al., 1986; Ladd et al., 1981).

At Provost, the total of 16% legume ^{15}N recovery at harvest was comparable to findings of other researchers who report recoveries of 10 - 34% in the first subsequent barley or wheat crop (Azam et al., 1986; Ladd et al., 1981, 1983; Muller and Sundman, 1988; Ta and Faris, 1990). This recovery means that the legumes supplied 4.4 kg N ha^{-1} (16% of 27.6 kg ha^{-1}) to the barley crop which, at harvest, contained approximately 107 kg N ha^{-1} (Table 3-2). The N derived from the legume, therefore, accounted for only 4.1% of the barley's N. Apparently, the main benefit of the pea green manure is in its contribution to long-term soil fertility.

The 5.3% recovery in the barley at Rimbey was less than expected. This observation may, in part, be the result of the greater potential mineralization of the Rimbey soil (see Chapter 2). The potential mineralization of the soil determines the ^{15}N atom % enrichment of the plant available nitrogen and consequently, dictates the enrichment of the crop. The greater the soil's potential mineralization, the more the legume-derived $^{15}NO_3^-$ will be diluted by soil-derived $^{14}NO_3^-$ (Ladd et al., 1983). Calculation of the ^{15}N atom % enrichment of the mineral fraction of the soil at barley seeding (mean of bloom treatments) supported this hypothesis with a lower percentage at Rimbey (0.586%) compared to Provost (0.937%). Another explanation for the low ^{15}N recovery in the barley at Rimbey was the apparent loss of ^{15}N from the 0-30 cm soil layer. With the wet

conditions, leaching and possibly denitrification would have been the primary processes of N loss. Poor barley vigor may also have limited N and ^{15}N uptake from the soil.

Incorporation of full bloom legumes resulted in closer synchrony between mineral N availability and crop demand. Cereal grains can absorb 90% of the nitrogen needed for maturity before they are half-grown (Salisbury and Ross, 1985). Therefore, to be most efficiently utilized by the barley crop, the N from the legume should be available in mineral form between the time of barley germination and the end of vegetative development. Our observations indicated that more legume-derived mineral ^{15}N was available at the beginning of this crucial period following incorporation of full bloom legumes. The higher ^{15}N recoveries in the barley roots and straw following this treatment were further evidence of the more timely availability of legume-derived N.

Many studies document that the chemical composition of forages changes as the plants mature (Walton, 1983). For example, Trevino et al. (1987) report a decrease in proteins, sugars and starch coupled with an increase in cellulose, hemicellulose and lignin in the leaves and stems of peas (*Pisum sativum* x *P. arvense*) between early pod filling and pod ripening. We had expected that the N content would be greater and the C:N ratio smaller in peas at 10% bloom compared to full bloom. Our analyses, however, indicated that these growth stages were similar in C and N content. Therefore, the two residues must have differed in some other respect to account for differences in their decomposition dynamics. Muller et al. (1988) found little change in the C, N and ethanol soluble fractions between 2 and 3 month old subterranean clover. Cellulose and lignin content, however, increased with the growth stages sampled. Furthermore, Amato et al. (1983) report that although the leaves and roots of two *Medicago* species had similar C:N ratios, a greater proportion of leaf ^{15}N was mineralized shortly after soil incorporation compared to root ^{15}N. This difference was attributed to a greater proportion of leaf ^{15}N in readily metabolizable forms. Therefore, residues with similar C and N content may have varied amounts of resistant structural and readily metabolizable labile nitrogenous compounds.

Mathematical models of plant residue decomposition based on the partitioning of residues into labile and resistant fractions suggest that differences in overall decomposition result from differences in the proportion of labile to recalcitrant material (Hunt, 1977; McGill et al., 1981; Wieder and Lang, 1982). The lower percentage of ^{15}N retained in the 10% bloom residues at the September 1989 sampling date at each site may indicate that this material had a larger labile or easily metabolizable component. The differences in ^{15}N recovery at this sampling were larger than could be explained by the additional 9 to 15 days of decomposition gained by earlier incorporation

(Rimbey and Provost, respectively) We assume that only the recalcitrant fraction of both 10% bloom and full bloom legume residues remained by the spring of 1990. From the lack of significant differences between decomposition rate constants for the 1990 sampling dates, we infer that, over these dates, decomposition of the resistant legume component followed similar trends for both bloom stages and at both sites. It should be noted that single site, single treatment equations were based on only three data points. Nevertheless, although the number of data points is small, these results appear to be consistent with the theory that the recalcitrant fractions of different plant materials have similar decomposition rates.

In conclusion, the 10% bloom and full bloom pea shoots were not significantly different in dry matter production, C content or N content. More N was, however, released from the 10% bloom residues directly following soil incorporation suggesting that the younger pea material may have had a larger proportion of easily metabolizable labile components. Although legume bloom stage at incorporation had no influence on barley dry matter yield, N content or ^{15}N recovery in the grain, significantly more ^{15}N was recovered in the barley straw and roots during vegetative growth following full bloom incorporation. This observation may be the result of a closer synchrony between the appearance of legume-derived mineral ^{15}N and early N demand by the barley. N losses (leaching/denitrification), poor crop vigor and the greater potential N mineralization rate of the Rimbey soil appeared to limit ^{15}N uptake by barley at this site. At Provost, 16% of legume N was recovered by the subsequent barley crop which supplied 4.1% of the barley's N requirement. The main benefit of the green manure, therefore, may be in building long-term soil fertility. Neither bloom stage nor site had a significant effect on decay rate constants for the recalcitrant fraction of legume residues over the time intervals of our observations. These findings are consistent with the theory that decomposition of the recalcitrant fraction of plant residues can be described by a single exponential equation.

3.5 LITERATURE CITED

Amato, M., Ladd, J.N, Ellington, A., Ford, G., Mahoney, J.E., Taylor, A.C. and Walsgott, D. 1987. Decompositon of plant material in Australian soils. IV: Decomposition *in situ* of ^{14}C and ^{15}N-labelled legume and wheat materials in a range of southern Australian soils. Aust. J. Soil Res. 25:95-105.

Amato, M., Jackson, R.B., Butler, J.H.A. and Ladd, J.N. 1983. Decomposition of plant materials in Australian soils. II: Residual organic ^{14}C and ^{15}N from legume plant parts decomposing under field and laboratory conditions. Aust. J. Soil Res. 21:563-70.

Azam, F., Malik, K.A. and Sajjad, M.I. 1986. Uptake by wheat plants and turnover within soil fractions of residual N from leguminous plant material and inorganic fertilizer. Plant and Soil 95:97-108.

Biederbeck, V.O. and Slinkard, A.E. 1988. Effect of annual legume green manures on yield and quality of wheat on a brown loam. Pages 345-361 *in* Proceedings of the Soils and Crops Workshop. Saskatoon, Saskatchewan. Feb 18-19,, 1988.

Brooks, P.D., Stark, J.M., McInteer, B.B. and Preston, T. 1989. Diffusion method to prepare soil extracts for automated nitrogen-15 analysis. Soil Sci. Soc. Am. J. 53:1707-1711.

Computer Associates. 1990. CA-Cricket Graph for Microsoft Windows User's Guide. Computer Associates International, Inc., San Diego, California, U.S.A.

Greenhouse, S.W. and Geisser, S. 1959. On methods in the analysis of profile data. Psychometrika 24:95-112.

Hunt, H.W. 1977. A simulation model for decomposition in grasslands. Ecol. 58:469-484.

Jenkinson, D.S. and Powlson, D.S. 1976. The effects of biocidal treatments on metabolism in soil V. A method for measuring soil biomass. Soil Biol. Biochem. 8:209-213.

Jensen, T.L. and Timmermans, J. 1987. Conservation Tillage. Alberta Agriculture Agdex 516-3.

Keeney, D.R. and Nelson, D.W. 1982. Nitrogen-Inorganic Forms. Pages 643-693 *in* A.L. Page, R.H. Miller, D.R. Keeney, eds. Methods of Soil Analysis. Part 2-Chemical and Microbiological Properties, 2nd Ed. ASA-SSSA, Madison, WI, USA.

Ladd, J.N., Amato, M., Jackson, R.B. and Butler, J.H.A. 1983. Utilization by wheat crops of nitrogen from legume residues decomposing in soils in the field. Soil Biol. Biochem. 15:231-238.

Ladd, J.N., Oades, J.M. and Amato, M. 1981. Distribution and recovery of nitrogen from legume residues decomposing in soils sown to wheat in the field. Soil Biol. Biochem. 13:251-256.

McGill, W.B., Hunt, H.W., Woodmansee, R.G. and Reuss, J.O. 1981. Phoenix-A model of the dynamics of carbon and nitrogen in grass-land soils *in* F.E. Clark and T. Rosswall, eds. Terrestrial Nitrogen Cycles. Ecol. Bull. (Stockholm) 33:49-115.

Muller, M.M. and Sundman, V. 1988. The fate of nitrogen (^{15}N) released from different plant materials during decomposition under field conditions. Plant and Soil 105:133-139.

Muller, M.M., Sundman, V., Soininvaara, O. and Merilainen, A. 1988. Effect of chemical composition on the release of nitrogen from agricultural plant materials decomposing in soil under field conditions. Biol. Fertil. Soils 6:78-83.

Salisbury, F.B. and Ross, C.W. 1985. Plant Physiology (3rd edition). Wadsworth Publishing Company, Belmont, California, U.S.A.

SAS Institute. 1985. SAS user's guide: Statistics, Version 5. SAS Institute, Cary, North Carolina, U.S.A.

Shen, S.M., Pruden, G. and Jenkinson, D.S. 1984. Mineralization and immobilization of nitrogen in fumigated soil and the measurement of microbial biomass nitrogen. Soil Biol. Biochem. 16:437-444.

Steel, R.G.D. and Torrie, J.H. 1980. Principles and Procedures of Statistics: A Biometrical Approach. 2nd ed. McGraw-Hill, Inc., USA.

Ta, T.C and Faris, M.A. 1990. Availability of N from ^{15}N-labeled alfalfa residues to three succeeding barley crops under field conditions. Soil Biol. Biochem. 22:835-838.

Tottman, D.R and Broad, H. 1987. The decimal code for the growth stages of cereals, with illustrations. Ann. Appl. Biol. 110:441-454.

Trevino, J., Centeno, C. and Cabanero, R. 1987. The chemical composition of pea plant parts as related to harvesting time. Anim Feed Sci. Technol. 16:305-309.

Walton, P.D. 1983. Production and Management of Cultivated Forages. Reston Publishing Company, Inc., Reston, Virginia.

Weider, R.K. and Lang, G.E. 1982. A critique of the analytical methods used in examining decomposition data obtained from litter bags. Ecol. 63:1636-1642.

CHAPTER 4

Is there a correlation among factors used to estimate soil microbial biomass?[1]

4.1 INTRODUCTION

Amato and Ladd (1988) propose an assay for microbial biomass C and N based on the release of ninhydrin-reactive N (α-amino N + NH_4^+-N) from soils held under $CHCl_3$ vapor for 10 days. The release of ninhydrin-reactive N (NRN) was calibrated against biomass C as estimated by the chloroform fumigation-incubation technique (CFI) of Jenkinson and Powlson (1976). From a range of 25 pasture soils (0-7.5 cm), the coefficient of correlation between the release of NRN and biomass C was greatest in soils which had been incubated for 44 or 66 weeks prior to fumigation (r=0.96, 0.91) and was less in soils incubated for only 2 weeks prior to fumigation (r=0.79). Amato and Ladd (1988), therefore, used data from the soils which had been conditioned for 44 and 66 weeks to derive the relationship, biomass C (ug C g^{-1}soil) = 21 x NRN (ug N g^{-1}soil), yet this relation is applied to fresh and conditioned soils alike (Van Gestel et al., 1992). This relationship has also not been tested in soils below 7.5 cm depth. Is it valid to use the same relation with conditioning periods that differ from that used to develop it, and with subsurface soils? Here I report on the correlation between the flush of CO_2-C (CO_2-C evolved from fumigated soil - CO_2-C evolved from nonfumigated soil), the flush of mineral N and the flush of NRN following fumigation of fresh soils sampled at two sites and at two depths.

4.2 MATERIALS AND METHODS

Soil samples were collected from field experimental sites: one in the Dark Brown Chernozemic zone (DBC) and the other in the Grey Luvisol Luvisolic zone (GLL) of Alberta. These sites formed part of a larger investigation and are described in Chapter 2. Briefly, field pea was incorporated as green manure in the fall of 1989 and barley seeded the following spring. Soils from the 0-15 cm and 15-30 cm layers (8 replicates of each) were sampled three times during the barley growing

---

[1] A version of this chapter has been accepted for publication in Applied Soil Ecology

season. Barley roots and partially decomposed legume residues were removed by hand picking and soil sieving (2 mm). Moist subsamples (approximately 25 g oven-dry) were adjusted to 55% water-holding capacity (WHC) and were: (i) incubated at 23°C for 10 days in 1.9 L glass jars together with 20 mL of 2.5 *M* NaOH, (ii) fumigated with $CHCl_3$ for 24 hours and then incubated for 10 days as in (i); or (iii) fumigated with $CHCl_3$ vapor for 10 days. CO_2-C recovered in the NaOH solution was measured by autotitration to pH 8.1 following addition of $BaCl_2$. The flush of CO_2 was calculated as $CO_{2fumigated} - CO_{2nonfumigated}$. All soil samples were extracted with 2 *M* KCl (5:1 v/w) and subsamples of extracts from nonfumigated and fumigated (24 hours) soils were analyzed for NH_4^+-N and NO_3^--N with a Technicon AutoAnalyzer (Keeney and Nelson, 1982). The flush of mineral N was calculated as mineral $N_{fumigated}$ - mineral $N_{nonfumigated}$. Subsamples of extracts from nonfumigated and fumigated (10 days) soils were analyzed for NRN by mixing 0.5 mL aliquots with 3.5 mL 2 M KCl and 2 mL ninhydrin reagent (Sigma Chemicals). Samples were heated in a water bath (100°C) for 15 minutes, cooled and mixed with 5 mL of 50% ethanol. NRN was determined by reading absorbances at 570 nm and comparing to *l*-leucine standards. The flush of NRN was calculated as $NRN_{fumigated} - NRN_{nonfumigated}$.

4.3 RESULTS AND DISCUSSION

Biomass C estimated from the flush of NRN was consistently greater than biomass C estimated from the flush of CO_2-C, although this difference was only significant in the GLL soil (Table 4-1). Biomass N estimated by NRN was significantly greater in all cases as compared to biomass N estimated from the flush of mineral N.

Although the coefficients of correlation were lower than those reported by Amato and Ladd (1988), correlation among primary factors used to calculate biomass C and N was significant in the 0-15 cm soil samples (Figure 4-1). Regression of the flush of NRN against biomass C (flush of CO_2-C / 0.45) (Jenkinson and Ladd, 1981), fitting the intercept through zero, gave the following relationship: biomass C (ug C g^{-1}soil) = 17.8 (±0.8) x NRN (ug N g^{-1}soil) (r = 0.62). Greater coefficients of correlation between the flushes of CO_2-C, mineral N and NRN have been reported in studies with conditioned topsoils. For example, Sparling and Zhu (1993) conditioned 24 soils (0-10 cm) from western Australia for 7 days at 22°C and 40% WHC before fumigating and found significant correlations (r=0.81-0.93) among flushes of CO_2-C, mineral N and NRN. Carter (1991) collected soils from three tillage sites (0-5 cm) in Atlantic Canada, stored the field moist samples at 4°C and then conditioned them for 2 days at 25°C and 50-55% WHC prior to fumigation. Again,

significant correlations (r=0.78-0.98) were observed among flushes of CO_2-C, mineral N and NRN. Soil conditioning typically precedes CFI to reduce interference from actively decomposing residues but, does the conditioned biomass represent the biomass at sampling? Reports of both net increases and net decreases in microbial biomass and metabolic activity in response to incubation (Van Gestel et al., 1992; Jenkinson and Powlson, 1976) suggest that it may not.

Table 4-1. Flushes of CO_2-C, mineral N and NRN and corresponding biomass C and N estimates[a]

		Concentration (ug g^{-1} soil)							
		DBC				GLL			
		0-15 cm		15-30 cm		0-15 cm		15-30 cm	
CO_2-C	Fumigated	273.6 (67)		140.8 (68)		190.8 (34)		95.2 (25)	
	Nonfum.	103.4 (43)		79.8 (77)		85.1 (20)		31.9 (18)	
	Biomass C[b]	378.2 **a** (133)		135.6 **a** (149)		234.9 **b** (66)		140.7 **b** (38)	
Mineral N	Fumigated	48.1 (12)		16.5 (8)		37.6 (7)		18.9 (8)	
	Nonfum.	15.3 (9)		5.5 (4)		16.4 (10)		7.1 (6)	
	Biomass N[c]	48.2 **d** (11)		16.2 **d** (6)		31.2 **d** (8)		17.4 **d** (6)	
NRN	Fumigated	22.9 (5)		12.4 (5)		19.8 (4)		12.4 (3)	
	Nonfum.	3.7 (2)		3.1 (2)		4.8 (2)		3.9 (1)	
	Biomass C[d]	403.2 **a** (86)		195.3 **a** (94)		315.0 **a** (81)		178.5 **a** (86)	
	Biomass N[e]	59.5 **c** (13)		28.8 **c** (14)		46.5 **c** (12)		26.4 **c** (13)	

[a] Mean and (standard deviation)
[b] Biomass C = flush of CO_2-C/0.45 (Jenkinson and Ladd. 1980)
[c] Biomass N = flush of mineral N/0.68 (Shen et al., 1984)
[d] Biomass C = flush of NRN * 21
[e] Biomass N = flush of NRN * 3.1
Biomass values within a column followed by the same letter do not differ significantly according to paired t-tests ($P<0.05$).

Correlation among flushes was not significant in the 15-30 cm samples (Figure 4-1). Of the few publications that report on the correlation between the NRN method and other methods of biomass analysis (Sparling and Zhu, 1993; Carter, 1991; Joergensen and Brookes, 1990; Amato and Ladd, 1988), none has included soil samples from below 10 cm. Relatively high levels of $CaCO_3$ in the 15-30 cm DBC soil may have interfered with CO_2 evolution. Separate statistical analysis of the 15-30 cm GLL data, however, also indicated nonsignificant correlation among

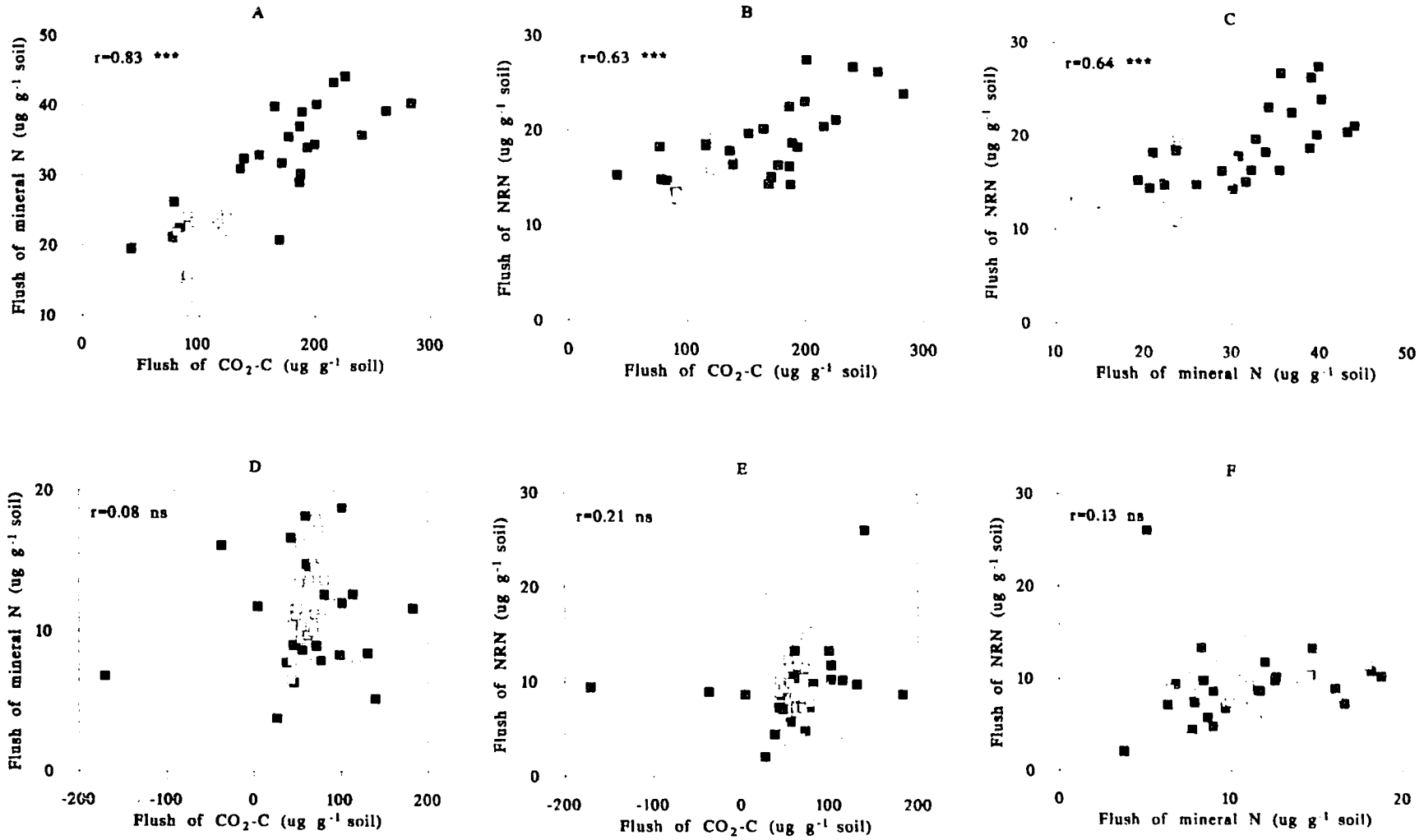

Figure 4-1. Correlation among flushes of CO_2-C, mineral N and NRN following fumigation of a DBC (■) and a GLL (□) soil at the 0-15 cm sampling depth (A-C) and the 15-30 cm sampling depth (D-F). Correlation significant at: ***<0.01, **<0.05, *<0.1, ns=not significant.

factors. Furthermore, $CaCO_3$ interference does not explain the poor correlation between the flush of mineral N and NRN.

Another consideration is that soils with lower initial biomass, as would be the case with subsurface soils, recover more slowly after fumigation (Muramoto et al., 1982). The transformation of lyzed cell materials to CO_2 and NH_4^+ is the result of immobilization-mineralization processes requiring active recolonizers. In contrast, the transformation of these cellular materials to extractable NRN is mainly the result of exo-cellular protease activity. Slow microbial recovery in fumigated subsoils would be more likely to delay mineralization processes than exo-cellular hydrolysis reactions.

The flush of NRN in the 15-30 cm soils was significantly ($P<0.05$) correlated to the 'noncorrected' CO_2-C evolved from fumigated soils. Sparling and Zhu (1993) also found a higher degree of correlation between the flush of NRN and CO_2-C ($r=0.95$) evolved from fumigated soils compared to the corrected flush of CO_2-C ($r=0.81$). This may suggest that CO_2 evolution from the nonfumigated soils was erratic which is substantiated by proportionately larger standard deviations for CO_2-C evolved from nonfumigated soils compared to fumigated soils (Table 4-1). A possible explanation becomes evident when considering the physiological state of the microbial population: the scarcity of accessible substrate at depth would be expected to result in more aged and resting cells. These cells would have lower CO_2 production per unit biomass C compared to younger cells (Anderson and Domsch, 1978). Once sieved and exposed to ambient conditions, these samples may have variable responses, some experiencing a longer lag period before becoming active while others may be able to take immediate advantage of newly accessible substrate. Fumigated samples would have relatively more abundant and possibly more homogeneous substrate (lyzed cells) resulting in less erratic mineralization patterns by recolonizing microbes.

In the original publication describing the NRN assay for biomass analysis, Amato and Ladd (1988) refer to the relationship: biomass C = 21 x the release of NRN. In fact, Amato and Ladd (1988) used the 'noncorrected' quantity of NRN extracted from fumigated soils to correlate against CFI-biomass C. Although the meaning of 'the release of NRN' is vague in the original publication, it is clearly stated as, 'NRN extracted from fumigated soils' in an accompanying publication (Ladd and Amato, 1988). In the present study, the correlation between 'noncorrected' NRN extracted from fumigated soils and the flush of CO_2-C ($r=0.56$) was weaker than the correlation between corrected values in the 0-15 cm samples (Figure 4-1). In the 15-30 cm

samples, the correlation between 'noncorrected' NRN and the flush of CO_2-C (r=0.20) was similar to that calculated with corrected NRN.

More recently, Amato and Ladd (1994) calculated net release of NRN by subtracting the NRN extracted from nonfumigated, nonincubated control soils from the NRN extracted from soils fumigated with $CHCl_3$ vapor for 10 days. Most other studies employing the NRN technique include 24 hour fumigation and calculation of the flush of NRN as NRN extracted from fumigated soil minus NRN extracted either from soil at time = 0 or at time = 24 hours (Carter, 1991; Joergensen and Brookes, 1990; Sparling and Zhu, 1993; Sparling et al., 1993). In the present study, the flush of NRN was calculated as NRN extracted from soil fumigated for 10 days minus NRN extracted from soil incubated for 10 days. In retrospect, because of the variable responses of NRN in nonfumigated incubated soils, sometimes increasing (Chapter 5) and sometimes decreasing (Van Gestel et al., 1992), a more appropriate control would have been the NRN extracted from soil at time = 0.

In summary, flushes of CO_2-C, mineral N and NRN were significantly correlated in the 0-15 cm depth of the two soils investigated. For these samples the relationship between biomass C (estimated by CFI) and the release of NRN was similar to that reported by Amato and Ladd (1988). The coefficients of correlation were lower than those reported elsewhere with conditioned topsoils. Correlation among flushes was not significant in the 15-30 cm samples except when the 'noncorrected' flush of CO_2-C was used. Consideration of the physiological state of the microbial biomass in subsoils may explain some of these observations. The relationship between the release of NRN from fumigated soil with biomass measured by CFI, may be strongest for soils and conditions similar to those from which the relationship was developed. Broader applications would benefit from a comprehensive examination of how the nature or strength of such a relationship varies with length of soil conditioning, soil sampling depth, and metabolic state of soil microbial communities at the time of sampling.

4.4 LITERATURE CITED

Amato, M. and Ladd, J.N. 1994. Application of the ninhydrin-reactive N assay for microbial biomass in acid soils. Soil Biol. Biochem. 26:1109-1115.

Amato, M. and Ladd, J.N. 1988. Assay for microbial biomass based on ninhydrin-reactive nitrogen in extracts of fumigated soils. Soil Biol. Biochem. 20:107-114.

Anderson, J.P.E. and Domsch, K.H. 1978. A physiological method for the quantitative measurement of microbial biomass in soils. Soil Biol. Biochem. 10:215-221.

Carter, M.R. 1991. Ninhydrin-reactive N released by the fumigation-extraction method as a measure of microbial biomass under field conditions. Soil Biol. Biochem. 23:139-143.

Jenkinson, D.S. and Ladd, J.N. 1981. Microbial biomass in soil: measurement and turnover. Pages 417-471 *in* E.A. Paul and J.N. Ladd, eds. Soil Biochemistry, Volume 5. Marcel Dekker, New York, USA.

Jenkinson, D.S and Powlson, D.S. 1976. The effects of biocidal treatments on metabolism in soil-V. A method for measuring soil biomass. Soil Biol. Biochem. 8:209-213.

Joergensen, R.G. and Brookes, P.C. 1990. Ninhydrin-reactive nitrogen measurements of microbial biomass in 0.5M K_2SO_4 soil extracts. Soil Biol. Biochem. 22:1023-1027.

Keeney, D.R. and Nelson, D.W., 1982. Nitrogen-Inorganic Forms. Pages 643-693 *in* A.L. Page, R.H. Miller and D.R. Keeney, eds. Methods of Soil Analysis. Part 2-Chemical and Microbiological Properties, 2nd Ed. ASA-SSSA, Madison, WI, USA.

Ladd, J.N. and Amato, M. 1988. Relationships between biomass ^{14}C and soluble organic ^{14}C of a range of fumigated soils. Soil Biol. Biochem. 20:115-116.

Marumoto, T., Anderson, J.P.E. and Domsch, K.H. 1982. Mineralization of nutrients from soil microbial biomass. Soil Biol. Biochem. 14:469-475.

Shen, S.M., Pruden, G. and Jenkinson, D.S. 1984. Mineralization and immobilization of nitrogen in fumigated soil and the measurement of microbial biomass nitrogen. Soil Biol. Biochem 16:437-444.

Sparling, G. and Zhu, C. 1993. Evaluation and calibration of biochemical methods to measure microbial biomass C and N in soils from western Australia. Soil Biol. Biochem. 25:1793-1801.

Sparling, G., Gupta, V.V.S.R. and Zhu, C. 1993. Release of ninhydrin-reactive compounds during fumigation of soil to estimate microbial C and N. Soil Biol. Biochem. 25:1803-1805.

Van Gestel, M., Ladd, J.N. and Amato, M. 1992. Microbial biomass responses to seasonal change and imposed drying regimes at increasing depths of undisturbed topsoil profiles. Soil Biol Biochem. 24:103-111.

CHAPTER 5

Decomposition of pea shoot in soil: a laboratory incubation

5.1 INTRODUCTION

The English dictionary defines decomposition as 'breaking up and separating into simple parts' (Longman, 1978). Decomposition of organic materials in soil, however, is a much more complex process because the organics are part of a cycle. For example, an amino acid contained within a plant residue could be assimilated by a microorganism thus maintaining its chemical composition but physically existing in another form of biota. Juma and McGill (1986) characterize decomposition in soil as a combination of physical breakdown, biochemical transformation and biophysical stabilization of organic material. A general description of plant residue decomposition would be the physical and/or chemical and/or biological transformation of plant materials to something other than their original state. By its vagueness, this definition indicates the breadth of processes involved in decomposition.

Decomposition of plant residues in soil is one of the key processes in nutrient cycling (Coleman and Hendrix, 1988). Unfortunately, the loss of original plant material cannot be directly measured in soil because non-decomposed materials are similar to inherent soil organic matter. One of the most common indirect methods of measuring plant residue decomposition involves monitoring $^{14}CO_2$ evolved or ^{14}C remaining in soil following the addition of ^{14}C-labelled residues (Juma and McGill, 1986). Actual decomposition, however, is not accounted for by this method because C mineralization is only one step in the decomposition process. Other steps include the activities of exo-cellular enzymes, microbial uptake of small molecular weight compounds to form new cellular or exo-cellular microbial material (Paul and Clark, 1989), predation by microfauna (Hunt, 1987) and stabilization of partially decomposed materials within the soil matrix (Juma and McGill, 1986). Quantifying the decomposition of nitrogenous materials is even more challenging because mineral N is not released from the soil like CO_2 but is recycled among mineral and organic forms. Measurements of organic ^{15}N remaining in soil or the accumulation of mineral ^{15}N, therefore, are even less representative of actual decomposition than are measurements of organic ^{14}C remaining or $^{14}CO_2$ evolved.

One approach to quantifying plant residue decomposition is to consider the mechanisms involved. Soil microflora are responsible for most of the heterotrophic activity through which residues are transformed (Heal and Dighton, 1986) and are themselves comprised of elements originating from decomposing residues. Consequently, we can look to microbial immobilization as the earliest stage of the decomposition process in which plant-derived compounds can be distinguished from the rest of the soil organic matter. By monitoring plant-derived ^{15}N in the microbial biomass, mineral and organic soil components, it is possible to identify pathways of elemental movement and gross rates of transfers and transformations (Nason and Myrold, 1991) This is true over the short-term only, however, because over long periods, isotopes equilibrate with all parts of the system through which they circulate. These isotopic data can then be used to develop and evaluate[1] mechanistic simulation models designed to mimic plant residue decomposition and subsequent transformations in soil.

Three simulation models (sets of hypotheses[2]) of plant residue decomposition are described in Chapter 6. The objective of the present chapter was to obtain and analyze critically sets of independent experimental data which were to be used for evaluation of those simulation models. This involved monitoring the flux of plant-derived ^{15}N through the microbial biomass and inorganic soil components, as well as the overall dynamics of these components in two soils amended with ^{15}N-labelled pea residue. Data were then compared to findings in the literature.

5.2 MATERIALS AND METHODS

Growth of ^{15}N-labelled Legume Material

The procedure for growing ^{15}N-labelled peas (*Pisum sativum* 'Sirius') was as described in Chapter 3 except that plants were grown in a greenhouse and fed a modified nutrient solution which included the equivalent of 115 kg N ha^{-1} as $(^{15}NH_4)_2SO_4$ (13.8% ^{15}N atom abundance). Plants were harvested at full bloom (June 20, 1991) and the roots separated from the shoots. Subsamples of shoots were lyophilized (Freeze Mobile 6) and ground to a fine powder in a Brinkmann ultra-high-speed mill. Shoots were analyzed for C, N and ^{15}N as described in Chapter 3. Pea shoots contained

---

[1] evaluate refers to a statistical or subjective comparison of simulated output and experimental observations of common variables over time.

[2] hypotheses are ideas which attempt to explain observations and may be expressed in the form of words or pictures or as mathematical equations. Mechanistic simulation models can be considered as statements of hypotheses.

41.1% C, 2.4% N, 11.7% ^{15}N atom abundance. Shoots were analyzed for lignin by refluxing with 72% H_2SO_4 for 3 hours and correcting the mass of the remaining insoluble residue for ash content (AOAC, 1990). Shoots were 4.9% lignin.

Incubation

Soil samples (0 - 15 cm) were collected on August 11, 1991 from fallow fields near the experimental sites described in Chapter 2: one from the Dark Brown Chernozemic (DBC) soil zone and the other from the Grey Luvisol Luvisolic (GLL) soil zone. Soil properties are shown in Table 5-1. The DBC soil was collected from an upper slope position and, therefore, had a lower clay content compared to the DBC soil used in Chapters 2, 3 and 4. Field-moist soil was sieved (2 mm) and stored overnight at 23°C. Triplicate 25 g subsamples were weighed into 50 mL polystyrene beakers and moistened to 55% water-holding capacity (WHC) which was equivalent to 31% water content for the DBC soil and 29% for the GLL soil. Soils were amended with 11.9 ± 0.2 mg ground pea shoot which was proportional to the amount of pea material per mass of soil used in related field experiments (Chapters 2 and 3). Individual beakers containing amended and non-amended samples were placed inside 1.9 L glass jars with screw cap lids; the bottom of the jars contained water to maintain high relative humidity and prevent soils from drying. Samples were incubated in the dark at 23°C. NaOH (2.5 *M*) traps were used to estimate cumulative CO_2 production. NaOH traps were replaced on days 0, 1, 2, 9, 16, 23, 30, 37, 51, 65 and 81.

Soil Analysis

Further replicates of amended and non-amended soils were incubated in 1.9 L jars and were destructively sampled on days 1, 2, 12, 22, 40, and 81. Jars were aerated every 7 days to insure aerobic conditions. At each date, triplicate samples of soil were either: (1) immediately extracted with 2*M* KCl (5:1 v/w), (2) used for biomass C and N determination, or (3) dried at 70°C. NH_4^+-N and NO_3^--N in KCl extracts were analyzed with a Technicon AutoAnalyzer (Keeney and Nelson, 1982). The remainder of the extracts were prepared for ^{15}N analysis by the ^{15}N diffusion method of Brooks et al. (1989). Biomass C and N were determined by the ninhydrin-reactive N (NRN) assay (Amato and Ladd, 1988) as described in Chapter 4. Biomass N was calculated as 3.1 times the flush of NRN following fumigation. It was assumed that the ^{15}N atom % abundance of the NH_4^+-N extracted from fumigated samples represented that of the microbial biomass. Total N and ^{15}N analyses were performed on the ANA-SIRA system as described in Chapter 3.

Statistical Analysis

Experimental data (combining observations taken over the 81 days) were analyzed using the ANOVA procedure of Microsoft Excel Version 5.0 (Microsoft Corporation, 1993). A NLIN procedure of SAS (SAS, 1985) was used to generate one and two-component first order equations to describe trends in microbial biomass N and ^{15}N data. One-component equations were considered adequate to represent trends unless the residual sum of squares (RSS) was significantly reduced by using the two-component equation. Significance was determined by comparing a computed F-statistic (= ($RSS_{one\text{-}component}$ - $RSS_{two\text{-}component}$) / residual mean $square_{two\text{-}component}$) to an F-value at $P<0.05$ with 1 and n-p degrees of freedom, where n=number of data points and p=number of parameters (Robinson, 1985).

Table 5-1. Properties of the Chernozemic and Luvisolic soils used in the laboratory incubation

Sample	Total C[a] (%)	Total N[b] (%)	pH[c]	Clay[d] (%)	Sand[d] (%)	^{15}N atom abundance (%)
DBC	2.82	0.23	7.3	19.5	45.3	0.3644
GLL	2.60	0.25	6.2	12.5	46.7	0.3685

[a] Determined by dry oxidation in LECO induction furnace.
[b] Determined by Dumas combustion.
[c] Determined in 1:2 soil:H_2O (mass:volume) mixture by glass electrode.
[d] Determined by hydrometer method.

5.3 RESULTS

Data for observed variables are plotted in Figures 5-1 through 5-3. Data points in these graphs were not joined because observations were made at points in time and, as such, do not necessarily indicate trends in the variables between observed times. In general, caution should be used when interpolating lines over time-course data points.

Microbial biomass N was significantly greater in the DBC soil compared to the GLL soil (Figure 5-1; Table 5-2). Overall, the addition of pea shoot did not significantly increase microbial biomass N in either soil. Biomass values in all soils declined after day 12 of the incubation. The percent of original biomass N remaining after 81 days was 59% in the DBC soil and 40% in the GLL soil. Mineral N was significantly greater in the GLL soil compared to the DBC soil (Figure 5-1; Table 5-2). Overall, mineral N was not significantly different between amended and non-amended soils although, it did appear to be greater in the amended soils on day 81. N mineralized

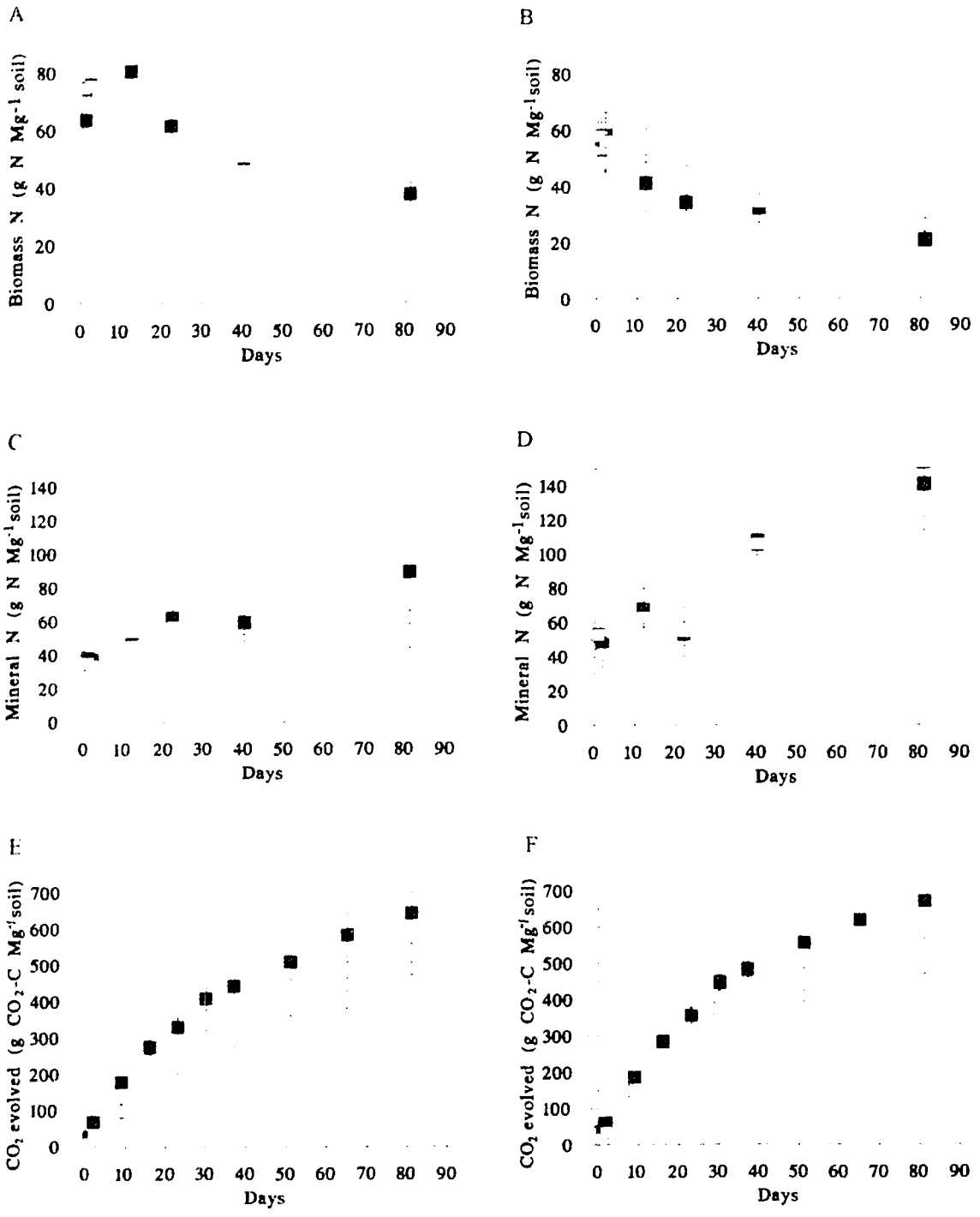

Figure 5-1. Microbial biomass N in (A) DBC and (B) GLL; mineral N in (C) DBC and (D) GLL; CO_2 evolved from (E) DBC and (F) GLL. ■, amended with pea shoot; □, nonamended. Error bars indicate standard deviation, n=3.

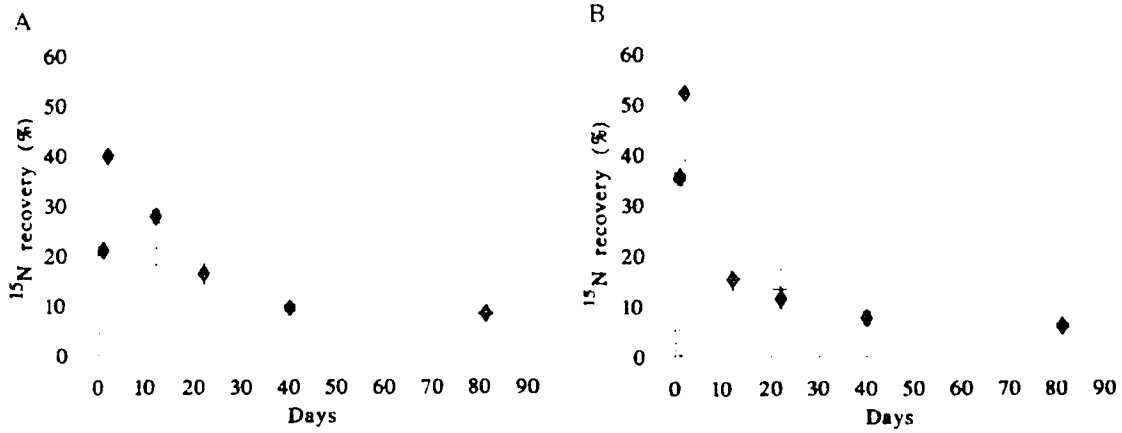

Figure 5-2 ^{15}N recovery in (A) DBC and (B) GLL soils. ◆, microbial biomass N; ◇, mineral N. Error bars indicate standard deviation. n=3.

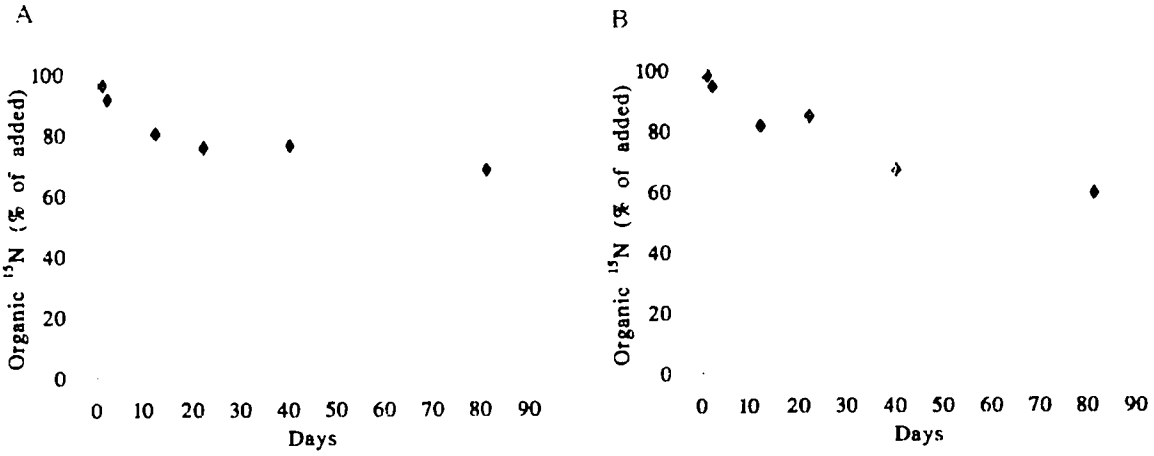

Figure 5-3. Transformation of plant residue ^{15}N in (A) DBC and (B) GLL soils. ◆, Total ^{15}N - mineral ^{15}N; ◇, Total ^{15}N - (microbial biomass ^{15}N + mineral ^{15}N)

Table 5-2. ANOVA results for combined 81 day incubation data

	Biomass N	Mineral N	Cum. CO_2	N min. rate / soil N	C min. rate / soil C	^{15}N rec. in biomass N	^{15}N rec. in mineral N
Site	***	***	NS	NS	NS	NS	NS
Amendment	NS	NS	**	NS	**	---	---

The difference between means is significant at: ***, P<0.001; **, P<0.01; *, P<0.05; NS, not significantly different.

in response to amendment (day 81: mineral $N_{amended}$ - mineral $N_{non\text{-}amended}$) accounted for 236% and 201% of N added as pea residue in the DBC in the GLL soil, respectively. This means that amendment increased mineralization of native soil N by 23 and 19 g N Mg^{-1}soil. Mineralization rate and mineralization rate normalized to soil N were not significantly different between soils or treatments (Table 5-2). N immobilization was evident in both soils early in the incubation (Figure 5-1). Cumulative CO_2 (Figure 5-1), respiration rate and respiration rate normalized to soil C were not significantly different between soils but were greater in the amended treatments (Table 5-2). The main respiratory response was observed on days 1 and 2. After day 20, respiration rates were similar between treatments. CO_2 evolved in response to amendment ($CO_{2amended}$ - $CO_{2non\text{-}amended}$) accounted for 78% and 60% of C added as pea residue in the DBC and GLL soil, respectively. Recovery of pea-derived ^{15}N in the whole soil was >92% after 81 days. There was no significant difference between soils in either the recovery of pea-derived ^{15}N in the biomass N or the recovery of pea-derived ^{15}N in the mineral N (Figure 5-2; Table 5-2). On day 81, however, the DBC biomass contained more ^{15}N than did the GLL biomass.

The net decay of microbial biomass N (from peak value to day 81) was best described by single component first-order kinetics which can be expressed as:

$$A_t = A_0 e^{-kt}$$

where A_t = microbial biomass N (g N Mg^{-1}soil) at time t (days), A_0 = microbial biomass N at t = 0 (time of peak value) and k = first-order rate constant (day^{-1}) (Table 5-3). Peak values (between 40% and 52%) of plant-derived ^{15}N were recovered in the biomass on day 2 in both soils (Figure 5-2). Decay of ^{15}N-labelled biomass between day 2 and 81 was best described by single component first order kinetics (Table 5-3). The rate constant for the decay of ^{15}N-labelled biomass was greater than that of total biomass N.

Table 5-3. First order decay parameters for microbial biomass

Soil	Variable	Amendment	A_0	k (day^{-1})	r^2	Half-life (days)
DBC	biomass N	none	75	9.9E-3	0.79	70
	biomass N	pea shoot	80	1.4E-2	0.89	50
	biomass ^{15}N	pea shoot	40	3.8E-2	0.95	18
GLL	biomass N	none	58	1.5E-2	0.93	46
	biomass N	pea shoot	59	1.7E-2	0.89	41
	biomass ^{15}N	pea shoot	52	9.7E-2	0.96	7

Because the loss of ^{15}N from the original plant residues cannot be measured directly, decomposition must be inferred from indirect measurements. The transformation of ^{15}N-labelled pea residue was represented in two ways (Figure 5-3). The initial rate of transformation was much greater when recovery of ^{15}N in the biomass was included. Transformation of plant-derived ^{15}N into non-microbial organic forms was evident in both representations.

5.4 DISCUSSION

Biomass N Dynamics

At the beginning of the incubation, biomass N as a proportion of soil organic N was 3.2% for the DBC and 2.4% for the GLL soil. These values were within the expected range (Hassink, 1994; Sparling and Zhu, 1993) and are consistent with general observations of greater proportions of soil N as biomass in soils of higher clay content (Hassink, 1994). Considering the variability of reported biomass values in comparable studies (Table 5-4), the percentage decline in biomass N in the present study (Figure 5-1) was not unrealistic. For example, Voroney and Paul (1984) report that 72% of the original soil biomass N remained after 42 days of incubation. This percentage is less than that observed in the present study at 40 days. Ladd et al. (1992) also report substantial decreases in biomass N during incubation with glucose and $(NH_4)_2SO_4$. As with the present study, the greater loss was observed in the soil with lower clay content (Vertisol 50% clay; Alfisol 10% clay). West et al. (1986) incubated 'fresh' soils and found variable responses in biomass C and N depending on the sampling site and the season in which samples were collected.

One could speculate that some of the apparent decline in microbial biomass was the result of 'artificially' high values at the start of the incubation. As reported in Chapter 2, pre-incubation soil conditions and sample preparation can influence results from studies under controlled environments. Soil samples, which were collected from fallow fields in August, probably contained little available substrate and, consequently, a largely inactive microbial population. The mechanical disturbance of sieving, as well as wetting the soils to 55% WHC may have stimulated microbial growth by increasing accessibility to previously protected substrates (Van Veen et al., 1984). N immobilization was evident in both amended and nonamended soils early in the incubation indicating that a substrate with a fairly wide C:N ratio was being utilized. Further to this argument,

the mean values of biomass N reported in Chapter 4 for similar soils (estimated by NRN and mineral N flush) were approximately 70% of the day 1 incubation values.

Table 5-4. Change in microbial biomass upon incubation as reported in the literature

Source of data	Voroney and Paul. 1984	Ladd et al., 1992		West et al., 1986
Soil description	Dark Brown Chernozemic	Vertisol	Alfisol	Silt loam pasture soil
Soil conditioning	'incubated 1 month'	'stored at 4°C'		none
Incubation period	42 days	112 days		7 days
Moisture content	50 kPa	40% WHC		50% WHC
Temperature	21°C	25°C		25°C
Amendment	NO_3^- (150 ug N g^{-1})	Glucose (1000 ug C g^{-1}) + $(NH_4)_2SO_4$ (36 ug N g^{-1})		none
Biomass analysis	Fumigation-incubation	Ninhydrin-reactive N		Fumigation-incubation
Biomass C remaining	92%	NR*	NR	43% to 94%
Biomass N remaining	72%	83%	56%	82% to 134%

* NR=not reported.

Analysis of Assumptions in Ninhydrin-Reactive N Technique

Was the decrease in biomass during incubation real or was it an artifact of the methodology employed? The NRN technique includes the following assumptions: (1) the cellular content of ninhydrin-reactive compounds (α-amino acid and NH_4^+) is constant and can be related to biomass C by a factor of 21 and to biomass N by a factor of 3.1, and (2) the degradation of nitrogenous compounds released from chloroform-lysed cells (i.e. protease activity) is independent of pre-incubation soil conditions and is comparable among soils held under chloroform vapour for 10 days. NRN extracted from fumigated samples decreased during the latter portion of the incubation in all cases. This decrease was expected as biomass declines. The observed fluctuation and increase in NRN extracted from non-fumigated samples, however, was not expected (Figure 5-4) and is in contrast to Van Gestel et al.'s (1992) observations of a decrease in NRN upon soil incubation. An increase in non-fumigated NRN decreases the size of the calculated flush of NRN and consequently decreases the estimation of biomass N. The increase in NRN was largely due to an increase in α-amino acids and secondarily to an increase in NH_4^+. Some of the accumulation may have been the result of microbial predation by amoebae and bacterivorous nematodes. Excess N in

both faunal groups is released solely as NH_4^+ and, although most of nitrogenous wastes (feces and dead animals) of amoebae are released as NH_4^+, about 48% of bacterivorous nematode waste is in organic form (Hunt et al., 1987). Some of this organic material could have contributed to the increase in α-amino acids over the 81 days of incubation.

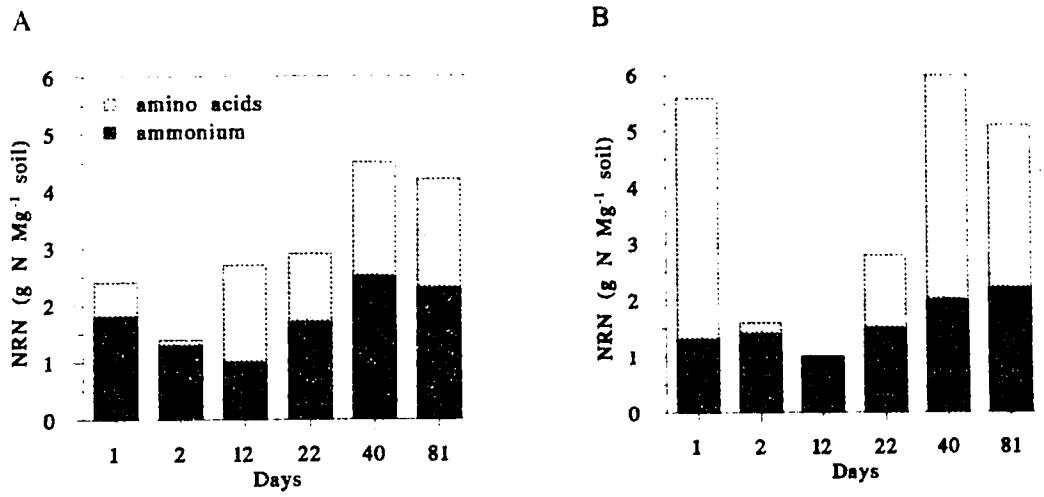

Figure 5-4. Ninhydrin -reactive N extracted from non-fumigated DBC soil (A) non-amended and (B) amended with pea residue.

When developing a conversion factor between the release of NRN and biomass C, Amato and Ladd (1988) found a good correlation between biomass C, as determined from the flush of CO_2 following fumigation, and NRN in soils that had been incubated for 44 and 66 weeks. They found a lower and much more variable ratio of biomass C:NRN in soils that had been incubated for 2 weeks. Was there a qualitative change in microbial cells, the older cells containing less NRN? Older cultures of *Fusarium oxysporum* were found to have significantly lower N content and significantly lower k_c and k_n values compared to younger cultures (Ross et al., 1987). The lower k_c and k_n values reflect a decrease in mycelial cytoplasmic content, the cytoplasmic material being the source of C and N mineralized upon incubation. The cytoplasm is also the main source of NRN compounds following fumigation. Assuming the conversion factor of 21 is appropriate for older cells such as those found in soils incubated for 44 or 66 weeks, it is possible that a smaller conversion factor may be more appropriate for younger cells such as those found in recently amended soils.

Estimating biomass by measuring the release of NRN requires comparable protease activity in different soils and under different environmental conditions. Evidence already exists of variable protease activity in different soils (Sparling et al., 1993). The magnitude of the NRN flush increases with soil water content and is affected by soil pH: activity optima were observed in the pH range 7.8-8.4 (Amato and Ladd, 1994). Protease activity is not always correlated to total numbers of bacteria and is proposed to be specific to a small fraction of the microbial community (Watanabe and Hayano, 1995). Shifts in species composition may, therefore, influence protease activity. Furthermore, there is evidence that protease activity may fluctuate with growth stage. In cultured isolates of *Frankia*, exo-cellular proteinase activity increased dramatically shortly before the peak in exponential growth (Muller, 1991). The specificity of the enzymes also changed (e.g. proline-specific aminopeptidase was no longer produced). Nutrient status also influences protease activity: C starved cells are reported to have higher rates of internal protein cycling (Mason and Egli, 1993).

Response to Amendment with Pea Residue

There were no significant increases in microbial biomass N or mineral N in response to amendment with pea residue over the 81 days of incubation. By day 81, however, amendment had resulted in an apparent 'priming effect' on N mineralization. Both the amended DBC and GLL soils had similar small increases in the quantity of native soil N mineralized. Considerable controversy exists regarding the indirect benefits of legume residues but it is suggested that, in addition to their value as a direct source of plant-available N, legume residues improve crop productivity by enhancing the availability of soil N (Azam et al., 1993).

Purposely low concentrations of plant residue were added to these soils (196 g C Mg^{-1}soil) in order to minimize distortion of soil dynamics. Input of plant materials mimicked the field situation. This is in contrast to studies in which large quantities of plant residue are added resulting in significant and sustained increases in microbial biomass. For example, Ocio and Brookes (1990) incubated soil with wheat straw at 8260 g C Mg^{-1}soil and noted a 50% to 100% increase in biomass by day 13 which was sustained until the end of the experiment (day 35). Similarly, Thomsen (1993) observed an 82% increase in biomass following the addition of barley straw at 2700 g C Mg^{-1}soil. For comparison, the highest barley straw yield observed during the present study was 1260 g C Mg^{-1}soil (Chapter 3).

Respiration was the only measured variable that showed a significant response to amendment and then only on the first two or three sampling dates. In fact, peak recovery of pea-derived ^{15}N in the microbial biomass was observed after only 2 days. More measurements during the first few days of incubation would have been useful to elucidate decomposition dynamics further. In a comparable laboratory incubation with ^{15}N-labelled maize residues (C:N = 41; 542 g C Mg^{-1}soil) decomposing in a fine sandy loam, peak recovery (34%) of plant-derived ^{15}N in the biomass was not observed until day 14 (Voroney, 1983).

Transformation of Pea Residue ^{15}N

With its rapid uptake by the microbial biomass, the pea shoot behaved much like a simple substrate. Glucose, for example, was observed to have maximum recovery in the biomass after 2 days of incubation (Ladd et al., 1992). A possible explanation for the ready availability of the pea N lies in the preparation of the plant material: grown in a greenhouse and harvested at bloom, it contained little lignin and was immediately freeze-dried and then ground to a fine powder. In both the previously mentioned experiments (Voroney, 1983; Amato and Ladd, 1980), the plant material was air-dried and chopped into 1-2 mm pieces. Freeze-dried plant material most closely resembles fresh material and freeze-drying is suggested to be the more appropriate method for mineralization studies when compared to oven drying (Moorhead et al., 1988).

Grinding plant materials appears to have contrasting effects on mineralization rate. Over a 98 day soil incubation, ground (<0.2 mm in cyclone mill) lentil green manure evolved similar amounts of CO_2 as cut (1 cm) green manure (Bremer et al., 1991). Grinding, however, increased CO_2 evolution from lentil and wheat straw. Grinding increases the residue's surface area and disrupts plant structure, thus increasing microbial accessibility. Apparently grinding the lentil green manure, which had the least amount of resistant material to begin with, did not make it significantly more susceptible to microbial attack.

Initial transformation of plant residue, as represented by the appearance of plant-derived ^{15}N in the microbial biomass and mineral soil components, was very rapid: 50 - 60% transformation in the first two days of incubation. In contrast, when represented by the accumulation of plant-derived N in the mineral component only, less than 10% transformation was estimated after two days. This type of discrepancy emphasizes the importance of considering mechanisms when assigning rates to complex processes.

N mineralization and immobilization occur simultaneously in the soil and, therefore, mineral N is in continuous flux. This is problematic when attempting to elucidate actual rates such as gross mineralization rate. A similar problem is evident when attempting to estimate decomposition rate from the amount of plant-derived N in the microbial biomass because the biomass is in flux with not only the mineral but also the organic soil component. Plant-derived N may be released from microbes as organic waste and this, plus inactivated cells, becomes incorporated into soil organic matter. Furthermore, not all plant residue N is necessarily mineralized or even taken up by microorganisms. Some of the N present in the more resistant structural components (aromatic compounds) of plant residues may be abiotically incorporated into soil humus. This should also be included in the decomposition equation. Again, it is imperative that mechanisms be considered when assigning rates to complex transformation processes.

Interaction Between Microbial Biomass and Soil Properties

Soil characteristics influence microbial dynamics (Amato and Ladd, 1992; Ladd et al., 1992). Examining microbial biomass decay in the DBC and GLL soils, gives some insight to interactions among microbes, substrate and habitat. Following amendment, microbial biomass in both soils had a shorter half-life compared to non-amended soils. Van Veen et al. (1984) suggest that each soil has a specific maximum capacity to protect microorganisms. Microbial biomass in excess of the protective capacity, such as that present in response to readily available substrate additions, is subject to rapid turnover. The shorter half-life of the ^{15}N-labelled biomass in comparison to total biomass N is further evidence toward a faster turnover of recently immobilized N (Azam et al., 1989; Ladd et al., 1985).

The rate of decay of microbial biomass N was greater in the GLL soil compared to the DBC soil (Table 5-3). Biomass ^{15}N also decayed more quickly in the GLL soil and, as a result, less ^{15}N was retained by the GLL biomass on day 81 of the incubation (Figure 5-2). These observations are in agreement with previous findings of a faster turnover of C and N in the microbial biomass of coarse-textured soils compared to fine-textured soils (Ladd et al., 1992). This has been attributed to predation: soils with coarser texture impose less physical restrictions on the ability of soil fauna to graze on microbes, thereby increasing faunal-induced mineralization of microbial C and N (Rutherford and Juma, 1992). Similar trends were observed in Luvisolic and Chernozemic soils collected from the field (Chapter 2).

Conclusion

The decline in biomass N was comparable to that observed in several other studies, although the question remains as to whether the decline was 'real' or an artifact of the technique employed to measure it. Amendment with pea residue did not elicit a significant response in biomass N, cumulative mineral N or N mineralization rate possibly as a result of the relatively low concentration of added substrate. Mineral N concentrations on day 81, however, suggest that amendment did cause a 'priming effect' resulting in the mineralization of an additional 19-23 g native soil N Mg^{-1}soil. The rate of pea residue N transformation, as estimated from the recovery of plant-derived ^{15}N in the soil microbial biomass and mineral components, was initially very rapid: 50-60% in the first 2 days of incubation. Transformation dynamics would have been better elucidated had more observations been made during the first few days of the incubation. Recently immobilized biomass N, possibly that in excess of the soil's protective capacity, had a faster turnover compared to 'steady-state' biomass N. Further evidence was found to support the hypothesis of faster turnover of biomass C and N in coarse-textured soils compared to fine-textured soils.

5.5 LITERATURE CITED

Amato, M. and Ladd, J.N. 1994. Application of the ninhydrin-reactive N assay for microbial biomass in acid soils. Soil Biol. Biochem. 26:1109-1115.

Amato, M. and Ladd, J.N. 1992. Decomposition of ^{14}C-labelled glucose and legume material in a range of soils: Properties influencing the accumulation of organic residues and microbial biomass C. Soil Biol. Biochem. 24:455-464.

Amato, M and Ladd, J.N. 1988. Assay for microbial biomass based on ninhydrin-reactive nitrogen in extracts of fumigated soils. Soil Biol. Biochem. 20:107-114.

Amato, M. and Ladd, J.N. 1980. Studies of nitrogen immobilization and mineralization in calcareous soils. V. Formation and distribution of isotope-labelled biomass during decomposition of ^{14}C- and ^{15}N-labelled plant material. Soil Biol. Biochem. 12:405-411.

Association of Official Analytical Chemists. 1990. Official Methods of Analysis. Association of Official Analytical Chemists, Inc., Arlington, Virginia, USA.

Azam, F., Simmons, F.W. and Mulvaney, R.L. 1993. Mineralization of N from plant residues and its interaction with native soil N. Soil Biol. Biochem. 25:1787-1792.

Azam, F., Mulvaney, R.L. and Stevenson, F.J. 1989. Synthesis of ^{15}N-labelled microbial biomass in soil in situ and extraction of biomass N. Biol. Fertil. Soils 7:180-185.

Bremer, E., van Houtum, W. and van Kessel, C. 1991. Carbon dioxide evolution from wheat and lentil residues as affected by grinding, added nitrogen, and the absence of soil. Biol. Fertil. Soils 11:221-227.

Brooks, P.D., Stark, J.M., McInteer, B.B. and Preston, T. 1989. Diffusion method to prepare soil extracts for automated nitrogen-15 analysis. Soil Sci. Soc. Am. J. 53:1707-1711.

Coleman, D.C. and Hendrix, P.F. 1988 Agroecosystem processes. Pages 149-170 *in* L.R. Pomeroy and J.J. Alberts, eds. Concepts of Ecosystem Ecology: A Comparitive View. Springer-Verlag, New York, USA.

Hassink, J. 1994. Effect of soil texture on the size of the microbial biomass and on the amount of C and N mineralized per unit of microbial biomass in Dutch grassland soils. Soil Biol. Biochem. 26:1573-1581.

Heal, O.W. and Dighton, J. 1986. Nutrient cycling and decomposition in natural terrestrial ecosystems. Pages 14-73 *in* M.J. Mitchell and J.P. Nakas, eds. Microfloral and Faunal Interactions in Natural and Agro-ecosystems. Martinus Nijhoff/Dr W. Junk Publishers, Dordrecht, The Netherlands.

Hunt, H.W., Coleman, D.C., Ingham, E.R., Ingham, R.E., Elliott, E.T., Moore, J.C., Rose, S.L., Reid, C.P.P. and Morley, C.R. 1987. The detrital food web in a shortgrass prairie. Biol. Fertil. Soils 3:57-68.

Juma, N.G. and McGill, W.B. 1986. Decomposition and nutrient cycling in agro-ecosystems. Pages 74-136 *in* M.J. Mitchell and J.P. Nakas, eds. Microfloral and Faunal Interactions in Natural and Agro-ecosystems. Martinus Nijhoff/Dr W. Junk Publishers, Dordrecht, The Netherlands.

Keeney, D.R. and Nelson, D.W., 1982. Nitrogen-Inorganic Forms. Pages 643-693 *in* A.L. Page, R.H. Miller and D.R. Keeney, eds. Methods of Soil Analysis. Part 2-Chemical and Microbiological Properties, 2nd Ed. ASA-SSSA, Madison, WI, USA.

Ladd, J.N., Jocteur-Monrozier, L. and Amato, M. 1992. Carbon turnover and nitrogen transformations in an alfisol and vertisol amended with [U-^{14}C] glucose and [^{15}N] ammonium sulfate. Soil Biol. Biochem. 24:359-371.

Ladd, J.N., Amato, M. and Oades, J.M. 1985. Decomposition of plant material in Australian soils. III. Residual organic and microbial biomass C and N from isotope-labelled legume material and soil organic matter, decomposing under field conditions. Aust. J. Soil Res. 23:603-611.

Longman Dictionary of Contemporary English. 1978. P. Procter, ed. Pitman Press, Bath, Great Britain.

Mason, C.A. and Egli, T. 1993. Dynamics of microbial growth in the decelerating and stationary phase of batch culture. Pages 81-102 *in* S. Kjelleberg, ed. Starvation in Bacteria. Plenum Press, New York, USA.

Microsoft Corporation. 1993. User's Guide: Microsoft Excel Version 5.0. Microsoft Corporation, USA. 786 pp.

Moorhead, K.K., Graetz, D.A. and Reddy, K.R. 1988. Mineralization of carbon and nitrogen from freeze- and oven-dried plant material added to soil. Soil Sci. Soc. Am. J. 52:1343-1346.

Muller, A., Benoist, P., Diem, H.G. and Schwencke, J. 1991. Age-dependent changes in extracellular proteins, aminopeptidase and proteinase activities in *Frankia* isolate BR. J. Gen. Microbiol. 137:2787-2796.

Nason, G.E. and Myrold, D.D. ^{15}N in soil research: appropriate application of rate estimation procedures. Agric. Ecosystems Environ. 34:427-441.

Ocio, J.A. and Brookes, P.C. 1990. An evaluation of methods for measuring the microbial biomass in soils following recent additions of wheat straw and the characterization of the biomass that develops. Soil Biol. Biochem. 22:685-694.

Paul, E.A. and Clark, F.E. 1989. Soil Microbiology and Biochemistry. Academic Press, Inc., San Diego, USA.

Robinson, J. A. 1985. Determining microbial kinetic parameters using non-linear regression analysis: advantages and limitations in microbial ecology. Adv. Microb. Ecol. 8:61-114.

Ross, D.J., Sparling, G.P. and West, A.W. 1987. Influence of *Fusarium oxysporum* age on proportions of C, N and P mineralized after chloroform fumigation in soil. Aust. J. Soil Res. 25:563-566.

Rutherford, P.M. and Juma, N.G. 1992. Influence of texture on habitable pore space and bacterial-protozoan populations in soil. Biol. Fertil. Soils 12:221-227.

Sparling, G.P., Gupta, V.V.S.R. and Zhu, C. 1993. Release of ninhydrin-reactive compounds during fumigation of soil to estimate microbial C and N. Soil Biol. Biochem. 25:1803-1805.

Sparling, G. and Zhu C. 1993. Evaluation and calibration of biochemical methods to measure microbial biomass C and N in soils from western Australia. Soil Biol. Biochem. 25:1793-1801.

Statistical Analysis System Institute, Inc. 1985. SAS user's guide: Statistics. Version 5 ed. SAS Institute, Inc., Cary, NC. 956 pp.

Thomsen, I.K. 1993. Turnover of ^{15}N-straw and NH_4NO_3 in a sandy loam soil: effects of straw disposal and N fertilization. Soil Biol. Biochem. 25:1561-1566.

Van Gestel, M., Ladd, J.N. and Amato, M., 1992. Microbial biomass responses to seasonal change and imposed drying regimes at increasing depths of undisturbed topsoil profiles. Soil Biol. Biochem. 24:103-111.

Van Veen, J.A., Ladd, J.N. and Frissel, M.J. 1984. Modelling C and N turnover through the microbial biomass in soil. Plant and Soil 76:257-274.

Voroney, R.P. 1983. Decomposition of crop residues. Ph.D. Thesis. University of Saskatchewan, Canada.

Voroney, R.P. and Paul, E.A. 1984. Determination of k_C and k_N *in situ* for calibration of the chloroform fumigation-incubation method. Soil Biol. Biochem. 16:9-14.

Watanabe, K. and Hayano, K. 1995. Seasonal variation of soil protease activities and their relation to proteolytic bacteria and *Bacillus* spp. in paddy field soil. Soil Biol. Biochem. 27:197-203.

West, A.W., Ross, D.J. and Cowling, J.C. 1986. Changes in microbial C, N, P and ATP contents, numbers and respiration on storage of soil. Soil Biol. Biochem. 18:141-148.

CHAPTER 6

Evaluation of three simulation models used to describe plant residue decomposition in soil[1]

6.1 INTRODUCTION

Transformation of organic matter in the soil-plant system[2] is a complex, dynamic process involving biological, chemical, and physical components. Mathematical representation of complex processes allows information from experiments to be integrated into a system model. Defining components of a natural system, and more importantly the links among components, challenges our understanding of a system and identifies areas where more information is required. To improve models, one must be able to distinguish and retain valid hypotheses and dismiss invalid ones. Two problems arise in evaluating models, however. First, there is a lack of consensus as to which statistical methods are appropriate when comparing model output to observed natural phenomena (Wallach and Goffinet, 1989). Is it quantitatively correct to compare many simulated variables to data sets with few variables? Often statistical comparisons are avoided and subjective means are used to evaluate model performance, graphing simulated and observed data and 'eyeing' the goodness of fit (Grant et al., 1993; McGill et al., 1981; Verberne et al., 1990). Two quantitative methods which have been used for model evaluation are the goodness of fit method (Whitmore, 1991) and the figure-of-merit function (Molina et al., 1990). The goodness of fit method is used for evaluating the difference between replicated data and simulated values of a single variable (e.g. microbial biomass N). The figure-of-merit function is used for comparing alternate models by ranking the correspondence between experimental data and simulated values of many variables.

The second problem in evaluating models is in the nature of the comparison between alternate models designed to simulate the same system. Comparing two system models yields little insight into which of the structural or kinetic features of one model might give it greater predictive accuracy or mechanistic integrity compared to the other. Specific hypotheses within the system models must be compared (Hunt and Parton, 1986) and evaluated against experimental data.

---

[1] A version of this chapter will be submitted to Ecological Modelling.

[2] system refers to a group of related parts working together; for example, a community within an ecosystem or a group of linked algorithms in a simulated ecosystem.

Failure of a model to replicate a natural phenomenon identifies an invalid hypothesis. Sensitivity to specific structural or kinetic features can also be evaluated by comparing the behavior of alternate models.

My objective was to evaluate systematically the plant residue decomposition algorithms[3] from three published models. These plant residue decomposition submodels were taken from Ecosys (Grant et al., 1993), Phoenix (McGill et al., 1981) and Verberne et al (1990) and will subsequently be referred to as ECO, PHO and VER. The three submodels differ both structurally and kinetically. Structurally, ECO partitions plant residues into four biochemical components, all of which are solubilized before either being taken up by soil microbes or abiotically adsorbed to soil organic matter (Figure 6-1). PHO, in contrast, partitions plant residues into two functional components: materials from these are either taken up by microbes or adsorbed to soil organic matter (humadification). VER partitions plant residues into three functional components: two of these are taken up by microbes while the third is directly incorporated into soil organic matter. The models differ kinetically in the types of equations used (first order, Michaelis-Menten) and in the factors which control the rates of transformation.

To evaluate the submodels, I sequentially 'plugged' each of them into a single base model which described soil dynamics thus testing only one aspect of the model: the hypothesized mechanisms of residue decomposition. I statistically evaluated ECO, PHO and VER in terms of their ability to mimic experimental data absolutely and relative to one another. Experimental data were from my laboratory incubations of ^{15}N-labelled plant residues (Chapter 5) and two other laboratory incubations of plant residues as reported in the literature.

6.2 MATERIALS AND METHODS

The Base Model

The base model and all three plant decomposition submodels were programmed with Stella II simulation software (High Performance Systems, 1994) and run on an hourly time-step using Euler's integration method. Stella II equations for the base model and the three submodels are listed in Appendix A. The base model which describes C, ^{14}N and ^{15}N transformations in soil, is a simplified version of the soil component from Ecosys (Grant et al., 1993) (Figure 6-2). This model

[3] algorithm refers to a list of mathematical operations which are carried out in a fixed order.

explicitly represents the activities of soil microorganisms as essential to the dynamics of soil organic matter transformation. Three organic substrates (groups of kinetically similar materials) are represented in the model: plant residue, active soil organic matter and passive soil organic matter[4]. Each substrate has an asso iated soluble component and associated microbial biomass. The microbial biomass is resolved into labile, resistant and storage components. Active microbial biomass is assumed to contain all the labile biomass in the system. Its composition is 55% labile and 45% resistant (Figure 6-3). The remainder of the resistant microbial material represents quiescent (dormant or non-viable) biomass. The storage component of microbial biomass represents exo-cellular 'coatings' of readily available polysaccharides.

Figure 6-1. Structure of plant residue decomposition submodels: (A) ECO, (B) PHO and (C) VER. Microbial biomass, adsorbed and active organic matter are components of the base model shown in Figure 6-2.

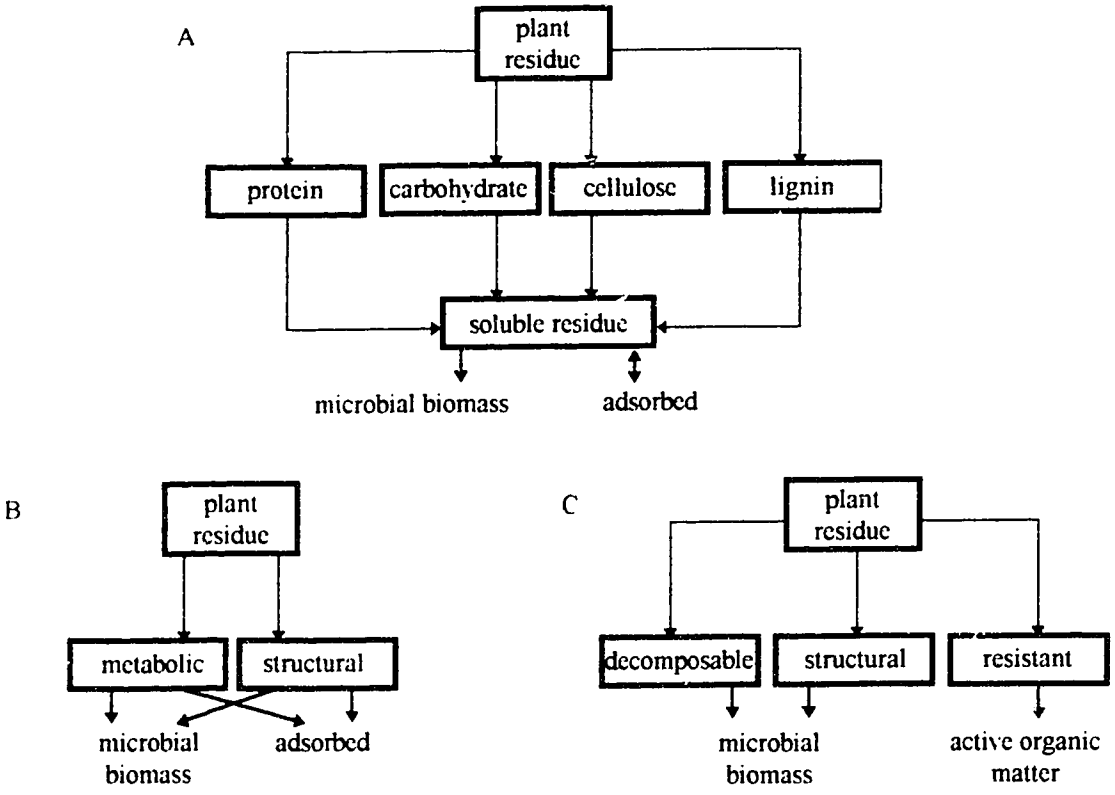

[4] active and passive soil organic matter refers to a conceptual division of organic matter into two kinetically homogenous components. Active organic matter has a greater turnover rate than passive organic matter.

Figure 6-2. General structure of base model for soil functions. As shown here, 'microbial biomass' represents both live and inactivated biomass. The *respiration* flow is used for C simulation and the *mineralization immobilization* flow is used for N simulation. Note: *sorption* refers to both adsorption/precipitation and desorption/dissolution.

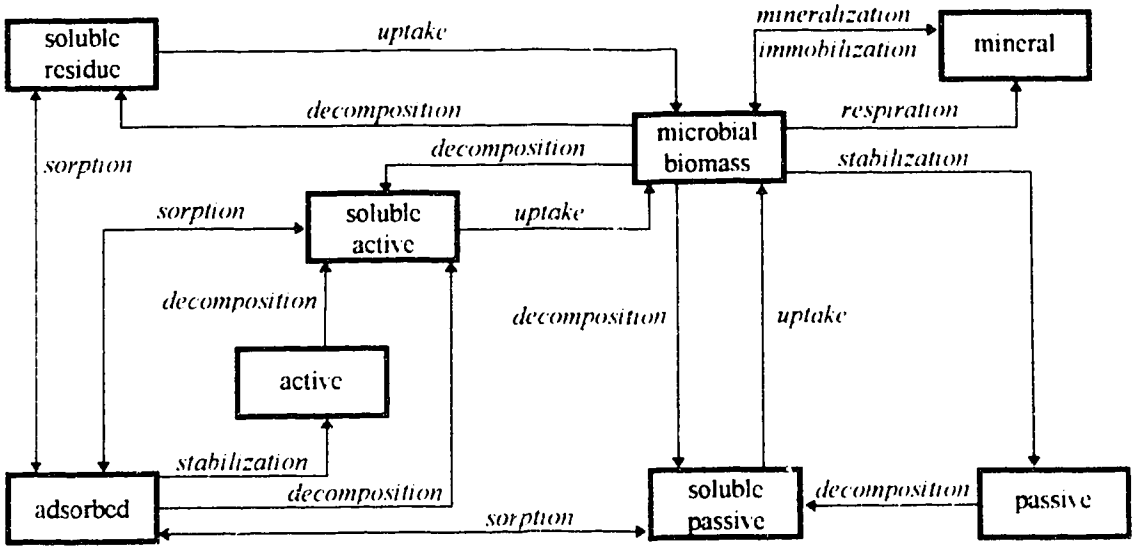

Figure 6-3. The concept of active biomass (55% labile + 45% resistant).

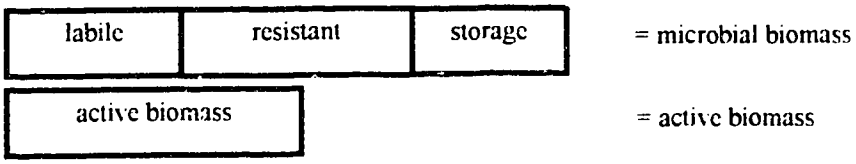

The simplified version of Ecosys differs from the original in the following: only one soil layer (0-15 cm) was represented, only one adsorbed pool was represented, animal manure was not included as an organic substrate, and oxygen and water were considered non-limiting to growth-related processes.

Although each submodel was designed to function within its own system model, the algorithms describing the loss of material from plant residue were considered to be sufficiently mechanistic and, thereby, independent of the respective system models to be separated. The rate at which material leaves the plant residue, therefore, is representative of the rate at which this process would have occurred in the original system model. See Appendix A for details on parameters in original models.

ECO Submodel for Plant Residue Decomposition

ECO (Grant et al., 1993) partitions plant residues into biochemical components (protein, carbohydrate, cellulose and lignin) based on chemical analysis of representative plant samples (Figure 6-1). These biochemical components are treated as homogeneous, independent and exhibiting different resistance to microbial decomposition. The N in each component is calculated by dividing the C in each component by a constant C:N ratio. The C:N ratios are: 3.125 for protein, 500 for carbohydrate, 500 for cellulose and 100 for lignin. The C in each component is subject to decomposition by first order kinetics as a function of active microbial biomass. For example, protein decomposition (g C Mg^{-1}soil h^{-1}) is described by:

$$Dprotein\ C = 1.00 * actmic\ C * (protein\ C / Tplant\ C) * ftg * fdplant\ C \quad (6\text{-}1)$$

where

1.00 = specific rate constant for decomposition of protein C (g C g^{-1}actmic C h^{-1}) (1.00 for carbohydrate C, 0.15 for cellulose C, 0.025 for lignin C)

actmic C = active microbial biomass C in soil (g C Mg^{-1}soil)

protein C = C in the form of plant residue protein (g C Mg^{-1}soil)

Tplant C = total plant residue C remaining in soil (g C Mg^{-1}soil)

ftg = Arrhenius temperature function for growth-related processes (dimensionless)

fdplant C = density function relating concentration of active microbes to the quantity of substrate (dimensionless)

Density functions are defined for each substrate (plant, active organic matter, passive organic matter). The density function for plant material is:

$$fdplant\ C = Tplant\ C / \{Tplant\ C + 75 * (1.0 + [actmic\ C] / 25)\} \quad (6\text{-}2)$$

where:

[actmic C] = aqueous concentration of active microbial biomass C (g C Mg^{-1} available H_2O)

75 = Michaelis-Menten constant describing substrate concentration at half V_{max} for plant residue decomposition (g C Mg^{-1}soil)

25 = inhibition constant for plant residue decomposition (g C Mg^{-1} available H_2O)

The 'aqueous concentration' of active microbial biomass refers to the mass of active microbial C per mass of 'available' soil water. Water held at potentials below -50 MPa is

considered unavailable as a medium for enzyme activity (Papendick and Campbell, 1981). At a given moisture content, the mass of water held at potentials above -50 MPa varies with soil texture. Using observed values for matric potential (-0.5 MPa and -1.5 MPa) and corresponding water contents for representative sand, silt loam and clay soils, I calculated values for 'a' and 'b' from the following relationship (Papendick and Campbell, 1981):

$$\Psi = a * \theta^{-b} \qquad (6\text{-}3)$$

where:

Ψ = matric potential (MPa)

θ = water content (Mg H_2O Mg^{-1} soil)

a, b = constants for given soil texture

The constant 'a' was calculated as 9.75E-..., 5.14E... and 3.33E-4 for sand, silt loam and clay, respectively. The constant 'b' was calculated as 3.0..., 4.56 and 6.25 for sand, silt loam and clay, respectively. I used equation 6-3 to calculate water content at a matric potential of -50 MPa for each soil texture and calculated available water as the difference between soil water content and water held below -50 MPa.

The products of decomposition of the plant residue biochemical components are transferred to a soluble residue pool[5] (Figure 6-1; 6-2). C in this pool and the other soluble pools (soluble active and soluble passive (Figure 6-1)) may become part of the adsorbed soil component or be taken up by microbes. Microbial uptake of C from all soluble pools is based on the microbial requirement for C (maintenance and growth respiration) and the availablilty of soluble C. Microbial uptake of C from the soluble residue pool (g C Mg^{-1}soil h^{-1}) is calculated by:

$$Usoll\ C = MIN(Rmmic1, Rspecific1) + \{Rgmic1 / (1 - 0.6)\} \qquad (6\text{-}4)$$

where:

MIN is a function that returns the minimum of the variables in the following brackets

Rmmic1 = maintenance respiration of microbes associated with plant residue, referred to as microbial biomass 1 (g C Mg^{-1}soil h^{-1})

Rgmic1 = growth respiration of microbes associated with plant residue (g C Mg^{-1}soil h^{-1})

Rspecific1 = specific respiration of microbes associated with plant residue (g C Mg^{-1}soil h^{-1})

---

[5] pools refer to conceptual reservoirs of kinetically similar yet chemically diverse materials and are represented as rectangles in the Stella software. Kinetically similar pools are not always physically associated in soil.

0.6 = efficiency of utilization of plant residues by microbial biomass 1 (dimensionless)

$$Rmmic1 = (2E\text{-}3 * labmic1\ C + 1E\text{-}4 * resmic1\ C) * ftm \quad (6\text{-}5)$$

where:

2E-3 = specific maintenance respiration of labile microbial biomass 1 at 30°C (g C g^{-1} labmic1 C h^{-1})

labmic1 C = labile microbial biomass associated with plant residue (g C Mg^{-1}soil)

1E-4 = specific maintenance respiration of resistant microbial biomass at 30°C (g C g^{-1} resmic1 C h^{-1})

resmic1 C = resistant microbial biomass associated with plant residue (g C Mg^{-1}soil)

ftm = temperature function for maintenance processes (dimensionless)

$$Rgmic1 = MAX(0, Rspecific1 - Rmmic1) \quad (6\text{-}6)$$

$$Rspecific1 = 0.25 * actmic1\ C * [soluble1\ C]/(35 + [soluble1\ C]) * ftg * fcnratio \quad (6\text{-}7)$$

where:

0.25 = specific respiration at saturating soluble1 C and 30°C (g C g^{-1} actmic C h^{-1})

[soluble1 C] = aqueous concentration of soluble C associated with plant residue (g C Mg^{-1} available H_2O)

35 = [soluble1 C] when growth respiration is half of maximum (g C Mg^{-1} available H_2O)

fcnratio = function of microbial C:N associated with plant residue (dimensionless)

$$fcnratio = actmic1\ NC / (actmicNC + 0.044) \quad (6\text{-}8)$$

where:

actmic1 NC = N:C ratio of active microbial biomass associated with plant residue

0.044 = N:C ratio of active microbial biomass associated with plant residue when uptake is half of maximum (g N g^{-1}C)

PHO Submodel for Plant Residue Decomposition

In the original version of Phoenix (McGill et al., 1981), separate algorithms were included for fungi and bacteria (=bacteria + actinomycetes). In order for the PHO submodel to 'connect' to the base model, fungi and bacteria were combined assuming a 4:1 ratio of fungal biomass:bacterial biomass (g C m^{-2}) (McGill et al., 1981, p.86). PHO partitions plant residues into two functional components: a metabolic component which mineralizes or decomposes rapidly, and a structural component which is more resistant to decomposition due to lack of N, chemical recalcitrance, or enzymatic inhibition (Figure. 6-1). The metabolic component is considered to contain DNA, RNA, small molecules, and most of the enzymes and therefore, the C:N ratio of this component is set at 5. The structural component is considered to contain cellulosic and lignified structures plus cell walls and some exo-cellular polysaccharides and has a C:N ratio of 150. The fraction of plant residue C which is structural (F_s) and that which is metabolic (1 - F_s) is calculated from the C:N ratio of the original plant residue by:

$$F_s = (1/\text{plant CN} - 1/5) / (1/150 - 1/5) \quad (6\text{-}9)$$

where:

plant CN = C:N ratio of original plant material (g C g^{-1}N)

5 = C:N ratio of metabolic component (g C g^{-1}N)

150 = C:N ratio of structural component (g C g^{-1}N)

The metabolic component is considered to be in soil solution and, therefore, microbial uptake of metabolic C (g C Mg^{-1}soil h^{-1}) follows Michaelis-Menten kinetics:

$$\text{Umet C} = 0.18 * \text{Tmic C} * [\text{met C}] / (92 + [\text{met C}]) * \text{ftg} \quad (6\text{-}10)$$

where:

0.18 = maximum uptake rate of metabolic component (h^{-1})

Tmic C = total microbial biomass C (g C Mg^{-1}soil)

[met C] = aqueous concentration of metabolic C (g C $Mg^{-1}H_2O$)

92 = [met C] when uptake is half of maximum (g C $Mg^{-1}H_2O$)

ftg = Arrhenius temperature function for growth-related processes (dimensionless)

Metabolic C in solution may undergo adsorption (g C Mg^{-1}soil h^{-1}) to become part of the adsorbed soil component:

$$\text{Amet C} = 0.044 * [\text{met C}] * \text{soil } H_2O * \text{ftg} \quad (6\text{-}11)$$

where:

0.044 = rate constant for adsorption of plant metabolic component (h^{-1})

soil H_2O = gravimetric soil moisture (Mg H_2O Mg^{-1}soil)

ftg = Arrhenius temperature function for growth-related processes (dimensionless)

Decomposition products of the structural component are either assimilated by microbes (97.5%) or undergo 'humadification' and are transferred to the adsorbed soil component (2.5%). Decomposition of structural C (g C Mg^{-1}soil h^{-1}) follows first order kinetics:

$$\text{Dstr C} = 0.0083 * \text{Tmic C} * \text{fcnratio} * \text{fdstr C} * \text{ftg} \quad (6\text{-}12)$$

where:

0.0083 = maximum decomposition rate of structural component (h^{-1})

fdstr C = density function relating total microbial biomass to the quantity of structural plant material (dimensionless)

$$\text{fdstr C} = 1 / \{1 + 13.27 (\text{Tmic C} / \text{str C})^{1.44}\} \quad (6\text{-}13)$$

where:

str C = structural C (g C Mg^{-1}soil)

13.27 = K_1 value for top 14 cm of soil (dimensionless), see Appendix A

1.44 = K_2 value for top 14 cm of soil (dimensionless), see Appendix A

VER Submodel for Plant Residue Decomposition

VER (Verberne et al., 1990) partitions plant residues into three components: a decomposable component representing carbohydrates and proteins, a structural component representing cellulose and hemicellulose, and a resistant component representing lignified structural material (Figure 6-1). The partitioning of plant residue among the components is based on the C:N ratio of the original plant residue and is presented as a graphical relationship. Each component has a constant C:N ratio: 6 for decomposable, 150 for structural, 100 for resistant and decomposes by first order kinetics. Decomposable and structural materials are transferred to microbes, while the resistant fraction is directly incorporated into the soil organic matter. Microbial uptake of decomposable C (g C Mg^{-1}soil h^{-1}) is independent of microbial biomass and is calculated by:

$$Udec\ C = 0.0093 * dec\ C \qquad (6\text{-}14)$$

where:

0.0093 = specific rate of uptake of decomposable C (h^{-1})

dec C = decomposable C (g C Mg^{-1}soil)

The microbial uptake of structural C (g Mg^{-1}soil h^{-1}) is regulated solely by the fraction of resistant material remaining in the plant residues:

$$Ustr\ C = 0.0044^{\{-3.0\ Fres\ C\ (Fstr\ C\ -\ Fres\ C)\}} * str\ C \qquad (6\text{-}15)$$

where:

0.0044 = specific rate of uptake of structural C (h^{-1})

Fres C = fraction of residue C which is resistant (dimensionless)

Fstr C = fraction of residue C which is structural (dimensionless)

str C = structural C (g C Mg^{-1}soil)

The resistant plant residue component is abiotically stabilized (g C Mg^{-1}soil h^{-1}) as active soil organic matter:

$$Sres\ C = 0.00084^{\{-3.0\ Fres\ C\ (Fstr\ C\ -\ Fres\ C)\}} * res\ C \qquad (6\text{-}16)$$

where:

0.00084 = specific rate of stabilization of resistant component (h^{-1})

res C = resistant C (g C Mg^{-1}soil)

Initialization Values

An 81 day laboratory incubation of ^{15}N-labelled pea shoot in two soils provided most of the experimental data for model evaluation. Details of pea growth and soil incubations are given in Chapter 5. Observed variables used for statistical analysis of model output included three replicate measures of biomass N, mineral N, biomass ^{15}N recovery, mineral ^{15}N recovery, and CO_2 evolution.

Soil and plant residue initialization values were required by the models. Soil inputs included total C, initial mineral N, background ^{15}N atom abundance, clay and sand content, gravimetric soil moisture and temperature (Table 6-1). The base model calculates initial microbial biomass C as a fraction of total soil C. When experimentally determined initial values of microbial

biomass C differed from those calculated by the model, adjustments were made to the resistant fractions of the microbial biomass associated with the active and passive soil organic matter. In this way, the active microbial C (= labile biomass C / 0.55) was always initiated as a constant fraction of total soil C. These values allowed the model to be initialized close to equilibrium (R.F. Grant, pers. comm.).

All three plant decomposition submodels required total plant residue C input (196 g C Mg^{-1} soil, calculated as dry mass x C content) and percent ^{15}N atom abundance (11.7%, analytically determined). PHO and VER further required the C:N ratio of the whole plant material (17.13). ECO required the biochemical analysis of the pea shoot. The pea shoot was separated into water-soluble and water-insoluble components, each of which were analyzed for C and N content (details in Chapter 7). The water-soluble component was assumed to contain soluble protein and carbohydrates. Protein was calculated as 6.25 x N and was assumed to be 50% C. The remaining C in the soluble component was assumed to be in the form of carbohydrates. The water-insoluble component was assumed to contain insoluble protein, cellulose and lignin. As for the soluble component, protein C was calculated as 6.25 x N x 50%. Lignin content was analytically determined (Chapter 5) and lignin was assumed to be 50% C. The remaining C was assigned to cellulose. The fraction of plant residue C in each component calculated by this method is shown in Table 6-1.

Further experimental data for model evaluation were taken from Ocio et al. (1991) and from Amato and Ladd (1980). Initialization values are shown in Table 6-1. Observed variables were biomass N and recovery of ^{15}N in biomass. Observed measurements were reported as mean values in both publications and, therefore, the goodness of fit method of model evaluation, which requires replicated data, could not be used. Only the chi-square statistic was used for these data (see 'Statistical Analysis').

Table 6-1. Initialization values for simulations of plant residue decomposition

Variable	Chapter 5 DBC	Chapter 5 GLL	Ocio et al., 1991	Amato and Ladd, 1980
Soil C (g C Mg^{-1} soil)	28200	26000	9000	14500
Biomass C (g C Mg^{-1} soil)	500	390	313[a]	250
Mineral N (g N Mg^{-1} soil)	35	53	2.5	not reported
Clay (%)	19.5	12.5	35	47
Sand (%)	46.3	45.8	10	25
Moisture (Mg H_2O Mg^{-1} soil)	0.29	0.30	0.27	0.18
Temperature (°C)	23	23	25	25
Plant residue	pea shoot	pea shoot	wheat straw	medic leaves
Residue input (g C Mg^{-1} soil)	196	196	4219	806
Residue C:N	17.13	17.13	56	8.7
Residue ^{15}N atom abundance	11.70	11.70	1.24	4.47
Protein[b] (g C g^{-1} C)	0.17	0.17	0.06[c]	0.36[d]
Carbohydrate[b] (g C g^{-1} C)	0.23	0.23	0.25[c]	0.17[d]
Cellulose[b] (g C g^{-1} C)	0.53	0.53	0.55[c]	0.40[d]
Lignin[b] (g C g^{-1} C)	0.07	0.07	0.14[c]	0.07[d]

[a] Assuming biomass C:N = 6.8.
[b] Biochemical components represented as C in each component / total plant residue C.
[c] Fractionation of wheat residue from Broder and Wagner, 1988.
[d] Fractionation of medic residue from Amato et al., 1983.

Statistical Analysis

The goodness of fit method (Whitmore, 1991) was used to evaluate the submodels' ability to simulate values of single variables (microbial biomass N, mineral N, ^{15}N recovery in biomass and mineral N and CO_2 evolution). This method partitions the sum of squares of the differences between measurement and simulation into two components: one calculated from the differences between the simulation and the mean of replicate measurements (lack of fit) and the other calculated from the variance within each set of replicate measurements (pure error). If lack of fit is not significantly larger than pure error then the data present no grounds for rejecting the model (F-statistic). The submodels were ranked with the lowest F_{LOFIT} (= mean square due to lack of fit / mean square due to error) as best fitting.

A further least squares method, χ^2, was used to rank overall performance of the submodels. The standard deviation of each variable was used as a scaling factor to account for

differences in the magnitude of the residuals among variables. The following figure-of-merit function was used (Molina et al., 1990):

$$\chi^2 = (\Sigma_j \Sigma_m [(Y_{jm} - Y_j(m,A))/SD_j]^2)/DF \quad (6\text{-}17)$$

where:

j = state variable index (microbial biomass N, mineral N, ^{15}N recovery in biomass and mineral N and CO_2 evolved)

m = sampling index (1, 2, 12, 22, 40 and 81 days)

Y_{jm} = observed experimental values

$Y_j(m,A)$ = simulated values given the set of model parameters, A

SD_j = standard deviation of the Yj observations (scaling factor)

DF = degrees of freedom

Controversy exists as to what form of experimental data, cumulative[6] or incremental[7], should be used with least-squares methods of model evaluation (Hess and Schmidt, 1995). Therefore, both forms of DBC and GLL data were used for submodel evaluation by the goodness of fit method. For reasons indicated in the 'Discussion', data sets consisting of cumulative values of biomass N, mineral N, ^{15}N recovery in biomass and mineral N, and incremental values of CO_2 evolution were used for submodel evaluation by the chi-square method.

6.3 RESULTS

Observed and simulated values of DBC soil variables in cumulative form are shown in Figure 6-4. Values of two DBC soil variables in incremental form are shown in Figure 6-5. For graphical purposes only, incremental experimental data were transformed to daily rates by dividing the incremental value by the number of days between successive measurements and plotting at the midpoint between the two data collection times. Similar results were observed for DBC and GLL simulations and, therefore, only DBC data are shown. For statistical purposes, incremental experimental data were not transformed to daily rates.

---

[6] cumulative refers to the quantity of a variable present at each sampling date (e.g. total biomass present at time=t).

[7] incremental refers to the change in a variable between successive sampling dates (e.g. change in biomass between t-1 and t).

A

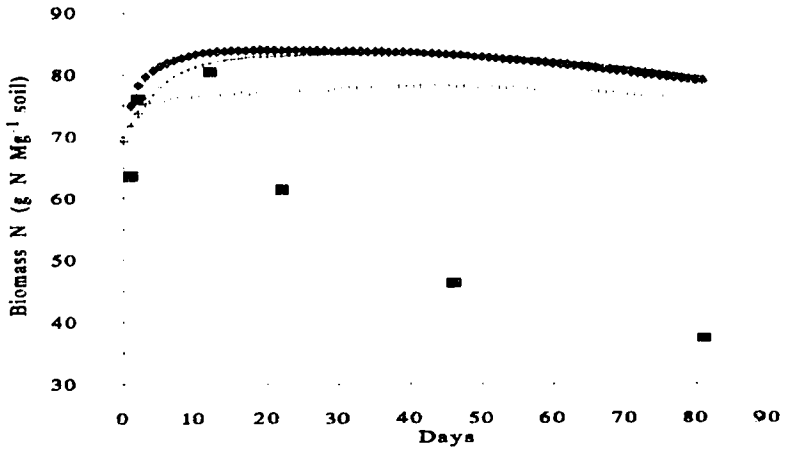
Biomass N (g N Mg-1 soil)
90
80
70
60
50
40
30
0
10
20
30
40
50
60
70
80
90
Days

B

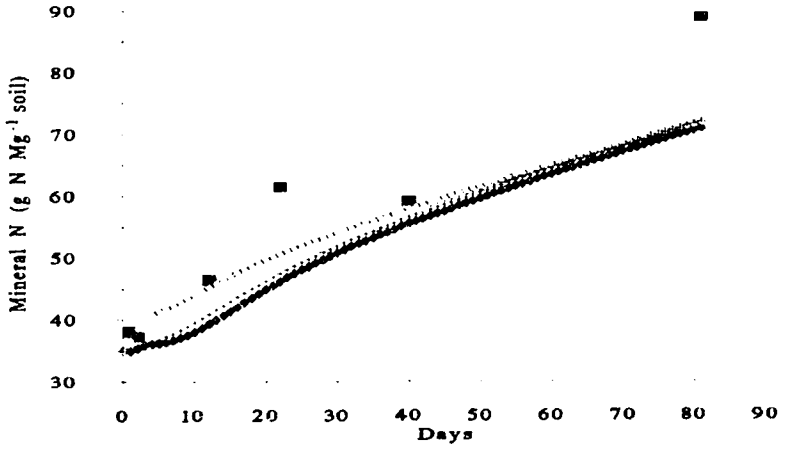
Mineral N (g N Mg-1 soil)
90
80
70
60
50
40
30
0
10
20
30
40
50
60
70
80
90
Days

C

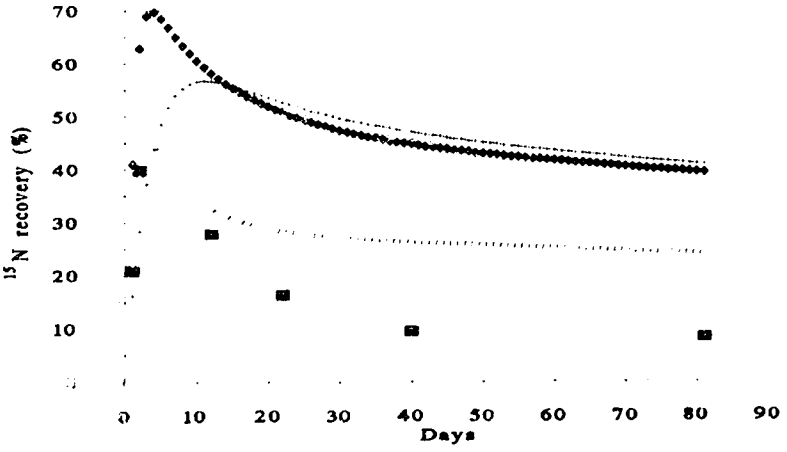
15N recovery (%)
70
60
50
40
30
20
10
0
10
20
30
40
50
60
70
80
90
Days

D

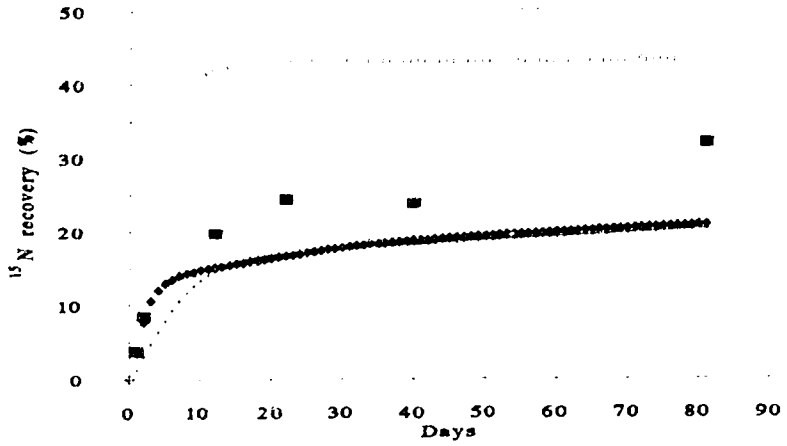

E

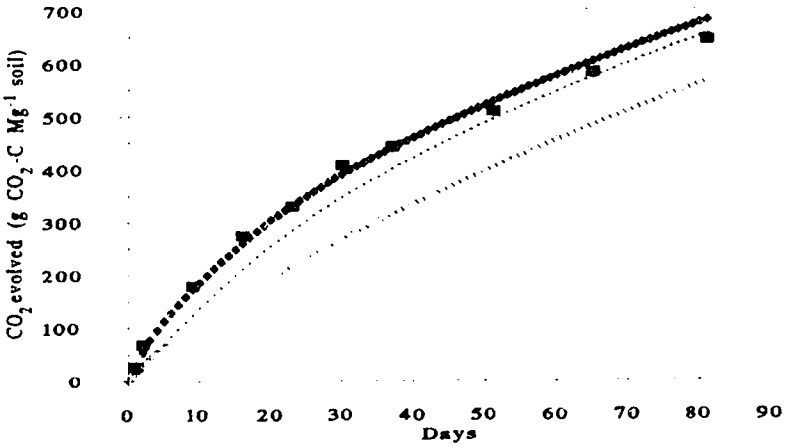

Figure 6-4. Observed (■) and simulated values (◆, ECO; ◇, PHO; +, VER) of (A) microbial biomass N, (B) mineral N, (C) ^{15}N recovery in microbial biomass N, (D) ^{15}N recovery in mineral N and (E) CO_2 evolved from a Dark Brown Chernozemic soil amended with ^{15}N-labelled pea shoots.

A

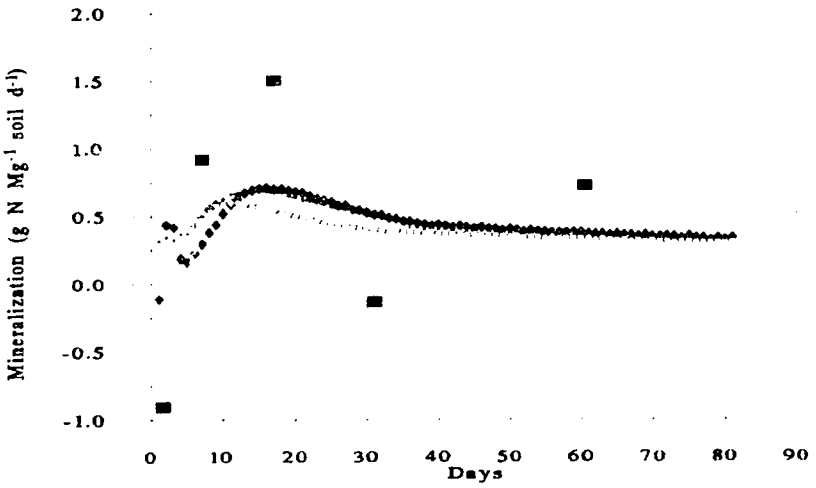

B

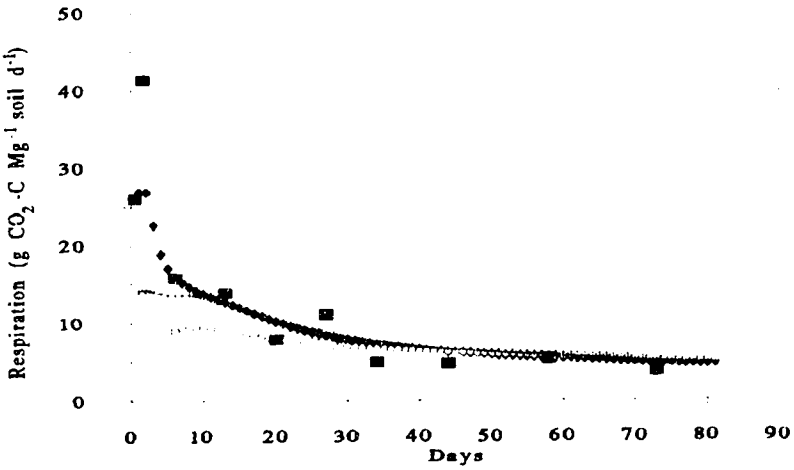

Figure 6-5. Observed (■) and simulated values (◆, ECO; ◇, PHO; +, VER) of (A) N mineralization rate and (B) respiration rate in a Dark Brown Chernozemic soil amended with ^{15}N-labelled pea shoots.

Table 6-2. Goodness of fit method to evaluate submodels (DBC and GLL experimental data)

Soil	Variable	F_{LOFTI} for accumulation			F_{LOFTI} for incremental change		
		ECO	PHO	VER	ECO	PHO	VER
DBC	Biomass N	53	40	53	10	11	11
	Mineral N	8	6	7	2	2	2
	Biomass ^{15}N recovery	74	10	67	1	1	11
	Mineral ^{15}N recovery	17	109	21	2	8	2
	CO_2	1	17	3	4	11	6
GLL	Biomass N	57	42	55	3	3	4
	Mineral N	38	37	36	13	13	13
	Biomass ^{15}N recovery	53	18	62	4	6	16
	Mineral ^{15}N recovery	63	342	74	28	60	31
	CO_2	12	233	59	7	25	13

The lowest F_{LOFTI} indicates the best fitting submodel for either cumulative or incremental change in the given variable.

The decline in biomass N was not well simulated by any of the models (Figure 6-4 (A)). Statistically, PHO best represented the cumulative experimental data and all three submodels were similar in their fit to incremental biomass N data (Table 6-2). Trends in mineral N data were fairly well simulated and all three submodels were statistically similar for both cumulative and incremental data (Figure 6-4 (B); 6-5 (A); Table 6-2). The pattern of ^{15}N recovery in the microbial biomass was simulated by ECO and PHO (Figure 6-4 (C)) and both submodels were statistically similar for incremental data; cumulative data were best represented by PHO (Table 6-2). ECO and VER best represented ^{15}N recovery in the mineral N (Figure 6-4 (D); Table 6-2). Accumulation of and incremental change in CO_2 were best simulated by ECO (Figure 6-4 (E); 6-5 (B); Table 6-2). Tabular F-values ($P<0.05$) with the appropriate degrees of freedom were 3.00 for biomass, mineral N and ^{15}N data and 2.35 for CO_2 data. Comparison of these F-values to F_{LOFTI} values in Table 6-2 indicated that the majority of simulated variables, especially in the GLL soil, were significantly different from observed values suggesting that submodels 'could almost certainly be improved' (Whitmore, 1991).

Observed and simulated cumulative data from Ocio et al. (1991) are shown in Figure 6-6 and observed and simulated cumulative data from Amato and Ladd (1980) are shown in Figure 6-7. The chi-square method was used to rate overall submodel performance for DBC, GLL, Ocio et

al. (1991) and Amato and Ladd (1980) data (Table 6-3). The PHO submodel best fit the experimental data from DBC and GLL soils. ECO best fit data from Ocio et al. (1991) and VER best fit data from Amato and Ladd (1980).

Table 6-3. Chi-square method to rank the submodels' overall correspondence to experimental data

		Chi-square		
Experimental data	Number of variables	ECO	PHO	VER
DBC	5	1.7	1.1	1.6
GLL	5	1.7	1.4	1.8
Ocio et al. (1991)	2	31	39	119
Amato and Ladd (1980)	2	99	23	15

The lowest χ^2 in a row indicates the best fitting submodel for that set of experimental data.

Distinct differences among submodels were observed for simulated values of pea shoot C and N (Figure 6-8). The initial value of residue N was different among submodels. Each submodel calculates the N in various plant components by dividing the C in each component by a constant C:N ratio as described in 'Materials and Methods'. As a result, the amount of simulated pea shoot residue N accompanying the input of 196 g of residue C was 11.10 g N for ECO, 11.45 g N for PHO and 12.56 g N for VER. An obvious change in kinetics was evident in PHO at approximately day 3 when the metabolic component of the residue had been completely decomposed (Figure 6-8). Overall, the disappearance of plant residue C was much slower in PHO compared to ECO and VER. The disappearance of residue N was more rapid in ECO and PHO as compared to VER (Figure 6-8).

The simulated fluxes through various soil components further demonstrated differences among submodels (Figure 6-9; Table 6-4). PHO had the slowest overall rate of decomposition with the largest amounts of ^{14}N and ^{15}N remaining in the residue by day 81. PHO had consistently the smallest amount of ^{14}N entering (flux 2 + flux 3 + flux 6) and leaving (flux 4 + flux 5) the microbial biomass while VER had the largest amount of ^{15}N entering and leaving the microbial biomass. The submodels were similar in ^{14}N mineralized (flux 5), but PHO had greater ^{15}N mineralized. ECO had greater ^{14}N immobilization (flux 6); ^{15}N immobilization was similar among submodels.

A

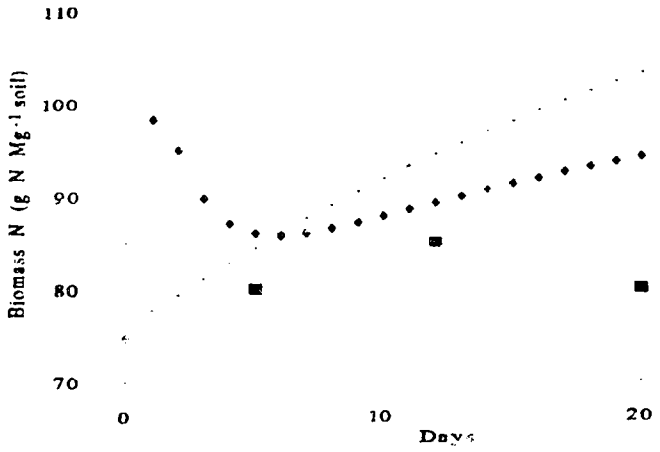

B

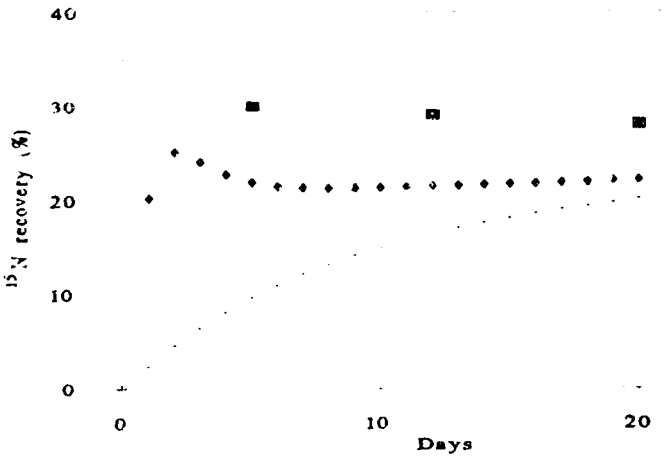

Figure 6-6. Observed (■) and simulated values (◆, ECO; ◇, PHO; +, VER) of (A) microbial biomass N and (B) ^{15}N recovery in microbial biomass N of a silty clay loam soil amended with ^{15}N-labelled wheat straw. Observed data from Ocio et al. (1991).

A

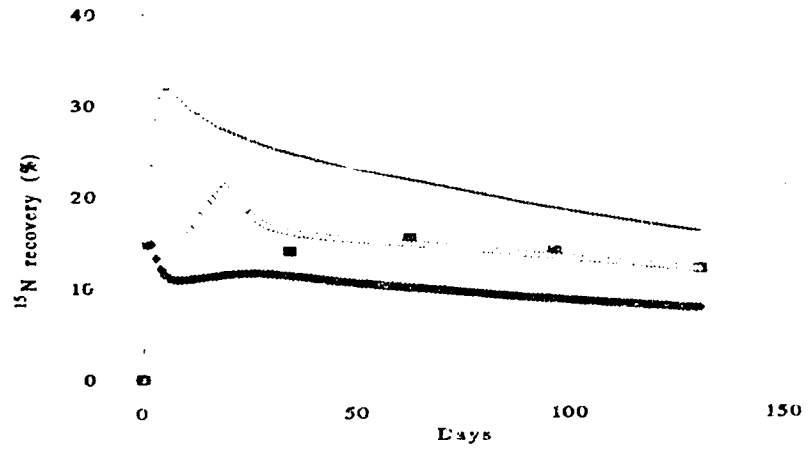

B

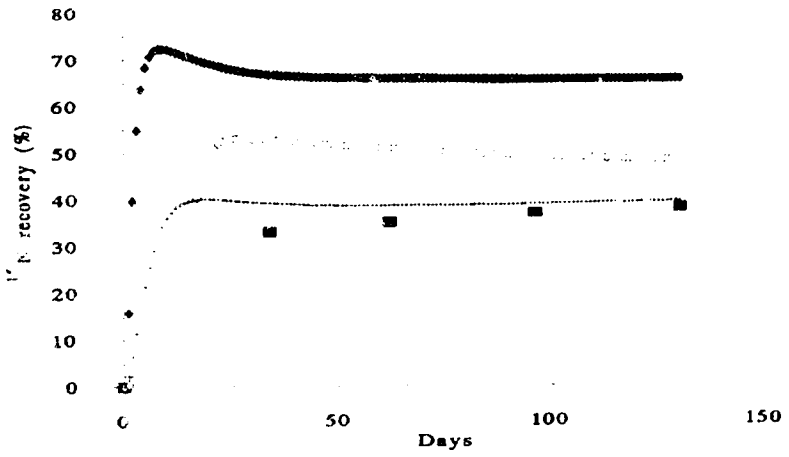

Figure 6-7. Observed (■) and simulated values (◆, ECO; ◇, PHO; +, VER) of (A) ^{15}N recovery in microbial biomass N and (B) ^{15}N recovery in mineral N of a vertisol amended with ^{15}N-labelled medic leaves. Observed data from Amato and Ladd (1980).

A

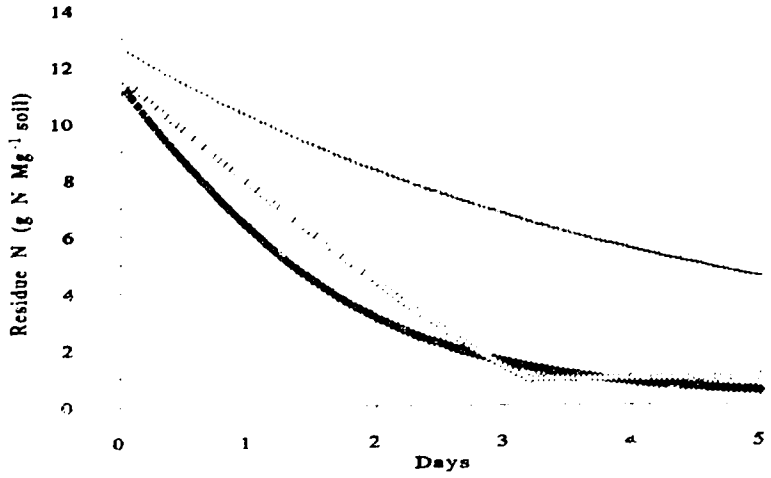

B

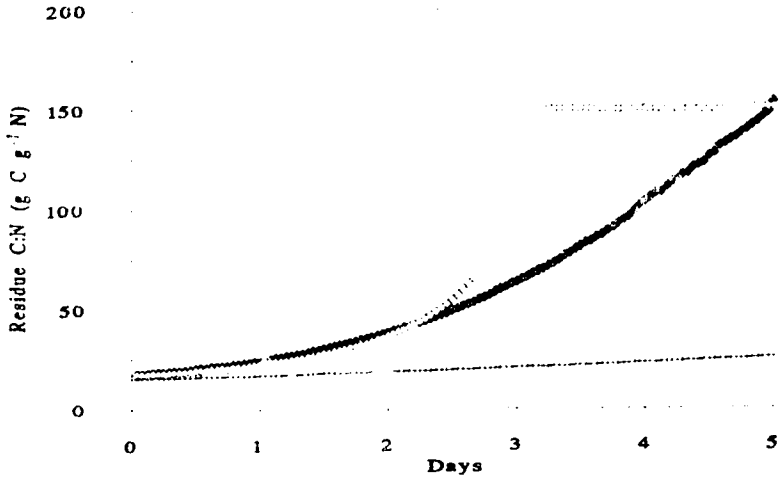

Figure 6-8. Simulated values (◆, ECO; ◇, PHO; +, VER) of (A) N remaining in plant residue and (B) C:N ratio of remaining plant residue during first 5 days of simulated incubation of a Dark Brown Chernozemic soil amended with ^{15}N-labelled pea residue.

Figure 6-9. Schematic of simulated N fluxes (see Table 6-4). 'Soil organic matter' represents soluble, adsorbed, active and passive organic matter and 'microbial biomass' represents both live and inactivated biomass.

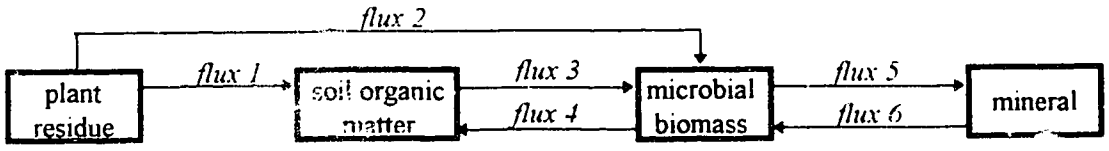

Table 6-4. Comparison of simulated N fluxes after 81 days (g N Mg^{-1} soil)

Isotope	Submodel	Residue[a]	Flux 1	Flux 2	Flux 3	Flux 4	Flux 5	Flux 6
				DBC soil				
^{14}N	ECO	0.0	9.8	----[b]	161	118	40	4.4
	PHO	0.6	0.1	9.4	140	108	38	2.3
	VER	0.1	0.1	10.9	152	118	39	2.8
^{15}N	ECO	0.00	1.30	----	2.68	1.69	0.43	0.03
	PHO	0.08	0.01	1.25	1.17	1.35	0.74	0.03
	VER	0.02	0.01	1.44	1.54	1.91	0.45	0.02
				GLL soil				
^{14}N	ECO	0.0	9.8	----	169	115	43	4.4
	PHO	0.6	0.1	9.4	145	105	40	2.1
	VER	0.1	0.1	10.9	159	114	42	2.5
^{15}N	ECO	0.00	1.30	----	2.84	1.71	0.51	0.03
	PHO	0.08	0.01	1.25	1.33	1.40	0.79	0.02
	VER	0.02	0.01	1.44	1.74	1.96	0.53	0.02

[a] N remaining as plant residue
[b] Pathway not represented in submodel

C mineralized in response to amendment ($CO_{2amended}$ - $CO_{2non\text{-}amended}$) was greater in simulations compared to observed values (Table 6-5). In contrast, N mineralized in response to amendment was less in simulations compared to observed values.

Table 6-5. Mineralization response to amendment with pea shoot at 81 days

Submodel	% of added C mineralized		% of added N mineralized	
	DBC	GLL	DBC	GLL
Observed	78	60	236	201
ECO	148	162	90	124
PHO	89	97	95	115
VER	135	147	88	114

6.4 DISCUSSION

Statistical Assumptions

In developing kinetic models, parameter values must be estimated such that equations represent the processes under study. Functions which best represent biological behavior are often non-linear with respect to their parameters[8] (Robinson, 1985) and require non-linear parameter estimation techniques. Commonly, least-squares techniques are used which involve minimizing some objective function such as the residual sum of squares (Robinson, 1985) or chi-square (Molina et al., 1990). Similarly, models can be ranked in terms of these functions: the lower the value of the function, the better the fit of the model to the experimental data. Assumptions implicit in least-squares analysis are that all errors associated with the experimental data are independent, are normally distributed and have a constant variance (Ott, 1984). This implies that the data themselves must also be independent. As a result, strong argument exists against the use of cumulative data and the integrated form of equations to obtain parameter estimates (Hess and Schmidt, 1995; Ellert and Bettany, 1988). For example, Hess and Schmidt (1995) compared the fit of cumulative CO_2 data to a model in integral form to the fit of discrete (incremental) CO_2 data to the same model in differential form. The use of the integral model and cumulative data produced correlated residuals and, therefore, violated the assumptions implicit in least-squares analysis. Furthermore, integral

[8] non-linear with respect to parameters refers to the non-linear response in a variable when a parameter is changed in a linear fashion.

models fit to cumulative data gave low values of the standard deviation associated with each parameter estimate thus 'giving the researcher a false sense of security' (Hess and Schmidt, 1995). They concluded that analyses of CO_2 evolution data are only statistically valid when discrete, independent data and differential model forms are used.

This raises the question: what constitutes independent data? Studies of biological processes often involve collecting data in time series and these types of data are often correlated. Most would agree that cumulative CO_2 data are not independent. A large value early in the time-sequence increases the value of all subsequent data points. This type of correlation is the result of the form in which data are presented (cumulative vs incremental). Repeated measures on the same sample over time (such as mycelial mass determined from the same fungal sample at daily intervals) are also not independent, especially if measurements are taken close together (Gurevitch and Chester, 1986). This type of correlation occurs because the characteristics of a single sample do not change randomly but are linked to characteristics earlier in time. Independent data, therefore, must be independent both in form of presentation and in sampling technique. Because components of complex systems, such as soil, are interrelated in space and time, is it ever possible to collect independent time series data from such a system? Consider, for example, microbial biomass in response to incubation. Two subsamples are taken from a homogenous soil sample and are incubated under identical conditions. Microbial biomass is destructively measured in sample A on day 1 and in sample B on day 2. Are these data independent? I would argue that, because the experimental units (sample A and B) are physically separate, these data can be considered independent. However, had the initial larger soil sample been incubated and then subsamples taken for biomass analysis on days 1 and 2, then the biomass data would not have been independent.

For successively measured variables such as CO_2 evolution, incremental data have been suggested to comply with the assumptions underlying least-squares analysis (Hess and Schmidt, 1995; Ellert and Bettany, 1988). Incremental data are not, however, necessarily independent. For example, consider a single soil sample which is incubated together with a substrate. Incremental CO_2 evolution is determined every hour. Biomass increases in response to the substrate and, therefore, assuming constant or increasing activity (CO_2 per unit biomass C), more CO_2 is evolved between hour 2 and 3 compared to that evolved between hour 1 and 2. I would argue that these data, although incremental, are not independent. The incremental form of these data is, however, more appropriate for least-squares analysis than the cumulative form.

I concluded that the most appropriate experimental data to use for submodel evaluation by least-squares analysis were the cumulative values of biomass N, mineral N, ^{15}N recovery in biomass and mineral N (as determined on days 1, 2, 12, 22, 40 and 81) and the incremental values of CO_2 evolved (10 increments between 0 and 81 days as reported in 'Materials and Methods'). In addition to the arguments given above, using different forms of these data is further supported by the nature of the variables. Biomass N and mineral N are in continuous flux with each other and with the rest of the soil environment and, therefore, the mass of microorganisms or the amount of mineral N at a given time is the net result of a number of processes. In contrast, CO_2 is removed from the soil system and is, therefore, a gross measure and qualitatively distinct from dynamic variables such as biomass N or mineral N. It should be noted that mineral N was determined by destructive sampling. Had mineral N been measured by successive leaching from the same samples, as was the case with Ellert and Bettany (1988), then incremental data would have been more appropriate for statistical analysis.

Data generated by simulation models are not independent over time. Firstly, equations are in the integral form (Euler's method of integration used in Stella II):

$$\text{variable}_t = \text{variable}_{t-dt} + dt * \text{flows} \qquad (6\text{-}18)$$

where variable_t = value of variable at time t, variable_{t-dt} = value of variable at previous time-step and flows = positive or negative change in the variable over time. Secondly, simulated data have no associated error terms. Independence among error and, therefore, among data, cannot be tested. Consequently, both the cumulative and incremental forms of simulated data are equally valid. The independence of experimental data must, therefore, be confirmed and the independent form compared to the appropriate simulated output for least-squares analysis. Because simulated data have no associated error, I have not found an objective means of comparing models without evaluating each against experimental data.

Classically, the chi-square method is used for analyzing categorical data (Ott, 1984). For example, 100 soil samples could be categorized into 2 groups: those with pH>7and those with pH<7. Assume, from previous experience, 25% of the samples are expected to fall into the pH>7 category. The chi-square statistic tests the null hypothesis that the number of samples observed in each category is the same as the number expected. The expression $(Ob - Ex)^2/Ex$, where Ob is the observed value for each category and Ex is the corresponding expected value, is calculated for each category. These quotients are summed over all categories to determine χ^2. Molina et al. (1990) suggest a modified chi-square statistic for analyzing the goodness of fit between simulated data and

experimental data. For this analysis, simulated data represent observed values and experimental data represent expected values. Time represents the categories into which the data fall. Two questions arise: first, is it valid to use the value of an observed or simulated data point (e.g. 10 g biomass N Mg^{-1}soil) in place of a count of the number of samples fitting into a category and second, is it valid to segment a continuous variable such as time into discrete categories? I would suggest that the modified chi-square statistic is valid for ranking alternate models in terms of correspondence between experimental and simulated data. The modified chi-square should not, however, be confused with the classical chi-square, nor should it be compared to tabulated critical values of χ^2. Molina et al. (1990), in fact, do not use chi-square as a means of testing hypotheses but rather as a least squares function to be minimized for parameter optimization.

The Quality of Data

Quantitative methods of evaluating simulation models are only as good as the experimental data allow. Ideally, experimental values for all variables in a system and their dynamics over short intervals should be collected for model evaluation. Because this is not feasible, experiments must be designed to best distinguish among alternate hypotheses (models). Although correlation between simulated output and experimental data is not proof of correlation to actual mechanisms, the more specific the data, the better the chances of falsifying a hypothesis. Consequently, ^{14}C and ^{15}N tracer data are particularly useful because isotopic data can identify pathways of elemental movement and quantify gross rates of transfers or transformations (Nason and Myrold, 1991). This is true over the short-term only as over long periods, isotopes equilibrate with all parts of the system through which they circulate.

Timing of observations is also critical. Most measurements should be taken when the experimental system is actively responding to perturbation. Estimates of the half-lives of plant residue carbohydrates in soil range between 0.69 - 3.5 days for the easily decomposable fraction and between 6.9 - 69 days for the more slowly decomposable fraction (Juma and Paul, 1981; McGill et al., 1981; Vanbuuge et al., 1990). I, therefore, expected to monitor initial rapid decomposition between days 1 and 3 and slower decomposition between days 12 and 40. In retrospect, more measurements should have been made in the first 10 days of incubation as this is the time when differences among the submodel simulations of ^{15}N dynamics were most evident. Later in the simulations, the influence of the plant decomposition submodel was overshadowed by the base

model and variables began to converge. Simulated values of integrated variables, such as mineral N, N mineralization rate and respiration rate converged by approximately day 45 of the simulation.

Submodel Hypotheses

Developing simulation models to describe plant residue decomposition in soil is problematic because the loss of original plant material cannot be directly measured in soil. Two methods used to overcome this problem are: (1) regression analysis on the C mineralization curve (where rate of mineralization is considered equal to rate of decomposition) and (2) the calculation of microbial growth on residues (Juma and McGill, 1986). Regression analysis yields information on the number of components involved and specific rate constants but does not yield information on mechanisms of transformation. This type of analysis can be used to develop decomposition equations as used in the VER submodel which are based on the assumption that the concentration of the substrate rather than the biological capacity is rate-limiting (Verberne et al., 1990).

Calculation of microbial growth yields information on total decomposition and the formation of microbial material. Both ECO and PHO explicitly represent the activities of soil microorganisms in the decomposition process. ECO partitions residues into biochemical components, each of which is assigned a specific decomposition rate and efficiency of utilization. This approach does not take into account that chemically homogeneous components (e.g. cellulose) may have different kinetics due to chemical and/or physical stabilization with other plant or soil components. The functional approach in PHO is based on observations of similar decomposition dynamics among labile fractions of various materials and among recalcitrant fractions of various materials (Hunt, 1977) (Wieder and Lang, 1982). A problem with this approach is that rate constants for the transformation of functional components are difficult to determine experimentally because these components are chemically heterogeneous and cannot be physically isolated.

Submodel Evaluations Based on DBC and GLL Soil Data

According to the F_{LOFIT} statistic, almost all simulated variables were significantly different from observed data. This indicates that mechanisms described in the models are not flexible enough to allow the models to function under conditions different from those used to calibrate them. The short-coming may be in the base model or in the submodels or perhaps both. A comparison of submodels was still informative, however, because the importance of the plant residue decomposition submodel to the behavior of soil variables in the short-term was verified.

None of the submodels simulated the decline in biomass N (Figure 6-4 (A)). This was most likely the result of model initialization procedures as outlined above in 'Initialization Values.' Experimentally determined biomass C was 500 g Mg^{-1}soil for the DBC soil. Based on total soil C, however, the base model initialized microbial C at 251 g Mg^{-1}soil. The remainder of experimentally determined microbial biomass was simulated as resistant biomass associated with the active and passive soil organic matter. Consequently, the ratio of resistant:labile biomass was approximately 22. In contrast, the base model initializes this ratio at approximately 11. The resistant biomass is slower to decay under limiting environments and, therefore, overall microbial biomass remained fairly constant.

The microbial biomass is the earliest stage of the transformation process in which plant-derived compounds can be distinguished from the rest of the soil organic matter and, therefore, the recovery of plant-derived ^{15}N in the biomass is the most sensitive variable for detecting differences in residue decomposition dynamics. Experimentally, more than 20% of pea-derived ^{15}N was recovered in the microbial biomass on day 1 and approximately 40% on day 2 (Figure 6-4 (C)). Simulated data also indicate a rapid uptake of plant ^{15}N with recoveries between 16-30% on day 1 and 28-59% on day 2. Statistically, PHO best simulated the recovery of ^{15}N in the biomass (Table 6-2). In this submodel, 73% of pea shoot C was partitioned as structural and the remaining 27% as metabolic (equation (6-9)). With set C:N ratios of 150 for the structural component and 5 for the metabolic component, 8% of total N was partitioned as structural and 92% as metabolic. Consequently, the vast majority of N was quickly available to microbes. PHO was developed with an emphasis on the physiological response of microorganisms to substrate and environment. I would speculate that this emphasis gave PHO an advantage over the other two submodels in terms of simulating substrate availability to microorganisms. PHO, however, overestimated the ^{15}N recovery in mineral N (Figure 6-4 (D)). The high values were the result of rapid N mineralization in the first 3 or 4 days as the microbial biomass compensated for the influx of residue material with a C:N ratio of about 5. In the models, the microbial C:N ratio is maintained at 4.5 for labile biomass and 7.5 for resistant biomass by transferring excess N to the mineral pool (Appendix A). Experimentally, a range of biomass C:N ratios in response to substrate have been reported (Voroney and Paul, 1984)

ECO and VER both had overall greater recovery of ^{15}N in the biomass and lower recovery in the mineral component compared to PHO (Figure 6-4 (C, D)). More plant residue C entered the biomass than the residue N (C:N approximately 10) and, therefore, the biomass 'grew' and

retained more ^{15}N. Readily available C resulted in the early peak in respiration rate giving ECO the best fit to respiration data (Figure 6-5 (B)).

Examining experimental data for the first 2 days of the incubation, the C:N ratio of immediately available substrate can be estimated. The 40% recovery of residue-derived ^{15}N in the biomass on day 2 (Figure 6-4 (C)) represents approximately 4.6 g of residue N Mg^{-1}soil. Cumulative CO_2 over this period was 70 g C Mg^{-1}soil (Figure 6-4 (E)). Assuming a C utilization efficiency of 60%, a total of 70/0.40 or 175 g C Mg^{-1}soil would have been processed by microorganisms. These calculations indicate that the C:N ratio of available substrate was approximately 175:4.6 or 38. This may explain the net immobilization of N observed prior to day 2 (Figure 6-4 (B)). In contrast, simulated substrate C:N ratios ranged from 5 to 10.

On day 2 of the DBC soil incubation, approximately 50% of pea shoot ^{15}N was recovered in the microbial biomass and mineral soil fractions (Figure 6-4 (C, D)). This indicates that at least 50% of plant residue N had been decomposed. Simulated values from ECO and PHO also indicated that more than 50% of N had been transferred out of the residue pool by day 2 (Figure 6-8 (B)). Both of these submodels employ Michaelis-Menten kinetics for the uptake of readily available soluble compounds (equations (6-7) and (6-10)). The first order kinetics used in VER were too sluggish to accurately represent this phenomenon (equation (6-14)).

An abrupt change in the rate of residue C and N decomposition was evident in PHO at approximately day 3 when the metabolic component of the residue was exhausted and kinetics switched from mainly Michaelis-Menten to exclusively first order (equation (6-12)). This exemplifies the difference between the functional and biochemical approach to decomposition. ECO simulates a more gradual change in residue C and N which is more in keeping with typical decomposition curves (Paul and Clark, 1989) and the general concept of decomposition as a continuum (Bosatta and Agren, 1985).

In PHO, most of the simulated C in pea shoots was partitioned as structural and decomposed very slowly in contrast to the rapid disappearance of C as simulated by ECO (Figure 6-8 (A)). From an incubation of ^{14}C-labelled medic leaves in soil, Amato and Ladd (1980) reported that, by day 34, 51% of medic-derived ^{14}C had been respired. In a similar experiment, 70% of medic-derived ^{14}C had been respired after 140 days. Residual ^{14}C remaining in the soil may have been in the form of non-decomposed plant residues and/or microbially 'processed' organics. In either case, this experimental evidence suggests that PHO's simulated decomposition of residue C

is unrealistically slow. Whether ECO's simulated C decomposition is too rapid cannot be ascertained from these experimental data.

Submodel Evaluations Based on Data From the Literature

All three submodels overestimated biomass N following addition of wheat straw (Figure 6-6 (A)). An assumption in the base model is that incoming plant residues have an associated biomass: additional labile biomass C is set at 0.02 * residue C and additional resistant biomass C is also set at 0.02 * residue C. Therefore, the simulated 4219 g residue C Mg^{-1}soil would bring with it approximately 84 g labile biomass C Mg^{-1}soil (C:N = 4.5) and 84 g resistant biomass C Mg^{-1}soil (C:N = 7.5) and a total of 30 g biomass N Mg^{-1}soil. The simulation models were initialized with biomass N values of 46 g N Mg^{-1}soil as reported by Ocio et al. (1991) for non-amended soils, however, with the large input of biomass associated with the wheat straw, the biomass N immediately increased to almost 75 g N Mg^{-1}soil. The quantity of biomass C added to the soil with large inputs of residue C may require re-evaluation.

The initial burst of biomass N simulated by ECO (Figure 6-6 (A)) was in response to readily available proteins. Because the proteins accounted for only 6% of the total wheat straw C (Table 6-1), N quickly became limiting and the biomass declined. By day 5, more slowly decomposing residues sustained a gradual increase in biomass N. In contrast to the simulated overestimation of biomass N, simulated values of ^{15}N recovery in the biomass were lower than observed values in all three submodels (Figure 6-6 (B)). The duality in dynamics of overall biomass N and biomass ^{15}N is further evidence in support of isotopic data to discern among processes in integrated systems

Simulation of ^{15}N in the microbial biomass following soil incubation with labelled medic leaves indicated a peak in ^{15}N recovery prior to the first experimental data point at 34 days (Figure 6-7 (A)). In their publication, Amato and Ladd (1980) show a graph of their observations similar to Figure 6-7 (A). In their graph, however, the data points are joined with the line beginning at 0% ^{15}N recovery at day 0. As a result, Amato and Ladd (1980) report that the peak recovery of ^{15}N in the biomass occurred at 62 days. This representation of the data is misleading in two ways: firstly, data points in time-course graphs should not be joined because the points do not necessarily represent the trends of the variables between observations. Secondly, the observations were not well timed. The medic leaves were a readily available source of N for the soil microorganisms and maximum recovery of ^{15}N in the biomass should have been expected much sooner than 34 days. In

the present study, approximately 40% of pea-derived ^{15}N was recovered in the DBC biomass after only 2 days (Figure 6-4 (C)). These data emphasize the importance of appropriate timing when measuring dynamic variables

ECO simulated a rapid mineralization of ^{15}N and an accompanying low recovery in biomass (Figure 6-7). Protein and carbohydrates were readily available from the medic leaves. Protein, however, made up the majority of the initial substrate (36% of medic C compared to 17% of medic C as carbohydrate (Table 6-1)) resulting in an over abundance of N. Hence, the rapid N mineralization.

Mineralization Response to Amendment

Experimental CO_2 evolved in response to amendment over 81 days was equivalent to 60-78% of C added residue (Table 6-5). Bremer et al. (1991) also reported 60% of lentil green manure C recovered over 100 days of incubation in soil. With the exception of PHO, all the submodels simulated a greater mineralization of C than could be accounted for by the added plant residue which would suggest that pulsed residue additions result in an overall decrease in soil organic C (Table 6-5). This is contradictory to current soil conservation strategies which recommend incorporating crop residues to increase soil organic matter. Some observations do, however, suggest that plant residue additions increase CO_2 evolution from indigenous sources (Parnas, 1975). Dalenberg and Jager (1989) postulated that this 'priming effect' was caused by an enhanced turnover of C in the microbial biomass. The positive priming effect caused by ryegrass incubating in soil, however, could not be explained by changes in the size of the native biomass and it was suggested that ligninases and cellulases produced by the microorganisms degrading the ryegrass also decomposed some of the native soil organic matter (Wu et al., 1993). In the simulation data, the biomass increased in response to residue additions and, because decomposition of soil active and passive organic matter in the base model is a function of active biomass C, the rate of mineralization of these soil pools was increased. As noted, the models overestimated biomass and, apparently, overestimated C mineralization as well.

As discussed in Chapter 5, pea residue additions caused an apparent increase in the mineralization of native soil N in both DBC and GLL soils. Simulated data, however, indicate only a slight increase in N mineralization in the GLL soil (Table 6-5). This soil had a smaller biomass and, therefore, less N was required for cell growth and maintenance. Examining N fluxes, the GLL biomass had a greater influx of N from soil organic matter compared to the DBC biomass. This

may be the influence of clay content: the GLL soil had less clay and, therefore, less of the inactivated microbial cells would be stabilized. Instead, these materials would be readily available for microbial uptake from the soluble pools. Greater internal N cycling would result in a greater rate of N mineralization

Conclusion

Rigorous guidelines for evaluating simulation models have not been established. The procedure involves more than statistically quantifying differences between observed and simulated variables. Even for this task, certain statistical assumptions must be satisfied: independent experimental data, for example. Time series data collected from integrated biological systems are often correlated and the question remains as to what constitutes truly independent data. Because data sets for model evaluation commonly consist of relatively few measured variables, the sensitivity and timing of measurements are critical. Isotopic data and short intervals between measurements at a time when the system is actively responding to perturbation are most informative. More credit should be given to models which accurately simulate the most sensitive variables in the process under study. Examining plant residue decomposition, for example, ^{15}N recovery in biomass was the most sensitive variable. Unfortunately, too few measurements were taken in the first few days of residue decomposition to accurately distinguish whether plant decomposition submodels were statistically valid or not.

In addition to quantitative considerations, conceptual integrity should also be evaluated. To what extent does a model mechanistically represent the natural system? Finally, there are practical considerations such as model accessibility. Questions such as, 'Is the model user-friendly and well documented?' or, 'How much computing power is required to run the model?' are valid factors in evaluating a simulation model.

In my evaluation of three plant residue decomposition submodels, I confirmed that simulated dynamics of plant-derived N within the microbial and mineral soil fractions were sensitive to structural and kinetic differences among submodels. The initial rapid microbial assimilation of residue N observed experimentally was also evident in simulated data and appeared to be best represented by Michaelis-Menten kinetics. Overall, however, the models appeared more sluggish than the natural system. Simulated CO_2 evolution suggested that pulsed addition of readily decomposable residues to soil increases the mineralization of indigenous soil C. Although this

phenomenon was not supported by the DBC and GLL experimental data, it has been previously reported and may be the result of increased enzymatic activity following microbial 'priming'

6.5 LITERATURE CITED

Amato, M. and Ladd, J N. 1980. Studies of nitrogen immobilization and mineralization in calcareous soils. V. Formation and distribution of isotope-labelled biomass during decomposition of ^{14}C- and ^{15}N-labelled plant material. Soil Biol. Biochem. 12:405-411.

Amato, M., Jackson, R.B., Butler, J.H.A. and Ladd, J.N. 1983. Decomposition of plant materials in Australian soils. I. Residual organic ^{14}C and ^{15}N from legume plant parts decomposing under field and laboratory conditions. Aust. J. Soil Res., 21:563-570.

Rosatta, E. and Agren, G.I. 1985. Theoretical analysis of decomposition of heterogeneous substrates. Soil Biol. Biochem. 17:601-610.

Bremer, E., van Houtum, W. and van Kessel, C. 1991. Carbon dioxide evolution from wheat and lentil residues as affected by grinding, added nitrogen, and the absence of soil. Biol. Fertil Soils 11:221-227.

Broder, M.W. and Wagner, G.H. 1988. Microbial colonization and decomposition of corn, wheat, and soybean residue. Soil Sci. Soc. Am. J. 52:112-117.

Dalenberg, J.W. and Jager, G. 1989. Priming effect of some organic additions to ^{14}C-labelled soil Soil Biol. Biochem. 21:443-448.

Ellert, B.H. and Bettany, J.R. 1988. Comparison of kinetic models for describing net sulfur and nitrogen mineralization. Soil Sci. Soc. Am. J. 52:1692-1702.

Grant, R.F., Juma, N.G. and McGill, W.B. 1993. Simulation of carbon and nitrogen transformations in soil: mineralization. Soil Biol. Biochem. 25:1317-1329.

Gurevitch, J. and Chester, S.T. Jr. 1986. Analysis of repeated measures experiments. Ecology 67:251-255.

Hess, T.F. and Schmidt, S.K. 1995. Improved procedure for obtaining statistically valid parameter estimates from soil respiration data. Soil Biol. Biochem. 27:1-7.

High Performance Systems. 1994. Stella II Technical Documentation. High Performance Systems, Inc., Hanover, NH.

Hunt, H.W. 1977. A simulation model for decomposition in grasslands. Ecol. 58:469-484.

Hunt, H.W. and Parton, W.J. 1986. The role of modeling in research on microfloral and faunal interactions in natural and agroecosystems. Pages 443-494 *in* M.J. Mitchell and J.P. Nakas, eds. Microfloral and Faunal Interactions in Natural and Agro-ecosystems. Martinus Nijhoff/Dr W. Junk Publishers, Dordrecht, The Netherlands.

Juma, N.G. and McGill, W.B. 1986. Decomposition and nutrient cycling in agro-ecosystems. Pages 74-136 *in* M.J. Mitchell and J.P. Nakas, eds. Microfloral and Faunal Interactions in Natural and Agro-ecosystems. Martinus Nijhoff/Dr W. Junk Publishers, Dordrecht, The Netherlands.

Juma,N.G. and Paul, E.A. 1981. Use of tracers and computer simulation techniques to assess mineralization and immobilization of soil nitrogen. Pages 145-170 *in* M.J. Frissel and J.A

van Veen, eds. Simulation of Nitrogen Behaviour of Soil-Plant Systems. Pudoc, Centre for Agricultural Publishing and Documentation, Wageningen, The Netherlands.

McGill, W.B., Hunt, H.W., Woodmansee, R.G. and Reuss, J.O. 1981. Phoenix-A model of the dynamics of carbon and nitrogen in grassland soils *in* F.E. Clark and T. Rosswall, eds. Terrestrial Nitrogen Cycles. Ecol. Bull. (Stockholm) 33:49-115.

Molina, J.A.E., Hadas, A. and Clapp, C.E. 1990. Computer simulation of nitrogen turnover in soil and priming effect. Soil Biol. Biochem. 22:349-353.

Nason, G.E. and Myrold, D.D. 1991. ^{15}N in soil research: appropriate application of rate estimation procedures. Agric. Ecosystems Environ. 34:427-441.

Ocio, J.A., Martinez, J. and Brookes, P.C. 1991. Contribution of straw-derived N to total microbial biomass N following incorporation of cereal straw to soil. Soil Biol. Biochem. 23:655-659.

Ott, L. 1984. An Introduction to Statistical Methods and Data Analysis. PWS Publishers, Boston, Massachusetts, USA.

Papendick, R.I. and Campbell, G.S. 1981. Theory and measurement of water potential. Pages 1-22 *in* J.F. Parr, W.R. Gardner and L.F. Elliott, eds. Water Potential Relations in Soil Microbiology. SSSA Special Publication No. 9, Madison, WI.

Parnas, H. 1975. Model for decomposition of organic material by microorganisms. Soil Biol Biochem. 7:161-169.

Paul, E.A. and Clark, F.E. 1989. Soil Microbiology and Biochemistry. Academic Press, Inc., San Diego, USA.

Robinson, J. A. 1985. Determining microbial kinetic parameters using non-linear regression analysis: advantages and limitations in microbial ecology. Adv. Microb. Ecol. 8:61-114.

Verberne, E.L.J., Hassink, J., De Willigen, P., Groot, J.J.R. and Van Veen, J.A. 1990. Modelling organic matter dynamics in different soils. Netherlands Journal of Agricultural Science 38:221-238.

Voroney, R.P. and Paul, E.A. 1984. Determination of k_C and k_N *in situ* for calibration of the chloroform fumigation-incubation method. Soil Biol. Biochem. 16:9-14.

Wallach, D. and Goffinet, B. 1989. Mean squared error of prediction as a criterion for evaluating and comparing system models. Ecol. Modelling 44:299-306.

Weider, R.K. and Lang, G.E. 1982. A critique of the analytical methods used in examining decomposition data obtained from litter bags. Ecol. 63:1636-1642.

Whitmore, A.P. 1991. A method for assessing the goodness of computer simulation of soil processes. J. Soil Sci. 42:289-299.

Wu, J., Brookes, P.C. and Jenkinson, D.S. 1993. Formation and destruction of microbial biomass during the decomposition of glucose and ryegrass in soil. Soil Biol. Biochem. 25:1435-1441.

CHAPTER 7

Spatial relationships and decomposition

7.1 INTRODUCTION

Microbial utilization of plant residues is influenced by their chemical composition and physical accessibility. Empirical indices have been suggested to relate attributes of plant residues to their decomposition dynamics in soil. It is generally accepted that residues with low C:N ratios decompose more rapidly than residues with high C:N ratios. In addition, increases in lignin content (Muller et al., 1988) and polyphenol concentrations (Palm and Sanchez, 1991) have been correlated to decreases in the rate of residue decomposition. Combinations of attributes such as C:N ratio, lignin content and carbohydrate content have also been related to C mineralization of root materials (Herman et al., 1977). More recently, the proportions of plant residue C and N in readily available, water-soluble components have been linked to early decomposition dynamics (Cogle et al., 1989; Reinertsen et al., 1984).

Spatial relationships at the pedon, organism and molecular level also influence residue decomposition (McGill and Myers, 1987). For example, at the pedon level, plant residues placed on the soil surface are not as quickly decomposed as those mixed into the soil (Cogle et al., 1989). At the organism level, decomposition occurs in microenvironments which bring together substrate and decomposer under hospitable moisture and aeration regimes. Structural plant components, such as lignin and cellulose, are postulated to serve as both habitat and substrate (McGill et al., 1981). The concentration of microorganisms in and around particulate residues may increase microbial efficiency or, alternatively at high densities may decrease efficiency through competition for space and nutrients. Finally, at the molecular level, interactions among spatially associated polymers result in unique decomposition rates for unique structures (McGill and Myers, 1987). For example, labile cytoplasmic compounds may be physically protected by their position within membranes and cell walls or by reaction with these resistant organics.

We assumed that freeze-drying and grinding pea residues would destroy the cellular integrity of the plant materials yet maintain the physical association between crystallized cytoplasmic components and structural components. We separated the water-soluble and insoluble components from these residues and added them to soil alone or in combination. By monitoring

microbial assimilation of ^{15}N, as well as ^{15}N and C mineralization from these materials, we hoped to compare microbial utilization of spatially associated or spatially separated plant components in soil. Furthermore, we assessed the ability of two plant residue decomposition submodels, ECO and PHO, to account for differences in the spatial arrangement of plant residues and their components.

7.2 MATERIALS AND METHODS

Analysis of Pea Residues

This experiment was run concurrently with that described in Chapter 5. Full bloom ^{15}N-labelled peas (*Pisum sativum* 'Sirius') were separated into shoots and roots, lyophilized and ground to a fine powder in a Brinkmann ultra-high-speed mill. Scanning electron microscopy was used to examine physical aspects of ground pea residues at various levels of magnification (Figure 7-1). The shoots and roots were separated into water-soluble and water-insoluble fractions by extraction in a mortar with a pestle and potassium phosphate buffer (0.02*M*, pH 7) (Knowles and Ries, 1981). Ten mL of buffer were used for 200 mg of plant material. The resulting slurry was centrifuged at 10,000 x g at 4°C for 30 minutes. The supernatant was removed and the remaining pellet washed with 4 mL of buffer and recentrifuged at 10,000 x g for 30 minutes. Supernatants were combined. The proportion of insoluble pea component was determined by extracting, washing and centrifuging a known mass of whole plant material then drying (70°C) and weighing the remaining pellet. The soluble component was assumed to be the difference between whole and insoluble mass. Further subsamples of supernatant and pellet were dried at 70°C and, along with whole shoot and root samples, were analyzed for total C, total N and ^{15}N as described for shoot materials (Chapter 5). It was assumed that the salt from the phosphate buffer was recovered in the supernatant and, therefore, the mass of the soluble fraction and hence its C and N contents were corrected for the mass of salt used in the extraction. The composition of pea materials is shown in Table 7.1.

The mass of C represented by each plant component was calculated as dry mass x C content. Biochemical fractionation of the plant materials was calculated as follows: The water-soluble component was assumed to contain soluble protein and carbohydrates. Protein was calculated as 6.25 x N and was assumed to be 50% C. The remaining C in the soluble component was assumed to be in the form of carbohydrates. The water-insoluble component was assumed to contain insoluble protein, cellulose and lignin. As for the soluble component, protein C was calculated as 6.25 x N x 50%. Lignin content was analytically determined (4.9% in shoot; 5.2% in

root (AOAC, 1990)) and lignin was assumed to be 50% C. The remaining C was assigned to cellulose.

Incubation

DBC soil samples (25 g) were placed in 50 mL polystyrene beakers and either left non-amended or amended with one of the following: (1) 11.9 ± 0.2 mg non-fractionated ground pea shoot, (2) water-soluble fraction of pea shoot (S-SH), (3) water-insoluble fraction of pea shoot (IN-SH), (4) water-soluble plus insoluble fractions of pea shoot (SIN-SH), (5) 11.9 ± 0.2 mg non-fractionated ground pea root, (6) water-soluble pea root (S-RT), (7) water-insoluble pea root (IN-RT) and, (8) water-soluble plus insoluble fractions of pea root (SIN-RT). The water-soluble and water-insoluble fractions were added in amounts equivalent to what was estimated to be present in 11.9 mg of non-fractionated plant material. Appropriate aliquots of water-soluble or insoluble materials were adjusted to a total volume of 1.1 mL with phosphate buffer and gently mixed into the soil. For the soluble plus insoluble treatment, the fractions were added separately to the soil in smaller volumes of phosphate buffer but so that the sum of buffer was also 1.1 mL. Ground pea shoot and root were mixed into the soil and 1.1 mL of phosphate buffer poured onto the soil surface. Soils were moistened to 55% water-holding capacity (WHC) with deionized water.

Table 7-1. Characteristics of pea components

Component	Dry mass as % of whole	Carbon[a] (%)	Nitrogen[b] (%)	C:N ratio	^{15}N atom abundance (%)
		Pea shoot			
Whole	100	41.1	2.40	17.1	11.7
Water-soluble	34	31.7	2.19	14.5	11.1
Water-insoluble	66	39.0	1.91	20.4	11.4
		Pea root			
Whole	100	37.5	2.37	15.8	8.8
Water-soluble	25	22.1	2.73	8.1	8.9
Water-insoluble	75	32.2	1.71	18.8	9.8

[a] Determined by dry oxidation in LECO induction furnace.
[b] Determined by Dumas combustion.

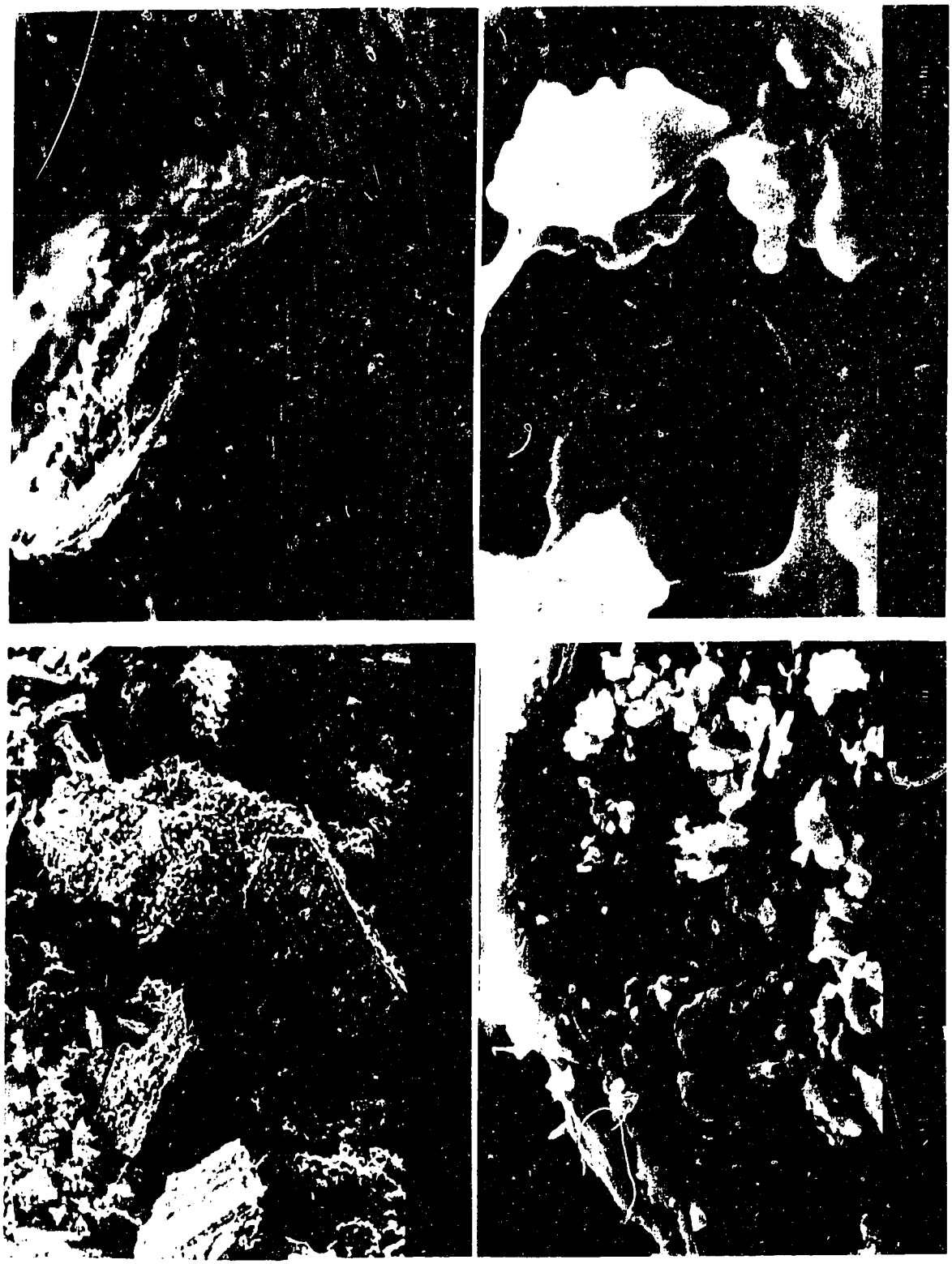

Figure 7-1. Scanning electron microscopy images of freeze-dried and ground pea shoot. For reference, a spherical bacterial cell is approximately 1 um in diameter.

Soils were incubated at 23 °C for 81 days as described in Chapter 5. Microbial biomass N, biomass ^{15}N, mineral N and mineral ^{15}N, as well as CO_2 production were all analyzed in triplicate as described in Chapter 5.

Computer Simulations

ECO and PHO submodels were examined for sensitivity toward spatial arrangement of plant residue components by comparing simulations of whole plant residues to simulations of the separate soluble and insoluble residue components. Initialization values were analytically determined (Table 7-2). For ECO, biochemical fractionation of soluble and insoluble components was estimated as described above. For PHO, the metabolic pool was assumed to represent soluble residue components and the structural pool, insoluble residue components. The fraction of plant C in the structural residue pool (F_s) was assumed to equal the C in the insoluble fraction divided by the C in the soluble + insoluble fractions. The C:N ratios of the metabolic and structural components were set to the analytically determined C:N ratio of the soluble and insoluble residue components, respectively.

Table 7-2. Initialization values for simulations of plant residue decomposition

	Shoot	S-SH	IN-SH	Root	S-RT	IN-RT
Residue input[a] (g C Mg^{-1} soil)	196	50	124	178	26	115
Protein[b] (g C g^{-1} C)	0.17	0.20	0.16	0.21	0.39	0.16
Carbohydrate (g C g^{-1} C)	0.23	0.80	0.00	0.11	0.61	0.00
Cellulose (g C g^{-1} C)	0.53	0.00	0.75	0.59	0.00	0.73
Lignin (g C g^{-1} C)	0.07	0.00	0.09	0.09	0.00	0.11
F_s[c]	0.71	0.00	1.00	0.82	0.00	1.00
$C:N_{metabolic}$	14.47	14.47	-----	8.06	8.06	-----
$C:N_{structural}$	20.40	-----	20.40	18.84	-----	18.84

[a] Residue input = dry mass as percent of whole x dry mass added to soil x C content.
[b] Biochemical components represented as C in each component / total residue C.
[c] Fraction of plant C in the structural component.

7.3 RESULTS

Experimental Data

The recovery of pea ^{15}N in the soil ranged from 92-117% ^{15}N recovery in the mineral, microbial and non-microbial organic (NMO) fractions, as a percent of total soil ^{15}N, is shown in Figure 7-2. The dynamics of ^{15}N assimilation by the microbial biomass were markedly different between the whole shoot or root treatments and the water-soluble plus insoluble treatments. On day 2, approximately 90% of the SIN-SH ^{15}N and 60% of the SIN-RT ^{15}N were recovered in the microbial biomass. A similar pattern of microbial recovery was evident for the insoluble treatments. Both net mineralization and net immobilization of ^{15}N were observed in most treatments at some point during the incubation. As evidenced by the increase in ^{15}N recovery in the NMO soil fraction following large recoveries in the microbial biomass, it appears that plant-derived N, once it had passed through the biomass, was left in the soil as 'processed' organics.

Combining all sampling dates, there were no significant differences (ANOVA, $P<0.05$) among treatments in microbial biomass N or mineral N. Amendment did not distort the system.

Incremental CO_2 data of non-amended soils were subtracted from incremental CO_2 data of amended soils and were transformed to daily rates by dividing the incremental value by the number of days between successive measurements. Rates were normalized by dividing by the mass of residue C added in each treatment. The resulting rates were plotted at the midpoint between the two data collection times (Figure 7-3). Cumulative CO_2 evolved in response to plant residue decomposition (i.e. when rate of evolution in amended was greater than that in non-amended) was calculated as a percent of residue C added (Figure 7-4). The respiratory response to amendment was observed up to day 16 for pea shoots and shoot components. The response was also observed up to day 16 for pea roots but varied for the other root treatments. The response to S-RT was only evident on the first two sampling dates whereas the response to IN-RT and SIN-RT was not evident until the third sampling date. The greatest respiratory response was observed in the first 24 hours of the S-SH and S-RT treatments: CO_2 evolved during this period accounted for over 20% of the soluble C added to soil. At day 16, CO_2 evolved accounted for approximately 60% of the shoot C added and 30% of the root C added. Generally, respiration rates were greater in the whole shoot treatment compared to SIN-SH. In comparison, rates were greater for whole root on the first 2 or 3 sampling dates after which, rates were greater for the SIN-RT treatment. Respiratory response to amendment was not evident beyond 27 days for any treatment.

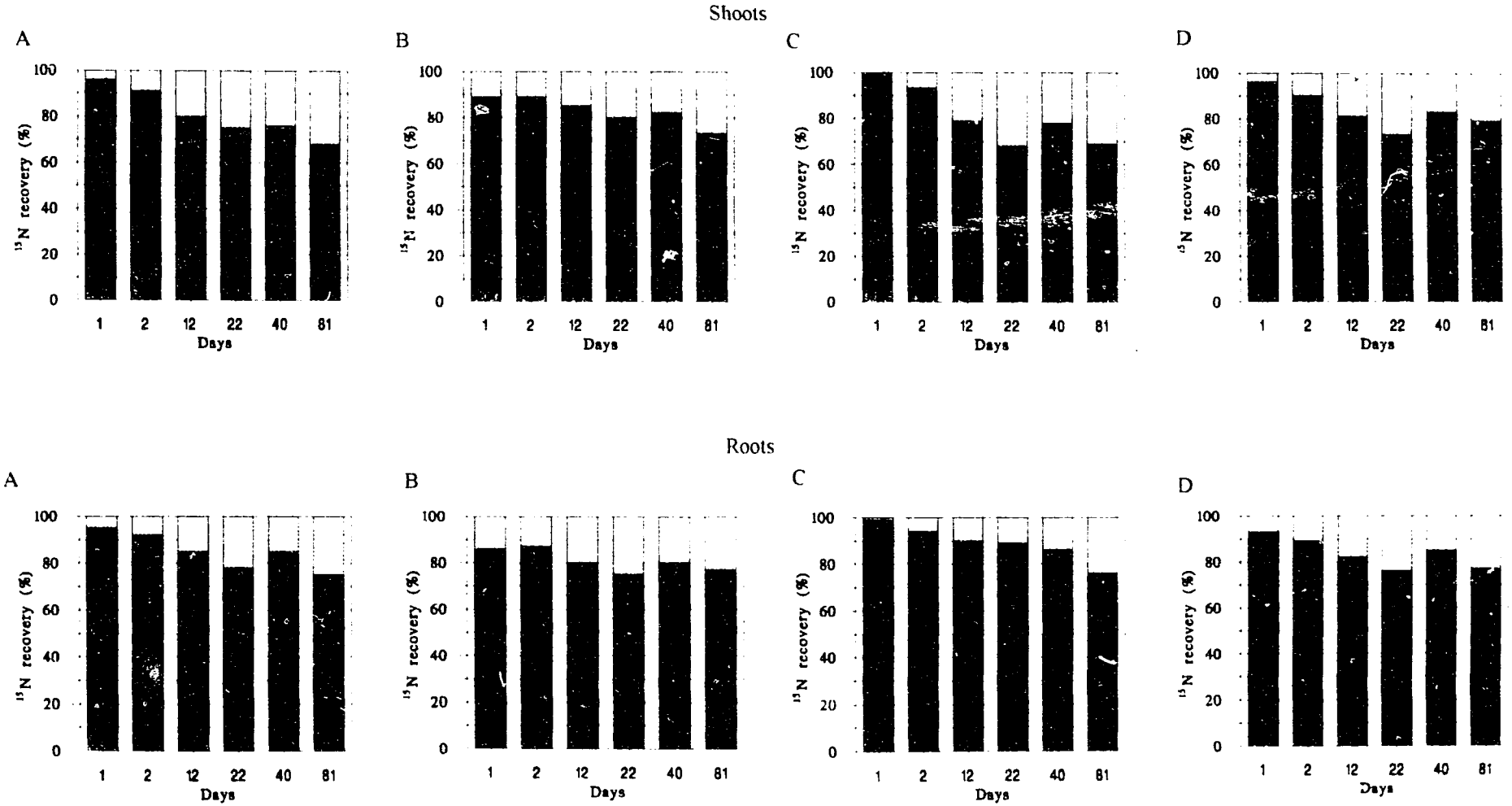

Figure 7-2. ^{15}N recovery (as a percent of total soil ^{15}N) in the mineral, microbial and non-microbial organic (NMO) fractions of a Dark Brown Chernozemic soil amended with the (A) whole, (B) soluble component, (C) insoluble component, (D) soluble + insoluble components of ^{15}N-labelled pea shoots and ^{15}N-labelled pea roots.

A

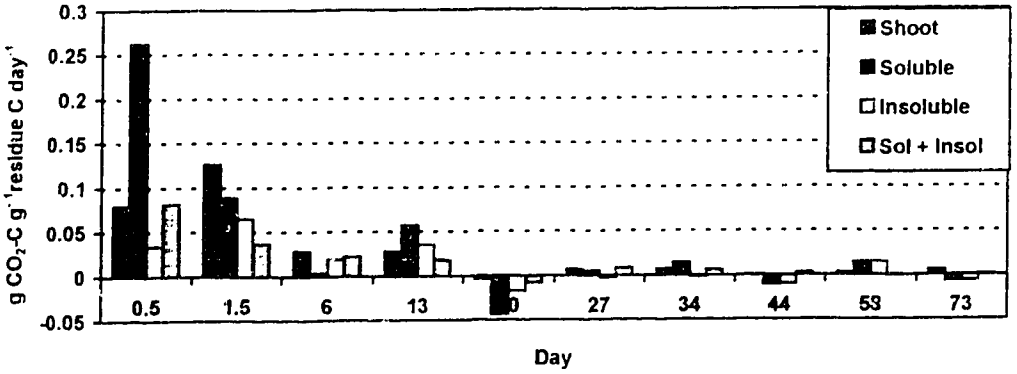

B

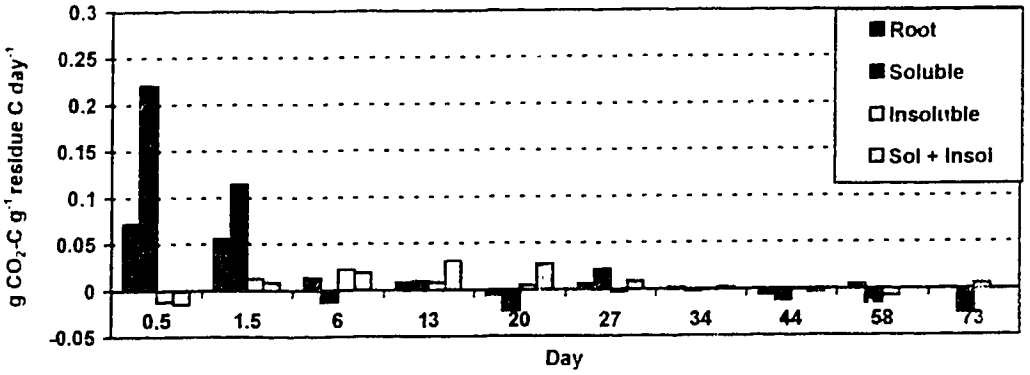

Figure 7-3. Rate of CO_2 evolution (corrected for basal rate) following amendment with (A) pea shoots and shoot components and (B) pea roots and root components.

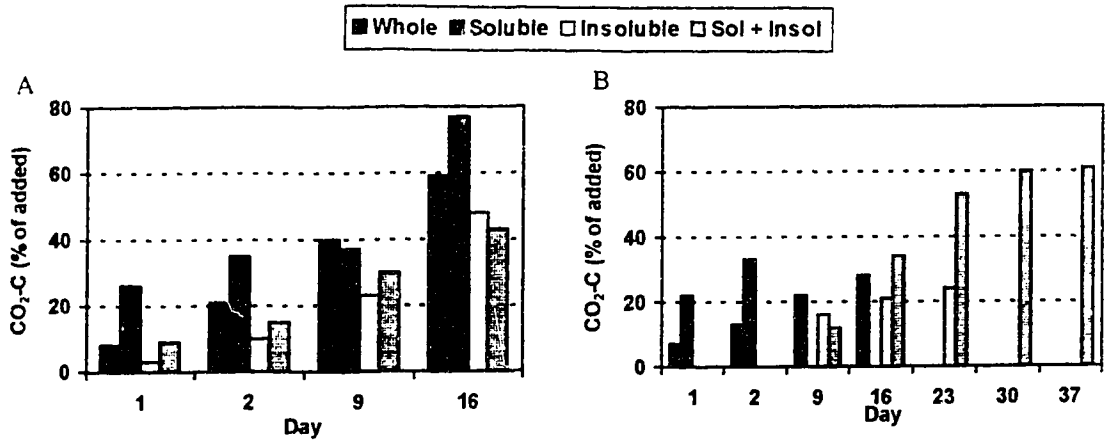

Figure 7-4. Respiratory response to amendment with (A) pea shoots and shoot components and (B) pea roots and root components. Values were calculated by subtracting the non-amended respiration from the respiration of amended incubations and dividing by the mass of residue C added (x 100%).

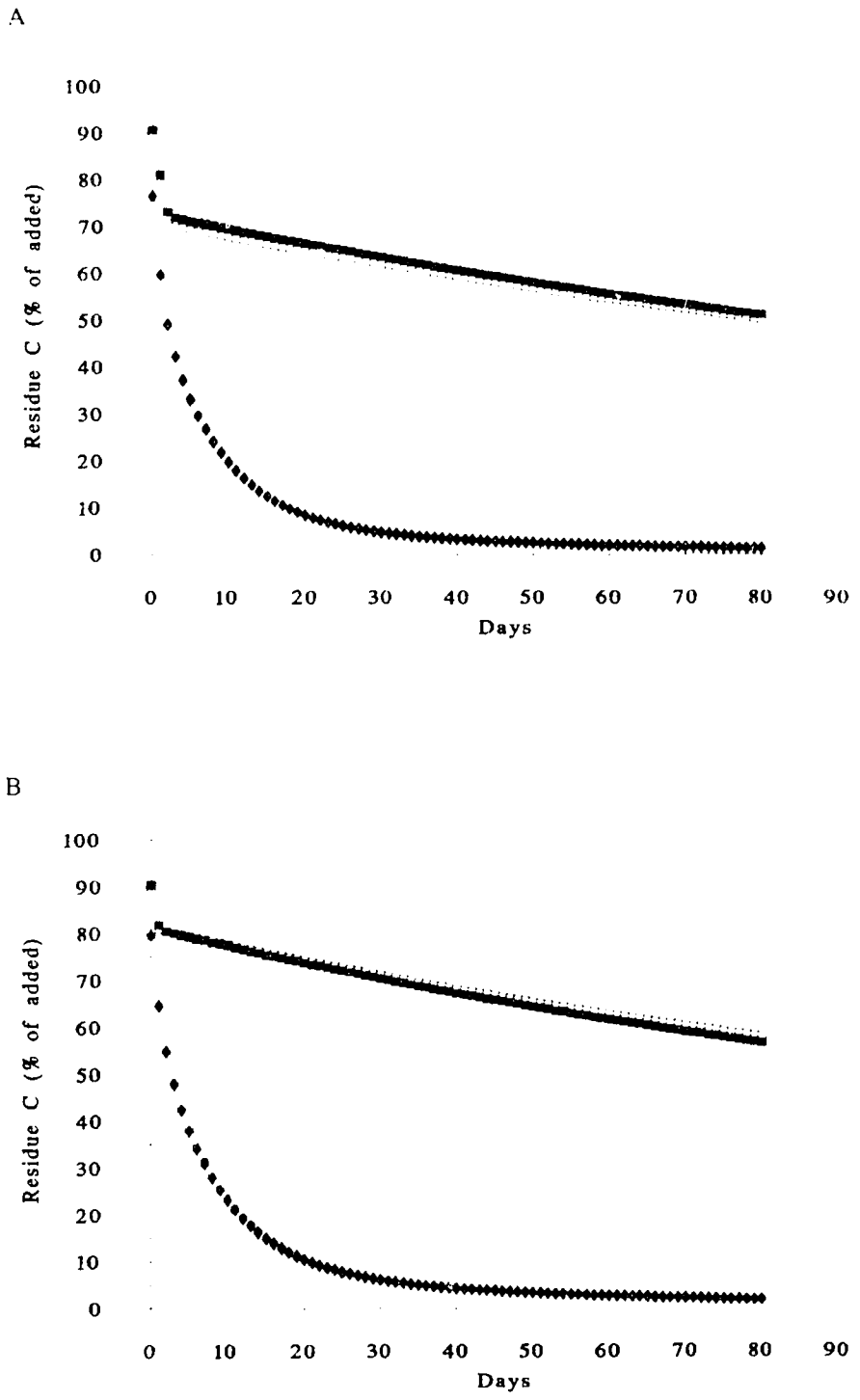

Figure 7-5. Simulated values of (A) pea shoot C remaining and (B) pea root C remaining. ◆. ECO and ■. PHO whole plant residue. ◇. ECO and □. PHO sum of soluble and insoluble components of plant residue.

Simulated Data

C remaining in plant residues was calculated as the arithmetic sum of soluble C and insoluble C remaining and was compared to values generated from simulations of whole plant residues (Figure 7-5). Neither ECO nor PHO showed any difference in plant C decomposition between soluble + insoluble and whole plant residue. Reasons for differences in C decomposition dynamics between ECO and PHO are discussed in Chapter 6.

7.4 DISCUSSION

Composition of Pea Residues

Scanning electron microscopy images confirmed that freeze-drying and grinding pea residues did destroy cellular integrity (Figure 7-1). Furthermore, these images show the residue landscapes at a scale relevant to microorganisms. Ample habitat opportunities were evident within and around structural materials and we suggest that displaced cytoplasmic materials coated the outside, as well as inside surfaces of these materials.

Pea shoots were more abundant in ^{15}N compared to roots (Table 7-1). Furthermore, the water-insoluble fractions, especially of roots, were more abundant in ^{15}N compared to the water-soluble fractions. Yoneyama and Kaneko (1989) also reported a lower abundance of ^{15}N in the roots of *Brassica campestris* plants grown hydroponically and fed ^{15}N-labelled nitrate. Isotopic discrimination is not believed to be associated with N transport because neither diffusion nor mass flow are subject to isotopic fractionation (Shearer and Kohl, 1986). Yoneyama and Kaneko (1989) suggest that the enzymatic reduction of nitrate is the critical step in isotopic fractionation: the products of enzymatic reactions (amino acids and proteins) have lower levels of heavier isotopes. Nitrate taken up from solution is translocated from roots to shoots. Amino acids less abundant in ^{15}N are returned to the root through the phloem for the synthesis of organic compounds. Our findings of greater ^{15}N abundance in the insoluble fraction of roots compared to the soluble, however, seem to contradict this hypothesis. The greater ^{15}N abundance of the insoluble fraction may have delayed the overall microbial recovery of ^{15}N from the whole root treatment.

The C:N ratios of the water-soluble fractions of pea ranged from 8.1 for pea roots to 14.5 for peas shoots (Table 7-1). Wheat straw with initial C:N ratios of 36 to 238, contained water-soluble fractions with C:N ratios from 9 to 63 (Reinertsen et al., 1984). Furthermore, the C:N ratio

of the soluble fraction of green manure lentil was 9 while that of mature lentil straw was 24 (Bremer et al., 1991). The water-soluble component of plant residues is considered to be readily available to decomposers (Cogle et al., 1989). Apparently, the soluble nature of this component, and not its C:N ratio, determines decomposability.

The cold water-extractable C accounted for 25% of total shoot C and 15% of total root C. In comparison, cold water-extractable N accounted for similar proportions (29 - 31%) of total N in both shoots and roots (Table 7-1). The roots of *Medicago littoralis* and *Medicago truncatula* were also reported to have a smaller proportion of water-extractable C compared to leaves: 13% for roots compared to 24% for leaves (Amato et al., 1983). Furthermore, grass roots have been reported to contain low concentrations of soluble carbohydrates (Herman et al., 1977). The root nodules of cowpea, on the other hand, contain relatively large proportions of soluble C and N (Franzluebbers et al., 1994). Pea roots in the present study had few nodules because plants were grown in sterile sand and fed a N-rich nutrient solution.

Dynamics of Soluble and Insoluble Components

The ^{15}N recovery data do not allow distinction among treatments in terms of the rates of transformations because the intervals between observations were too long. The timing of static measurements of dynamic systems is critical and must be matched to the rate of the process under study. Maximum recovery of soluble ^{15}N was expected between 1 and 2 days whereas maximum recovery of insoluble ^{15}N was expected between days 12 and 40 (Chapter 6). Apparently, transformation rates were more rapid than expected. The rapid rates of CO_2 evolution in the S-SH and S-RT treatments prior to 24 hours suggest that the soluble C was quickly mineralized. The water-soluble C fraction of wheat straw was also readily mineralizable with respired ^{14}C-CO_2 accounting for 40% of applied ^{14}C after 4 days (Cogle et al., 1989). Although ^{15}N data do not show a dramatic recovery of soluble N in the microbial biomass on day 1, it is possible that a substantial portion of the ^{15}N had already passed through the biomass by this time. Soluble pea N would, after all, have accounted for only a small fraction (approximately 5%) of biomass N. The recovery of ^{15}N in the soil mineral component of the soluble treatments also suggests activity prior to 24 hours.

After day 2, the rate of CO_2 evolution in the soluble treatments was similar to the other treatments suggesting that microorganisms had transformed the soluble compounds into materials which decomposed more slowly. Cogle et al. (1989) also noted that the half-life of ^{14}C originating from the soluble fraction of wheat straw increased during the first 4 days of incubation so that,

between days 4 and 15, the half-life was similar to that of intact straw. Cytoplasmic materials from bacterial cells also showed biphasic decomposition in soil indicating their reaction with soil components such as phenolics (Juma and McGill, 1986).

Rapid microbial assimilation of ^{15}N originating from the insoluble fraction of pea shoots and, to a lesser extent, that originating from pea roots, was evident between day 1 and 2 (Figure 7-2). Respiration rates, however, did not correspond well to these ^{15}N data. On day 2, for example, the respiratory response to the IN-SH treatment accounted for 10% of C added (Figure 7-4). Assuming a maximum microbial efficiency of 60%, at least another 15% was present as microbial biomass or its by-products. In total approximately 25% of the substrate's C would have been processed by microorganisms. This value is in contrast to the 90% recovery of substrate ^{15}N in the microbial biomass on day 2. This is possible only if the N in the insoluble compounds was preferentially utilized by microorganisms over the C in these compounds. Water-insoluble N was assumed to be in the form of proteins. Conjugated proteins, such as lipoproteins, would be insoluble because of their association with fats or cholesterol (Wade, 1987) but the N in these proteins may still be readily available to microorganisms. Furthermore, C in some structures may become resistant to microbial utilization by its association with less active soil components. Perhaps accessible N was cleaved and the remaining C structures were directly incorporated into soil organic matter. The phenyl propanoid structure of lignin, for example, lends itself to oxidative coupling of phenols with components of soil humus. These phenomena deserve further investigation.

Influence of Spatial Arrangement on ^{15}N Dynamics and C Mineralization

Although rates of N transformation cannot be distinguished from the ^{15}N data, it can be ascertained that the dynamics of ^{15}N recovery in the microbial biomass were changed by separating the substrate into soluble and insoluble components. The microbial assimilation of soluble + insoluble ^{15}N appeared to reflect dynamics of each component added separately, as would be expected. The whole shoot is more of a mystery. Is the peak in microbial ^{15}N recovery before or after day 2? Analysis of the respiration data suggested that, during the first two days of incubation, more C from whole plant residues was mineralized compared to C from soluble + insoluble residue components: this was especially evident for root materials. In addition, by day 2, the mass of C respired from the whole shoot and whole root treatments accounted for more than twice the mass of C respired from the S-SH and S-RT treatments, respectively suggesting that both soluble and

insoluble materials were being mineralized. One could speculate, therefore, that the peak in microbial recovery of whole residue ^{15}N was prior to day 2 and that the decomposition of pea residues was enhanced by maintaining a physical association between soluble and insoluble components. This would support the hypothesis of structural plant materials providing both habitat and substrate to microorganisms (McGill et al., 1981). If there is contact between decomposer and substrate, then the efficiency of enzymatic catabolism of both soluble and insoluble substrates would be enhanced. At high microbial density, however, efficiency may be reduced through competition for space and nutrients or by the production of inhibitory substances such as antibiotics (McGill et al., 1981).

The hypothesis of structural plant components protecting labile components from microbial attack and thus delaying decomposition of intact residues is widely accepted (Cogle et al., 1989; Muller et al., 1988). Physical protection of labile cytoplamic components within membranes and cell walls requires intact cellular structure (Juma and McGill, 1986). Because cells were disrupted by freeze-drying and grinding pea residues, this type of physical protection was not a factor in the whole residue treatments. Structural components also protect labile components from rapid decomposition by forming resistant complexes. For example, N mineralization may be lowered in the presence of high concentrations of polyphenols, due to the binding of mineralized N into an insoluble organic compound (Tian et al., 1992). Partially altered plant lignins and other phenolic materials are abundant in soil (Juma and McGill, 1986). The S-SH and S-RT compounds were as likely to complex with indigenous resistant soil compounds as with adjacent plant compounds.

Reinertsen et al. (1984) concluded that the biomass produced during the utilization of the initial available C fraction of wheat straw has a significant influence on the overall rate of decomposition in the initial stages. Collins et al. (1990) noted that wheat residue mixes containing quickly and slowly decomposable components decomposed more quickly than would be expected from the decomposition rates of individual parts. They postulated that bridging of fungal hyphae from substrate-rich components may enable some fungi to produce enzymes necessary for utilization of complex substrates. Both of these examples demonstrate the importance of the spatial association of decomposers with their substrate. As microbes cluster around particulate residues, they quickly utilized the readily available nutrients and the energy released from these nutrients spurs on decomposition of the more resistant substrates. Separating the soluble and insoluble plant components dilutes nutrient concentrations within the soil matrix and reduces the efficiency of the decomposers.

Differences Between the Decomposition of Shoots and Roots

Root C mineralization was slower than that of shoot C (Figure 7-4). Jawson and Elliott (1986) also reported slower C mineralization of wheat roots compared to straw and showed that the difference in CO_2-C evolved during the first 6 days of incubation was nearly equivalent to the difference in water soluble C content of the plant materials. During the first 9 days of incubation, the ratio of % pea shoot C respired / % pea root C respired was approximately 1.9 (Figure 7-4). The ratio of soluble C in the pea shoot / soluble C in pea root was 1.7. The difference in C mineralization in pea residues, therefore, could also be related to initial soluble C content. Similar results were reported for the decomposition of *Medicago littoralis* leaves, stems and roots (Amato et al., 1983). Differences in the C mineralization of SIN-SH compared to SIN-RT are more difficult to explain.

Submodel Performance

ECO partitions residues into biochemical components, each of which is assigned a specific decomposition rate. Chemical or physical interaction with other plant or soil components is not expected to change the decomposition rates. The functional approach in PHO partitions residues into labile and resistant fractions. Although this approach recognizes cellular structure, it does not allow for exchange between labile and resistant fractions.

Both ECO and PHO contain 'density functions' which represent the idea of plant residues providing both substrate and habitat to microorganisms. In ECO, the density function applies to all biochemical components (protein, carbohydrate, cellulose and lignin) and is based on the ratio of the aqueous concentration of active microbial C to total plant residue C remaining in soil. In PHO, the density function applies only to the structural plant components and is based on the ratio of total microbial C to structural C. Neither submodel, however, could account for differences in residue decomposition resulting from the spatial arrangement of residue components and their proximity to decomposers. Spatial phenomena may be one of the most challenging aspects of simulation modelling.

Conclusion

SEM images confirmed that freeze-drying and grinding pea residues disrupted plant cells and also suggested that structural residue components could serve as microbial habitats. The water-soluble fraction of plant residues was readily utilized by soil microorganisms: apparently the soluble nature of this component and not its C:N ratio, determined decomposability. ^{15}N data suggest that

insoluble N was also rapidly assimilated by the microbial biomass although, C mineralization data do not concur. This is possible only if N in insoluble compounds was preferentially utilized over C in these compounds. It was postulated that the decomposition of pea residues was enhanced by maintaining a physical association between soluble and insoluble components, thereby increasing decomposer efficiency. The capacity to simulate spatial relationships would greatly improve existing ecosystem simulation models. Further work is required in this area.

7.5 LITERATURE CITED

Amato, M., Jackson, R.B., Butler, J.H.A. and Ladd, J.N. 1983. Decomposition of plant materials in Australian soils. I. Residual organic ^{14}C and ^{15}N from legume plant parts decomposing under field and laboratory conditions. Aust. J. Soil Res. 21:563-570.

Association of Official Analytical Chemists. 1990. Official Methods of Analysis. Association of Official Analytical Chemists, Inc., Arlington, Virginia, USA.

Bremer, E., van Houtum, W. and van Kessel, C. 1991. Carbon dioxide evolution from wheat and lentil residues as affected by grinding, added nitrogen, and the absence of soil. Biol. Fertil. Soils 11:221-227.

Cogle, A.L., Saffigna, P.G. and Strong, W.M. 1989. Carbon transformations during wheat straw decomposition. Soil Biol. Biochem. 21:367-372.

Collins, H.P., Elliott, L.F., Rickman, R.W., Bezdicek, D.F. and Papendick, R.I. 1990. Decomposition and interactions among wheat residue components. Soil Sci. Soc. Am. J. 54:780-785.

Franzluebbers, K. Weaver, R.W., Juo, A.S.R. and Franzluebbers, A.J. 1994. Carbon and nitrogen mineralization from cowpea plant parts decomposing in moist and in repeatedly dried and wetted soil. Soil Biol. Biochem. 26:1379-1387.

Herman, W.A., McGill, W.B. and Dormaar, J.F. 1977. Effects of initial chemical composition on decomposition of roots of three grass species. Can. J. Soil Sci. 57:205-215.

Jawson, M.D. and Elliott, L.F. 1986. Carbon and nitrogen transformations during wheat straw and root decomposition. Soil Biol. Biochem. 18:15-22.

Juma, N.G. and McGill, W.B. 1986. Decomposition and nutrient cycling in agro-ecosystems. Pages 74-136 *in* M.J. Mitchell and J.P. Nakas, eds. Microfloral and Faunal Interactions in Natural and Agro-ecosystems. Martinus Nijhoff/Dr W. Junk Publishers, Dordrecht, The Netherlands.

Knowles, N.R. and Ries, S.K. 1981. Rapid growth and apparent total nitrogen increases in rice and corn plants following applications of triacontanol. Plant Physiol. 68:1279-1284.

McGill, W.B. and Myers, R.J.K. 1987. Controls on dynamics of soil and fertilizer nitrogen. Pages 73-99 *in* Soil Fertility and Organic Matter as Critical Components of Production Systems. SSSA Spec. Pub. no. 19.

McGill, W.B., Hunt, H.W., Woodmansee, R.G. and Reuss, J.O. 1981. Phoenix-A model of the dynamics of carbon and nitrogen in grassland soils *in* F E. Clark and T. Rosswall, eds. Terrestrial Nitrogen Cycles. Ecol. Bull. (Stockholm) 33:49-115.

Muller, M.M., Sundman, V., Soininvaara, O. and Merilaninen, A. 1988. Effect of chemical composition on the release of nitrogen from agricultural plant materials decomposing in soil under field conditions. Biol. Fertil. Soils 6:78-83.

Palm, C.A. and Sanchez, P.A. 1991. Nitrogen release from the leaves of some tropical legumes as affected by their lignin and polyphenolic contents. Soil Biol. Biochem. 23:83-88.

Reinertsen, S.A., Elliott, L.F., Cochran, V.L. and Campbell, G.S. 1984. Role of available carbon and nitrogen in determining the rate of wheat straw decomposition. Soil Biol. Biochem. 16:459-464.

Shearer, G. and Kohl, D.H. 1986. N_2-fixation in field settings: estimations based on natural ^{15}N abundance. Aust. J. Plant Physiol. 13:699-756.

Tian, G., Kang, B.T. and Brussaard, L. 1992. Biological effects of plant residues with contrasting chemical compositions under humic tropical conditions - decomposition and nutrient release. Soil Biol. Biochem. 24:1051-1060.

Wade, L.G. 1987. Organic Chemistry. Prentice-Hall, Inc. New Jersey, USA.

Yoneyama, T. and Kaneko, A. 1989. Variations in the natural abundance of ^{15}N in nitrogenous fractions of komatsuna plants supplied with nitrate. Plant Cell Physiol. 30:957-962.

CHAPTER 8

Synthesis

8.1 DECOMPOSITION WITHIN AN ECOSYSTEM FRAMEWORK

Organic matter decomposition and nutrient cycling at specific sites under specific conditions have been studied extensively. Most of these observations, however, cannot be extrapolated to other ecosystems. Rather than building an inventory of empirical site-specific data, we must work toward elucidating mechanisms within processes and the influence of regulatory factors on these mechanisms. To be applied most broadly, the flux of energy and nutrients within an ecosystem should be examined at the level of the agents of transformation. In soil, the microbial biomass is the primary biological agent of organic matter transformation and is largely regulated by the properties of its substrate and the physico-chemical environment.

Elucidating mechanisms at the microbial level remains a challenge, especially within a heterogeneous matrix such as soil. Hierarchy theory, the systematic organization of observations at specific levels of resolution, is a useful framework in which to examine interactions within and links between levels of resolution (McGill and Myers, 1987). Mechanistic simulation models, those which are structured to be analogous to the real system under study, exemplify this framework: their purpose is to account for behavior at one hierarchical level by describing the elements of a more detailed level (Hunt and Parton, 1986). With the proper links, observations from soil samples under controlled laboratory conditions and even field-scale observations could be simulated from algorithms representing interactions at the microbial level. Failure of a model to mimic natural phenomena would indicate that one or more hypotheses in that model must be invalid.

In my dissertation I have focused on the microbial biomass as the driving force behind the decomposition process. Chemical properties of plant residues, specifically the proportion of labile components, as well as the spatial relationship between labile and structural components were shown to regulate microbial utilization. Microbial activity (as determined by N mineralization per unit biomass N) was linked to soil clay content. Through simulation modelling, the impact of change in biomass size and activity on the rest of the soil system was evident. Only by studying the process of plant residue decomposition at the level of the agents of transformation and within the context of an integrated ecosystem will its interconnections and implications be fully understood.

8.2 CONCLUSIONS

1. Although 10% bloom and full bloom pea shoots were not significantly different in dry matter production, C or N content, more N was released from the 10% bloom residues directly following soil incorporation. It was suggested that the younger pea material had a larger proportion of easily metabolizable labile components.
2. Legume bloom stage at incorporation had no influence on barley dry matter yield, N content or ^{15}N recovery in the grain, however, significantly more ^{15}N was recovered in the barley straw and roots during vegetative growth following full bloom incorporation. This observation may be the result of a closer synchrony between the appearance of legume-derived mineral ^{15}N and early N demand by the barley.
3. At Provost (DBC) 16% of full bloom legume N was recovered in the subsequent barley crop. This legume-derived N supplied approximately 4.1% of the barley's N at harvest. The main benefit of legume green manure, therefore, may be in building long-term soil fertility.
4. Under laboratory conditions, the rate of pea residue N transformation, as estimated from the recovery of plant-derived ^{15}N in the soil microbial biomass and mineral components, was initially very rapid: 50-60% in the first 2 days of incubation.
5. The water-soluble C and N from pea residues was rapidly mineralized and ^{15}N data suggest that insoluble N was also rapidly assimilated by the microbial biomass. Apparently, there was a preferential microbial uptake of N from insoluble components compared to C in these components.
6. It was postulated that the decomposition of pea residues was enhanced by maintaining a physical association between soluble and insoluble components, thereby increasing decomposer efficiency. The simulation submodels, ECO and PHO, could not account for differences in residue decomposition resulting from differences in the spatial arrangement of the residues' soluble and insoluble components.
7. The fate of N from plant residues was distinguished best among diverse soils on the basis of normalized rates of flow through selected soil components (e.g. mg N mineralized g^{-1} soil microbial N), rather than on the basis of accumulation in these components.
8. Our observations supported previous reports of higher normalized N mineralization rates in Luvisolics compared to Chernozemics under controlled environments and were consistent with the hypothesis that higher rates are associated with soils of lower clay content.

9. Under laboratory conditions, amendment with pea shoot caused a 'priming effect' resulting in the mineralization of an additional 19-23 g native soil N Mg^{-1}soil over 81 days.
10. Simulated CO_2 evolution suggested that pulsed addition of a readily decomposable residue to soil increases the mineralization of indigenous soil C. Although this phenomenon was not supported by our experimental data, it has been previously reported and may be the result of increased enzymatic activity following microbial 'priming'.
11. Recently immobilized biomass N, possibly that in excess of the soil's protective capacity, had a faster turnover compared to 'steady state' biomass N.
12. Flushes of CO_2-C, mineral N and ninhydrin-reactive N (NRN) were significantly correlated in the 0-15 cm depth of the two soils investigated. Correlation among flushes was not significant in the 15-30 cm samples except when the 'noncorrected' flush of CO_2-C was used. We concluded that the relationship between the flush of NRN and biomass measured by CFI, may be strongest for soils and conditions similar to those from which the relationship was developed. Broader applications would benefit from a comprehensive examination of how the nature or strength of such a relationship varies with length of soil conditioning, soil sampling depth, and metabolic state of soil microbial communities at the time of sampling.
13. The simulated dynamics of plant-derived N within the microbial and mineral soil fractions were sensitive to structural and kinetic differences among three plant residue decomposition submodels, ECO, PHO and VER. The rapid microbial assimilation of residue N observed experimentally was also evident in simulated data. Overall, however, the models appeared more sluggish than the natural system. Unfortunately, too few measurements were taken in the first few days of residue decomposition to accurately distinguish whether plant decomposition submodels were statistically valid or not.
14. Quantitatively evaluating model performance emphasized the importance of appropriate experimental data. Least squares analysis requires independent experimental data for model evaluation. Time series data collected from integrated biological systems are often correlated and the question remains as to what constitutes truly independent data. Because data sets for model evaluation commonly consist of relatively few measured variables, the sensitivity and timing of measurements are critical. Isotopic data and short intervals between measurements at a time when the system is actively responding to perturbation are most informative.

8.3 FURTHER CONSIDERATIONS

1. More studies of decomposition from the perspective of microbial metabolism of plant constituents is required. The apparent preferential microbial utilization of N in insoluble compounds compared to C in these compounds is one aspect of this issue deserving further investigation.
2. Microbial biomass estimation techniques should be further evaluated under various conditions. For meaningful comparisons among published findings, some degree of methodological standardization would be appropriate, especially regarding the length and environment of the soil conditioning period.
3. Simulation models are often not evaluated in situations other than those for which they were developed. Rather than developing new models around data sets, varied independent data sets should be used to evaluate systematically hypotheses within existing models.
4. Although it is not practical to represent individual pores or individual microorganisms in simulation models designed to represent ecosystems, representation of spatial phenomena in some capacity should be considered.
5. Research findings should be more than topics for discussion among academics; they should be shared with potential users. The role of extension services within the agricultural and environmental sectors should not be underestimated.

8.4 LITERATURE CITED

Hunt, H.W. and Parton, W.J. 1986. The role of modeling in research on microfloral and faunal interactions in natural and agroecosystems. Pages 443-494 *in* M.J. Mitchell and J.P. Nakas, eds. Microfloral and Faunal Interactions in Natural and Agro-ecosystems. Martinus Nijhoff/Dr W. Junk Publishers, Dordrecht, The Netherlands.

McGill, W.B. and Myers, R.J.K. 1987. Controls on dynamics of soil and fertilizer nitrogen. Pages 73-99 *in* Soil Fertility and Organic Matter as Critical Components of Production Systems. SSSA Spec. Pub. no. 19.

APPENDIX A

Simulation model equations and schematics

Stella II software was used to program the simulation models. Equations for the base model, ECO, PHO and VER follow. Refer to the schematics at the end of the equations section to see how sectors, submodels, stocks, flows and converters are arranged. Stella II allows modelling on three layers. The *sector* layer is the simplest view of the model and only sectors are visible. Sectors are arbitrary boundaries which surround groups of related equations. The *model* layer shows all the main stocks, flows and converters. Stocks represent state variables and are shown as rectangles in the schematics. Flows represent movement of materials, in this case C, ^{14}N and ^{15}N. In the schematics, flows are shown as hollow arrows with attached circular 'valves' and can be either single or double headed for one and two-way flows, respectively. Converters are shown as circles. Converters hold supplemental information required to run the model and may be stock-related, flow-related or external input-related. Finally, thin black connecting arrows link variables that are interdependent. The *submodel* layer shows further details about certain stocks. On the model layer, stocks with associated submodels are shown as larger rectangles surrounding a smaller striped rectangle. The submodel layer shows secondary stocks, flows and converters.

The first set of equations are for the combination of base model and ECO. Following are equations for the submodels PHO and VER. Each set of equations are arranged alphabetically within stock, flow and converter groupings.

The following standard designations are used throughout the code:

1. The nature of the flow is defined by the first letter of its code: D=decomposition, U=microbial uptake, R=respiration, M=N mineralization, Z=N immobilization, A=adsorption desorption, S=physical chemical stabilization, C=chemical stabilization.
2. Similar stocks and flows are associated with each of the three organic substrates. These stocks and flows have the same codes except for a numerical designation: 1 refers to plant residue, 2 refers to active organic matter and 3 refers to passive organic matter. For example, soluble1 C is the soluble C stock associated with plant residue, soluble2 C is the soluble C stock associated with active organic matter and, soluble3 C is the soluble C stock associated with passive organic matter.
3. Flows that connect stocks on the model layer to the submodel layer have the same codes except that, on the submodel layer, the code is followed by one or more prime symbols (').

BASE MODEL + ECO PLANT DECOMPOSITION SUBMODEL

The base model is a version of ECOSYS (Grant et al., 1993) and was translated from FORTRAN into Stella II.

Stocks

active_C(t) = active_C(t - dt) + (Cads_C - Dact_C) * dt
INIT active_C = 0.45*(organic_C-
(adsorbed_C+soluble1_C+soluble2_C+soluble3_C+labcor1_C+labcor2_C+labcor3_C+labmic1_C+labmic2_C+labmic3_C+rescor1_C+rescor2_C+rescor3_C+resmic1_C+resmic2_C+resmic3_C)) {g C Mg^{-1}soil}
DOCUMENT: Active organic matter.

active_N14(t) = active_N14(t - dt) + (Cads_N14 - Dact_N14) * dt
INIT active_N14 = active_C 10.5*(1-nat_atab) {g N14 Mg^{-1}soil}
DOCUMENT: Active organic matter.

active_N15(t) = active_N15(t - dt) + (Cads_N15 - Dact_N15) * dt
INIT active_N15 = active_C 10.5*nat_atab {g N15 Mg^{-1}soil}
DOCUMENT: Active organic matter.

adsorbed_C(t) = adsorbed_C(t - dt) + (Asol2_C + Asol1_C + Asol3_C - Cads_C - DadsC) * dt
INIT adsorbed_C = Qadsorb {g C Mg^{-1}soil}
DOCUMENT: Adsorbed organic matter.

adsorbed_N14(t) = adsorbed_N14(t - dt) + (Asol2_N14 + Asol1_N14 + Asol3_N14 - Cads_N14 - Dads_N14) * dt
INIT adsorbed_N14 = adsorbed_C 10*(1-nat_atab) {g N14 Mg^{-1}soil}
DOCUMENT: Adsorbed organic matter.

adsorbed_N15(t) = adsorbed_N15(t - dt) + (Asol2_N15 + Asol1_N15 + Asol3_N15 - Cads_N15 - Dads_N15) * dt
INIT adsorbed_N15 = adsorbed_C 10*nat_atab {g N15 Mg^{-1}soil}
DOCUMENT: Adsorbed organic matter.

carbohy_C(t) = carbohy_C(t - dt) + (car_C - Dplant_C') * dt
INIT carbohy_C = 0 {g C Mg^{-1}soil}
DOCUMENT: Plant residue carbohydrate.

carbohy_N14(t) = carbohy_N14(t - dt) + (car_N14 - Dplant_N14') * dt

INIT carbohy_N14 = 0 {g N14 Mg^{-1}soil}
DOCUMENT: Plant residue carbohydrate

carbohy_N15(t) = carbohy_N15(t - dt) + (car_N15 - Dplant_N15") * dt
INIT carbohy_N15 = 0 {g N15 Mg^{-1}soil}
DOCUMENT: Plant residue carbohydrate.

cellulose_C(t) = cellulose_C(t - dt) + (cel_C - Dplant_C") * dt
INIT cellulose_C = 0 {g C Mg^{-1}soil}
DOCUMENT: Plant residue cellulose.

cellulose_N14(t) = cellulose_N14(t - dt) + (cel_N14 - Dplant_N14") * dt
INIT cellulose_N14 = 0 {g N14 Mg^{-1}soil}
DOCUMENT: Plant residue cellulose.

cellulose_N15(t) = cellulose_N15(t - dt) + (cel_N15 - Dplant_N15") * dt
INIT cellulose_N15 = 0 {g N15 Mg^{-1}soil}
DOCUMENT: Plant residue cellulose.

CO2(t) = CO2(t - dt) + (Rmic_C) * dt
INIT CO2 = 0 {g C Mg^{-1}soil}
DOCUMENT: CO2-C respired by microbial biomass.

labcor1_C(t) = labcor1_C(t - dt) + (Dlab1_C - Dmic1_C") * dt
INIT labcor1_C = 0.0015*plant_Cin {g C Mg^{-1}soil}
DOCUMENT: Labile fraction of microbial corpses.

labcor1_N14(t) = labcor1_N14(t - dt) + (Dlab1_N14 - Dmic1_N14') * dt
INIT labcor1_N14 = labcor1_C 4.5*(1-nat_atab) {g N14 Mg^{-1}soil}
DOCUMENT: Labile fraction of microbial corpses.

labcor1_N15(t) = labcor1_N15(t - dt) + (Dlab1_N15 - Dmic1_N15') * dt
INIT labcor1_N15 = labcor1_C 4.5*nat_atab {g N15 Mg^{-1}soil}
DOCUMENT: Labile fraction of microbial residue.

labcor2_C(t) = labcor2_C(t - dt) + (Dlab2_C - Dmic2_C') * dt
INIT labcor2_C = 0.00025*(0.45*organic_C) {g C Mg^{-1}soil}
DOCUMENT: Labile fraction of microbial corpses.

labcor2_N14(t) = labcor2_N14(t - dt) + (Dlab2_N14 - Dmic2_N14") * dt
INIT labcor2_N14 = labcor2_C 4.5*(1-nat_atab) {g N14 Mg^{-1}soil}
DOCUMENT: Labile fraction of microbial corpses.

labcor2_N15(t) = labcor2_N15(t - dt) + (Dlab2_N15 - Dmic2_N15') * dt
INIT labcor2_N15 = labcor2_C 4.5*nat_atab {g N15 Mg soil}
DOCUMENT: Labile fraction of microbial residue.

labcor3_C(t) = labcor3_C(t - dt) + (Dlab3_C - Dmic3_C') * dt
INIT labcor3_C = 0.00005*(0.55*organic_C) {g C Mg^{-1}soil}
DOCUMENT: Labile fraction of microbial corpses.

labcor3_N14(t) = labcor3_N14(t - dt) + (Dlab3_N14 - Dmic3_N14") * dt
INIT labcor3_N14 = labcor3_C 4.5*(1-nat_atab) {g N14 Mg^{-1}soil}
DOCUMENT: Labile fraction of microbial corpses.

labcor3_N15(t) = labcor3_N15(t - dt) + (Dlab3_N15 - Dmic3_N15') * dt
INIT labcor3_N15 = labcor3_C 4.5*nat_atab {g N15 Mg^{-1}soil}
DOCUMENT: Labile fraction of microbial residue.

labmic1_C(t) = labmic1_C(t - dt) + (flab1_C + Ustglab1_C - Dlab1_C - Smic_C' - Rmic_C') * dt
INIT labmic1_C = 0.02*plant_Cin {g C Mg^{-1}soil}
DOCUMENT: Labile fraction of microbial biomass.

labmic1_N14(t) = labmic1_N14(t - dt) + (flab1_N14 + Zlab1_N14 - Dlab1_N14 - Smic_N14' - Mmic_N14') * dt
INIT labmic1_N14 = labmic1_C 4.5*(1-nat_atab) {g N14 Mg^{-1}soil}
DOCUMENT: Labile fraction of microbial biomass.

labmic1_N15(t) = labmic1_N15(t - dt) + (flab1_N15 + Zlab1_N15 - Dlab1_N15 - Smic_N15' - Mmic_N15') * dt
INIT labmic1_N15 = labmic1_C 4.5*nat_atab {g N15 Mg^{-1}soil}
DOCUMENT: Labile fraction of microbial biomass.

labmic2_C(t) = labmic2_C(t - dt) + (flab2_C + Ustglab2_C - Dlab2_C - Smic_C'' - Rmic_C'') * dt
INIT labmic2_C = 0.001*(0.45*organic_C) {g C Mg^{-1}soil}
DOCUMENT: Labile fraction of microbial biomass.

labmic2_N14(t) = labmic2_N14(t - dt) + (flab2_N14 + Zlab2_N14 - Dlab2_N14 - Smic_N14'' - Mmic_N14'') * dt
INIT labmic2_N14 = labmic2_C 4.5*(1-nat_atab) {g N14 Mg^{-1}soil}
DOCUMENT: Labile fraction of microbial biomass.

labmic2_N15(t) = labmic2_N15(t - dt) + (flab2_N15 + Zlab2_N15 - Dlab2_N15 - Smic_N15'' - Mmic_N15'') * dt
INIT labmic2_N15 = labmic2_C 4.5*nat_atab {g N15 Mg^{-1}soil}
DOCUMENT: Labile fraction of microbial biomass.

labmic3_C(t) = labmic3_C(t - dt) + (flab3_C + Ustglab3_C - Dlab3_C - Smic_C'' - Rmic_C'') * dt
INIT labmic3_C = 0.0001*(0.55*organic_C) {g C Mg^{-1}soil}
DOCUMENT: Labile fraction of microbial biomass.

labmic3_N14(t) = labmic3_N14(t - dt) + (flab3_N14 + Zlab3_N14 - Dlab3_N14 - Smic_N14'' - Mmic_N14'') * dt
INIT labmic3_N14 = labmic3_C 4.5*(1-nat_atab) {g N14 Mg^{-1}soil}
DOCUMENT: Labile fraction of microbial biomass.

labmic3_N15(t) = labmic3_N15(t - dt) + (flab3_N15 + Zlab3_N15 - Dlab3_N15 - Smic_N15'' - Mmic_N15'') * dt
INIT labmic3_N15 = labmic3_C 4.5*nat_atab {g N15 Mg^{-1}soil}
DOCUMENT: Labile fraction of microbial biomass.

lignin_C(t) = lignin_C(t - dt) + (lig_C - Dplant_C'') * dt
INIT lignin_C = 0 {g C Mg^{-1}soil}
DOCUMENT: Plant residue lignin.

lignin_N14(t) = lignin_N14(t - dt) + (lig_N14 - Dplant_N14'') * dt
INIT lignin_N14 = 0 {g N14 Mg^{-1}soil}
DOCUMENT: Plant residue lignin.

lignin_N15(t) = lignin_N15(t - dt) + (lig_N15 - Dplant_N15'') * dt
INIT lignin_N15 = 0 {g N15 Mg^{-1}soil}
DOCUMENT: Plant residue lignin.

miedum_C(t) = miedum_C(t - dt) + (Usol3_C' + Usol2_C' + Usol1_C' + Umic3_C + Umic2_C + Umic1_C) * dt
INIT miedum_C = 0 {g C Mg^{-1}soil}
DOCUMENT: Dummy pool.

miedum_N14(t) = miedum_N14(t - dt) + (Usol2_N14' + Usol3_N14' + Usol1_N14' + Umic2_N14 + Umic1_N14 + Umic3_N14) * dt
INIT miedum_N14 = 0 {g N14 Mg^{-1}soil}
DOCUMENT: Dummy pool holding microbial biomass before partitioning it among populations.

miedum_N15(t) = miedum_N15(t - dt) + (Usol1_N15' + Usol3_N15' + Usol2_N15' + Umic3_N15 + Umic2_N15 + Umic1_N15) * dt
INIT miedum_N15 = 0 {g N15 Mg^{-1}soil}
DOCUMENT: Dummy pool holding microbial biomass before partitioning it among populations.

miedum1_C(t) = miedum1_C(t - dt) + (Umic1_C - fres1_C - flab1_C - fstg1_C) * dt
INIT miedum1_C = 0 {g C Mg^{-1}soil}
DOCUMENT: Dummy pool holding microbial biomass before separating it into labile and resistant fractions

miedum1_N14(t) = miedum1_N14(t - dt) + (Umic1_N14 - fres1_N14 - flab1_N14) * dt
INIT miedum1_N14 = 0 {g N14 Mg^{-1}soil}
DOCUMENT: Dummy pool holding microbial biomass before separating it into labile and resistant fractions

miedum1_N15(t) = miedum1_N15(t - dt) + (Umic1_N15 - fres1_N15 - flab1_N15) * dt
INIT miedum1_N15 = 0 {g N15 Mg^{-1}soil}
DOCUMENT: Dummy pool holding microbial biomass before separating it into labile and resistant fractions of population 1

miedum2_C(t) = miedum2_C(t - dt) + (Umic2_C - fres2_C - flab2_C - fstg2_C) * dt
INIT miedum2_C = 0 {g C Mg^{-1}soil}
DOCUMENT: Dummy pool holding microbial biomass before separating it into labile and resistant fractions

miedum2_N14(t) = miedum2_N14(t - dt) + (Umic2_N14 - fres2_N14 - flab2_N14) * dt
INIT miedum2_N14 = 0 {g N14 Mg^{-1}soil}
DOCUMENT: Dummy pool holding microbial biomass before separating it into labile and resistant fractions of biomass.

miedum2_N15(t) = miedum2_N15(t - dt) + (Umic2_N15 - fres2_N15 - flab2_N15) * dt
INIT miedum2_N15 = 0 {g N15 Mg^{-1}soil}
DOCUMENT: Dummy pool holding microbial biomass before separating it into labile and resistant fractions of population 2

miedum3_C(t) = miedum3_C(t - dt) + (Umic3_C - fres3_C - flab3_C - fstg3_C) * dt
INIT miedum3_C = 0 {g C Mg^{-1}soil}
DOCUMENT: Dummy pool holding microbial biomass before separating it into labile and resistant fractions.

miedum3_N14(t) = miedum3_N14(t - dt) + (Umic3_N14 - fres3_N14 - flab3_N14) * dt
INIT miedum3_N14 = 0 {g N14 Mg^{-1}soil}
DOCUMENT: Dummy pool holding microbial biomass before separating it into labile and resistant fractions biomass.

miedum3_N15(t) = miedum3_N15(t - dt) + (Umic3_N15 - fres3_N15 - flab3_N15) * dt
INIT miedum3_N15 = 0 {g N15 Mg^{-1}soil}
DOCUMENT: Dummy pool holding microbial biomass before separating it into labile and resistant fractions of population 3.

microbial_C = rescor1_C + resmic1_C + miedum1_C + miedum_C + miedum3_C + resmic3_C + stgmic3_C + labmic3_C + labcor3_C + rescor3_C + miedum2_C + resmic2_C + stgmic2_C + labmic2_C + labcor2_C + rescor2_C + labmic1_C + stgmic1_C + labcor1_C

microbial_N14 = rescor3_N14 + resmic3_N14 + miedum3_N14 + miedum_N14 + miedum2_N14 + resmic2_N14 + mindum2_N14 + mindum_N14 + mindum1_N14 + labmic1_N14 + miedum1_N14 + resmic1_N14 + rescor1_N14 + labcor1_N14 + mindum3_N14 + labmic3_N14 + labcor3_N14 + labmic2_N14 + labcor2_N14 + rescor2_N14

microbial_N15 = labmic1_N15 + miedum1_N15 + miedum_N15 + miedum3_N15 + resmic3_N15 + mindum3_N15 + mindum_N15 + mindum2_N15 + labmic2_N15 + miedum2_N15 + resmic2_N15 + rescor2_N15 + labcor2_N15 + mindum1_N15 + resmic1_N15 + rescor1_N15 + labmic3_N15 + labcor3_N15 + rescor3_N15 + labcor1_N15

mindum_N14(t) = mindum_N14(t - dt) + (Zmin_N14' - Zmic2_N14 - Zmic1_N14 - Zmic3_N14) * dt
INIT mindum_N14 = 500 {g N14 Mg^{-1}soil}
DOCUMENT: Dummy pool holding mineral N before partitioning it among microbial populations.

mindum_N15(t) = mindum_N15(t - dt) + (Zmin_N15' - Zmic2_N15 - Zmic3_N15 - Zmic1_N15) * dt
INIT mindum_N15 = 1000 {g N15 Mg^{-1}soil}
DOCUMENT: Dummy pool holding mineral N before partitioning it among microbial populations.

mindum1_N14(t) = mindum1_N14(t - dt) + (Zmic1_N14 - Zlab1_N14 - Zres1_N14) * dt
INIT mindum1_N14 = 1000 {g N14 Mg^{-1}soil}
DOCUMENT: Dummy pool holding immobilized N before designating it as part of the labile or resistant microbial population 1. Initialized at a high value because total immobilization is dependant on labile + resistant immobilization and therefore Zmic is calculated AFTER Zlab and Zres.

mindum1_N15(t) = mindum1_N15(t - dt) + (Zmic1_N15 - Zlab1_N15 - Zres1_N15) * dt
INIT mindum1_N15 = 1000 {g N15 Mg^{-1}soil}
DOCUMENT: Dummy pool holding immobilized N before designating it as part of the labile or resistant microbial population 1. Initialized at a high value because total immobilization is dependant on labile + resistant immobilization and therefore Zmic is calculated AFTER Zlab and Zres.

mindum2_N14(t) = mindum2_N14(t - dt) + (Zmic2_N14 - Zlab2_N14 - Zres2_N14) * dt
INIT mindum2_N14 = 1000 {g N14 Mg^{-1}soil}
DOCUMENT: Dummy pool holding immobilized N before designating it as part of the labile or resistant microbial biomass of population 2. Initialized at a high value because total immobilization is dependant on labile + resistant immobilization and therefore Zmic is calculated AFTER Zlab and Zres.

mindum2_N15(t) = mindum2_N15(t - dt) + (Zmic2_N15 - Zlab2_N15 - Zres2_N15) * dt
INIT mindum2_N15 = 1000 {g N15 Mg^{-1}soil}
DOCUMENT: Dummy pool holding immobilized N before designating it as part of the labile or resistant microbial biomass of population 2. Initialized at a high value because total immobilization is dependant on labile + resistant immobilization and therefore Zmic is calculated AFTER Zlab and Zres.

mindum3_N14(t) = mindum3_N14(t - dt) + (Zmic3_N14 - Zlab3_N14 - Zres3_N14) * dt
INIT mindum3_N14 = 1000 {g N14 Mg^{-1}soil}
DOCUMENT: Dummy pool holding immobilized N before designating it as part of the labile or resistant microbial population 3. Initialized at a high value because total immobilization is dependant on labile + resistant immobilization and therefore Zmic is calculated AFTER Zlab and Zres.

mindum3_N15(t) = mindum3_N15(t - dt) + (Zmic3_N15 - Zlab3_N15 - Zres3_N15) * dt
INIT mindum3_N15 = 1000 {g N15 Mg^{-1}soil}
DOCUMENT: Dummy pool holding immobilized N before designating it as part of the labile or resistant microbial population 3. Initialized at a high value because total immobilization is dependant on labile + resistant immobilization and therefore Zmic is calculated AFTER Zlab and Zres.

mineral_N14(t) = mineral_N14(t - dt) + (Mmic_N14 - Zmin_N14) * dt
INIT mineral_N14 = INITmin_N*(1-nat_atab) {g N14 Mg^{-1}soil}
DOCUMENT: Soluble mineral N.

```
mineral_N15(t) = mineral_N15(t - dt) + (Mmic_N15 - Zmin_N15) * dt
INIT mineral_N15 = INITmin_N*nat_atab {g N15 Mg-1soil}
DOCUMENT: Soluble mineral N.

passive_C(t) = passive_C(t - dt) + (Smic_C - Dpas_C) * dt
INIT passive_C = 0.55*(organic_C-
(adsorbed_C+soluble1_C+soluble2_C+soluble3_C+labmic1_C+resmic1_C+labcor1_C+rescor1_C+labmic2_C+resmic2_C+labcor2_C
rescor2_C+labmic3_C+resmic3_C+labcor3_C+rescor3_C)) {g C Mg-1soil}
DOCUMENT: Passive organic matter.

passive_N14(t) = passive_N14(t - dt) + (Smic_N14 - Dpas_N14) * dt
INIT passive_N14 = passive_C/10.5*(1-nat_atab) {g N14 Mg-1soil}
DOCUMENT: Passive organic matter.

passive_N15(t) = passive_N15(t - dt) + (Smic_N15 - Dpas_N15) * dt
INIT passive_N15 = passive_C/10.5*nat_atab {g N15 Mg-1soil}
DOCUMENT: Passive organic matter.

plant_C = protein_C + pltdum_C + lignin_C + cellulose_C + carbohy_C

plant_N14 = protein_N14 + pltdum_N14 + lignin_N14 + cellulose_N14 + carbohy_N14

plant_N15 = protein_N15 + pltdum_N15 + lignin_N15 + cellulose_N15 + carbohy_N15

pltdum_C(t) = pltdum_C(t - dt) + (plantC_in' - pro_C - lig_C - cel_C - car_C) * dt
INIT pltdum_C = 0 {g C Mg-1soil}
DOCUMENT: Dummy pool holding incoming plant materials before separating them into biochemical components

pltdum_N14(t) = pltdum_N14(t - dt) + (plant_N14in' - pro_N14 - lig_N14 - cel_N14 - car_N14) * dt
INIT pltdum_N14 = 0 {g N14 Mg-1soil}
DOCUMENT: Dummy pool holding incoming plant materials before separating them into biochemical components

pltdum_N15(t) = pltdum_N15(t - dt) + (plantN15_in' - pro_N15 - lig_N15 - cel_N15 - car_N15) * dt
INIT pltdum_N15 = 0 {g N15 Mg-1soil}
DOCUMENT: Dummy pool holding incoming plant materials before separating them into biochemical components

protein_C(t) = protein_C(t - dt) + (pro_C - Dplant_C') * dt
INIT protein_C = 0 {g C Mg-1soil}
DOCUMENT: Plant residue protein.

protein_N14(t) = protein_N14(t - dt) + (pro_N14 - Dplant_N14') * dt
INIT protein_N14 = 0 {g N14 Mg-1soil}
DOCUMENT: Plant residue protein.

protein_N15(t) = protein_N15(t - dt) + (pro_N15 - Dplant_N15') * dt
INIT protein_N15 = 0 {g N15 Mg-1soil}
DOCUMENT: Plant residue protein.

rescor1_C(t) = rescor1_C(t - dt) + (Dres1_C - Dmic1_C") * dt
INIT rescor1_C = 0.0015*plant_Cin {g C Mg-1soil}
DOCUMENT: Resistant fraction of microbial corpses.

rescor1_N14(t) = rescor1_N14(t - dt) + (Dres1_N14 - Dmic1_N14") * dt
INIT rescor1_N14 = rescor1_C/7.5*(1-nat_atab) {g N14 Mg-1soil}
DOCUMENT: Resistant fraction of microbial corpses.

rescor1_N15(t) = rescor1_N15(t - dt) + (Dres1_N15 - Dmic1_N15") * dt
INIT rescor1_N15 = rescor1_C/7.5*nat_atab {g N15 Mg-1soil}
DOCUMENT: Resistant fraction of microbial corpses.

rescor2_C(t) = rescor2_C(t - dt) + (Dres2_C - Dmic2_C") * dt
INIT rescor2_C = 0.0015*(0.45*organic_C) {g C Mg-1soil}
DOCUMENT: Resistant fraction of microbial corpses.

rescor2_N14(t) = rescor2_N14(t - dt) + (Dres2_N14 - Dmic2_N14') * dt
INIT rescor2_N14 = rescor2_C/7.5*(1-nat_atab) {g N14 Mg-1soil}
DOCUMENT: Resistant fraction of microbial corpses.

rescor2_N15(t) = rescor2_N15(t - dt) + (Dres2_N15 - Dmic2_N15") * dt
INIT rescor2_N15 = rescor2_C/7.5*nat_atab {g N15 Mg-1soil}
```

DOCUMENT: Resistant fraction of microbial corpses

rescor3_C(t) = rescor3_C(t - dt) + (Dres3_C - Dmic3_C") * dt
INIT rescor3_C = 0.0005*(0.55*organic_C) {g C Mg^{-1}soil}
DOCUMENT: Resistant fraction of microbial corpses.

rescor3_N14(t) = rescor3_N14(t - dt) + (Dres3_N14 - Dmic3_N14") * dt
INIT rescor3_N14 = rescor3_C/7.5*(1-nat_atab) {g N14 Mg^{-1}soil}
DOCUMENT: Resistant fraction of microbial corpses.

rescor3_N15(t) = rescor3_N15(t - dt) + (Dres3_N15 - Dmic3_N15") * dt
INIT rescor3_N15 = rescor3_C/7.5*nat_atab {g N15 Mg^{-1}soil}
DOCUMENT: Resistant fraction of microbial corpses.

resmic1_C(t) = resmic1_C(t - dt) + (fres1_C + Ustgres1_C - Dres1_C - Smic_C" - Rmic_C") * dt
INIT resmic1_C = 0.02*plant_Cin {g C Mg^{-1}soil}
DOCUMENT: Resistant fraction of microbial biomass.

resmic1_N14(t) = resmic1_N14(t - dt) + (fres1_N14 + Zres1_N14 - Dres1_N14 - Smic_N14"" - Mmic_N14"") * dt
INIT resmic1_N14 = resmic1_C/7.5*(1-nat_atab) {g N14 Mg^{-1}soil}
DOCUMENT: Resistant fraction of microbial biomass.

resmic1_N15(t) = resmic1_N15(t - dt) + (fres1_N15 + Zres1_N15 - Dres1_N15 - Smic_N15" - Mmic_N15") * dt
INIT resmic1_N15 = resmic1_C/7.5*nat_atab {g N15 Mg^{-1}soil}
DOCUMENT: Resistant fraction of microbial biomass.

resmic2_C(t) = resmic2_C(t - dt) + (fres2_C + Ustgres2_C - Dres2_C - Smic_C"" - Rmic_C"") * dt
INIT resmic2_C = 0.015*(0.45*organic_C)/94 {g C Mg^{-1}soil}
DOCUMENT: Resistant fraction of microbial biomass.

resmic2_N14(t) = resmic2_N14(t - dt) + (fres2_N14 + Zres2_N14 - Dres2_N14 - Smic_N14"" - Mmic_N14"") * dt
INIT resmic2_N14 = resmic2_C/7.5*(1-nat_atab) {g N14 Mg^{-1}soil}
DOCUMENT: Resistant fraction of microbial biomass.

resmic2_N15(t) = resmic2_N15(t - dt) + (fres2_N15 + Zres2_N15 - Dres2_N15 - Smic_N15"" - Mmic_N15"") * dt
INIT resmic2_N15 = resmic2_C/7.5*nat_atab {g N15 Mg^{-1}soil}
DOCUMENT: Resistant fraction of microbial biomass.

resmic3_C(t) = resmic3_C(t - dt) + (fres3_C + Ustgres3_C - Dres3_C - Smic_C"" - Rmic_C"") * dt
INIT resmic3_C = 0.003*(0.55*organic_C)/27 {g C Mg^{-1}soil}
DOCUMENT: Resistant fraction of microbial biomass.

resmic3_N14(t) = resmic3_N14(t - dt) + (fres3_N14 + Zres3_N14 - Dres3_N14 - Smic_N14" - Mmic_N14") * dt
INIT resmic3_N14 = resmic3_C/7.5*(1-nat_atab) {g N14 Mg^{-1}soil}
DOCUMENT: Resistant fraction of microbial biomass.

resmic3_N15(t) = resmic3_N15(t - dt) + (fres3_N15 + Zres3_N15 - Dres3_N15 - Smic_N15"" - Mmic_N15"") * dt
INIT resmic3_N15 = resmic3_C/7.5*nat_atab {g N15 Mg^{-1}soil}
DOCUMENT: Resistant fraction of microbial biomass.

soluble1_C(t) = soluble1_C(t - dt) + (Dmic1_C + Dplant_C - Usol1_C - Asol1_C) * dt
INIT soluble1_C = 0.001*plant_Cin {g C Mg^{-1}soil}
DOCUMENT: Organic matter in soil solution.

soluble1_N14(t) = soluble1_N14(t - dt) + (Dmic1_N14 + Dplant_N14 - Usol1_N14 - Asol1_N14) * dt
INIT soluble1_N14 = soluble1_C/10*(1-nat_atab) {g N14 Mg^{-1}soil}

soluble1_N15(t) = soluble1_N15(t - dt) + (Dmic1_N15 + Dplant_N15 - Usol1_N15 - Asol1_N15) * dt
INIT soluble1_N15 = soluble1_C/10*nat_atab {g N15 Mg^{-1}soil}

soluble2_C(t) = soluble2_C(t - dt) + (DadsC + Dact_C + Dmic2_C - Asol2_C - Usol2_C) * dt
INIT soluble2_C = 0.00005*(0.45*organic_C) {g C Mg^{-1}soil}
DOCUMENT: Organic matter in soil solution.

soluble2_N14(t) = soluble2_N14(t - dt) + (Dact_N14 + Dads_N14 + Dmic2_N14 - Asol2_N14 - Usol2_N14) * dt
INIT soluble2_N14 = soluble2_C/10*(1-nat_atab) {g N14 Mg^{-1}soil}

soluble2_N15(t) = soluble2_N15(t - dt) + (Dact_N15 + Dads_N15 + Dmic2_N15 - Asol2_N15 - Usol2_N15) * dt
INIT soluble2_N15 = soluble2_C/10*nat_atab {g N15 Mg^{-1}soil}

soluble3_C(t) = soluble3_C(t - dt) + (Dpas_C + Dmic3_C - Asol3_C - Usol3_C) * dt

INIT soluble3_C = 0.000005*(0.55*organic_C) {g C Mg^{-1}soil}
DOCUMENT: Organic matter in soil solution.

soluble3_N14(t) = soluble3_N14(t - dt) + (Dpas_N14 + Dmic3_N14 - Usol3_N14 - Asol3_N14) * dt
INIT soluble3_N14 = soluble3_C*10*(1-nat_atab) {g N14 Mg^{-1}soil}

soluble3_N15(t) = soluble3_N15(t - dt) + (Dpas_N15 + Dmic3_N15 - Usol3_N15 - Asol3_N15) * dt
INIT soluble3_N15 = soluble3_C*10*nat_atab {g 15 Mg^{-1}soil}
DOCUMENT: Organic matter in soil solution.

stgmic1_C(t) = stgmic1_C(t - dt) + (fstg1_C - Ustglab1_C - Ustgres1_C) * dt
INIT stgmic1_C = 0 {g C Mg^{-1} soil}
DOCUMENT: Microbial storage as exocellular material.

stgmic2_C(t) = stgmic2_C(t - dt) + (fstg2_C - Ustglab2_C - Ustgres2_C) * dt
INIT stgmic2_C = 0 {g C Mg^{-1} soil}
DOCUMENT: Microbial storage as exocellular material.

stgmic3_C(t) = stgmic3_C(t - dt) + (fstg3_C - Ustglab3_C - Ustgres3_C) * dt
INIT stgmic3_C = 0 {g C Mg^{-1} soil}
DOCUMENT: Microbial storage as exocellular material.

TimmobilizedN14(t) = TimmobilizedN14(t - dt) + (RimmN14) * dt
INIT TimmobilizedN14 = 0
DOCUMENT: Total N14 immobilized.

TimmobilizedN15(t) = TimmobilizedN15(t - dt) + (RimmN15) * dt
INIT TimmobilizedN15 = 0
DOCUMENT: Total N15 immobilized.

TmicinC(t) = TmicinC(t - dt) + (RmicinC) * dt
INIT TmicinC = 0
DOCUMENT: Total input of non-plant residue C into microbial biomass.

TmicinN14(t) = TmicinN14(t - dt) + (RmicinN14) * dt
INIT TmicinN14 = 0
DOCUMENT: Total input of non-plant residue N14 into microbial biomass.

TmicinN15(t) = TmicinN15(t - dt) + (RmicinN15) * dt
INIT TmicinN15 = 0
DOCUMENT: Total input of non-plant residue N15 into microbial biomass.

TmicoutC(t) = TmicoutC(t - dt) + (RmicoutC) * dt
INIT TmicoutC = 0
DOCUMENT: Total C output from microbial biomass.

TmicoutN14(t) = TmicoutN14(t - dt) + (RmicoutN14) * dt
INIT TmicoutN14 = 0
DOCUMENT: Total N14 output from microbial biomass.

TmicoutN15(t) = TmicoutN15(t - dt) + (RmicoutN15) * dt
INIT TmicoutN15 = 0
DOCUMENT: Total N15 output from microbial biomass.

Tmineralized_N15(t) = Tmineralized_N15(t - dt) + (RminN15) * dt
INIT Tmineralized_N15 = 0
DOCUMENT: Total N15 mineralized.

TmineralizedN14(t) = TmineralizedN14(t - dt) + (RminN14) * dt
INIT TmineralizedN14 = 0
DOCUMENT: Total N14 mineralized.

TplantN15_in(t) = TplantN15_in(t - dt) + (FplantN15_in) * dt
INIT TplantN15_in = 0 {g N15 Mg^{-1}soil}
DOCUMENT: Total plant residue N15 added to soil.

Flows

Asol1_C = IF(Qadsorb>adsorbed_C) THEN(0.001*MIN(soluble1_C,Qadsorb-adsorbed_C)) ELSE(0.0001*MAX(-adsorbed_C,Qadsorb-adsorbed_C)) {g C Mg^{-1}soil h^{-1};

DOCUMENT: Rate of adsorption and desorption of soluble organics.
0.001 equilibrium rate of adsorption {h^{-1}}
0.0001 equilibrium rate of desorption {h^{-1}}

Asol1_N14 = IF(Asol1_C>0) THEN(Asol1_C*(sol1_N/soluble1_C)*(soluble1_N14/sol1_N)) ELSE(Asol1_C*(adsorbed_N/adsorbed_C)*(adsorbed_N14/adsorbed_N)) {g N14 Mg^{-1}soil h^{-1}}
DOCUMENT: Rate of adsorption and desorption of soluble organics.

Asol1_N15 = IF(Asol1_C>0) THEN(Asol1_C*(sol1_N/soluble1_C)*(soluble1_N15/sol1_N)) ELSE(Asol1_C*(adsorbed_N/adsorbed_C)*(adsorbed_N15/adsorbed_N)) {g N15 Mg^{-1}soil h^{-1}}
DOCUMENT: Rate of adsorption and desorption of soluble organics.

Asol2_C = IF(Qadsorb>adsorbed_C) THEN(0.001*MIN(soluble2_C,Qadsorb-adsorbed_C)) ELSE(0.0001*MAX(-adsorbed_C,Qadsorb-adsorbed_C)) {g C Mg^{-1}soil h^{-1}}
DOCUMENT: Rate of adsorption and desorption of soluble organics.
0.001 equilibrium rate of adsorption {h^{-1}}
0.0001 equilibrium rate of desorption {h^{-1}}

Asol2_N14 = IF(Asol2_C>0) THEN(Asol2_C*(sol2_N/soluble2_C)*(soluble2_N14/sol2_N)) ELSE(Asol2_C*(adsorbed_N/adsorbed_C)*(adsorbed_N14/adsorbed_N)) {g N14 Mg^{-1}soil h^{-1}}
DOCUMENT: Rate of adsorption and desorption of soluble organics.

Asol2_N15 = IF(Asol2_C>0) THEN(Asol2_C*(sol2_N/soluble2_C)*(soluble2_N15/sol2_N)) ELSE(Asol2_C*(adsorbed_N/adsorbed_C)*(adsorbed_N15/adsorbed_N)) {g N15 Mg^{-1}soil h^{-1}}
DOCUMENT: Rate of adsorption and desorption of soluble organics.

Asol3_C = IF(Qadsorb>adsorbed_C) THEN(0.001*MIN(soluble3_C,Qadsorb-adsorbed_C)) ELSE(0.0001*MAX(-adsorbed_C,Qadsorb-adsorbed_C)) {g C Mg^{-1}soil h^{-1}}
DOCUMENT: Rate of adsorption and desorption of soluble organics.
0.001 equilibrium rate of adsorption {h^{-1}}
0.0001 equilibrium rate of desorption {h^{-1}}

Asol3_N14 = IF(Asol3_C>0) THEN(Asol3_C*(sol3_N/soluble3_C)*(soluble3_N14/sol3_N)) ELSE(Asol3_C*(adsorbed_N/adsorbed_C)*(adsorbed_N14/adsorbed_N)) {g N14 Mg^{-1}soil h^{-1}}
DOCUMENT: Rate of adsorption and desorption of soluble organics.

Asol3_N15 = IF(Asol3_C>0) THEN(Asol3_C*(sol3_N/soluble3_C)*(soluble3_N15/sol3_N)) ELSE(Asol3_C*(adsorbed_N/adsorbed_C)*(adsorbed_N15/adsorbed_N)) {g N15 Mg^{-1}soil h^{-1}}
DOCUMENT: Rate of adsorption and desorption of soluble organics.

Cads_C = 0.5E-4*adsorbed_C*ftg {g C Mg^{-1}soil h^{-1}}
DOCUMENT: Rate of chemical stabilization of adsorbed component to active organic matter.
0.5E-4 specific rate of stabilization {h^{-1}}

Cads_N14 = Cads_C*(adsorbed_N/adsorbed_C)*(adsorbed_N14/adsorbed_N) {g N14 Mg^{-1}soil h^{-1}}
DOCUMENT: Rate of chemical stabilization of adsorbed component to active organic matter.

Cads_N14 = Cads_C*(adsorbed_N/adsorbed_C)*(adsorbed_N14/adsorbed_N) {g N14 Mg^{-1}soil h^{-1}}
DOCUMENT: Rate of chemical stabilization of adsorbed component to active organic matter.

Cads_N15 = Cads_C*(adsorbed_N/adsorbed_C)*(adsorbed_N15/adsorbed_N) {g N15 Mg^{-1}soil h^{-1}}
DOCUMENT: Rate of chemical stabilization of adsorbed component to active organic matter.

car_C = fcarC*plantC_in' {g C Mg^{-1}soil h^{-1}}
DOCUMENT: Carbohydrate entering soil system.

car_N14 = car_C/carCN*(1-plant_atab) {g N14 Mg^{-1}soil h^{-1}}
DOCUMENT: Carbohydrate entering soil system.

car_N15 = car_C/carCN*plant_atab {g N15 Mg^{-1}soil h^{-1}}
DOCUMENT: Carbohydrate entering soil system.

cel_C = fcelC*plantC_in' {g C Mg^{-1}soil h^{-1}}
DOCUMENT: Cellulose entering soil system.

cel_N14 = cel_C/celCN*(1-plant_atab) {g N14 Mg^{-1}soil h^{-1}}
DOCUMENT: Cellulose entering soil system.

cel_N15 = cel_C/celCN*plant_atab {g N15 Mg^{-1}soil h^{-1}}
DOCUMENT: Cellulose entering soil system.

Dact_C = 0.02*actmic_C*fdactiveC*ftg {g C Mg^{-1}soil h^{-1}}
DOCUMENT: Rate of decomposition of active organic matter.
0.02 specific rate of decomposition of active C {g C g^{-1}actmic C h^{-1}}

Dact_N14 = Dact_C*(active_N/active_C)*(active_N14/active_N) {g N14 Mg^{-1}soil h^{-1}}
DOCUMENT: Rate of decomposition of active organic matter.

Dact_N15 = Dact_C*(active_N/active_C)*(active_N15/active_N) {g N15 Mg^{-1}soil h^{-1}}
DOCUMENT: Rate of decomposition of active organic matter.

Dads_N14 = DadsC*(adsorbed_N/adsorbed_C)*(adsorbed_N14/adsorbed_N) {g N14Mg^{-1}soil h^{-1}}
DOCUMENT: Rate of decomposition of adsorbed organic matter.

Dads_N15 = DadsC*(adsorbed_N/adsorbed_C)*(adsorbed_N15/adsorbed_N) {g N15 Mg^{-1}soil h^{-1}}
DOCUMENT: Rate of decomposition of adsorbed organic matter.

DadsC = MIN(0.5*adsorbed_C,0.024*actmic_C*fdadsorbedC*ftg) {g C Mg^{-1}soil h^{-1}}
DOCUMENT: Rate of decomposition of adsorbed organic matter.
0.024=specific rate of decomposition of adsorbed organic matter {g C g^{-1}actmic C h^{-1}}

Dlab1_C = Ilabmic1_C-Smic_C' {g C Mg^{-1}soil h^{-1}}
DOCUMENT: Rate of transfer of inactivated labile microbial biomass to microbial corpses.

Dlab1_N14 = Dlab1_C*(labmic1_N/labmic1_C)*(labmic1_N14/labmic1_N) {g N14 Mg^{-1}soil h^{-1}}
DOCUMENT: Rate of transfer of inactivated labile microbial biomass to microbial corpses.

Dlab1_N15 = Dlab1_C*(labmic1_N/labmic1_C)*(labmic1_N15/labmic1_N) {g N15 Mg^{-1}soil h^{-1}}
DOCUMENT: Rate of transfer of inactivated labile microbial biomass to microbial corpses.

Dlab2_C = Ilabmic2_C-Smic_C'' {g C Mg^{-1}soil h^{-1}}
DOCUMENT: Rate of transfer of inactivated labile microbial biomass to microbial corpses.

Dlab2_N14 = Dlab2_C*(labmic2_N/labmic2_C)*(labmic2_N14/labmic2_N) {g N14 Mg^{-1}soil h^{-1}}
DOCUMENT: Rate of transfer of inactivated labile microbial biomass to microbial corpses.

Dlab2_N15 = Dlab2_C*(labmic2_N/labmic2_C)*(labmic2_N15/labmic2_N) {g N15 Mg^{-1}soil h^{-1}}
DOCUMENT: Rate of transfer of inactivated labile microbial biomass to microbial corpses.

Dlab3_C = Ilabmic3_C-Smic_C''' {g C Mg^{-1}soil h^{-1}}
DOCUMENT: Rate of transfer of inactivated labile microbial biomass to microbial corpses.

Dlab3_N14 = Dlab3_C*(labmic3_N/labmic3_C)*(labmic3_N14/labmic3_N) {g N14 Mg^{-1}soil h^{-1}}
DOCUMENT: Rate of transfer of inactivated labile microbial biomass to microbial corpses.

Dlab3_N15 = Dlab3_C*(labmic3_N/labmic3_C)*(labmic3_N15/labmic3_N) {g N15 Mg^{-1}soil h^{-1}}
DOCUMENT: Rate of transfer of inactivated labile microbial biomass to microbial corpses.

Dmic1_C = Dmic1_C' + Dmic1_C'' {g C Mg^{-1}soil h^{-1}}
DOCUMENT: Decomposition rate of microbial corpses.

Dmic1_C' = 0.10*rescor1_C/miccor1_C*Pmiccor1 {g C Mg^{-1}soil h^{-1}}
DOCUMENT: Rate of decomposition of resistant microbial corpses.
0.10=specific rate of decomposition of resistant microbial corpses {g g^{-1}actmic C h^{-1}}

Dmic1_C'' = 0.5*labcor1_C/miccor1_C*Pmiccor1 {g C Mg^{-1}soil h^{-1}}
DOCUMENT: Rate of decomposition of labile microbial corpses.
0.5=specific rate of decomposition of labile microbial corpses {g g^{-1}actmic C h^{-1}}

Dmic1_N14 = Dmic1_N14' + Dmic1_N14'' {g N14 Mg^{-1}soil h^{-1}}
DOCUMENT: Total decomposition rate of microbial corpses.

Dmic1_N14' = Dmic1_C'*(rescor1_N/rescor1_C)*(rescor1_N14/rescor1_N) {g N14 Mg^{-1}soil h^{-1}}
DOCUMENT: Rate of decomposition of labile microbial corpses.

Dmic1_N14'' = Dmic1_C'*(rescor1_N/rescor1_C)*(rescor1_N14/rescor1_N) {g N14 Mg^{-1}soil h^{-1}}
DOCUMENT: Rate of decomposition of resistant microbial corpses.

Dmic1_N15 = Dmic1_N15' + Dmic1_N15'' {g N15 Mg^{-1}soil h^{-1}}
DOCUMENT: Decomposition rate of microbial corpses.

Dmic1_N15' = Dmic1_C''*(labcor1_N/labcor1_C)*(labcor1_N15/labcor1_N) {g N15 Mg^{-1}soil h^{-1}}

DOCUMENT: Rate of decomposition of labile microbial corpses.

Dmic1_N15" = Dmic1_C"*(rescor1_N/rescor1_C)*(rescor1_N15/rescor1_N) {g N15 Mg^{-1}soil h^{-1}}
DOCUMENT: Rate of decomposition of resistant microbial corpses.

Dmic2_C = Dmic2_C' + Dmic2_C" {g C Mg^{-1}soil h^{-1}}
DOCUMENT: Decomposition rate of microbial corpses.

Dmic2_C' = 0.5*labcor2_C/miccor2_C*Pmiccor2 {g C Mg^{-1}soil h^{-1}}
DOCUMENT: Rate of decomposition of labile microbial corpses.
0.5: specific rate of decomposition of labile microbial corpses {g g^{-1}actmic C h^{-1}}

Dmic2_C" = 0.10*rescor2_C/miccor2_C*Pmiccor2 {g C Mg^{-1}soil h^{-1}}
DOCUMENT: Rate of decomposition of resistant microbial corpses.
0.10: specific rate of decomposition of resistant microbial corpses {g g^{-1}actmic C h^{-1}}

Dmic2_N14 = Dmic2_N14' + Dmic2_N14" {g N14 Mg^{-1}soil h^{-1}}
DOCUMENT: Decomposition rate of microbial corpses.

Dmic2_N14' = Dmic2_C"*(rescor2_N/rescor2_C)*(rescor2_N14/rescor2_N) {g N14 Mg^{-1}soil h^{-1}}
DOCUMENT: Rate of decomposition of resistant microbial corpses.

Dmic2_N14" = Dmic2_C"*(labcor2_N/labcor2_C)*(labcor2_N14/labcor2_N) {g N14 Mg^{-1}soil h^{-1}}
DOCUMENT: Rate of decomposition of labile microbial corpses.

Dmic2_N15 = Dmic2_N15' + Dmic2_N15" {g N15 Mg^{-1}soil h^{-1}}
DOCUMENT: Decomposition of microbial corpses.

Dmic2_N15' = Dmic2_C"*(labcor2_N/labcor2_C)*(labcor2_N15/labcor2_N) {g N15 Mg^{-1}soil h^{-1}}
DOCUMENT: Rate of decomposition of labile microbial corpses.

Dmic2_N15" = Dmic2_C"*(rescor2_N/rescor2_C)*(rescor2_N15/rescor2_N) {g N15 Mg^{-1}soil h^{-1}}
DOCUMENT: Rate of decomposition of resistant microbial corpses.

Dmic3_C = Dmic3_C' + Dmic3_C" {g C Mg^{-1}soil h^{-1}}
DOCUMENT: Decomposition rate of microbial corpses.

Dmic3_C' = 0.5*labcor3_C/miccor3_C*Pmiccor3 {g C Mg^{-1}soil h^{-1}}
DOCUMENT: Rate of decomposition of labile microbial corpses.
0.5: specific rate of decomposition of labile microbial corpses {g g^{-1}actmic C h^{-1}}

Dmic3_C" = 0.10*rescor3_C/miccor3_C*Pmiccor3 {g C Mg^{-1}soil h^{-1}}
DOCUMENT: Rate of decomposition of resistant microbial corpses.
0.10: specific rate of decomposition of resistant microbial corpses {g g^{-1}actmic C h^{-1}}

Dmic3_N14 = Dmic3_N14' + Dmic3_N14" {g N14 Mg^{-1}soil h^{-1}}
DOCUMENT: Decomposition rate of microbial corpses

Dmic3_N14' = Dmic3_C"*(rescor3_N/rescor3_C)*(rescor3_N14/rescor3_N) {g N14 Mg^{-1}soil h^{-1}}
DOCUMENT: Rate of decomposition of resistant microbial corpses.

Dmic3_N14" = Dmic3_C"*(labcor3_N/labcor3_C)*(labcor3_N14/labcor3_N) {g N14 Mg^{-1}soil h^{-1}}
DOCUMENT: Rate of decomposition of labile microbial corpses.

Dmic3_N15 = Dmic3_N15' + Dmic3_N15" {g N15 Mg^{-1}soil h^{-1}}
DOCUMENT: Decomposition rate of microbial corpses.

Dmic3_N15' = Dmic3_C"*(labcor3_N/labcor3_C)*(labcor3_N15/labcor3_N) {g N15 Mg^{-1}soil h^{-1}}
DOCUMENT: Rate of decomposition of labile microbial corpses.

Dmic3_N15" = Dmic3_C"*(rescor3_N/rescor3_C)*(rescor3_N15/rescor3_N) {g N15 Mg^{-1}soil h^{-1}}
DOCUMENT: Rate of decomposition of resistant microbial corpses.

Dpas_C = 0.005*actmic_C*fdpassiveC*flg {g C Mg^{-1}soil h^{-1}}
DOCUMENT: Rate of decomposition of passive organic matter.
0.005: specific rate of decomposition of passive organic matter {g g^{-1}actmic C h^{-1}}

Dpas_N14 = Dpas_C*(passive_N/passive_C)*(passive_N14/passive_N) {g N14 Mg^{-1}soil h^{-1}}
DOCUMENT: Rate of decomposition of passive organic matter.

Dpas_N15 = Dpas_C*(passive_N/passive_C)*(passive_N15/passive_N) {g N15 Mg^{-1}soil h^{-1}}

DOCUMENT: Rate of decomposition of passive organic matter.

Dplant_C = Dplant_C' + Dplant_C" + Dplant_C"' + Dplant_C"" {g C Mg^{-1}soil h^{-1}}
DOCUMENT: Total decomposition rate of plant residues.

Dplant_C' = 1.00*protein_C TplantC*PplantC {g C Mg^{-1}soil h^{-1}}
DOCUMENT: Rate of decomposition of plant residue protein.
1.00 specific rate of decomposition of plant protein {g g^{-1}actmic C h^{-1}}

Dplant_C" = 1.00*carbohy_C TplantC*PplantC {g C Mg^{-1}soil h^{-1}}
DOCUMENT: Rate of decomposition of plant residue carbohydrate.
1.00 specific rate of decomposition of plant carbohydrate {g g^{-1}actmic C h^{-1}}

Dplant_C"' = 0.15*cellulose_C TplantC*PplantC {g C Mg^{-1}soil h^{-1}}
DOCUMENT: Rate of decomposition of plant residue cellulose.
0.15 specific rate of decomposition of plant cellulose {g g^{-1}actmic C h^{-1}}

Dplant_C"" = 0.025*lignin_C TplantC*PplantC {g C Mg^{-1}soil h^{-1}}
DOCUMENT: Rate of decomposition of plant residue lignin.
0.025=specific rate of decomposition of plant lignin {g g^{-1}actmic C h^{-1}}

Dplant_N14 = Dplant_N14' + Dplant_N14" + Dplant_N14"' + Dplant_N14"" {g N14 Mg^{-1}soil h^{-1}}
DOCUMENT: Total decomposition rate of plant residues.

Dplant_N14' = Dplant_C' proCN*(protein_N14/pro_N) {g N14 Mg^{-1}soil h^{-1}}
DOCUMENT: Rate of decomposition of plant residue protein.

Dplant_N14" = Dplant_C" carCN*(carbohy_N14 car_N) {g N14 Mg^{-1}soil h^{-1}}
DOCUMENT: Rate of decomposition of plant residue carbohydrate.

Dplant_N14"' = Dplant_C"' celCN*(cellulose_N14 cel_N) {g N14 Mg^{-1}soil h^{-1}}
DOCUMENT: Rate of decomposition of plant residue cellulose.

Dplant_N14"" = Dplant_C"" ligCN*(lignin_N14 lig_N) {g N14 Mg^{-1}soil h^{-1}}
DOCUMENT: Rate of decomposition of plant residue lignin.

Dplant_N15 = Dplant_N15' + Dplant_N15" + Dplant_N15"' + Dplant_N15"" {g N15 Mg^{-1}soil h^{-1}}
DOCUMENT: Total decomposition rate of plant residues.

Dplant_N15' = Dplant_C' proCN*(protein_N15/pro_N) {g N15 Mg^{-1}soil h^{-1}}
DOCUMENT: Rate of decomposition of plant residue protein.
Soil Input Sector

Dplant_N15" = Dplant_C" carCN*(carbohy_N15 car_N) {g N15 Mg^{-1}soil h^{-1}}
DOCUMENT: Rate of decomposition of plant residue carbohydrate.

Dplant_N15"' = Dplant_C"' celCN*(cellulose_N15 cel_N) {g N15 Mg^{-1}soil h^{-1}}
DOCUMENT: Rate of decomposition of plant residue cellulose.

Dplant_N15"" = Dplant_C"" ligCN*(lignin_N15 lig_N) {g N15 Mg^{-1}soil h^{-1}}
DOCUMENT: Rate of decomposition of plant residue lignin.

Dres1_C = Iresmic1_C-Smic_C" {g C Mg^{-1}soil h^{-1}}
DOCUMENT: Rate of transfer of inactivated resistant microbial biomass to microbial corpses.

Dres1_N14 = Dres1_C*(resmic1_N/resmic1_C)*(resmic1_N14/resmic1_N) {g N14 Mg^{-1}soil h^{-1}}
DOCUMENT: Rate of transfer of inactivated resistant microbial biomass to microbial corpses.

Dres1_N15 = Dres1_C*(resmic1_N/resmic1_C)*(resmic1_N15/resmic1_N) {g N15 Mg^{-1}soil h^{-1}}
DOCUMENT: Rate of transfer of inactivated resistant microbial biomass to microbial corpses.

Dres2_C = Iresmic2_C-Smic_C"' {g C Mg^{-1}soil h^{-1}}
DOCUMENT: Rate of transfer of inactivated resistant microbial biomass to microbial corpses.

Dres2_N14 = Dres2_C*(resmic2_N/resmic2_C)*(resmic2_N14/resmic2_N) {g N14 Mg^{-1}soil h^{-1}}
DOCUMENT: Rate of transfer of inactivated resistant microbial biomass to microbial corpses.

Dres2_N15 = Dres2_C*(resmic2_N/resmic2_C)*(resmic2_N15/resmic2_N) {g N15 Mg^{-1}soil h^{-1}}
DOCUMENT: Rate of transfer of inactivated resistant microbial biomass to microbial corpses.

Dres3_C = Iresmic3_C-Smic_C"" {g C Mg^{-1}soil h^{-1}}

DOCUMENT Rate of transfer of inactivated resistant microbial biomass to microbial corpses

Dres3_N14 Dres3_C*(resmic3_N/resmic3_C)*(resmic3_N14/resmic3_N) {g N14 Mg^{-1}soil h^{-1}}
DOCUMENT: Rate of transfer of inactivated resistant microbial biomass to microbial corpses.

Dres3_N15 Dres3_C*(resmic3_N/resmic3_C)*(resmic3_N15/resmic3_N) {g N15 Mg^{-1}soil h^{-1}}
DOCUMENT: Rate of transfer of inactivated resistant microbial biomass to microbial corpses.

flab1_C (1-fstorage)*0.55*Umic1_C {g C Mg^{-1}soil h^{-1}}
DOCUMENT: Fraction of substrate uptake assigned to labile microbial biomass.

flab1_N14 0.55*Umic1_N14 {g N14 Mg^{-1}soil h^{-1}}
DOCUMENT: Fraction of substrate uptake assigned to labile microbial biomass.

flab1_N15 0.55*Umic1_N15 {g N15 Mg^{-1}soil h^{-1}}
DOCUMENT: Fraction of substrate uptake assigned to labile microbial biomass.

flab2_C (1-fstorage)*0.55*Umic2_C {g C Mg^{-1}soil h^{-1}}
DOCUMENT: Fraction of substrate uptake assigned to labile microbial biomass.

flab2_N14 0.55*Umic2_N14 {g N14 Mg^{-1}soil h^{-1}}
DOCUMENT: Fraction of substrate uptake assigned to labile microbial biomass.

flab2_N15 0.55*Umic2_N15 {g N15 Mg^{-1}soil h^{-1}}
DOCUMENT: Fraction of substrate uptake assigned to labile microbial biomass.

flab3_C (1-fstorage)*0.55*Umic3_C {g C Mg^{-1}soil h^{-1}}
DOCUMENT: Fraction of substrate uptake assigned to labile microbial biomass.

flab3_N14 0.55*Umic3_N14 {g N14 Mg^{-1}soil h^{-1}}
DOCUMENT: Fraction of substrate uptake assigned to labile microbial biomass.

flab3_N15 0.55*Umic3_N15 {g N15 Mg^{-1}soil h^{-1}}
DOCUMENT: Fraction of substrate uptake assigned to labile microbial biomass.

FplantN15_in plantN15_in

fres1_C (1-fstorage)*0.45*Umic1_C {g C Mg^{-1}soil h^{-1}}
DOCUMENT: Fraction of substrate uptake assigned to resistant biomass.

fres1_N14 0.45*Umic1_N14 {g N14 Mg^{-1}soil h^{-1}}
DOCUMENT: Fraction of substrate uptake assigned to resistant biomass.

fres1_N15 0.45*Umic1_N15 {g N15 Mg^{-1}soil h^{-1}}
DOCUMENT: Fraction of substrate uptake assigned to resistant biomass.

fres2_C (1-fstorage)*0.45*Umic2_C {g C Mg^{-1}soil h^{-1}}
DOCUMENT: Fraction of substrate uptake assigned to resistant biomass.

fres2_N14 0.45*Umic2_N14 {g N14 Mg^{-1}soil h^{-1}}
DOCUMENT: Fraction of substrate uptake assigned to resistant biomass.

fres2_N15 0.45*Umic2_N15 {g N15 Mg^{-1}soil h^{-1}}
DOCUMENT: Fraction of substrate uptake assigned to resistant biomass.

fres3_C (1-fstorage)*0.45*Umic3_C {g C Mg^{-1}soil h^{-1}}
DOCUMENT: Fraction of substrate uptake assigned to resistant biomass.

fres3_N14 0.45*Umic3_N14 {g N14 Mg^{-1}soil h^{-1}}
DOCUMENT: Fraction of substrate uptake assigned to resistant biomass.

fres3_N15 0.45*Umic3_N15 {g N15 Mg^{-1}soil h^{-1}}
DOCUMENT: Fraction of substrate uptake assigned to resistant biomass.

fstg1_C fstorage*Umic1_C {g Mg^{-1}soil h^{-1}}
DOCUMENT: Fraction of uptake assigned to microbial storage.

fstg2_C fstorage*Umic2_C {g Mg^{-1}soil h^{-1}}
DOCUMENT: Fraction of uptake assigned to microbial storage.

fstg3_C fstorage*Umic3_C {g Mg^{-1}soil h^{-1}}

DOCUMENT: Fraction of uptake assigned to microbial storage.

Ilabmic1_C = IF(Rspecific1>Rmmic1) THEN(0.0125*labmic1_C*ftg) ELSE(0.0125*labmic1_C*ftg-Rmlabmic1*(Rmmic1-Rspecific1)/Rmmic1) {g C Mg^{-1}soil h^{-1}}
DOCUMENT: Inactivation of labile microbial biomass.
0.0125=specific inactivation at 30C {g C g^{-1}labmic C h^{-1}}

Ilabmic2_C = IF(Rspecific2>Rmmic2) THEN(0.0125*labmic2_C*ftg) ELSE(0.0125*labmic2_C*ftg-Rmlabmic2*(Rmmic2-Rspecific2)/Rmmic2) {g C Mg^{-1}soil h^{-1}}
DOCUMENT: Inactivation of labile microbial biomass.
0.0125=specific inactivation at 30C {g C g^{-1}labmic C h^{-1}}

Ilabmic3_C = IF(Rspecific3>Rmmic3) THEN(0.0125*labmic3_C*ftg) ELSE(0.0125*labmic3_C*ftg-Rmlabmic3*(Rmmic3-Rspecific3)/Rmmic3) {g C Mg^{-1}soil h^{-1}}
DOCUMENT: Inactivation of labile microbial biomass.
0.0125=specific inactivation at 30C {g C g^{-1}labmic C h^{-1}}

Iresmic1_C = IF(Rspecific1>Rmmic1) THEN(0.00035*resmic1_C*ftg) ELSE(0.00035*resmic1_C*ftg-Rmresmic1*(Rmmic1-Rspecific1)/Rmmic1) {g C Mg^{-1}soil h^{-1}}
DOCUMENT: Inactivation of resistant microbial biomass.
0.00035=specific inactivation at 30C {g C g^{-1}resmic C h^{-1}}

Iresmic2_C = IF(Rspecific2>Rmmic2) THEN(0.00035*resmic2_C*ftg) ELSE(0.00035*resmic2_C*ftg-Rmresmic2*(Rmmic2-Rspecific2)/Rmmic2) {g C Mg^{-1}soil h^{-1}}
DOCUMENT: Inactivation of resistant microbial biomass.
0.00035=specific inactivation at 30C {g C g^{-1}resmic C h^{-1}}

Iresmic3_C = IF(Rspecific3>Rmmic3) THEN(0.00035*resmic3_C*ftg) ELSE(0.00035*resmic3_C*ftg-Rmresmic3*(Rmmic3-Rspecific3)/Rmmic3) {g C Mg^{-1}soil h^{-1}}
DOCUMENT: Inactivation of resistant microbial biomass.
0.00035=specific inactivation at 30C {g C g^{-1}resmic C h^{-1}}

lig_C = fligC*plantC_in' {g C Mg^{-1}soil h^{-1}}
DOCUMENT: Lignin entering soil system.

lig_N14 = lig_C/ligCN*(1-plant_atab) {g N14 Mg^{-1}soil h^{-1}}
DOCUMENT: Lignin entering soil system.

lig_N15 = lig_C/ligCN*plant_atab {g N15Mg^{-1}soil h^{-1}}
DOCUMENT: Lignin entering soil system.

miccor1_C = labcor1_C+rescor1_C {g C Mg^{-1}soil}

miccor2_C = labcor2_C+rescor2_C {g C Mg^{-1}soil}

miccor3_C = labcor3_C+rescor3_C {g C Mg^{-1}soil}

Mmic_N14' = IF(labmic1_C/labmic1_N>4.5) THEN((labmic1_N-labmic1_C/4.5)*(labmic1_N14/labmic1_N)) ELSE(0) {g N14 Mg $^{-1}$soil h^{-1}}
DOCUMENT: Mineralization rate of 'excess' microbial N.
4.5=preferred C:N ratio of labmic

Mmic_N14" = IF(resmic3_C/resmic3_N>7.5) THEN((resmic3_N-resmic3_C/7.5)*(resmic3_N14/resmic3_N)) ELSE(0) {g N14 Mg $^{-1}$soil h^{-1}}
DOCUMENT: Rate of mineralization of 'excess' microbial N.
7.5=preferred C:N ratio of resmic

Mmic_N14''' = IF(labmic3_C/labmic3_N>4.5) THEN((labmic3_N-labmic3_C/4.5)*(labmic3_N14/labmic3_N)) ELSE(0) {g N14 Mg $^{-1}$soil h^{-1}}
DOCUMENT: Mineralization rate of 'excess' microbial N.
4.5=preferred C:N ratio of labmic

Mmic_N14'''' = IF(resmic2_C/resmic2_N>7.5) THEN((resmic2_N-resmic2_C/7.5)*(resmic2_N14/resmic2_N)) ELSE(0) {g N14 Mg $^{-1}$soil h^{-1}}
DOCUMENT: Rate of mineralization of 'excess' microbial N.
7.5=preferred C:N ratio of resmic

Mmic_N14''''' = IF(labmic2_C/labmic2_N>4.5) THEN((labmic2_N-labmic2_C/4.5)*(labmic2_N14/labmic2_N)) ELSE(0) {g N14 Mg $^{-1}$soil h^{-1}}
DOCUMENT: Mineralization rate of 'excess' microbial N.
4.5=preferred C:N ratio of labmic

Mmic_N14"" IF(resmic1_C resmic1_N 7.5) THEN((resmic1_N-resmic1_C 7.5)*(resmic1_N14 resmic1_N)) ELSE(0) {g N14 Mg $^{-1}$soil h^{-1}}
DOCUMENT: Rate of mineralization of 'excess' microbial N
7.5 preferred C:N ratio of resmic

Mmic_N15 Mmic_N15' + Mmic_N15" + Mmic_N15"" + Mmic_N15""" + Mmic_N15"""" {g N15 Mg^{-1}soil h^{-1}}
DOCUMENT: Total microbial mineralization rate.

Mmic_N15' IF(labmic1_C labmic1_N 4.5) THEN((labmic1_N-labmic1_C 4.5)*(labmic1_N15 labmic1_N)) ELSE(0) {g N Mg^{-1}soil h^{-1}}
DOCUMENT: Mineralization rate of 'excess' microbial N.
4.5 preferred C:N ratio of labmic

Mmic_N15" IF(resmic1_C resmic1_N 7.5) THEN((resmic1_N-resmic1_C 7.5)*(resmic1_N15 resmic1_N)) ELSE(0) {g N15 Mg $^{-1}$soil h^{-1}}
DOCUMENT: Rate of mineralization of 'excess' microbial N.
7.5 preferred C:N ratio of resmic

Mmic_N15"" IF(labmic2_C labmic2_N 4.5) THEN((labmic2_N-labmic2_C 4.5)*(labmic2_N15 labmic2_N)) ELSE(0) {g N Mg^{-1}soil h^{-1}}
DOCUMENT: Mineralization rate of 'excess' microbial N.
4.5 preferred C:N ratio of labmic

Mmic_N15""" IF(resmic2_C resmic2_N 7.5) THEN((resmic2_N-resmic2_C 7.5)*(resmic2_N15 resmic2_N)) ELSE(0) {g N15 Mg $^{-1}$soil h^{-1}}
DOCUMENT: Rate of mineralization of 'excess' microbial N.
7.5 preferred C:N ratio of resmic

Mmic_N15"""" IF(labmic3_C labmic3_N 4.5) THEN((labmic3_N-labmic3_C 4.5)*(labmic3_N15 labmic3_N)) ELSE(0) {g N Mg^{-1}soil h^{-1}}
DOCUMENT: Mineralization rate of 'excess' microbial N
4.5 preferred C:N ratio of labmic

Mmic_N15""" IF(resmic3_C resmic3_N 7.5) THEN((resmic3_N-resmic3_C 7.5)*(resmic3_N15 resmic3_N)) ELSE(0) {g N15 Mg $^{-1}$soil h^{-1}}
DOCUMENT: Rate of mineralization of 'excess' microbial N.
7.5 preferred C:N ratio of resmic

plant_N14in plant_Nin*(1-plant_atab) {g N14 Mg^{-1}soil h^{-1}}
DOCUMENT: Input of plant residue

plant_N14in' plant_N14in
DOCUMENT: Input of plant residue C

plantC_in plant_Cin
DOCUMENT: Total plant C added as residue

plantC_in' plantC_in
DOCUMENT: Input of plant residue C

plantN15_in plant_Nin*plant_atab {g N15 Mg^{-1}soil h^{-1}}
DOCUMENT: Input of plant residue.

plantN15_in' plantN15_in
DOCUMENT: Input of plant residue C.

Pmicocor1 actmic1_C*fdmicocorC*flg {g actmic C Mg^{-1}soil}
DOCUMENT: Potential decomposition rate of microbial corpses.

Pmicocor2 actmic2_C*fdmicocorC*flg {g actmic C Mg^{-1}soil}
DOCUMENT: Potential decomposition rate of microbial corpses.

Pmicocor3 actmic3_C*fdmicocorC*flg {g actmic C Mg^{-1}soil}
DOCUMENT: Potential decomposition rate of microbial corpses.

pro_C fproC*plantC_in' {g C Mg^{-1}soil h^{-1}}
DOCUMENT: Protein entering soil system.

pro_N14 (pro_C proCN)*(1-plant_atab) {g N14 Mg^{-1}soil h^{-1}}
DOCUMENT: Protein entering soil system

pro_N15 = (pro_C/proCN)*plant_atab {g N15 Mg^{-1}soil h^{-1}}
DOCUMENT: Protein entering soil system.

Rglabmic1 = 0.55*Rgmic1 {g C Mg^{-1}soil h^{-1}}
DOCUMENT: Growth respiration of labile microbial biomass.
0.55 fraction of active biomass which is labile

Rglabmic2 = 0.55*Rgmic2 {g C Mg^{-1}soil h^{-1}}
DOCUMENT: Growth respiration of labile microbial biomass.
0.55 fraction of active biomass which is labile

Rglabmic3 = 0.55*Rgmic3 {g C Mg^{-1}soil h^{-1}}
DOCUMENT: Growth respiration of labile microbial biomass.
0.55 fraction of active biomass which is labile

Rgmic1 = MAX(0,Rspecific1-Rmmic1) {g C Mg^{-1}soil h^{-1}}
DOCUMENT: Growth respiration of microbial biomass.

Rgmic2 = MAX(0,Rspecific2-Rmmic2) {g C Mg^{-1}soil h^{-1}}
DOCUMENT: Growth respiration of microbial biomass.

Rgmic3 = MAX(0,Rspecific3-Rmmic3) {g C Mg^{-1}soil h^{-1}}
DOCUMENT: Growth respiration of microbial biomass.

Rgresmic1 = 0.45*Rgmic1 {g C Mg^{-1}soil h^{-1}}
DOCUMENT: Growth respiration of resistant microbial biomass.
0.45 fraction of active biomass which is resistant.

Rgresmic2 = 0.45*Rgmic2 {g C Mg^{-1}soil h^{-1}}
DOCUMENT: Growth respiration of resistant microbial biomass.
0.45 fraction of active biomass which is resistant.

Rgresmic3 = 0.45*Rgmic3 {g C Mg^{-1}soil h^{-1}}
DOCUMENT: Growth respiration of resistant microbial biomass.
0.45 fraction of active biomass which is resistant.

RimmN14 = Zmin_N14
DOCUMENT: Rate of .N14 immobilization.

RimmN15 = Zmin_N15
DOCUMENT: Rate of .N15 immobilization.

Rmic_C = Rmic_C' + Rmic_C'' + Rmic_C''' + Rmic_C'''' + Rmic_C''''' + Rmic_C'''''' {g C Mg^{-1}soil h^{-1}}
DOCUMENT: Total microbial respiration rate.

Rmic_C' = Rmlabmic1 - Rglabmic1 {g C Mg^{-1}soil h^{-1}}
DOCUMENT: Maintenance and growth respiration of labile microbial biomass.

Rmic_C'' = Rmresmic1 - Rgresmic1 {g C Mg^{-1}soil h^{-1}}
DOCUMENT: Maintenance and growth respiration of resistant microbial biomass.

Rmic_C''' = Rmlabmic2 - Rglabmic2 {g C Mg^{-1}soil h^{-1}}
DOCUMENT: Maintenance and growth respiration of labile microbial biomass.

Rmic_C'''' = Rmresmic2 - Rgresmic2 {g C Mg^{-1}soil h^{-1}}
DOCUMENT: Maintenance and growth respiration of resistant microbial biomass.

Rmic_C''''' = Rmlabmic3 - Rglabmic3 {g C Mg^{-1}soil h^{-1}}
DOCUMENT: Maintenance and growth respiration of labile microbial biomass.

Rmic_C'''''' = Rmresmic3 - Rgresmic3 {g C Mg^{-1}soil h^{-1}}
DOCUMENT: Maintenance and growth respiration of resistant microbial biomass.

RmicinC = Usol1_C - Usol2_C - Usol3_C
DOCUMENT: Rate of input of non-plant residue C into microbial biomass.

RmicinN14 = Usol1_N14 - Usol2_N14 - Usol3_N14
DOCUMENT: Rate of input of non-plant residue N14 into microbial biomass.

RmicinN15 = Usol1_N15 - Usol2_N15 - Usol3_N15

DOCUMENT: Rate of input of non-plant residue N15 into microbial biomass.

RmicoutC = Dmic1_C + Dmic2_C + Dmic3_C + Rmic_C + Smic_C
DOCUMENT: Rate of output from microbial biomass.

RmicoutN14 = Dmic1_N14 + Dmic2_N14 + Dmic3_N14 + Smic_N14
DOCUMENT: Rate of output from microbial biomass.

RmicoutN15 = Dmic1_N15 + Dmic2_N15 + Dmic3_N15 + Smic_N15
DOCUMENT: Rate of output from microbial biomass.

RminN14 = Mmic_N14
DOCUMENT: Rate of N14 mineralization.

RminN15 = Mmic_N15
DOCUMENT: Rate of N15 mineralization.

Rmlabmic1 = 2E-3*labmic1_C*ftm {g C Mg^{-1}soil h^{-1}}
DOCUMENT: Maintenance respiration of labile microbial biomass.
2.0E-3 specific maintenance respiration at 30C {g C g^{-1}labmic h^{-1}}

Rmlabmic2 = 2E-3*labmic2_C*ftm {g C Mg^{-1}soil h^{-1}}
DOCUMENT: Maintenance respiration of labile microbial biomass.
2.0E-3 specific maintenance respiration at 30C {g C g^{-1}labmic h^{-1}}

Rmlabmic3 = 2E-3*labmic3_C*ftm {g C Mg^{-1}soil h^{-1}}
DOCUMENT: Maintenance respiration of labile microbial biomass.
2.0E-3 specific maintenance respiration at 30C {g C g^{-1}labmic h^{-1}}

Rmmic1 = Rmlabmic1 + Rmresmic1 {g C Mg^{-1}soil h^{-1}}
DOCUMENT: Maintenance respiration of microbial biomass.

Rmmic2 = Rmlabmic2 + Rmresmic2 {g C Mg^{-1}soil h^{-1}}
DOCUMENT: Maintenance respiration of microbial biomass.

Rmmic3 = Rmlabmic3 + Rmresmic3 {g C Mg^{-1}soil h^{-1}}
DOCUMENT: Maintenance respiration of microbial biomass.

Rmresmic1 = 1.0E-4*resmic1_C*ftm {g C Mg^{-1}soil h^{-1}}
DOCUMENT: Maintenance respiration of resistant microbial biomass.
1.0E-4 specific maintenance respiration at 30C {g C g^{-1}resmic C h^{-1}}

Rmresmic2 = 1.0E-4*resmic2_C*ftm {g C Mg^{-1}soil h^{-1}}
DOCUMENT: Maintenance respiration of resistant microbial biomass.
1.0E-4 specific maintenance respiration at 30C {g C g^{-1}resmic C h^{-1}}

Rmresmic3 = 1.0E-4*resmic3_C*ftm {g C Mg^{-1}soil h^{-1}}
DOCUMENT: Maintenance respiration of resistant microbial biomass.
1.0E-4 specific maintenance respiration at 30C {g C g^{-1}resmic C h^{-1}}

Rspecific1 = IF(soluble1_C>0) THEN(0.25*actmic1_C*((soluble1_C avail_H2O)/(soluble1_C avail_H2O+Csol1_C))*ftg*(actmic1_NC/(actmic1_NC+0.044))) ELSE (0) {g C Mg^{-1}soil h^{-1}}
DOCUMENT: Specific respiration given concentration of soluble substrate.
0.25 growth respiration at saturating soluble C and 30C {g C g^{-1}actmic C h^{-1}}
0.044 active microbial N:C ratio (C:N of 22.5) at which respiration is 0.5 of maximum {g N g^{-1}C}

Rspecific2 = 0.25*actmic2_C*((soluble2_C/avail_H2O)/(soluble2_C avail_H2O+Csol2_C))*ftg*(actmic2_NC/(actmic2_NC+0.044)) {g C Mg^{-1}soil h^{-1}}
DOCUMENT: Specific respiration given concentration of soluble substrate.
0.25 growth respiration at saturating soluble C and 30C {g C g^{-1}actmic C h^{-1}}
0.044 active microbial N:C ratio (C:N of 22.5) at which respiration is 0.5 of maximum {g N g^{-1}C}

Rspecific3 = 0.25*actmic3_C*((soluble3_C avail_H2O)/(soluble3_C avail_H2O+Csol3_C))*ftg*(actmic3_NC/(actmic3_NC+0.044)) {g C Mg^{-1}soil h^{-1}}
DOCUMENT: Specific respiration given concentration of soluble substrate.
0.25 growth respiration at saturating soluble C and 30C {g C g^{-1}actmic C h^{-1}}
0.044 active microbial N:C ratio (C:N of 22.5) at which respiration is 0.5 of maximum {g N g^{-1}C}
Mmic_N14 = Mmic_N14' + Mmic_N14'' + Mmic_N14''' + Mmic_N14'''' + Mmic_N14''''' {g N14 Mg^{-1}soil h^{-1}}
DOCUMENT: Total microbial mineralization rate.

Smic_C = Smic_C' + Smic_C" + Smic_C"' + Smic_C"" + Smic_C""" {g C Mg^{-1}soil h^{-1}}
DOCUMENT: Total microbial stabilization rate.

Smic_C' = Ilabmic1_C*(clay (0.40+clay)) {g C Mg^{-1}soil h^{-1}}
DOCUMENT: Rate of stabilization of inactivated labile microbial biomass in passive organic matter.
0.40 clay content at which stabilization is 0.5 of inactivation rate

Smic_C" = Iresmic1_C*(clay (0.40+clay)) {g C Mg^{-1}soil h^{-1}}
DOCUMENT: Rate of stabilization of inactivated resistant microbial biomass in passive organic matter.
0.40+clay content at which stabilization is 0.5 of inactivation

Smic_C"' = Ilabmic2_C*(clay (0.40+clay)) {g C Mg^{-1}soil h^{-1}}
DOCUMENT: Rate of stabilization of inactivated labile microbial biomass in passive organic matter.
0.40+clay content at which stabilization is 0.5 of inactivation rate

Smic_C"" = Iresmic2_C*(clay (0.40+clay)) {g C Mg^{-1}soil h^{-1}}
DOCUMENT: Rate of stabilization of inactivated resistant microbial biomass in passive organic matter
0.40+clay content at which stabilization is 0.5 of inactivation

Smic_C""" = Ilabmic3_C*(clay (0.40+clay)) {g C Mg^{-1}soil h^{-1}}
DOCUMENT: Rate of stabilization of inactivated labile microbial biomass in passive organic matter.
0.40+clay content at which stabilization is 0.5 of inactivation rate

Smic_C""" = Iresmic3_C*(clay (0.40+clay)) {g C Mg^{-1}soil h^{-1}}
DOCUMENT: Rate of stabilization of inactivated resistant microbial biomass in passive organic matter.
0.40+clay content at which stabilization is 0.5 of inactivation

Smic_N14 = Smic_N14' + Smic_N14" + Smic_N14"' + Smic_N14"" + Smic_N14""" {g N14 Mg^{-1}soil h^{-1}}
DOCUMENT: Total microbial stabilization rate.

Smic_N14' = Smic_C'*(labmic1_N/labmic1_C)*(labmic1_N14/labmic1_N) {g N14 Mg^{-1}soil h^{-1}}
DOCUMENT: Rate of stabilization of inactivated labile microbial biomass N in passive organic matter.

Smic_N14" = Smic_C"*(resmic3_N/resmic3_C)*(resmic3_N14/resmic3_N) {g N14 Mg^{-1}soil h^{-1}}
DOCUMENT: Rate of stabilization of inactivated resistant microbial biomass in passive organic matter.

Smic_N14"' = Smic_C"'*(labmic3_N/labmic3_C)*(labmic3_N14/labmic3_N) {g N14 Mg^{-1}soil h^{-1}}
DOCUMENT: Rate of stabilization of inactivated labile microbial biomass N in passive organic matter.

Smic_N14"" = Smic_C""*(resmic2_N/resmic2_C)*(resmic2_N14/resmic2_N) {g N14 Mg^{-1}soil h^{-1}}
DOCUMENT: Rate of stabilization of inactivated resistant microbial biomass in passive organic matter.

Smic_N14""" = Smic_C"'*(labmic2_N/labmic2_C)*(labmic2_N14/labmic2_N) {g N14 Mg^{-1}soil h^{-1}}
DOCUMENT: Rate of stabilization of inactivated labile microbial biomass N in passive organic matter.

Smic_N14""" = Smic_C"*(resmic1_N/resmic1_C)*(resmic1_N14/resmic1_N) {g N14 Mg^{-1}soil h^{-1}}
DOCUMENT: Rate of stabilization of inactivated resistant microbial biomass in passive organic matter.

Smic_N15 = Smic_N15' + Smic_N15" + Smic_N15"' + Smic_N15"" + Smic_N15""" {g N15 Mg^{-1}soil h^{-1}}
DOCUMENT: Total microbial stabilization rate.

Smic_N15' = Smic_C'*(labmic1_N/labmic1_C)*(labmic1_N15/labmic1_N) {g N Mg^{-1}soil h^{-1}}
DOCUMENT: Rate of stabilization of inactivated labile microbial biomass N in passive organic matter.

Smic_N15" = Smic_C"*(resmic1_N/resmic1_C)*(resmic1_N15/resmic1_N) {g N15 Mg^{-1}soil h^{-1}}
DOCUMENT: Rate of stabilization of inactivated resistant microbial biomass in passive organic matter.

Smic_N15"' = Smic_C"'*(labmic2_N/labmic2_C)*(labmic2_N15/labmic2_N) {g N Mg^{-1}soil h^{-1}}
DOCUMENT: Rate of stabilization of inactivated labile microbial biomass N in passive organic matter.

Smic_N15"" = Smic_C""*(resmic2_N/resmic2_C)*(resmic2_N15/resmic2_N) {g N15 Mg^{-1}soil h^{-1}}
DOCUMENT: Rate of stabilization of inactivated resistant microbial biomass in passive organic matter.

Smic_N15""" = Smic_C"'*(labmic3_N/labmic3_C)*(labmic3_N15/labmic3_N) {g N Mg^{-1}soil h^{-1}}
DOCUMENT: Rate of stabilization of inactivated labile microbial biomass N in passive organic matter.

Smic_N15""" = Smic_C"*(resmic3_N/resmic3_C)*(resmic3_N15/resmic3_N) {g N15 Mg^{-1}soil h^{-1}}
DOCUMENT: Rate of stabilization of inactivated resistant microbial biomass in passive organic matter

Umic1_C = Usol1_C' {g C Mg^{-1}soil h^{-1}}
DOCUMENT: Rate of uptake of soluble substrate by microbial biomass.

Umic1_N14 = Usol1_N14'
DOCUMENT: Rate of uptake of soluble substrate by microbial biomass.

Umic1_N15 = Usol1_N15'
DOCUMENT: Rate of uptake of soluble substrate by microbial biomass

Umic2_C = Usol2_C' {g C Mg^{-1}soil h^{-1}}
DOCUMENT: Rate of uptake of soluble substrate by microbial biomass

Umic2_N14 = Usol2_N14'
DOCUMENT: Rate of uptake of soluble substrate by microbial biomass.

Umic2_N15 = Usol2_N15'
DOCUMENT: Rate of uptake of soluble substrate by microbial biomass.

Umic3_C = Usol3_C' {g C Mg^{-1}soil h^{-1}}
DOCUMENT: Rate of uptake of soluble substrate by microbial biomass.

Umic3_N14 = Usol3_N14'
DOCUMENT: Rate of uptake of soluble substrate by microbial biomass.

Umic3_N15 = Usol3_N15'
DOCUMENT: Rate of uptake of soluble substrate by microbial biomass.

Usol1_C = MIN(Rmmic1,Rspecific1)*(Rgmic1 (1-eff1)) {g C Mg^{-1}soil h^{-1}}
DOCUMENT: Rate of uptake of soluble substrate by microbial biomass.

Usol1_C' = Usol1_C
DOCUMENT: Rate of uptake of soluble substrate by microbial biomass.

Usol1_N14 = MIN(soluble1_N14,Usol1_C*(sol1_N soluble1_C)*(soluble1_N14 sol1_N)) {g N14 Mg^{-1}soil h^{-1}}
DOCUMENT: Rate of uptake of soluble substrate by microbial biomass.

Usol1_N14' = Usol1_N14
DOCUMENT: Rate of uptake of soluble substrate by microbial biomass.

Usol1_N15 = MIN(soluble1_N15,Usol1_C*(sol1_N soluble1_C)*(soluble1_N15 sol1_N)) {g N15 Mg^{-1}soil h^{-1}}
DOCUMENT: Rate of uptake of soluble substrate by microbial biomass.

Usol1_N15' = Usol1_N15
DOCUMENT: Rate of uptake of soluble substrate by microbial biomass.

Usol2_C = MIN(Rmmic2,Rspecific2)*(Rgmic2 (1-eff2)) {g C Mg^{-1}soil h^{-1}}
DOCUMENT: Rate of uptake of soluble substrate by microbial biomass.

Usol2_C' = Usol2_C
DOCUMENT: Rate of uptake of soluble substrate by microbial biomass.

Usol2_N14 = MIN(soluble2_N14,Usol2_C*(sol2_N soluble2_C)*(soluble2_N14 sol2_N)) {g N14 Mg^{-1}soil h^{-1}}
DOCUMENT: Rate of uptake of soluble substrate by microbial biomass.

Usol2_N14' = Usol2_N14
DOCUMENT: Rate of uptake of soluble substrate by microbial biomass.

Usol2_N15 = MIN(soluble2_N15,Usol2_C*(sol2_N soluble2_C)*(soluble2_N15 sol2_N)) {g N15 Mg^{-1}soil h^{-1}}
DOCUMENT: Rate of uptake of soluble substrate by microbial biomass.

Usol2_N15' = Usol2_N15
DOCUMENT: Rate of uptake of soluble substrate by microbial biomass.

Usol3_C = MIN(Rmmic3,Rspecific3)*(Rgmic3 (1-eff3)) {g C Mg^{-1}soil h^{-1}}
DOCUMENT: Rate of uptake of soluble substrate by microbial biomass.

Usol3_C' = Usol3_C
DOCUMENT: Rate of uptake of soluble substrate by microbial biomass.

Usol3_N14 = MIN(soluble3_N14,Usol3_C*(sol3_N soluble3_C)*(soluble3_N14 sol3_N)) {g N14 Mg^{-1}soil h^{-1}}
DOCUMENT: Rate of uptake of soluble substrate by microbial biomass.

Usol3_N14' = Usol3_N14

DOCUMENT: Rate of uptake of soluble substrate by microbial biomass.

Usol3_N15 = MIN(soluble3_N15,Usol3_C*(sol3_N soluble3_C)*(soluble3_N15 sol3_N)) {g N15 Mg^{-1}soil h^{-1}}
DOCUMENT: Rate of uptake of soluble substrate by microbial biomass.

Usol3_N15' = Usol3_N15
DOCUMENT: Rate of uptake of soluble substrate by microbial biomass.

Ustglab1_C = 0.55*(0.002*stgmic1_C*ftg) {g C Mg^{-1}soil h^{-1}}
DOCUMENT: Uptake of storage carbon by labile microbial biomass.
0.55 fraction assigned to labile microbial biomass
0.002 specific rate of transfer {h^{-1}}

Ustglab2_C = 0.55*(0.002*stgmic2_C*ftg) {g C Mg^{-1}soil h^{-1}}
DOCUMENT: Uptake of storage carbon by labile microbial biomass.
0.55 fraction assigned to labile microbial biomass
0.002 specific rate of transfer {h^{-1}}

Ustglab3_C = 0.55*(0.002*stgmic3_C*ftg) {g C Mg^{-1}soil h^{-1}}
DOCUMENT: Uptake of storage carbon by labile microbial biomass.
0.55 fraction assigned to labile microbial biomass
0.002 specific rate of transfer {h^{-1}}

Ustgres1_C = 0.45*(0.002*stgmic1_C*ftg) {g C Mg^{-1}soil h^{-1}}
DOCUMENT: Uptake of storage carbon by resistant microbial biomass.
0.45 fraction assigned to resistant biomass
0.002 specific rate of transfer {h^{-1}}

Ustgres2_C = 0.45*(0.002*stgmic2_C*ftg) {g C Mg^{-1}soil h^{-1}}
DOCUMENT: Uptake of storage carbon by resistant microbial biomass.
0.45 fraction assigned to resistant biomass
0.002 specific rate of transfer {h^{-1}}

Ustgres3_C = 0.45*(0.002*stgmic3_C*ftg) {g C Mg^{-1}soil h^{-1}}
DOCUMENT: Uptake of storage carbon by resistant microbial biomass.
0.45 fraction assigned to resistant biomass
0.002 specific rate of transfer {h^{-1}}

Zlab1_N14 = IF(labmic1_C labmic1_N>4.5) THEN(MIN(mineral_N14,(labmic1_C/4.5-labmic1_N)*(mineral_N14/mineral_N)))
ELSE(0) {g N14 Mg^{-1}soil h^{-1}}
DOCUMENT: Rate of immobilization of mineral N by labmic C.

Zlab1_N15 = IF(labmic1_C labmic1_N>4.5) THEN(MIN(mineral_N15,(labmic1_C/4.5-labmic1_N)*(mineral_N15/mineral_N)))
ELSE(0) {g N15 Mg^{-1}soil h^{-1}}
DOCUMENT: Rate of immobilization of mineral N by labmic.

Zlab2_N14 = IF(labmic2_C labmic2_N>4.5) THEN(MIN(mineral_N14,(labmic2_C/4.5-labmic2_N)*(mineral_N14/mineral_N)))
ELSE(0) {g N14 Mg^{-1}soil h^{-1}}
DOCUMENT: Rate of immobilization of mineral N by labmic C.

Zlab2_N15 = IF(labmic2_C labmic2_N>4.5) THEN(MIN(mineral_N15,(labmic2_C/4.5-labmic2_N)*(mineral_N15/mineral_N)))
ELSE(0) {g N15 Mg^{-1}soil h^{-1}}
DOCUMENT: Rate of immobilization of mineral N by labmic.

Zlab3_N14 = IF(labmic3_C labmic3_N>4.5) THEN(MIN(mineral_N14,(labmic3_C/4.5-labmic3_N)*(mineral_N14/mineral_N)))
ELSE(0) {g N14 Mg^{-1}soil h^{-1}}
DOCUMENT: Rate of immobilization of mineral N by labmic C.

Zlab3_N15 = IF(labmic3_C labmic3_N>4.5) THEN(MIN(mineral_N15,(labmic3_C/4.5-labmic3_N)*(mineral_N15/mineral_N)))
ELSE(0) {g N15 Mg^{-1}soil h^{-1}}
DOCUMENT: Rate of immobilization of mineral N by labmic.

Zmic1_N14 = Zlab1_N14-Zres1_N14 {g N14 Mg^{-1}soil h^{-1}}
DOCUMENT: Rate of immobilization of mineral N by microbial biomass.

Zmic1_N15 = Zlab1_N15-Zres1_N15 {g N15 Mg^{-1}soil h^{-1}}
DOCUMENT: Rate of immobilization of mineral N by microbial biomass.

Zmic2_N14 = Zlab2_N14-Zres2_N14 {g N14 Mg^{-1}soil h^{-1}}
DOCUMENT: Rate of immobilization of mineral N by microbial biomass.

Zmic2_N15 = Zlab2_N15+Zres2_N15 {g N15 Mg^{-1}soil h^{-1}}
DOCUMENT: Rate of immobilization of mineral N by microbial biomass.

Zmic3_N14 = Zlab3_N14+Zres3_N14 {g N14 Mg^{-1}soil h^{-1}}
DOCUMENT: Rate of immobilization of mineral N by microbial biomass.

Zmic3_N15 = Zlab3_N15+Zres3_N15 {g N15 Mg^{-1}soil h^{-1}}
DOCUMENT: Rate of immobilization of mineral N by microbial biomass.

Zmin_N14 = Zmic1_N14+Zmic2_N14+Zmic3_N14 {g N14 Mg^{-1}soil h^{-1}}
DOCUMENT: Total microbial immobilization rate.

Zmin_N14' = Zmin_N14

Zmin_N15 = Zmic1_N15+Zmic2_N15+Zmic3_N15 {g N15 Mg^{-1}soil h^{-1}}
DOCUMENT: Total microbial immobilization rate.

Zmin_N15' = Zmin_N15

Zres1_N14 = IF(resmic1_C resmic1_N>7.5) THEN(MIN(mineral_N14,(resmic1_C/7.5-resmic1_N)*(mineral_N14/mineral_N))) ELSE(0) {g N14 Mg^{-1}soil h^{-1}}
DOCUMENT: Rate of immobilization of mineral N by resmic C.

Zres1_N15 = IF(resmic1_C resmic1_N>7.5) THEN(MIN(mineral_N15,(resmic1_C/7.5-resmic1_N)*(mineral_N15/mineral_N))) ELSE(0) {g N15 Mg^{-1}soil h^{-1}}
DOCUMENT: Rate of immobilization of mineral N by resmic.

Zres2_N14 = IF(resmic2_C resmic2_N>7.5) THEN(MIN(mineral_N14,(resmic2_C/7.5-resmic2_N)*(mineral_N14/mineral_N))) ELSE(0) {g N14 Mg^{-1}soil h^{-1}}
DOCUMENT: Rate of immobilization of mineral N by resmic C.

Zres2_N15 = IF(resmic2_C resmic2_N>7.5) THEN(MIN(mineral_N15,(resmic2_C/7.5-resmic2_N)*(mineral_N15/mineral_N))) ELSE(0) {g N15 Mg^{-1}soil h^{-1}}
DOCUMENT: Rate of immobilization of mineral N by resmic.

Zres3_N14 = IF(resmic3_C resmic3_N>7.5) THEN(MIN(mineral_N14,(resmic3_C/7.5-resmic3_N)*(mineral_N14/mineral_N))) ELSE(0) {g N14 Mg^{-1}soil h^{-1}}
DOCUMENT: Rate of immobilization of mineral N by resmic C.

Zres3_N15 = IF(resmic3_C resmic3_N>7.5) THEN(MIN(mineral_N15,(resmic3_C/7.5-resmic3_N)*(mineral_N15/mineral_N))) ELSE(0) {g N15 Mg^{-1}soil h^{-1}}
DOCUMENT: Rate of immobilization of mineral N by resmic.

Converters

active_atab = active_N15/active_N {g N15 g^{-1}N}

active_N = active_N14+active_N15 {g N Mg^{-1}soil}

active_rec = IF(TplantN15_in>0) THEN(active_N*(active_atab-nat_atab)/TplantN15_in)*100 ELSE(0) {%}
DOCUMENT: Recovery of plant residue N15 in active organic matter.

actmic_C = actmic1_C+actmic2_C+actmic3_C {g C Mg^{-1}soil}
DOCUMENT: Total active microbial biomass.

actmic1_C = labmic1_C*0.55 {g C Mg^{-1}soil}
DOCUMENT: Active microbial biomass is 55% labile.

actmic1_NC = (labmic1_N+(actmic1_C-labmic1_C)/(resmic1_C/resmic1_N))/actmic1_C {g N g^{-1}C}
DOCUMENT: N:C ratio of active microbial biomass.

actmic2_C = labmic2_C*0.55 {g C Mg^{-1}soil}
DOCUMENT: Active microbial biomass is 55% labile.

actmic2_NC = (labmic2_N+(actmic2_C-labmic2_C)/(resmic2_C/resmic2_N))/actmic2_C {g N g^{-1}C}
DOCUMENT: N:C ratio of active microbial biomass.

actmic3_C = labmic3_C*0.55 {g C Mg^{-1}soil}
DOCUMENT: Active microbial biomass is 55% labile.

actmic3_NC = (labmic3_N-(actmic3_C-labmic3_C)/(resmic3_C/resmic3_N))/actmic3_C {g N g^{-1}C}
DOCUMENT: N:C ratio of active microbial biomass

adsorbed_atab = adsorbed_N15/adsorbed_N {g N15 g^{-1}N}

adsorbed_N = adsorbed_N14-adsorbed_N15 {g N Mg^{-1}soil}

adsorbed_rec = IF(TplantN15_in>0) THEN(adsorbed_N*(adsorbed_atab-nat_atab)/TplantN15_in)*100 ELSE(0) {%}
DOCUMENT: Recovery of plant residue N15 in adsorbed component.

avail_H2O = soil_H2O-unavH2O_2 {Mg H2O Mg^{-1}dry soil}
DOCUMENT: Soil water held at potentials above -50MPa and, therefore, available for microbial use.

car_atab = IF(carbohy_N15>0) THEN(carbohy_N15/car_N) ELSE 0 {g N15 g^{-1}N}

car_N = carbohy_N14-carbohy_N15 {g N Mg^{-1}soil}

car_rec = IF(TplantN15_in>0) THEN(car_N*car_atab/TplantN15_in)*100 ELSE(0) {%}
DOCUMENT: Recovery of plant residue N15 in carbohydrate.

carCN = 500 {g C g^{-1}N}
DOCUMENT: Carbohydrate C:N ratio.

cel_atab = IF(cellulose_N15>0) THEN(cellulose_N15/cel_N) ELSE 0 {g N15 g^{-1}N}

cel_N = cellulose_N14-cellulose_N15 {g N Mg^{-1}soil}

cel_rec = IF(TplantN15_in>0) THEN(cel_N*cel_atab/TplantN15_in)*100 ELSE(0) {%}
DOCUMENT: Recovery of plant residue N15 in cellulose.

celCN = 500 {g C g^{-1}N}
DOCUMENT: Cellulose C:N ratio.

clay = 0.47 {Mg Mg^{-1}soil}
DOCUMENT: Soil clay content.

Csol1_C = 35 {g C Mg^{-1}avail H2O}
DOCUMENT: Concentration of soluble C {on an available H2O basis} when growth respiration is 0.5 of maximum.

Csol2_C = 35 {g C Mg^{-1}avail H2O}
DOCUMENT: Concentration of soluble C {on an available H2O basis} when growth respiration is 0.5 of maximum.

Csol3_C = 35 {g C Mg^{-1}avail H2O}
DOCUMENT: Concentration of soluble C {on an available H2O basis} when growth respiration is 0.5 of maximum

eff1 = 0.6
DOCUMENT: Microbial efficiency of substrate utilization.

eff2 = 0.6
DOCUMENT: Microbial efficiency of substrate utilization.

eff3 = 0.6
DOCUMENT: Microbial efficiency of substrate utilization.

fcarC = 0.17 {g C g^{-1}plant C}
DOCUMENT: Fraction of plant residue which is carbohydrate.
Total residue C - (protein C + cellulose C + lignin C)

fcelC = 0.40 {g C g^{-1}plant C}
DOCUMENT: Fraction of plant residue which is cellulose.
Measured (cellulose + hemicellulose)

fdactiveC = active_C/(active_C+75*(1.0+(actmic_C/avail_H2O)/25))*(active_C/(active_C+passive_C)) {dimensionless}
DOCUMENT: Density function for decomposition of active soil organic matter.
75=Michaelis constant for decomposition of active soil OM carbon {g C Mg^{-1}soil}
40=inhibition constant for active soil fraction {g C Mg^{-1}avail H2O}

fdadsorbedC = adsorbed_C/(adsorbed_C+75*(1.0+(actmic_C/avail_H2O)/25)) {dimensionless}
DOCUMENT: Density function for decomposition of adsorbed organic matter.
75=Michaelis constant for decomposition of adsorbed C {g C Mg^{-1}soil}
25=inhibition constant for adsorbed C {g C Mg^{-1}avail H2O}

fdmicorC Tmicorr_C (Tmicorr_C+75*(1.0+(actmic_C avail_H2O) 25)) {dimensionless}
DOCUMENT: Density function for decomposition of microbial residue.
75 Michaelis constant for decomposition of microbial residue carbon {g C Mg^{-1}soil}
25 inhibition constant for microbial residue {g C Mg^{-1}avail H2O}

fdpassiveC passive_C (passive_C+75*(1.0+(actmic_C avail_H2O) 25))*(passive_C (active_C+passive_C)) {dimensionless}
DOCUMENT: Density function for decomposition of passive soil organic matter.
75 Michaelis constant for decomposition of passive soil OM carbon {g C Mg^{-1}soil}
40 inhibition constant for passive fraction {g C Mg^{-1}avail H2O}

fdplantC TplantC (TplantC+75*(1.0+(actmic_C avail_H2O) 25)) {dimensionless}
DOCUMENT: Density function for decomposition of plant residue.
75 Michaelis constant for decomposition of plant residue carbon {g C Mg^{-1}soil}
20 inhibition constant for plant residue {g C Mg^{-1}avail H2O}

fligC 0.07 {g C g^{-1}plant C}
DOCUMENT: Fraction of plant residue which is lignin.
Measured

fproC 0.36 {g C g^{-1}plant C}
DOCUMENT: Fraction of plant residue which is protein.
Measured (N x 6.25)

fstorage 0 {g C g^{-1}C}
DOCUMENT: Fraction of residue C uptake which is stored by microbial biomass.

ftg Tk*(EXP(17.1127-57500/(Tk*8.3295)))/(1+EXP((192500-710*Tk)/(Tk*8.3295))+EXP((710*Tk-222500)/(Tk*8.3295)))
{dimensionless}
DOCUMENT: Temperature function (Arrhenius equation) for growth related processes.
17.1127 parameter selected such that ftg = 1.0 at 30C
57500 energy of activation {J mol^{-1}}
8.3295 universal gas constant {J mol^{-1} K^{-1}}
192500 energy of low temperature deactivation {J mol^{-1}}
222500 energy of high temperature deactivation {J mol^{-1}}
710 change in entropy {J mol^{-1} K^{-1}}

ftm 0.14*EXP(0.067*(Tk-273.16)) {dimensionless}
DOCUMENT: Temperature function for maintenance processes.
0.14 parameter selected such that ftm = 1.0 at 30C
0.067 parameter selected to give a Q10 of 2

INITmin_N 5 {g N Mg^{-1}soil}
DOCUMENT: Initial soluble mineral N content of soil.

labcor1_atab IF(labcor1_N>0) THEN(labcor1_N15/labcor1_N) ELSE(0) {g N15 g^{-1}N}

labcor1_N labcor1_N14+labcor1_N15 {g N Mg^{-1}soil}

labcor1_rec IF(TplantN15_in>0) THEN(labcor1_N*(labcor1_atab-nat_atab)/TplantN15_in)*100 ELSE(0) {%}
DOCUMENT: Recovery of plant residue N15 in labile microbial corpses.

labcor2_atab labcor2_N15/labcor2_N {g N15 g^{-1}N}

labcor2_N labcor2_N14+labcor2_N15 {g N Mg^{-1}soil}

labcor2_rec IF(TplantN15_in>0) THEN(labcor2_N*(labcor2_atab-nat_atab)/TplantN15_in)*100 ELSE(0) {%}
DOCUMENT: Recovery of plant residue N15 in labile microbial corpses.

labcor3_atab labcor3_N15/labcor3_N {g N15 g^{-1}N}

labcor3_N labcor3_N14+labcor3_N15 {g N Mg^{-1}soil}

labcor3_rec IF(TplantN15_in>0) THEN(labcor3_N*(labcor3_atab-nat_atab)/TplantN15_in)*100 ELSE(0) {%}
DOCUMENT: Recovery of plant residue N15 in labile microbial corpses.

labmic1_atab IF(labmic1_N>0) THEN(labmic1_N15/labmic1_N) ELSE (0) {g N15 g^{-1}N}

labmic1_N labmic1_N14+labmic1_N15 {g N Mg^{-1}soil}

labmic1_rec IF(TplantN15_in>0) THEN(labmic1_N*(labmic1_atab-nat_atab)/TplantN15_in)*100 ELSE(0) {%}

DOCUMENT: Recovery of plant residue N15 in labile microbial biomass.

labmic2_atab = labmic2_N15/labmic2_N {g N15 g^{-1}N}

labmic2_N = labmic2_N14+labmic2_N15 {g N Mg^{-1}soil}

labmic2_rec = IF(TplantN15_in>0) THEN(labmic2_N*(labmic2_atab-nat_atab)/TplantN15_in)*100 ELSE(0) {%}
DOCUMENT: Recovery of plant residue N15 in labile microbial biomass.

labmic3_atab = labmic3_N15/labmic3_N {g N15 g^{-1}N}

labmic3_N = labmic3_N14+labmic3_N15 {g N Mg^{-1}soil}

labmic3_rec = IF(TplantN15_in>0) THEN(labmic3_N*(labmic3_atab-nat_atab)/TplantN15_in)*100 ELSE(0) {%}
DOCUMENT: Recovery of plant residue N15 in labile microbial biomass.

lig_atab = IF(lignin_N15>0) THEN(lignin_N15/lig_N) ELSE 0 {g N15 g^{-1}N}

lig_N = lignin_N14+lignin_N15 {g N Mg^{-1}soil}

lig_rec = IF(TplantN15_in>0) THEN(lig_N*lig_atab/TplantN15_in)*100 ELSE(0) {%}
DOCUMENT: Recovery of plant residue N15 in lignin.

ligCN = 100 {g C g^{-1}N}
DOCUMENT: Lignin C:N ratio.

mic_atab = ((mic_rec/100*TplantN15_in)/mic_N)+0.003663)*100 {%}

mic_CN = mic_C/mic_N {g C g^{-1}N}
DOCUMENT: Microbial biomass C
N ratio.

mic_N = labmic1_N+labmic2_N+labmic3_N+resmic1_N+resmic2_N+resmic3_N {g N Mg^{-1}soil}
PplantC = actmic_C*fdplantC*ftg {g actmic C Mg^{-1}soil}
DOCUMENT: Potential decomposition of plant residue.

mic_rec = mic1_rec+mic2_rec+mic3_rec {%}

mic1_CN = (labmic1_C+resmic1_C+stgmic1_C)/(labmic1_N+resmic1_N) {g C g^{-1}N}
DOCUMENT: Microbial biomass C:N ratio.

mic1_N = labmic1_N+resmic1_N {g N Mg^{-1}soil}
mic2_CN = (labmic2_C+resmic2_C+stgmic2_C)/(labmic2_N+resmic2_N) {g C g^{-1}N}
DOCUMENT: Microbial biomass C:N ratio.

mic1_rec = labmic1_rec+resmic1_rec+labcor1_rec+rescor1_rec {%}

mic2_N = labmic2_N+resmic2_N {g N Mg^{-1}soil}
mic3_CN = (labmic3_C+resmic3_C+stgmic3_C)/(labmic3_N+resmic3_N) {g C g^{-1}N}
DOCUMENT: Microbial biomass C:N ratio.

mic2_rec = labmic2_rec+resmic2_rec+labcor2_rec+rescor2_rec {%}

mic3_N = labmic3_N+resmic3_N {g N Mg^{-1}soil}
mic_C = labmic1_C+labmic2_C+labmic3_C+resmic1_C+resmic2_C+resmic3_C+stgmic1_C+stgmic2_C+stgmic3_C {g C Mg^{-1}soil}
DOCUMENT: Total microbial C.

mic3_rec = labmic3_rec+resmic3_rec+labcor3_rec+rescor3_rec {%}

min_atab = mineral_atab*100 {%}

mineral_atab = IF(mineral_N>0) THEN(mineral_N15/mineral_N) ELSE (0) {g N15 g^{-1}N}

mineral_N = mineral_N14+mineral_N15 {g N Mg^{-1}soil}

mineral_rec = IF(TplantN15_in>0) THEN(mineral_N*(mineral_atab-nat_atab)/TplantN15_in)*100 ELSE(0) {%}
DOCUMENT: Recovery of plant residue N15 in mineral N.

nat_atab = 0.003663 {g N15 g^{-1}N}
DOCUMENT: Natural N15 atom abundance.

NMO rec passive rec+active rec+soluble rec+adsorbed rec {‰}

organic C 14500 {g C Mg^{-1}soil}
DOCUMENT: Soil organic carbon content.

passive atab passive N15 passive N {g N15 g^{-1}N}

passive N passive N14+passive N15 {g N Mg^{-1}soil}

passive rec IF(TplantN15 in>0; THEN(passive N*(passive atab-nat atab) TplantN15 in)*100 ELSE(0) {‰}
DOCUMENT: Recovery of plant residue N15 in passive organic matter.

plant atab 0.04473 {g N15 g^{-1}N}
DOCUMENT: Plant residue N15 atom abundance.

plant Cin PULSE(0,0,9000) {g C Mg^{-1}soil, time of addition, time of next addition}
DOCUMENT: Plant residue C added to soil.

plant CN (fproC+fcarC+fcelC+fligC) (fproC proCN+fcarC carCN+fcelC celCN+fligC ligCN) {g C g^{-1}N}
DOCUMENT: Plant residue C:N ratio.

plant Nin pro C proCN+car C carCN+cel C celCN+lig C ligCN {g N Mg^{-1}soil h^{-1}}

plant rec pro rec+car rec+cel rec+lig rec {‰}

pro atab IF(protein N15>0) THEN(protein N15 pro N) ELSE 0 {g N15 g^{-1}N}

pro N protein N14+protein N15 {g N Mg^{-1}soil}

pro rec IF(TplantN15 in>0) THEN(pro N*pro atab TplantN15 in)*100 ELSE(0) {‰}
DOCUMENT: Recovery of plant residue N15 in protein.

proCN 3.125 {g C g^{-1}N}
DOCUMENT: Protein C:N ratio.

Qadsorb ((2*TadsorbentC)*0.001*(((2*(soluble1 C+soluble2 C+soluble3 C)) avail H2O) 0.85)) 2 {g C Mg^{-1}soil}
DOCUMENT: Equilibrium amount of adsorbed organic C given amount in solution. This equation was formulated on a dry matter basis
0.001 partitioning coefficient between aqueous and sorbed fraction {Mg H20 Mg^{-1}soil}
0.85 Freundlich exponenT:2*TadsorbentC Tadsorbent dry matter
2*soluble C soluble dry matter

rescor1 atab IF(rescor1 N>0) THEN(rescor1 N15 rescor1 N) ELSE (0) {g N15 g^{-1}N}

rescor1 N rescor1 N14+rescor1 N15 {g N Mg^{-1}soil}

rescor1 rec IF(TplantN15 in>0) THEN(rescor1 N*(rescor1 atab-nat atab) TplantN15 in)*100 ELSE(0) {‰}
DOCUMENT: Recovery of plant residue N15 in resistant microbial corpses.

rescor2 atab rescor2 N15 rescor2 N {g N15 g^{-1}N}

rescor2 N rescor2 N14+rescor2 N15 {g N Mg^{-1}soil}

rescor2 rec IF(TplantN15 in>0) THEN(rescor2 N*(rescor2 atab-nat atab) TplantN15 in)*100 ELSE(0) {‰}
DOCUMENT: Recovery of plant residue N15 in resistant microbial corpses.

rescor3 atab rescor3 N15 rescor3 N {g N15 g^{-1}N}

rescor3 N rescor3 N14+rescor3 N15 {g N Mg^{-1}soil}

rescor3 rec IF(TplantN15 in>0) THEN(rescor3 N*(rescor3 atab-nat atab) TplantN15 in)*100 ELSE(0) {‰}
DOCUMENT: Recovery of plant residue N15 in resistant microbial corpses.

resmic1 atab IF(resmic1 N>0) THEN(resmic1 N15 resmic1 N) ELSE (0) {g N15 g^{-1}N}

resmic1 N resmic1 N14+resmic1 N15 {g N Mg^{-1}soil}

resmic1 rec IF(TplantN15 in>0) THEN(resmic1 N*(resmic1 atab-nat atab) TplantN15 in)*100 ELSE(0) {‰}
DOCUMENT: Recovery of plant residue N15 in resistant microbial biomass.

resmic2 atab resmic2 N15 resmic2 N {g N15 g^{-1}N}

resmic2_N = resmic2_N14+resmic2_N15 {g N Mg^{-1}soil}

resmic2_rec = IF(TplantN15_in>0) THEN(resmic2_N*(resmic2_atab-nat_atab)/TplantN15_in)*100 ELSE(0) {%}
DOCUMENT: Recovery of plant residue N15 in resistant microbial biomass.

resmic3_atab = resmic3_N15/resmic3_N {g N15 g^{-1}N}

resmic3_N = resmic3_N14+resmic3_N15 {g N Mg^{-1}soil}

resmic3_rec = IF(TplantN15_in>0) THEN(resmic3_N*(resmic3_atab-nat_atab)/TplantN15_in)*100 ELSE(0) {%}
DOCUMENT: Recovery of plant residue N15 in resistant microbial biomass.

sand = 0.25 {Mg Mg^{-1}soil}
DOCUMENT: Soil sand content.

soil_H2O = 0.18 {Mg H2O Mg^{-1}dry soil}
DOCUMENT: Soil gravimetric moisture content.

sol_3_atab = soluble3_N15/sol3_N {g N15 g^{-1}N}

sol_3_rec = IF(TplantN15_in>0) THEN(sol3_N*(sol_3_atab-nat_atab)/TplantN15_in)*100 ELSE(0) {%}
DOCUMENT: Recovery of plant residue N15 in soluble component.

sol1_atab = soluble1_N15/sol1_N {g N15 g^{-1}N}

sol1_N = soluble1_N14+soluble1_N15

sol1_rec = IF(TplantN15_in>0) THEN(sol1_N*(sol1_atab-nat_atab)/TplantN15_in)*100 ELSE(0) {%}
DOCUMENT: Recovery of plant residue N15 in soluble component.

sol2_atab = soluble2_N15/sol2_N {g N15 g^{-1}N}

sol2_N = soluble2_N14+soluble2_N15

sol2_rec = IF(TplantN15_in>0) THEN(sol2_N*(sol2_atab-nat_atab)/TplantN15_in)*100 ELSE(0) {%}
DOCUMENT: Recovery of plant residue N15 in soluble component.

sol3_N = soluble3_N14+soluble3_N15

soluble_N = sol1_N+sol2_N+sol3_N

soluble_rec = sol1_rec+sol2_rec+sol_3_rec {%}

TadsorbentC = organic_C+TplantC+(mic_C) {g C Mg^{-1}soil}
DOCUMENT: Total C which influences adsorption equilibrium.

temperature = 25 {degrees C}
DOCUMENT: Soil temperature.

Tk = temperature+273.15 {degrees K}
DOCUMENT: Soil temperature in degrees Kelvin

Tmiccor_C = miccor1_C+miccor2_C+miccor3_C {g C Mg^{-1}soil}
DOCUMENT: Total microbial corpse C.
PHO plant decomposition Submodel

TplantC = protein_C+carbohy_C+cellulose_C+lignin_C {g C Mg^{-1}soil}
DOCUMENT: Total plant C.

unavH2O_1 = IF(sand>0.50) THEN(0.051) ELSE(0.013) {Mg H2O Mg^{-1}soil}
DOCUMENT: Water held at potentials below -50MPa (and, therefore, not available to microbes) in sandy and silty soils
0.051=H2O in silty soil at -50MPa
0.013=H2O in sandy soil at -50MPa

unavH2O_2 = IF(clay>0.50) THEN(0.15) ELSE(unavH2O_1) {Mg H2O Mg^{-1}soil}
DOCUMENT: Water held at potentials below -50MPa (and, therefore, not available to microbes) in clay soils
0.15=H2O in clay soil at -50MPa

PHO PLANT DECOMPOSITION SUBMODEL

Modifications to the original Phoenix plant decomposition equations (McGill et al., 1981): Daily rates were converted to hourly rates. parmeters given separately for bacteria and fungi were combined assuming a 1:4 ratio. parameters given separately for soil layers were combined to give a mean for a 15 cm soil sample. For example, in fdstr, the value, 13.27, is adjusted from K_t values of 11.5 for the top 2 cm soil layer and 13.56 for the 2-6 cm and 6-14 cm soil layers so that $K_{t_{adjusted}} = (2/14) * 11.5 + (12/14) * 13.56 = 13.27$. The value, 1.44, is adjusted from K_2 values of 1.837 for the top 2 cm soil layer and 1.37 for the lower layers.

Stocks (PHO)

dum1_N14(t) = dum1_N14(t - dt) + (plant_N14in' - met_N14 - str_N14) * dt
INIT dum1_N14 = 0 {g N14 Mg^{-1}soil}
DOCUMENT: Dummy pool holding incoming plant materials before separating them into structural and metabolic components.

dum1_N15(t) = dum1_N15(t - dt) + (plant_N15in' - met_N15 - str_N15) * dt
INIT dum1_N15 = 0 {g N15 Mg^{-1}soil}
DOCUMENT: Dummy pool holding incoming plant materials before separating them into structural and metabolic components.

dumC1(t) = dumC1(t - dt) + (plantC_in' - met_C - str_C) * dt
INIT dumC1 = 0 {g C Mg^{-1}soil}
DOCUMENT: Dummy pool holding incoming plant materials before separating them into structural and metabolic components

metabolic_C(t) = metabolic_C(t - dt) + (met_C - Uplant_C' - Aplant_C') * dt
INIT metabolic_C = 0 {g C Mg^{-1}soil}
DOCUMENT: Metabolic plant residue.

metabolic_N14(t) = metabolic_N14(t - dt) + (met_N14 - Uplant_N14' - Aplant_N14') * dt
INIT metabolic_N14 = 0 {g N14 Mg^{-1}soil}
DOCUMENT: Metabolic plant residue.

metabolic_N15(t) = metabolic_N15(t - dt) + (met_N15 - Uplant_N15' - Aplant_N15') * dt
INIT metabolic_N15 = 0 {g N15 Mg^{-1}soil}
DOCUMENT: Metabolic plant residue.

plant_C = structural_C + dumC1 + metabolic_C

plant_N14 = metabolic_N14 + dum1_N14 + structural_N14

plant_N15 = metabolic_N15 + dum1_N15 + structural_N15

structural_C(t) = structural_C(t - dt) + (str_C - Uplant_C" - Aplant_C") * dt
INIT structural_C = 0 {g C Mg^{-1}soil}
DOCUMENT: Structural plant residue.

structural_N14(t) = structural_N14(t - dt) + (str_N14 - Uplant_N14" - Aplant_N14") * dt
INIT structural_N14 = 0 {g N14 Mg^{-1}soil}
DOCUMENT: Structural plant residue.

structural_N15(t) = structural_N15(t - dt) + (str_N15 - Uplant_N15" - Aplant_N15") * dt
INIT structural_N15 = 0 {g N15 Mg^{-1}soil}
DOCUMENT: Structural plant residue.

TplantN15_in(t) = TplantN15_in(t - dt) + (FplantN15_in) * dt
INIT TplantN15_in = 0 {g N15 Mg^{-1}soil}
DOCUMENT: Total plant residue N15 added to soil (sum of pulsed additions if relevant).

Flows (PHO)

Aplant_C = Aplant_C' + Aplant_C"
DOCUMENT: Rate of humadification of plant residue.

Aplant_C" = Uplant_C"*0.975*(1-0.975) {g C Mg^{-1}soil h^{-1}}
DOCUMENT: Rate of adsorption of plant residue structural component.
(1-0.975) =fraction of structural material which is adsorbed

Aplant_C" = 0.044*ftg*Cmet_C*soil_H2O {g C Mg^{-1}soil h^{-1}}
DOCUMENT: Rate of humadification of plant metabolic component
0.044 =rate constant for adsorption {h^{-1}}

Aplant_N14 = Aplant_N14' + Aplant_N14"
DOCUMENT: Rate of humadification of plant residue.

Aplant_N14' = (Aplant_C"*metCN)*(metabolic_N14*met_N) {g N14 Mg^{-1}soil h^{-1}}
DOCUMENT: Rate of adsorption of plant metabolic component.

Aplant_N14" = (Aplant_C"*strCN)*(structural_N14*str_N) {g N14 Mg^{-1}soil h^{-1}}
DOCUMENT: Rate of adsorption of plant residue structural component

Aplant_N15 = Aplant_N15' + Aplant_N15"
DOCUMENT: Rate of humadification of plant residue.

Aplant_N15' = (Aplant_C"*metCN)*(metabolic_N15*met_N) {g N15 Mg^{-1}soil h^{-1}}
DOCUMENT: Rate of adsorption of plant metabolic component.

Aplant_N15" = (Aplant_C"*strCN)*(structural_N15*str_N) {g N15 Mg^{-1}soil h^{-1}}
DOCUMENT: Rate of adsorption of plant residue structural component.

FplantN15_in = plant_N15in {g N15 Mg^{-1}soil h^{-1}}
DOCUMENT: Rate of addition of plant residue N15.

met_C = (1-Fs)*plantC_in' {g C Mg^{-1}soil h^{-1}}
DOCUMENT: Metabolic plant residue entering soil system

met_N14 = (met_C*metCN)*(1-plant_atab) {g N14 Mg^{-1}soil h^{-1}}
DOCUMENT: Metabolic plant residue entering soil system.

met_N15 = (met_C*metCN)*plant_atab {g N15 Mg^{-1}soil h^{-1}}
DOCUMENT: Metabolic plant residue entering soil system.

plant_N14in = plant_Nin*(1-plant_atab) {g N14 Mg^{-1}soil h^{-1}}
DOCUMENT: Input of plant residue.

plant_N14in' = plant_N14in
DOCUMENT: Input of plant residue (link between main and submodel).

plant_N15in = plant_Nin*plant_atab {g N15 Mg^{-1}soil h^{-1}}
DOCUMENT: Input of plant residue.

plant_N15in' = plant_N15in
DOCUMENT: Input of plant residue (link between main and submodel)

plant_Nin = (Fs*plant_Cin)/strCN+((1-Fs)*plant_Cin)/metCN {g N Mg^{-1}soil h^{-1}}
DOCUMENT: Single input of plant residue N.

str_C = Fs*plantC_in' {g C Mg^{-1}soil h^{-1}}
DOCUMENT: Structural plant residue entering soil system.

str_N14 = (str_C/strCN)*(1-plant_atab) {g N14 Mg^{-1}soil h^{-1}}
DOCUMENT: Structural plant residue entering soil system.

str_N15 = (str_C/strCN)*plant_atab {g N15 Mg^{-1}soil h^{-1}}
DOCUMENT: Structural plant residue entering soil system.

Uplant_C = Uplant_C' + Uplant_C"
DOCUMENT: Rate of uptake of plant residue.

Uplant_C' = ftg*(0.18*Cmet_C*mic_C)/(92+Cmet_C) {g C Mg^{-1}soil h^{-1}}
DOCUMENT: Rate of uptake of plant residue metabolic component.
0.18=maximum uptake rate {h^{-1}}
92=Cmet when uptake is 0.5 of maximum {g C $Mg^{-1}H2O$}

Uplant_C" = 0.975*0.0083*ftg*fdstr*fcnratio*mic_C {g C Mg^{-1}soil h^{-1}}
DOCUMENT: Rate of uptake of plant residue structural component.
0.975 = fraction of structural material taken up by microbes
0.0083=maximum uptake rate of structural component {h^{-1}}

Uplant_N14 = Uplant_N14' + Uplant_N14"
DOCUMENT: Rate of uptake of plant residue.

Uplant_N14' = (Uplant_C"*metCN)*(metabolic_N14*met_N) {g N14 Mg^{-1}soil h^{-1}}

DOCUMENT: Rate of uptake of plant residue metabolic component

U plant N14" (U plant C" strCN)*(structural N14 str N) {g N14 Mg^{-1}soil h^{-1}}
DOCUMENT: Rate of uptake of plant residue structural component

U plant N15 U plant N15' + U plant N15"
DOCUMENT: Rate of uptake of plant residue

U plant N15' (U plant C' metCN)*(metabolic N15 met N) {g N15 Mg^{-1}soil h^{-1}}
DOCUMENT: Rate of uptake of plant residue metabolic component.

U plant N15" (U plant C" strCN)*(structural N15 str N) {g N15 Mg^{-1}soil h^{-1}}
DOCUMENT: Rate of uptake of plant residue structural component.

Converters (PHO)

Cmet C 0.586*(metabolic C soil H2O) 0.161 {g C Mg^{-1}H2O}
DOCUMENT: Solution concentration of plant metabolic component.

fcnratio GRAPH(mic C mic N)
(0.00, 1.00), (5.00, 1.00), (10.0, 1.00), (15.0, 1.00), (20.0, 0.75), (25.0, 0.5), (30.0, 0.00)
DOCUMENT: Factor adjusting for the effect of microbial C:N ratio on decomposition and uptake of structural plant residue.

fdstr 1 (1+13.27*((mic C structural C) 1.44)) {dimensionless}
DOCUMENT: Density function for decomposition of structural plant residue.
13.27 (K1) {dimensionless}
1.44 (K2) {dimensionless}

Fs (1 plant CN^{-1} metCN) (1 $strCN^{-1}$ metCN) {dimensionless}
DOCUMENT: Fraction of C in the structural components of plant residue.

met atab IF(metabolic N15 0) THEN(metabolic N15 met N) ELSE 0 {g N15 g^{-1}N}

met N metabolic N14+metabolic N15 {g N Mg^{-1}soil}

met rec IF(TplantN15 in 0) THEN(met N*met atab TplantN15 in)*100 ELSE(0) {%}
DOCUMENT: Recovery of plant residue N15 in protein

metCN 5 {g C g^{-1}N}
DOCUMENT: C:N ratio of metabolic plant component

plant atab 0.117 {g N15 g^{-1}N}
DOCUMENT: Plant residue N15 atom abundance.

plant Cin PULSE(196,0,9000) {g C Mg^{-1}soil, time of addition, time of next addition}
DOCUMENT: Plant residue C added to soil.

plant CN 17.13 {g C g^{-1}N}
DOCUMENT: Original plant C:N ratio

plant rec met rec+str rec {%}

plantC in plant Cin {g C Mg $soil^{-1}$}
DOCUMENT: Input of plant residue (link between plant input sector and main model)

plantC in' plantC in
DOCUMENT: Input of plant residue (link between main and submodel).

str atab IF(structural N15 0) THEN(structural N15 str N) ELSE 0 {g N15 g^{-1}N}

str N structural N14+structural N15 {g N Mg^{-1}soil}

str rec IF(TplantN15 in 0) THEN(str N*str atab TplantN15 in)*100 ELSE(0) {%}
DOCUMENT: Recovery of plant residue N15 in carbohydrate.

strCN 150 {g C g^{-1}N}
DOCUMENT: C:N ratio of structural plant component.

TplantC metabolic C+structural C {g C Mg^{-1}soil}
DOCUMENT: Total plant C.

VER PLANT DECOMPOSITION SUBMODEL

Modifications to the original Verberne et al. (1990) plant decomposition equations. Daily rates were converted to hourly rates.

Stocks (VER)

decomposable_C(t) = decomposable_C(t - dt) + (dec_C - Uplant_C') * dt
INIT decomposable_C = 0 {g C Mg^{-1}soil}
DOCUMENT: Decomposable plant residue.

decomposable_N14(t) = decomposable_N14(t - dt) + (dec_N14 - Uplant_N14') * dt
INIT decomposable_N14 = 0 {g N14 Mg^{-1}soil}
DOCUMENT: Decomposable plant residue.

decomposable_N15(t) = decomposable_N15(t - dt) + (dec_N15 - Uplant_N15') * dt
INIT decomposable_N15 = 0 {g N15 Mg^{-1}soil}
DOCUMENT: Decomposable plant residue.

dum1_N14(t) = dum1_N14(t - dt) + (plant_N14in' - res_N14 - str_N14 - dec_N14) * dt
INIT dum1_N14 = 0 {g N14 Mg^{-1}soil}
DOCUMENT: Dummy pool holding incoming plant materials before separating them into components.

dum1_N15(t) = dum1_N15(t - dt) + (plant_N15in' - res_N15 - str_N15 - dec_N15) * dt
INIT dum1_N15 = 0 {g N15 Mg^{-1}soil}
DOCUMENT: Dummy pool holding incoming plant materials before separating them into components.

dumC1(t) = dumC1(t - dt) + (plantC_in' - res_C - str_C - dec_C) * dt
INIT dumC1 = 0 {g C Mg^{-1}soil}
DOCUMENT: Dummy pool holding incoming plant materials before separating them into components.

plant_C = resistant_C + dumC1 + structural_C + decomposable_C

plant_N14 = resistant_N14 + dum1_N14 + structural_N14 + decomposable_N14

plant_N15 = resistant_N15 + dum1_N15 + structural_N15 + decomposable_N15

resistant_C(t) = resistant_C(t - dt) + (res_C - Cplant_C') * dt
INIT resistant_C = 0 {g C Mg^{-1}soil}
DOCUMENT: Plant residue resistant component.

resistant_N14(t) = resistant_N14(t - dt) + (res_N14 - Cplant_N14') * dt
INIT resistant_N14 = 0 {g N14 Mg^{-1}soil}
DOCUMENT: Resistant plant residue.

resistant_N15(t) = resistant_N15(t - dt) + (res_N15 - Cplant_N15') * dt
INIT resistant_N15 = 0 {g N15 Mg^{-1}soil}
DOCUMENT: Resistant plant residue.

structural_C(t) = structural_C(t - dt) + (str_C - Uplant_C') * dt
INIT structural_C = 0 {g C Mg^{-1}soil}
DOCUMENT: Plant residue structural component.

structural_N14(t) = structural_N14(t - dt) + (str_N14 - Uplant_N14') * dt
INIT structural_N14 = 0 {g N14 Mg^{-1}soil}
DOCUMENT: Structural plant residue.

structural_N15(t) = structural_N15(t - dt) + (str_N15 - Uplant_N15') * dt
INIT structural_N15 = 0 {g N15 Mg^{-1}soil}
DOCUMENT: Structural plant residue.

TplantN15_in(t) = TplantN15_in(t - dt) + (FplantN15_in) * dt
INIT TplantN15_in = 0 {g N15 Mg^{-1}soil}
DOCUMENT: Total plant residue N15 added to soil.

Flows (VER)

Cplant_C = Cplant_C'
DOCUMENT: Rate of humadification of plant residue.

Cplant_C = 0.00084*EXP(-3.0*fdplant)*resistant_C {g C Mg^{-1}soil h^{-1}}
DOCUMENT: Rate of stabilization of resistant plant residue.
0.00084: specific rate of stabilization {h^{-1}}

Cplant_N14 = Cplant_N14'
DOCUMENT: Rate of humadification of plant residue

Cplant_N14' = (Cplant_C'/resCN)*(resistant_N14/res_N) {g N14 Mg^{-1}soil h^{-1}}
DOCUMENT: Rate of stabilization of plant resistant component.

Cplant_N15 = Cplant_N15'
DOCUMENT: Rate of humadification of plant residue.

Cplant_N15' = (Cplant_C'/resCN)*(resistant_N15/res_N) {g N15 Mg^{-1}soil h^{-1}}
DOCUMENT: Rate of stabilization of resistant plant residue.

dec_C = fdecC*plantC_in' {g C Mg^{-1}soil h^{-1}}
DOCUMENT: Decomposable plant residue entering soil system.

dec_C = fdecC*plantC_in' {g C Mg^{-1}soil h^{-1}}
DOCUMENT: Decomposable plant residue entering soil system.

dec_N14 = (dec_C/decCN)*(1-plant_atab) {g N14 Mg^{-1}soil h^{-1}}
DOCUMENT: Decomposable plant residue entering soil system.

dec_N14 = (dec_C/decCN)*(1-plant_atab) {g N14 Mg^{-1}soil h^{-1}}
DOCUMENT: Decomposable plant residue entering soil system

dec_N15 = (dec_C/decCN)*plant_atab {g N15 Mg^{-1}soil h^{-1}}
DOCUMENT: Decomposable plant residue entering soil system.

dec_N15 = (dec_C/decCN)*plant_atab {g N15 Mg^{-1}soil h^{-1}}
DOCUMENT: Decomposable plant residue entering soil system

FplantN15_in = plant_N15in

res_C = fresC*plantC_in' {g C Mg^{-1}soil h^{-1}}
DOCUMENT: Resistant plant residue entering soil system.

res_C = fresC*plantC_in' {g C Mg^{-1}soil h^{-1}}
DOCUMENT: Resistant plant residue entering soil system.

res_N14 = (res_C/resCN)*(1-plant_atab) {g N14 Mg^{-1}soil h^{-1}}
DOCUMENT: Resistant plant residue entering soil system.

res_N14 = (res_C/resCN)*(1-plant_atab) {g N14 Mg^{-1}soil h^{-1}}
DOCUMENT: Resistant plant residue entering soil system.

res_N15 = (res_C/resCN)*plant_atab {g N15 Mg^{-1}soil h^{-1}}
DOCUMENT: Resistant plant residue entering soil system.

res_N15 = (res_C/resCN)*plant_atab {g N15 Mg^{-1}soil h^{-1}}
DOCUMENT: Resistant plant residue entering soil system.

str_C = fstrC*plantC_in' {g C Mg^{-1}soil h^{-1}}
DOCUMENT: Structural plant residue entering soil system.

str_C = fstrC*plantC_in' {g C Mg^{-1}soil h^{-1}}
DOCUMENT: Structural plant residue entering soil system.

str_N14 = (str_C/strCN)*(1-plant_atab) {g N14 Mg^{-1}soil h^{-1}}
DOCUMENT: Structural plant residue entering soil system.

str_N14 = (str_C/strCN)*(1-plant_atab) {g N14 Mg^{-1}soil h^{-1}}
DOCUMENT: Structural plant residue entering soil system.

str_N15 = (str_C/strCN)*plant_atab {g N15 Mg^{-1}soil h^{-1}}
DOCUMENT: Structural plant residue entering soil system.

str_N15 = (str_C/strCN)*plant_atab {g N15 Mg^{-1}soil h^{-1}}
DOCUMENT: Structural plant residue entering soil system.

Uplant_C = Uplant_C' + Uplant_C"
DOCUMENT: Rate of uptake of plant residue.

Uplant_C' = 0.0044*EXP(-3.0*fdplant)*structural_C {g C Mg^{-1}soil h^{-1}}
DOCUMENT: Rate of microbial uptake of structural plant residue.
0.0044=specific rate of decomposition {h^{-1}}

Uplant_C" = 0.0093*decomposable_C {g C Mg^{-1}soil h^{-1}}
DOCUMENT: Rate of microbial uptake of decomposable plant residue.
0.0093=specific rate of decomposition {h^{-1}}

Uplant_N14 = Uplant_N14' + Uplant_N14"
DOCUMENT: Rate of uptake of plant residue.

Uplant_N14' = (Uplant_C'/strCN)*(structural_N14/str_N) {g N14 Mg^{-1}soil h^{-1}}
DOCUMENT: Rate of microbial uptake of structural plant residue.

Uplant_N14" = (Uplant_C"/decCN)*(decomposable_N14/dec_N) {g N14 Mg^{-1}soil h^{-1}}
DOCUMENT: Rate of decomposition of decomposable plant residue.

Uplant_N15 = Uplant_N15' + Uplant_N15"
DOCUMENT: Rate of uptake of plant residue.

Uplant_N15' = (Uplant_C'/strCN)*(structural_N15/str_N) {g N15 Mg^{-1}soil h^{-1}}
DOCUMENT: Rate of microbial uptake of structural plant residue.

Uplant_N15" = (Uplant_C"/decCN)*(decomposable_N15/dec_N) {g N15 Mg^{-1}soil h^{-1}}
DOCUMENT: Rate of microbial uptake of decomposable plant residue.

Converters (VER)

dec_atab = IF(decomposable_N15>0) THEN(decomposable_N15/dec_N) ELSE 0 {g N15 g^{-1}N}

dec_N = decomposable_N14+decomposable_N15 {g N Mg^{-1}soil}

dec_rec = IF(TplantN15_in>0) THEN(dec_N*dec_atab/TplantN15_in)*100 ELSE(0) {%}
DOCUMENT: Recovery of plant residue N15 in protein.

decCN = 6
DOCUMENT: Decomposable plant residue C:N ratio.

fdecC = GRAPH(plant_CN)
(0.00, 1.000), (5.00, 0.75), (10.0, 0.60), (15.0, 0.45), (20.0, 0.30), (25.0, 0.20), (30.0, 0.15), (35.0, 0.125), (40.0, 0.10), (45.0, 0.08), (50.0, 0.07), (55.0, 0.065), (60.0, 0.06), (65.0, 0.050)
DOCUMENT: Fraction of plant residue which is decomposable.

fdplant = IF(TplantC>0) THEN((resistant_C/TplantC)/(structural_C/TplantC+resistant_C/TplantC)) ELSE (1) {dimensionless}
DOCUMENT: Density function for decomposition of structural and resistant plant residue.

fresC = GRAPH(plant_CN)
(0.00, 0.00), (5.00, 0.00), (10.0, 0.00), (15.0, 0.01), (20.0, 0.1), (25.0, 0.15), (30.0, 0.18), (35.0, 0.195), (40.0, 0.2), (45.0, 0.22), (50.0, 0.23), (55.0, 0.235), (60.0, 0.24), (65.0, 0.25)
DOCUMENT: Fraction of plant residue which is resistant.

fstrC = GRAPH(plant_CN)
(0.00, 0.0), (5.00, 0.25), (10.0, 0.4), (15.0, 0.54), (20.0, 0.60), (25.0, 0.65), (30.0, 0.67), (35.0, 0.68), (40.0, 0.7), (45.0, 0.7), (50.0, 0.7), (55.0, 0.7), (60.0, 0.7), (65.0, 0.7)
DOCUMENT: Fraction of plant residue which is structural.

plant_atab = 0.117 {g N15 g^{-1}N}
DOCUMENT: Plant residue N15 atom abundance.

plant_Cin = PULSE(196,0,9000) {g C Mg^{-1}soil, time of addition, time of next addition}
DOCUMENT: Plant residue C added to soil.

plant_CN = 17.13 {g C g^{-1}N}
DOCUMENT: Plant C:N ratio.

plant_N14in = plant_Nin*(1-plant_atab) {g N14 Mg^{-1}soil }

DOCUMENT Input of plant residue

plant N14in' plant N14in
DOCUMENT Input of plant residue

plant N15in plant Nin*plant atab {g N15 Mg^{-1}soil}
DOCUMENT Input of plant residue

plant N15in' plant N15in
DOCUMENT Input of plant residue

plant Nin dec C/decCN+str C/strCN+res C/resCN {g N Mg^{-1}soil h^{-1}}

plant rec dec rec*res rec+str rec {%}

plantC in plant Cin
DOCUMENT Input of plant residue (amount, first pulse, pulse interval).

plantC in' plantC in
DOCUMENT Input of plant residue

res atab IF(resistant N15>0) THEN(resistant N15/res N) ELSE 0 {g N15 g^{-1}N}

res N resistant N14+resistant N15 {g N Mg^{-1}soil}

res rec IF(TplantN15 in>0) THEN(res N*res atab/TplantN15 in)*100 ELSE(0) {%}
DOCUMENT Recovery of plant residue N15 in carbohydrate.

resCN 100
DOCUMENT Resistant plant residue C:N ratio

str atab IF(structural N15>0) THEN(structural N15/str N) ELSE 0 {g N15 g^{-1}N}

str N structural N14+structural N15 {g N Mg^{-1}soil}

str rec IF(TplantN15 in>0) THEN(str N*str atab/TplantN15 in)*100 ELSE(0) {%}
DOCUMENT Recovery of plant residue N15 in cellulose

strCN 150
DOCUMENT Structural plant residue C:N ratio.

TplantC decomposable C+resistant C+structural C {g C Mg^{-1}soil}
DOCUMENT Total plant C

LITERATURE CITED

Grant, R.F., Juma, N.G. and McGill, W.B. 1993. Simulation of carbon and nitrogen transformations in soil: mineralization. Soil Biol. Biochem. 25:1317-1329.

McGill, W.B., Hunt, H.W., Woodmansee, R.G. and Reuss, J.O. 1981. Phoenix-A model of the dynamics of carbon and nitrogen in grassland soils *in* F.E. Clark and T. Rosswall, eds. Terrestrial Nitrogen Cycles. Ecol. Bull. (Stockholm) 33:49-115.

Verberne, E.L.J., Hassink, J., De Willigen, P., Groot, J.J.R. and Van Veen, J.A. 1990. Modelling organic matter dynamics in different soils. Netherlands Journal of Agricultural Science 38:221-238.

SCHEMATIC OF SELECTED COMPONENTS OF BASE MODEL + ECO PLANT DECOMPOSITION SUBMODEL

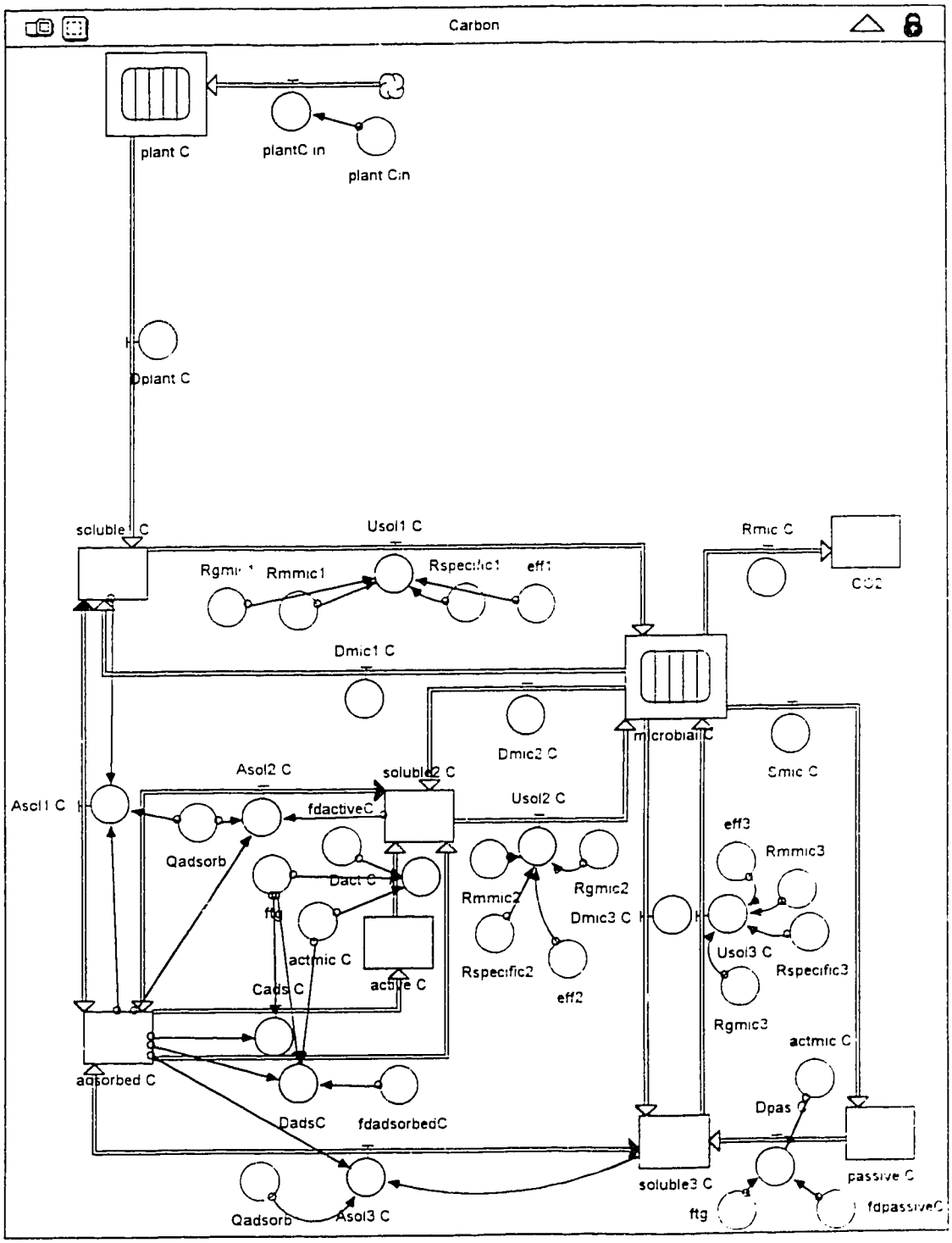

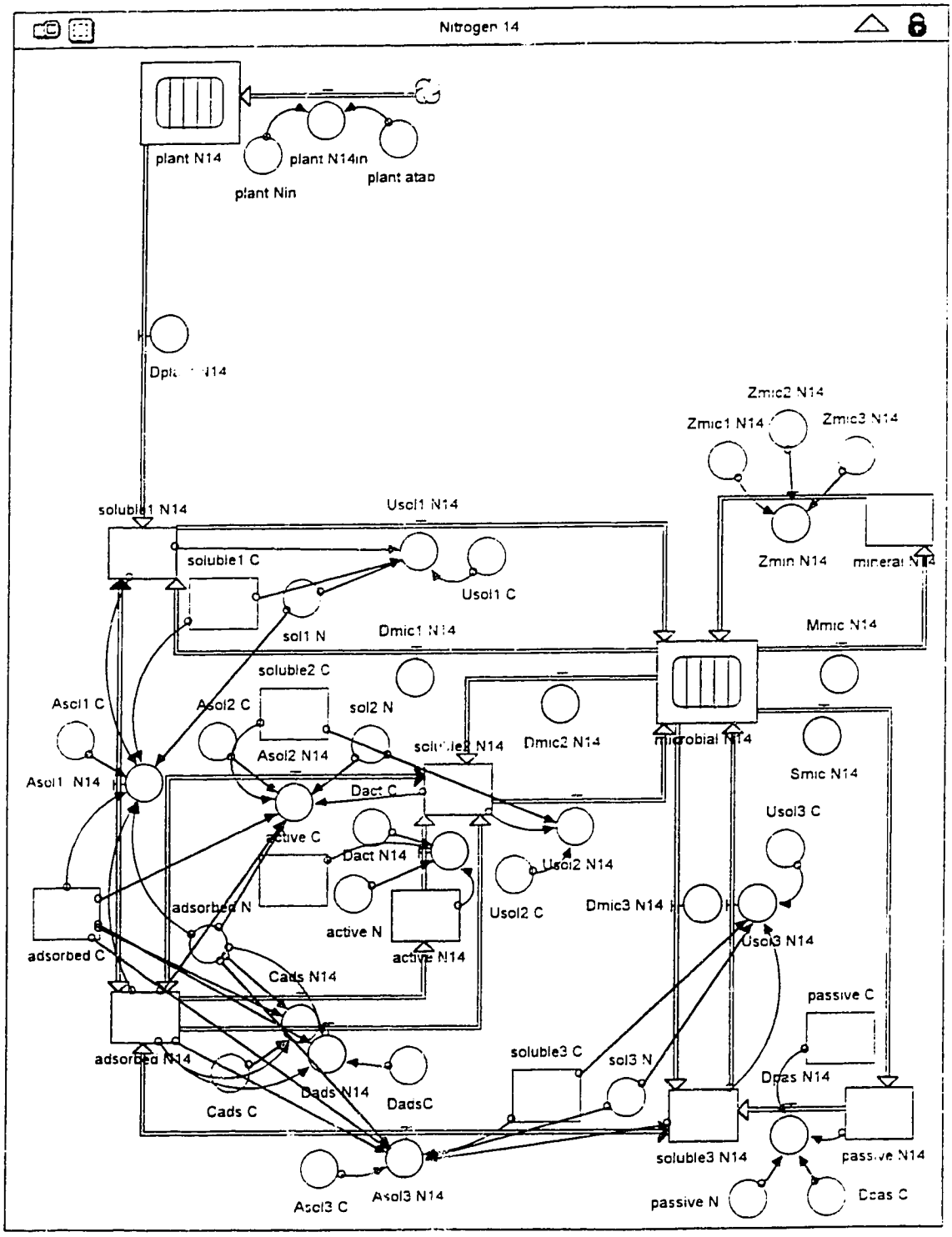
Nitrogen 14
plant N14
plant N14in
plant atap
plant Nin
Zmic2 N14
Zmic1 N14
Zmic3 N14
Zmin N14
Usol1 N14
soluble1 C
Usol1 C
sol1 N
Dmic1 N14
Mmic N14
soluble2 C
Asol1 C
Asol2 C
sol2 N
Asol2 N14
Dmic2 N14
Smic N14
Asol1 N14
Dact C
active C
Dact N14
Usol2 N14
Usol3 C
adsorbed N
active N
Usol2 C
Dmic3 N14
Usol3 N14
adsorbed C
active N14
Cads N14
passive C
soluble3 C
sol3 N
Dpas N14
Cads C
Dads N14
DadsC
soluble3 N14
passive N14
Asol3 C
Asol3 N14
passive N
Dpas C

Microbial C Submodel

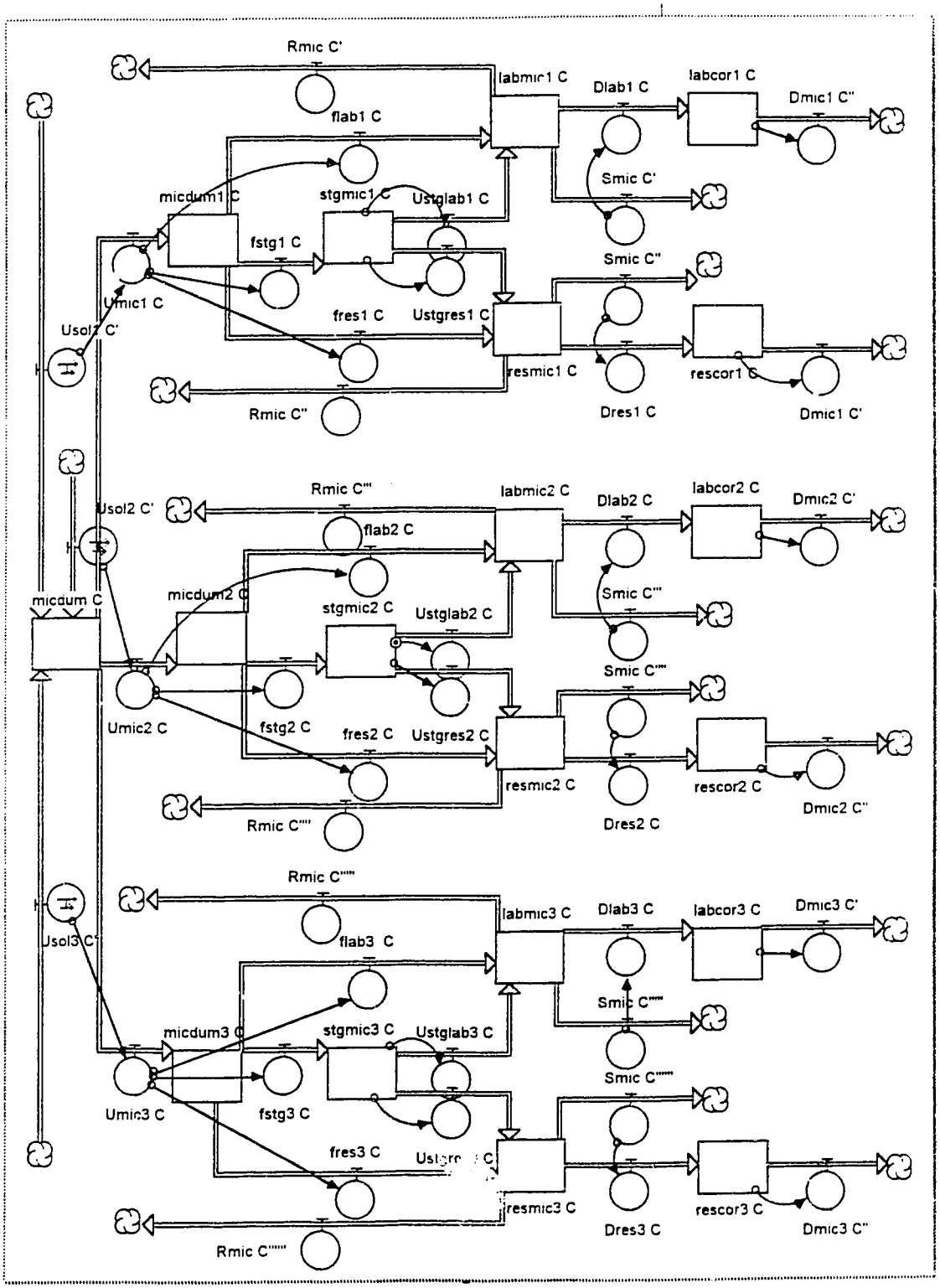

Microbial N14 Submodel